

Charles University

Faculty of Science

Study program: Physical Geography and Geoecology



Bc. et RNDr. Ondřej Hotový

Changes in snowmelt and rain-on-snow runoff in mountainous catchments

Změny v tání sněhu a odtoku při událostech deště na sněh v horských povodích

Doctoral thesis

Supervisor: doc. RNDr. Michal Jeníček, Ph.D.

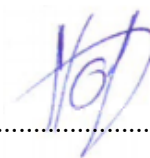
Prague, 2024

Declaration / Prohlášení:

I hereby declare that I have worked independently on the doctoral thesis and reported all the data sources and literature used in the thesis. This thesis has not been submitted to obtain any other academic title.

Prohlašuji, že jsem disertační práci vypracoval samostatně a všechny použité datové a informační zdroje jsem řádně citoval. Tato práce ani její podstatná část nebyla předložena k získání jiného nebo stejného akademického titulu.

August 5, 2024, in Prague



.....
Bc. et RNDr. Ondřej Hotový

Table of contents

Acknowledgements	5
Abstract	6
Abstrakt	7
List of publications	8
1 Scope of the thesis	9
2 Topic introduction	11
2.1 Hydrological role of snow	11
2.2 Snow accumulation and snowmelt	11
2.2.1 Snowpack energy balance method	12
2.2.2 Degree-day approach.....	13
2.2.3 Energy fluxes in different canopy structures	14
2.3 Rain-on-snow events	16
2.3.1 RoS principles	16
2.3.2 RoS-driven hydrological response	16
2.3.3 RoS occurrence in the current climate.....	16
2.4 Changes driven by climate change	17
2.4.1 Future snow	17
2.4.2 Future RoS.....	17
3 Materials and methods.....	20
3.1 Study areas	20
3.2 Data collecting and analyzing	20
3.2.1 Field measurements.....	20
3.2.2 Modeling approaches	21
3.2.3 HBV model.....	22
3.3 Identification of RoS events	24
4 Published research overview	25
4.1 Paper I	25
4.2 Paper II	26
4.3 Paper III.....	27
4.4 Paper IV.....	28
5 Discussion	30

5.1 Hydrological implications	30
5.2 Uncertain climate impacts	30
5.3 RoS identification.....	31
5.4 Data complexity in snow hydrology.....	32
5.5 Uncertainty in modeling approach	34
6 Outlook and conclusions	36
7 References	38
8 Supplements	46

Acknowledgements

This dissertation would not have been possible without the support, guidance, and encouragement of many individuals.

First and foremost, I would like to express my deepest gratitude to my advisor, Michal Jeníček, for his continuous encouragement, academic energy and insightful feedback throughout this research journey. Michal was always available to provide support on everything from administrative procedures to research and fieldwork planning. His expertise and patience have been invaluable in shaping this and previous works, as well as in my development as a scholar. After almost ten years of collaboration, I would say without doubt that choosing such a perfect supervisor was a crucial step for my future academic career. Thank you for all, Michal!

A special thanks go to my colleagues, fellow doctoral candidates and friends, whose camaraderie and intellectual exchanges have been a source of inspiration and motivation. I am particularly grateful to Vojtěch Vlach and Tomáš Kroczeck who made my studies funnier and shared the PhD worries with me. I would also like to thank my colleague Ondřej Nedělničev who was always willing to share his technical knowledge and support me in developing research ideas.

Finally, I am deeply grateful to my family for their unwavering support throughout this long journey. Without their encouragement and sacrifices, this would not have been possible. I am particularly grateful to my wife and daughter who faced my complaints about how to balance work, studies and family life the most often.

Finally, the research would not be performed without the direct financial support of the following agencies and projects: Charles University Grant Agency, project no. GAUK 272119 (Modelling of future effects of changes in snow storages on occurrence and extremity of runoff caused by rain-on-snow events); Czech Science Foundation, project no. 18-06217Y (Influence of seasonal snowpack on summer low flows: Climate change implications on hydrological drought) and project no. GAČR 23-06859K (MountSnow); Technology Agency of the Czech Republic, project no. SS02030040; Internal Grant Agency of Faculty of Environmental Sciences, Czech University of Life Sciences in Prague, project no. 20184236.

Abstract

Snowmelt dynamics and the frequency and intensity of rain-on-snow (RoS) events are expected to change in response to climate variations due to changes in precipitation, increase in air temperature and subsequent changes in the snow occurrence. Therefore, there is a need to understand the circumstances under which RoS events produce runoff and how the main drivers affect snowmelt.

This dissertation thesis compiles various types of research at different spatial and temporal scales, including the experimental site study and regional and international multi-catchment research. Mountainous catchments located in Central Europe were selected for the studies. Particular attention was paid to changes in elevation, with a specific focus on areas within the rain-snow transition zones where large changes in snow storage, snow dynamics and RoS occurrence typically occur due to warming climate. Various methodological approaches were used in the research ([Papers I-IV](#)). In our experimental study ([Paper I](#)), we assessed forest structure as an important parameter that significantly influences the amount of radiation fluxes that consequently affect snowpack energy balance and snowmelt rates. In [Papers II-IV](#), a conceptual hydrological HBV model was used to simulate runoff components. We then identified RoS days/events, evaluated trends and spatial and temporal changes in the RoS occurrence, and assessed the hydrological response resulting from these hydrological events using the data series simulated by the model. We also attributed changes in selected climate variables, particularly air temperature and precipitation, to simulated possible variations in RoS events in the future climate ([Paper IV](#)).

This research highlighted the different roles of shortwave and longwave radiation in different forest structures, as well as the influence of other components of the snowpack energy balance. The results presented in [Paper I](#) revealed that energy from rain might be very important when assessing snowmelt at daily and shorter temporal resolutions. Notable effects of gradual forest decay on snowmelt processes were also demonstrated in this study, showing a 50% increase in modeled snowmelt rates in the disturbed forest. Our elevation-based methods accounted for the fact that only a part of the catchment contributes to runoff during the specific RoS events due to the strong dependence of snowmelt on air temperature at specific elevations ([Paper II](#)). Analyses of the runoff response showed that most of the RoS events (82% in [Paper II](#), 72% in [Paper III](#)) did not cause a significant increase in runoff, highlighting the importance of the snowpack which can often prevent extreme runoff even when a large amount of rain occurs ([Paper II](#)). Nevertheless, notable climate change-driven RoS changes were identified and were highly variable across regions, elevations, and within the cold season ([Papers III](#) and [IV](#)). A significant decrease in RoS days (up to 75%) was projected for some lower-elevation sites. An increase in the number of RoS days was limited to higher elevations and the coldest winter months ([Papers III](#) and [IV](#)). Our projections also suggested that the RoS contribution to annual runoff will be considerably reduced; from the current 10% to 2-4% for the warmest projections in Czechia, and from 18% to 5-9% in Switzerland ([Paper IV](#)).

Although the overall impact of RoS on runoff is expected to be lower in the future, extreme hydrological response and flooding triggered by RoS events can still pose a significant flood risk. Therefore, understanding snowmelt processes and RoS behavior is essential for improving snowmelt models, effective water resource management, drought and flood forecasting and risk mitigation, especially in the face of climate change.

Keywords: snowmelt, rain-on-snow events, runoff, rain-snow transition zone, climate change

Abstrakt

Očekává se, že dynamika tání sněhu a četnost a intenzita událostí deště na sníh (*RoS events*) se bude měnit v reakci na změny klimatu, konkrétně v důsledku změn srážek, zvýšení teploty vzduchu a následných změn ve výskytu sněhové pokrývky. I proto je třeba porozumět tomu, jak tyto události generují odtok a jaké jsou hlavní faktory ovlivňující tání sněhu.

Tato disertační práce zahrnuje různé typy výzkumu napříč prostorovými a časovými měřítky, včetně experimentální studie a regionálního a mezinárodního výzkumu na větším počtu povodí. Pro účely výzkumu byla vybrána horská povodí nacházející se v regionu střední Evropy. Zvláštní pozornost byla věnována změnám v různých nadmořských výškách, se zvláštním zaměřením na oblasti v přechodové zóně déšť-sníh, kde v důsledku oteplování klimatu obvykle dochází k výrazným změnám v akumulaci a tání sněhu, ke změnám procesů uvnitř sněhové pokrývky a výskytu RoS. Při výzkumu byly použity různé metodické postupy ([články I-IV](#)). V naší experimentální studii ([článek I](#)) jsme analyzovali strukturu lesa jako jeden z důležitých parametrů, který významně ovlivňuje intenzitu radiačních toků, jež následně ovlivňují energetickou bilanci sněhové pokrývky a rychlost tání sněhu. V [článcích II-IV](#) byl k simulaci komponent odtoku použit konceptní hydrologický model HBV. Následně jsme identifikovali RoS dny/události, vyhodnotili trendy a prostorové a časové změny výskytu RoS a analyzovali hydrologickou odezvu vyvolanou těmito událostmi s použitím dat simulovaných modelem. Dále jsme změny vybraných klimatických proměnných, zejména teploty vzduchu a srážek, vztáhli k možným budoucím změnám událostí RoS ([článek IV](#)).

Tento výzkum poukázal na rozdílnou roli krátkovlnného a dlouhovlnného záření v různých strukturách lesa a také na vliv dalších složek energetické bilance sněhové pokrývky. Výsledky prezentované v [článku I](#) ukázaly, že energie z deště může být velmi významnou složkou při vyhodnocování tání sněhu v denním a kratším časovém horizontu. V této studii byl také prokázán významný vliv postupného rozpadu lesa na procesy tání sněhu, vykazující 50% nárůst modelované rychlosti tání sněhu v rozpadlém lese. Naše metody zohledňující nadmořskou výšku poukázaly na skutečnost, že během konkrétních událostí RoS přispívá k celkovému odtoku pouze část povodí, a to v důsledku závislosti tání sněhu na teplotě vzduchu v konkrétních nadmořských výškách ([článek II](#)). Analýzy odtokové odezvy ukázaly, že většina událostí RoS (82 % v [článku II](#), 72 % v [článku III](#)) nezpůsobila významné zvýšení odtoku, což zdůrazňuje význam sněhové pokrývky, která může často zabránit extrémnímu odtoku i při vyšších úhrnech dopadajících srážek ([článek II](#)). Přesto byly zjištěny významné změny v událostech RoS vyvolané změnami klimatických parametrů v souvislosti se změnou klimatu. Pozorované změny se významně lišily v závislosti na regionu, nadmořské výšce a období v průběhu zimy ([článek III](#) a [IV](#)). Naše prognózy také naznačují, že podíl RoS na ročním odtoku se v budoucnosti výrazně sníží; ze současných 10 % na 2-4 % pro nejteplejší projekce v Česku a z 18 % na 5-9 % ve Švýcarsku ([článek IV](#)).

Ačkoli se očekává, že celkový dopad RoS na odtok bude v budoucnu nižší, extrémní hydrologická reakce a povodně vyvolané RoS událostmi mohou nadále představovat významné povodňové riziko. Hlubší pochopení procesů tání sněhu a chování RoS je proto nezbytné pro zdokonalení hydrologických modelů, které zohledňují tání sněhu, a tím do budoucna zefektivit management vodních zdrojů, predikce sucha a povodňových stavů a zmírnění povodňového rizika.

Klíčová slova: tání sněhu, události deště na sníh, odtok, přechodová zóna déšť-sníh, klimatická změna

List of publications

The thesis summarizes the results of four papers published in well-recognized international Web-of-Science-indexed journals. All papers in the original journal form are attached in Supplement, overviews of published papers are included in Section 4. Quartiles in the list below are based on the AIS metric.

Paper I (IF 2023 = 2.8, Q1 in Water Resources)

Hotovy O, Jenicek M. 2020. The impact of changing subcanopy radiation on snowmelt in a disturbed coniferous forest. *Hydrological Processes* 34 (26): 5298-5314 <https://doi.org/10.1002/hyp.13936>

Author's contribution (85%): literature research, methodology, data collection, data processing, and analyses, results interpretation, figures, manuscript writing and editing, and correspondence with the journal.

Paper II (IF 2023 = 5.9, Q1 in Water Resources)

Juras R, Blöcher JR, Jenicek M, Hotovy O, Markonis Y. 2021. What affects the hydrological response of rain-on-snow events in low-altitude mountain ranges in Central Europe? *Journal of Hydrology* 603: 127002 <https://doi.org/10.1016/j.jhydrol.2021.127002>

Author's contribution (15%): modeling procedures, manuscript co-writing and editing.

Paper III (IF 2023 = 2.8, Q1 in Water Resources)

Hotovy O, Nedelcev O, Jenicek M. 2023. Changes in rain-on-snow events in mountain catchments in the rain-snow transition zone. *Hydrological Sciences Journal* 68 (4): 572-584 <https://doi.org/10.1080/02626667.2023.2177544>

Author's contribution (80%): literature research, methodology, data collection, data processing, and analyses, results interpretation, figures, manuscript writing and editing, and correspondence with the journal.

Paper IV (IF 2023 = 5.7, Q1 in Water Resources)

Hotovy O, Nedelcev O, Seibert J, Jenicek M. 2024. Rain-on-snow events in mountainous catchments under climate change. *Hydrology and Earth System Sciences* (under review)

Author's contribution (80%): literature research, methodology, data collection, data processing, and analyses, results interpretation, figures, manuscript writing and editing, and correspondence with the journal.

I, Michal Jeniček, agree with the author's contribution statements above

1 Scope of the thesis

This doctoral thesis assesses changes in mountain snowmelt and rain-on-snow (RoS) runoff in the context of climate change since variations in precipitation, the increase in air temperature and subsequent changes in the snow storage are likely to affect the behavior of extreme hydrological events in the future. Although these snowmelt topics have been widely studied recently, the real impact of changing climate variables on snowmelt processes, RoS frequency and related hydrological implications remain unclear, mainly due to their complex nature.

Four studies included within the thesis represent various types of research at different spatial and temporal scales (Fig. 1). The thesis aims to introduce different methodological approaches that can be applied in the research of mountain snowmelt at various spatial resolutions, from the experimental site study with the high detail on snowmelt processes and influencing factors to more generalized multi-catchment regional and international studies. We were particularly focused on the changes in lower-elevation mountain ranges that represent rain-snow transition areas where large changes in snow storage, snowmelt and RoS occurrence typically occur due to warming climate and landscape changes. Moreover, most European studies have had a limited focus on elevation which significantly influences the precipitation phase and snow cover. Therefore, our focus on differences across elevation zones addressed within the thesis is another important spatial dimension of this research.

The thesis contributes to the understanding of the snowmelt processes, the role of various factors and runoff responses driven by extreme meteorological events within rain-snow transition zones which is essential for effective water resource management, drought and flood prediction and risk mitigation, particularly in the face of climate change, which alters snowfall patterns and the onset and character of snowmelt.

Regarding the scope of the thesis, the **main research objectives** can be drawn as follows:

- 1) Analyzing main snowmelt drivers and their contribution to runoff
- 2) Evaluating the frequency and extremity of rain-on-snow events, their spatial and temporal changes and hydrological implications
- 3) Assessing the role of warming climate and landscape changes on snowmelt processes, runoff and rain-on-snow events

Research topic (method used)	Spatial scale		
	Local	Regional	National
Hydrological response, effect on runoff (Hydrological modeling, self-organizing maps)		Paper II Paper III	Paper IV
Future variations due to warming climate (Hydrological modeling, sensitivity analysis)			Paper IV
RoS trends (Hydrological modeling, trend analysis)		Paper III	
Interannual RoS variability (Hydrological modeling)		Paper II	
Influencing factors (Field observation, correlation analysis)	Paper I		Paper IV

Figure 1: PhD publications sorted by topic and spatial scale.

2 Topic introduction

2.1 Hydrological role of snow

Snow has a profound impact on many dimensions of human life and nature. Seasonal snowpack significantly influences catchment runoff and thus represents an essential component of the hydrological cycle, particularly in mountainous regions in humid climates. Most of the hydrological implications of snowpack are related to its ability to store a substantial amount of water from winter precipitation. Field experiments conducted by Juras *et al.* (2017) showed that snowpack temporarily stored up to 70% of incoming rainwater volume. This stored water is gradually released during the spring and summer as the snow melts. The gradual melting of snow provides a sustained source of water to rivers and streams, which is particularly important in regions that experience dry periods. Snowpack accumulated during the cold season affects groundwater recharge and thus influences spring runoff and summer low flows (Hammond *et al.*, 2018; Jenicek and Ledvinka, 2020; Vlach *et al.*, 2020). The amount of snow accumulated during the winter period together with the character of a subsequent snowmelt process significantly determines the availability of water in many regions, thus affecting agriculture, hydropower generation, water supply management and other related sectors.

Regarding the scope of this thesis, the effects of snow on flood risk are the most relevant to be highlighted here. There are both, positive and negative impacts of snow associated with flood generating – on the one hand, snowpack helps to mitigate the risk of flooding by temporarily storing water that would otherwise contribute to runoff (Würzer *et al.*, 2017; [Paper II](#)), on the other hand, rapid snowmelt under certain conditions, especially during rain-on-snow (RoS) events, can lead to increased runoff and potential severe flooding.

Understanding these hazardous events is therefore crucial for flood management and risk mitigation. Given the importance of snow mentioned above, an understanding the snow processes in general, as well as the role of various influencing factors, is essential for effective water resource management, particularly in the face of climate change, which alters snowfall patterns and the onset and character of snowmelt.

2.2 Snow accumulation and snowmelt

Snow accumulation intensity and snowmelt rates directly determine the volume of accumulated snow, and storage of water respectively. At local scales, snow accumulation and ablation are controlled by a number of factors (Fig. 2). These include 1) meteorological conditions (Assaf, 2007), such as air temperature, precipitation rate, air humidity, or wind speed, 2) local topography (Zheng *et al.*, 2016), including elevation, aspect and slope, and 3) canopy structure (Jenicek *et al.*, 2018; Lendzioch *et al.*, 2019; [Paper I](#)).

As investigated in several studies (Helgason and Pomeroy, 2012; Lundquist *et al.*, 2013; Broxton *et al.*, 2015; [Paper I](#)), the forest significantly influences the amount and distribution of individual energy fluxes and thus the snowpack energy balance (Section 2.2.1), snowpack physical properties and water volume (Musselman and Pomeroy, 2017; Roth and Nolin, 2017). Detailed analysis of the effect of sub-canopy snowmelt was provided in [Paper I](#) which concluded the important role of both radiation fluxes (shortwave and longwave radiation) in decreasing snowmelt rates which is consistent with the findings presented by Assaf (2007); Webster *et al.* (2016); Malle *et al.* (2019).

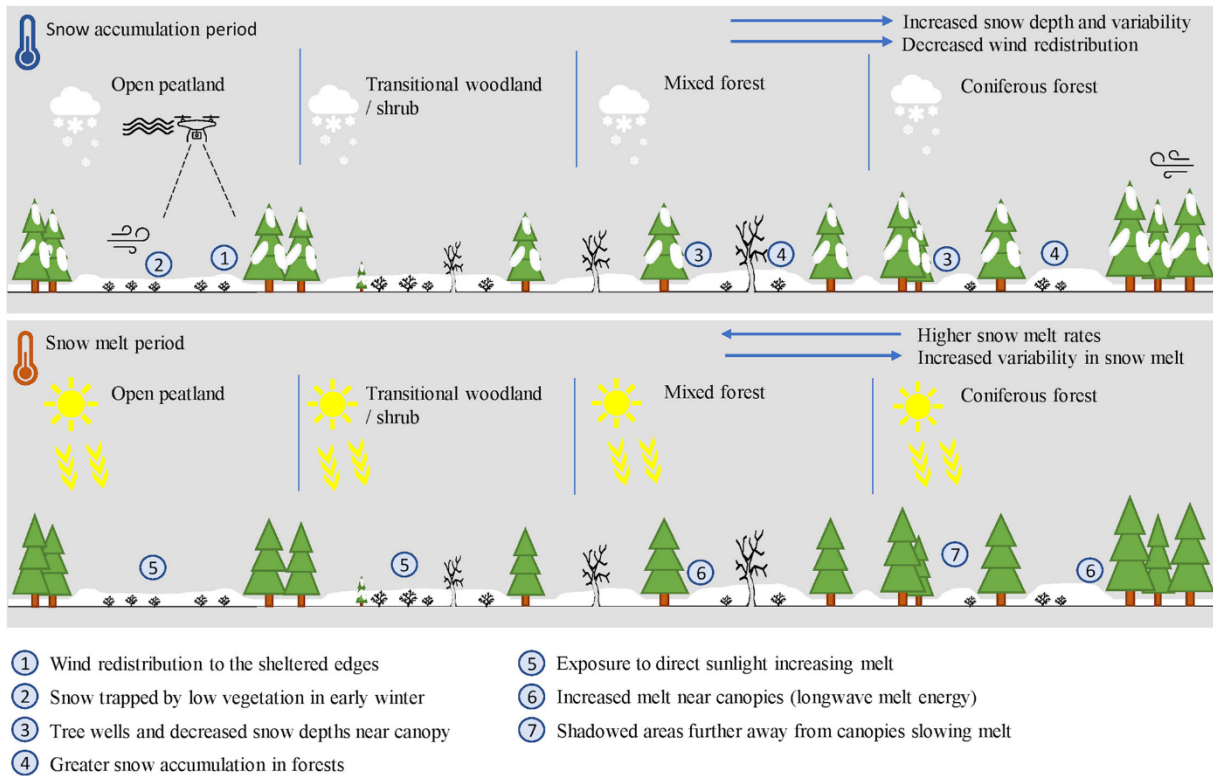


Figure 2: Snow accumulation and snowmelt processes for different land cover types observed by Meriö et al. (2023).

In addition, the canopy structure considerably affects the wind speed (Fig. 2), reducing the intensity of snow redistribution by the wind. Forest density also determines the interception rate which primarily controls the subcanopy snow accumulation. According to Helbig *et al.* (2019), through interception, up to 60% of the cumulative snowfall may be captured by tree crowns in coniferous forests during winter. A high interception rate combined with a reduced redistribution of snow by wind may lead to notable differences in the amount of accumulated snow between forested sites and open areas. This topic was addressed in detail in [Paper I](#) since understanding the effect of forests on snowmelt dynamics enables better estimates of snow and water storage and contributes to higher accuracy of spring flood forecasting (Hock, 2003).

There are basically two main methods used for snowmelt rate calculation – the complex snowpack energy balance method and the degree-day-based approach.

2.2.1 Snowpack energy balance method

The snowpack energy balance method is a comprehensive approach to understanding the snowpack behavior, in particular the snowmelt process. This method quantifies heat fluxes, various energy inputs and outputs, at the atmosphere-snow-soil ground interfaces and heat exchange within the snowpack (Singh and Singh, 2001) (Fig. 3). By considering all energy sources, this method allows accurate predictions of snowmelt and its subsequent effects on runoff response. However, the entire energy balance-based calculations require a high demand for detailed meteorological and hydrological data. This physically-based approach was applied in [Paper I](#) to calculate the main energy fluxes driving the snowmelt process in different environments (coniferous forest, disturbed coniferous forest, meadow).

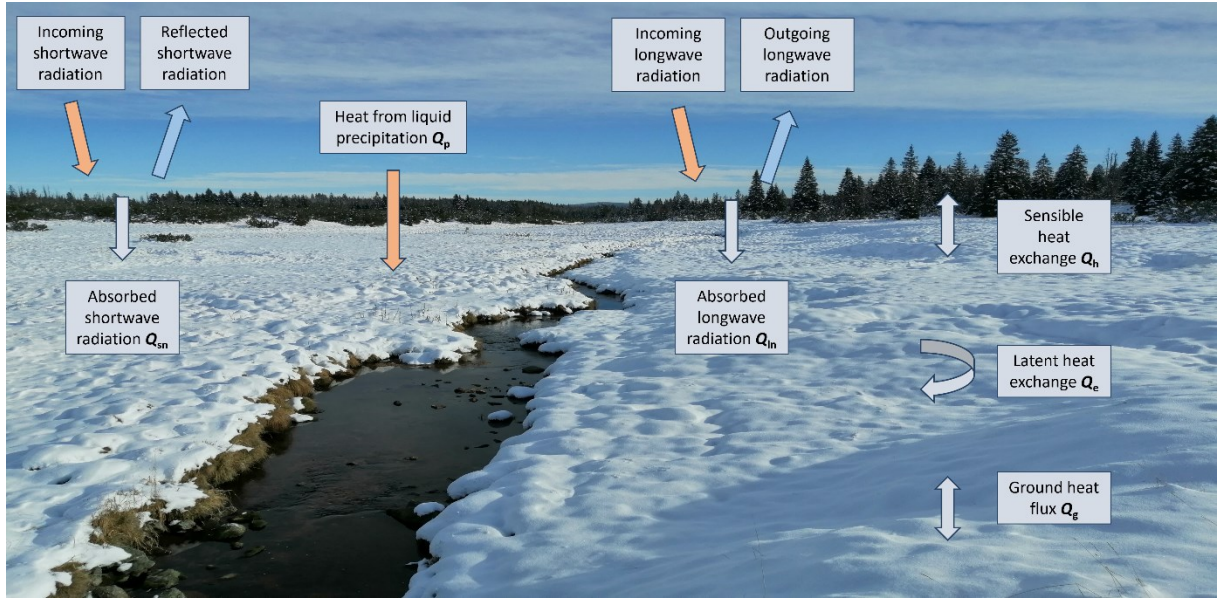


Figure 3: Scheme of individual energy fluxes within the complex snowpack energy balance (photo by author).

Equation (1) expresses the calculation of the total heat Q_m ($\text{W}\cdot\text{m}^{-2}$) available for snowmelt and refreezing based on a sum of six components. Positive values of Q_m represent snowpack energy gains resulting in gradual warming of the snowpack (snowmelt occurs when the snowpack temperature reaches 0°C within the entire snow profile). Negative Q_m values signify energy losses, resulting in a decrease of snowpack temperature (no snowmelt):

$$Q_m = Q_{ns} + Q_{nl} + Q_h + Q_e + Q_p + Q_g \quad (1)$$

where Q_{ns} is net shortwave radiation (SWR), including solar radiation that reaches the snow surface. Q_{nl} represents net longwave radiation (LWR) which encompasses the absorbed radiation emitted by the atmosphere and the earth's surface. Q_h is the sensible heat flux, meaning the energy exchange due to temperature differences between the air and the snow surface. Q_e represents the latent heat flux which involves the energy exchange due to phase changes of water. Q_p is the heat supplied by liquid precipitation (investigated in more detail in [Paper I](#)) and Q_g is the ground heat flux, attributing energy transfer between the snowpack and the ground beneath it. All components use the same unit ($\text{W}\cdot\text{m}^{-2}$).

Since the spatial and temporal variability of key components of the energy balance is important for the timing and intensity of runoff, the topic has been widely studied (Garvelmann *et al.*, 2015; Welch *et al.*, 2016), including the application of energy balance methods into the hydrological modeling (Ellis *et al.*, 2011; Helgason and Pomeroy, 2012; Gouttevin *et al.*, 2015) (Section 3.1.2). Several authors have focused on selected components in their studies, mainly on the role of radiative fluxes; SWR (Courbaud *et al.*, 2003; Reid *et al.*, 2014; Musselman *et al.*, 2015) and LWR (Iziomon *et al.*, 2003; Essery *et al.*, 2008; Webster *et al.*, 2016).

2.2.2 Degree-day approach

The degree-day approach represents the simplified energy balance of the snowpack (DeWalle and Rango, 2008). This approach is based on the principle that the amount of snowmelt is directly related to the accumulated temperature over time, providing a simplified yet effective way to model and predict snowmelt. The basic degree-day calculation is given by Equation (2):

$$M = m_f(T_a - T_b) \quad (2)$$

where M represents snowmelt volume ($\text{mm}\cdot\text{d}^{-1}$), T_a is air temperature, usually daily mean ($^{\circ}\text{C}$), T_b represents the critical temperature for snowmelt initiation ($^{\circ}\text{C}$). The critical temperature of 0°C is generally used for melt calculation, however, a wider range can be applied regarding the conditions and of the study area (Hock, 2003). m_f (alternatively DDF) is a melt factor or degree-day factor ($\text{mm}\cdot^{\circ}\text{C}^{-1}\cdot\text{d}^{-1}$) representing the decrease in snow water equivalent (SWE) per day caused by the air temperature (T_a) change by 1°C compared to the critical air temperature (T_b).

A wide range of melt factors can be found in the literature as different variables affect snowmelt. These include meteorological conditions (rainfall intensity, cloudiness, wind, humidity), snowpack properties (snow density, layering, snow surface contamination), site specifics (canopy structure, topography) and other factors (season). Most m_f values fall between 1 and $8 \text{ mm}\cdot^{\circ}\text{C}^{-1}\cdot\text{d}^{-1}$, according to DeWalle and Rango (2008).

The degree-day approach in its simple version was used in many recent studies (Freudiger *et al.*, 2014; Girons Lopez *et al.*, 2020). Jenicek *et al.* (2017) quantified the role of different forest types on snowmelt processes with the m_f ranging from 2.1 to $3.1 \text{ mm}\cdot^{\circ}\text{C}^{-1}\cdot\text{d}^{-1}$. A more complex degree-day calculation was applied in [Papers II-IV](#) where the HBV snow routine was used to simulate snow accumulation and snowmelt rates. This model routine uses an extended degree-day approach, that includes potential refreezing of meltwater and snow water holding capacity in its calculation (see Section 3.1.3 for more details).

Despite its limitations, the simplicity and effectiveness of the degree-day method make it an indispensable component of hydrological studies and applications. Temperature-index methods have been widely used in hydrological modeling to approximate snowpack energy exchange rather than using the more data-intensive energy-budget approaches (DeWalle and Rango, 2008).

2.2.3 Energy fluxes in different canopy structures

Specific scientific interest has been put on the contribution of the individual energy balance components regarding the differences in canopy structure ([Paper I](#)) as understanding the effects of forest cover on the sub-canopy energy balance is important for improving snowmelt models for accurate prediction of catchment runoff from forested catchments.

Based on the performed research, individual energy fluxes vary significantly among different canopy structures and there are considerable differences between forested sites and open non-forested areas. Thus, potential changes in forest structure, such as forest disturbances, may lead to significant changes in snowmelt dynamics and runoff conditions (Su *et al.*, 2017; Bartik *et al.*, 2019), with expected faster snowmelt (Moeser *et al.*, 2016; Förster *et al.*, 2018, [Paper I](#)). These differences can be mainly explained by (a) lower snow interception (Helbig *et al.*, 2019), (b) the increase in incoming SWR due to a lower shading effect of trees after forest disturbance (Pomeroy *et al.*, 2012; Malle *et al.*, 2019) and (c) the decrease in incoming LWR emitted by trees which is an important energy contributor (Essery *et al.*, 2008; Webster *et al.*, 2016; [Paper I](#)).

The results of our experimental study ([Paper I](#)) showed that SWR was the major energy source at the open site, while, in the dense coniferous forest, net SWR represented only 7% of the amount at the open site due to tree shading (Fig. 4). In contrast, net LWR was the dominant energy contributor at the healthy forest site (on average 41% of all energy fluxes) and thus contributed most to snowmelt.

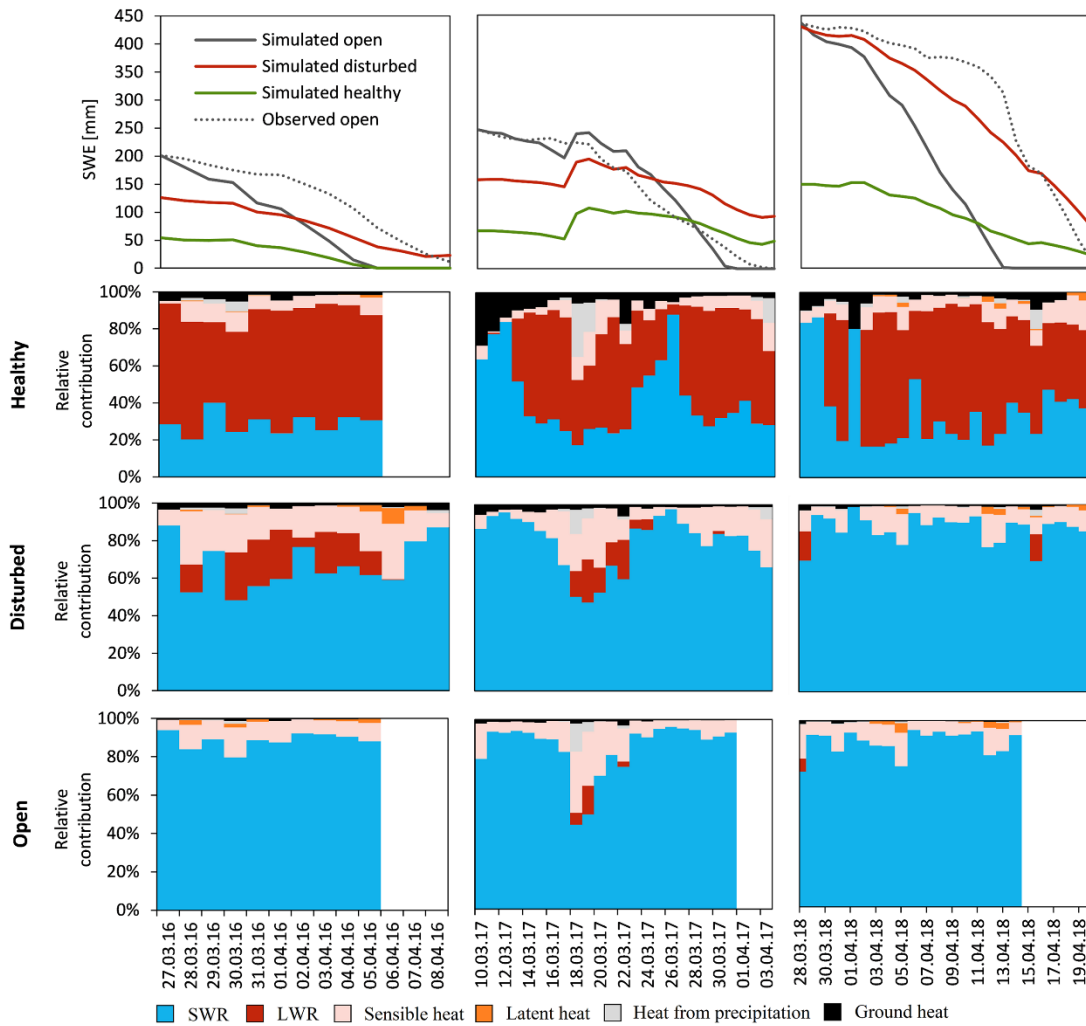


Figure 4: Simulated and observed SWE at individual study sites with different forest structures during the main spring snowmelt periods in seasons 2016, 2017 and 2018 (first line panels). Relative daily contribution of individual energy fluxes to snowmelt rates at the healthy forest site (second line panels), disturbed forest site (third line panels) and open site (fourth line panels) ([Paper I](#)).

Notable energy and snowmelt changes were identified in the disturbed forest within the 3 years of gradual forest decay (Fig. 4).

[Paper I](#) provided some interesting conclusions related to the turbulent energy exchange since we were specifically interested in the contribution of heat energy from rain. On a seasonal average, rainfall added rather a negligible amount of energy (up to 10%) to the snowpack. This supports the findings of other studies (Mazurkiewicz *et al.*, 2008; Trubilowicz and Moore, 2017; Li *et al.*, 2019). However, the increased importance of heat from the rain to snowmelt was found during the days with heavier precipitation, supporting the fact that energy from rain can be very important when assessing the snowpack energy balance at daily and shorter temporal resolutions (Würzer *et al.*, 2016; Juras *et al.*, 2017). This finding initiated our subsequent interest in rain-on-snow events ([Paper II-IV](#)).

2.3 Rain-on-snow events

2.3.1 RoS principles

Rain-on-snow (RoS) events occur when rain falls on snow, intensifying energy fluxes within the snowpack, and can substantially accelerate snowmelt (Garvelmann *et al.*, 2014; [Paper I](#)). These events represent an example of multiple meteorological factors acting together, as these meteorological situations are often accompanied by increased air temperature and windy conditions. During RoS events, turbulent (latent and sensible heat) fluxes within the entire snowpack energy balance (Section 2.2.1) are usually dominant (Würzer *et al.*, 2016). Such turbulent energy exchange processes are important when assessing the snowmelt on a daily (event) scale. Heat directly added by rain can contribute more than 25% of the total energy available for snowmelt on days with heavy rainfall (Jennings and Jones, 2015; [Paper I](#)). Furthermore, torrential rainfall events are often associated with additional turbulent heat input (Marks *et al.*, 1998; Garvelmann *et al.*, 2014), and longwave radiation that can further accelerate snowmelt (Sezen *et al.*, 2020). On longer (seasonal) scales, the radiation components (shortwave and longwave radiation) become more important ([Paper I](#)). The heat directly supplied by rain during RoS events tends to be a minor contributor to snowmelt – typically up to 10% of the total energy balance at longer time scales (Mazurkiewicz *et al.*, 2008; Trubilowicz and Moore, 2017; Li *et al.*, 2019, [Paper I](#)).

Moreover, RoS events affect important processes, parameters and mechanisms within the snowpack, including changes in snowpack saturation, an increase in liquid water content, and a decrease in snow albedo, which enhances the energy absorption of the snowpack. These secondary effects can persist for several days after the rainfall event and further accelerate snowmelt (Yang *et al.*, 2023).

2.3.2 RoS-driven hydrological response

Most RoS events do not directly lead to severe flooding because the snowpack, especially fresh snow, can store large amounts of rainwater, resulting in reduced or even zero runoff (Wayand *et al.*, 2015; [Paper II](#)). However, under certain conditions, these events can potentially trigger excessive runoff and widespread floods (Berghuijs *et al.*, 2019; Giron Lopez *et al.*, 2020; Brunner and Fischer, 2022). Elevated RoS-driven runoff is often more intense and short-lived compared to the thermally driven types of snowmelt and associated runoff, along with lower groundwater recharge and infiltration rates (Earman *et al.*, 2006).

The interaction of different influencing factors makes it difficult to accurately predict the effect of snow cover on runoff formation for an upcoming RoS event (Würzer *et al.*, 2016). Several studies (Garvelmann *et al.*, 2015; Würzer *et al.*, 2016; Brandt *et al.*, 2022; [Paper II](#)) indicated the strong influence of initial snowpack properties on runoff formation during RoS. Therefore, the behavior of rainwater within the snowpack is one of the important issues to be properly understood. Detailed analyses of rainwater behavior were performed by Surfleet and Tullos (2013), Juras *et al.* (2017), or Würzer *et al.* (2017).

2.3.3 RoS occurrence in the current climate

The most vulnerable regions of the world experience more than 10 RoS events per year (Cohen *et al.*, 2015; Suriano, 2022) (Fig. 5). The occurrence and intensity of RoS events have been widely studied in recent years, with the research mainly focused on North American catchments (Grenfell and Putkonen, 2008; Bieniek *et al.*, 2018; Musselman *et al.*, 2018; Crawford *et al.*, 2020), where maximum daily

runoff is associated with RoS events 80% of the time between January and May, according to Il Jeong and Sushama (2017). Several other studies have been conducted in Siberia (Bartsch *et al.*, 2010), Scandinavia (Pall *et al.*, 2019; Poschlod *et al.*, 2020; Mooney and Li, 2021), Central Europe (Freudiger *et al.*, 2014; Schirmer *et al.*, 2022; [Papers II-IV](#)), high mountain Asia (Yang *et al.*, 2022; Maina and Kumar, 2023), as well as in the terrestrial Arctic (Rennert *et al.*, 2009; Bartsch *et al.*, 2023).

RoS events have been in the focus of hydrologists in recent decades. Although the topic is gaining scientific interest, the complex RoS processes are still on the list of unsolved problems in hydrology proposed by Blöschl *et al.* (2019).

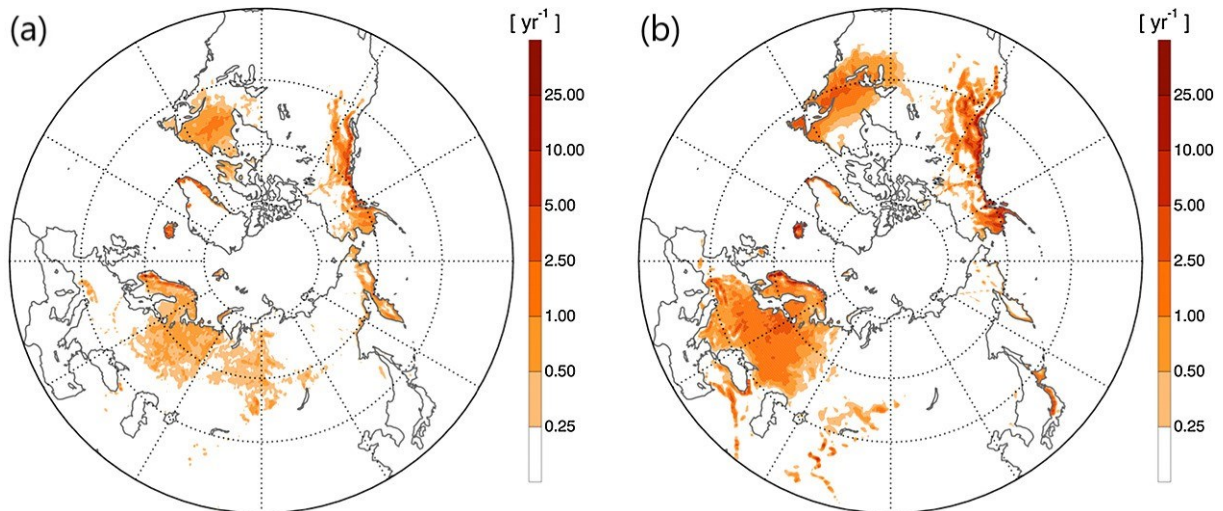


Figure 5: The number of RoS events across the Northern Hemisphere for September-November (a) and December-February (b) for the period 1979/1980 to 2013/2014 (Cohen *et al.*, 2015).

2.4 Changes driven by climate change

2.4.1 Future snow

Projected changes in climate variables will have a strong impact on snow-related hydrometeorological processes, including snow storage and snowmelt dynamics (Jennings *et al.*, 2018; Sezen *et al.*, 2020), variations in precipitation intensity and distribution, as well as a shift from snowfall to rain (Serquet *et al.*, 2011; Musselman *et al.*, 2018; Blahusiakova *et al.*, 2020; Li *et al.*, 2020). As a result, snow cover depth and the number of days with snow on the ground, snow density and snowfall fraction have already shown signs of decreasing trends in many regions of the world (Beniston and Stoffel, 2016; Marty *et al.*, 2017; Li *et al.*, 2020; Notarnicola, 2020; Nedelcev and Jenicek, 2021; Urban *et al.*, 2023) and are expected to be affected by gradual climate warming. Many studies predict a significant decrease in snow storage amounts and durations in the future (Notarnicola, 2020; Jenicek *et al.*, 2021; Nedelcev and Jenicek, 2021; Hale *et al.*, 2023). Snow-related changes are likely to become the main driver of interannual variability in future RoS occurrence (Suriano, 2022).

2.4.2 Future RoS

Since global temperature and precipitation patterns are changing the frequency and spatial distribution of RoS are also changing. Much of the current research focuses on highlighting the changes in RoS and snow conditions regarding ongoing climate change ([Paper IV](#)).

Recent studies have shown that the behavior and occurrence of RoS can be strongly determined by its spatial and temporal distribution (López-Moreno *et al.*, 2021). In general, the number of RoS events is expected to decline in low- and mid-latitude areas and low-elevation regions, primarily due to a shortening of the period with the snow on the ground (McCabe *et al.*, 2007; Surfleet and Tullos, 2013; Musselman *et al.*, 2018; Li *et al.*, 2019; López-Moreno *et al.*, 2021; Mooney and Li, 2021, [Paper III](#)). In contrast, RoS events are predicted to occur more frequently in the future due to an increase in the number of days with rain, triggered by increasing air temperature, in both high-latitude and high-elevation regions (Surfleet and Tullos, 2013; Morán-Tejeda *et al.*, 2016; Il Jeong and Sushama, 2017; Trubilowicz and Moore, 2017; Musselman *et al.*, 2018; Li *et al.*, 2019; Sezen *et al.*, 2020, [Paper IV](#)).

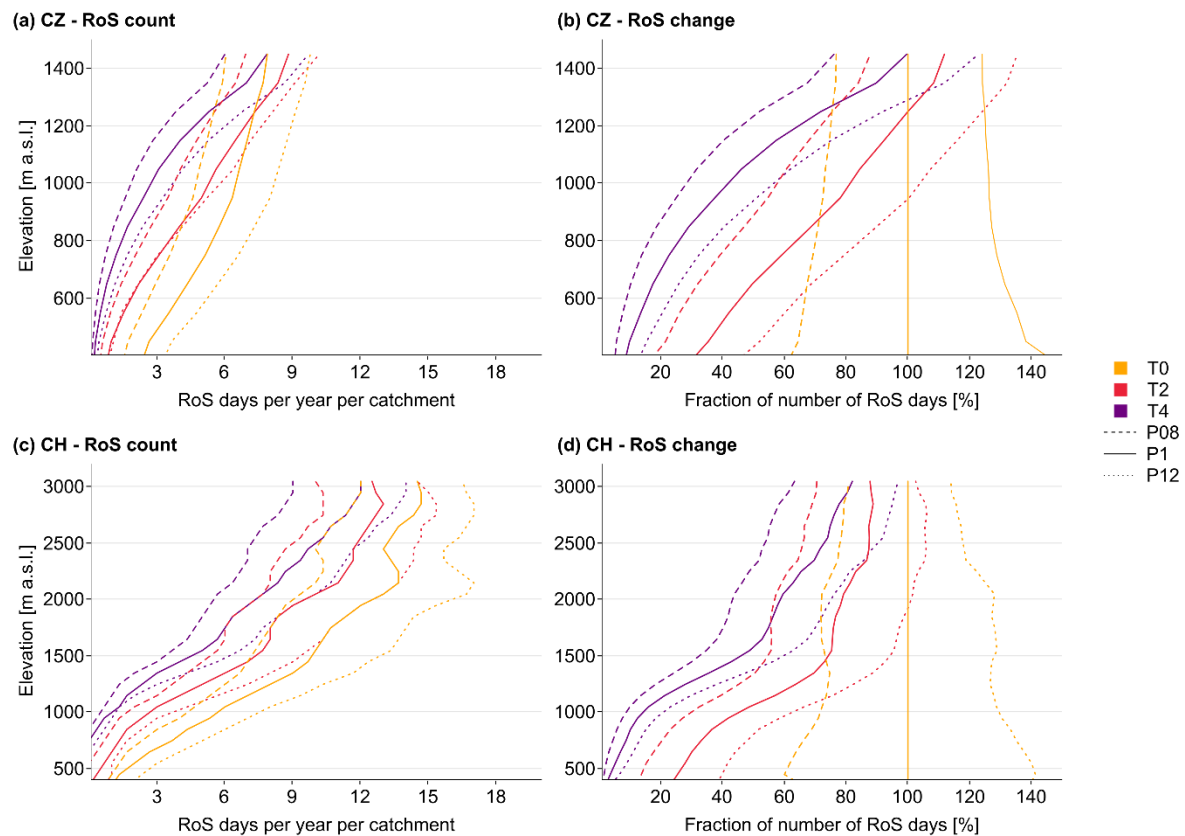


Figure 6: RoS day occurrence (a and c) and a fraction of the number of RoS days for selected projections compared to reference conditions T0_P1 (b and d) for distinct elevation zones in both Czech (a and b) and Swiss (c and d) regions. Line colors and styles represent selected temperature (T) and precipitation (P) projections ([Paper IV](#)).

In terms of temporal distribution, future projections for the humid mountain regions suggest an overall increase in RoS in the middle of the winter season (from November to March) as more precipitation will fall as rain rather than snow (Il Jeong and Sushama, 2017). A decrease in the number of RoS is expected in early and late winter due to the shortened period with existing snow cover (Hundechea *et al.*, 2017; Sezen *et al.*, 2020). Similar findings with varying spatial and temporal trends in RoS days for specific months of the winter season at different elevations were found in [Papers III](#) and [IV](#).

Despite increasing scientific interest, future climate change-driven changes in RoS are still subject to large uncertainties (López-Moreno *et al.*, 2021; Schirmer *et al.*, 2022) and there is still limited knowledge about the role of different climate variables controlling the RoS behavior, RoS dynamics

and RoS-driven runoff responses. The real impact of climate change on RoS events and their associated hydrological consequences remains unclear, mainly due to their complex nature (Sezen *et al.*, 2020; Mooney and Li, 2021; Myers *et al.*, 2023). Moreover, most European studies have had a limited focus on elevation, which significantly influences snow cover and precipitation phase and consequently RoS occurrence.

[Papers III](#) and [IV](#) addressed the aforementioned research gaps since understanding these specific spatial and temporal changes in RoS, with a particular focus on elevation (Fig. 6), and climate drivers is critical for future water management strategies to mitigate risks and impacts associated with RoS events. A wider area is expected to become vulnerable to RoS-related hazards in the future.

3 Materials and methods

3.1 Study areas

All studies included in the thesis shared the same geographical location within the region of central Europe, including mountainous catchments of various sizes and elevations. These catchments were selected because they are affected by snow, show near-natural runoff regimes and have no glacierized areas. Moreover, most of them represent areas in the rain-snow transition zones where large changes in snow storage and RoS occurrence typically occur. Table 1 summarizes the areas of interest within each paper with selected characteristics. Performed studies covered a range of temporal and spatial scales with different levels of detail, from detailed analyses of snowpack dynamics at the catchment scale to more generic assessments at the national or regional scale involving dozens of catchments.

The first study ([Paper I](#)) was carried out in the Ptaci Brook catchment (an experimental catchment of the Charles University, Prague) in the Bohemian Forest (Sumava National Park) in the southwestern part of Czechia. The second study ([Paper II](#)) was located in the two highest Czech mountain ranges, Krkonoše and Jeseníky mountains in the Sudetes region (southeastern Czechia). The third study ([Paper III](#)) extended this dataset by several other mountain ranges across Czechia. The last study ([Paper IV](#)) consisted of 93 mountainous catchments, including several mountain ranges in Czechia, and eastern Germany (located within the same cross-border mountain ranges), and an additional dataset containing catchments in Switzerland (located in three parts of the Alps) (Table 1).

Table 1: Summary of the study areas.

Study	Country	Catchment count	Elevation range [m a.s.l.]	Area range [km ²]	Time period	Spatial scale
Paper I	Czechia	1	1130-1150	4	2016-2018	Local
Paper II	Czechia	15	438-1603	3-181	2004-2014	Regional
Paper III	Czechia	40	295-1489	2-383	1965-2019	Regional
Paper IV	Czechia, Germany, Switzerland	93	269-3269	2-383	1980-2010	National

3.2 Data collecting and analyzing

3.2.1 Field measurements

Field measurements in snow hydrology are essential to accurately assess snowpack properties such as snow depth, snow density, and snow water equivalent (SWE), and to understand snowpack dynamics and snow processes in detail. Field campaigns provide critical data for predicting snowmelt rates and timing which are crucial for effective water resource management, flood forecasting, or agricultural planning. By collecting real-time and historical data, field measurements help to validate and calibrate hydrological models, thereby increasing their reliability (Sections 3.2.2 and 3.2.3).

Complex data collecting with dozens of field measurements over three consecutive winter seasons was the essential part of the research presented in [Paper I](#). Apart from basic manual snow measurements (including snow depth, snow density, and SWE measurements) during the main spring snowmelt periods, the studied experimental catchment (Ptaci Brook) is equipped with the automatic

measurements of snow depth and SWE, together with air, snow and soil temperature, precipitation, air moisture and shortwave and longwave radiation. The SWE data are collected directly in the study catchment using a Snow Pack Analyzer (SPA) device (Fig. 7). Three stripes (two placed horizontally, one placed diagonally) measure the electric impedance and provide the aggregate information about the ratio of liquid water, ice and air from the entire snow column.

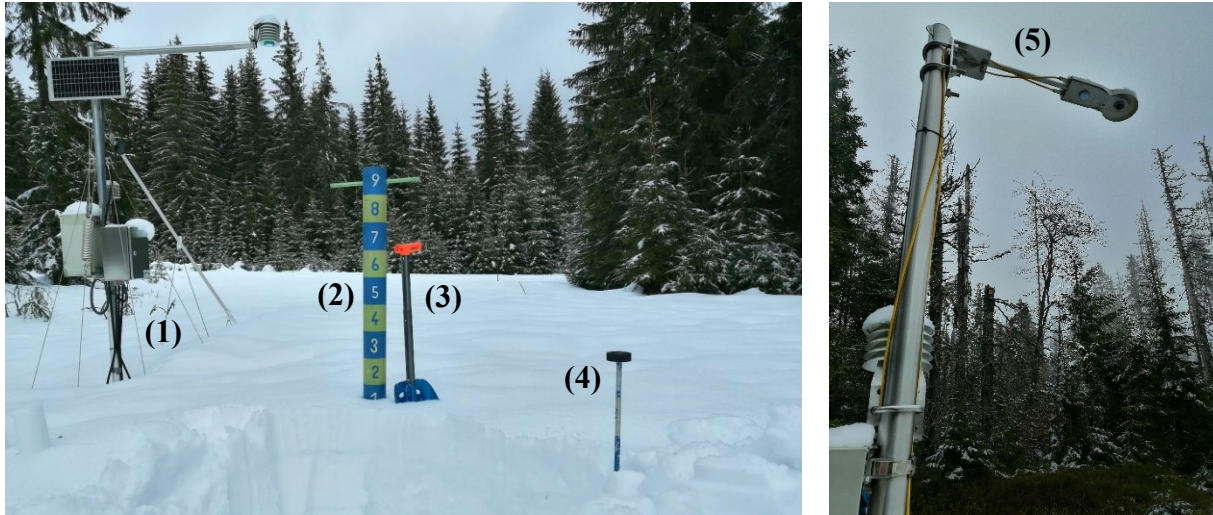


Figure 7: Selected equipment and devices used during the field campaigns in the Ptaci Brook catchment, Sumava National Park: Snow Pack Analyzer (1), snow tube (2), shovel (3), snow measuring stick (4), and radiometer (5) (photos by author).

Regarding the energy balance topic within the scope of [Paper I](#), another specific, not directly snow-related device called the CNR4 Net Radiometer (Fig. 7) was used for the assessment of incoming and reflected shortwave (SWR) and longwave (LWR) radiation at plots with different canopy structures. This device uses pyranometers (for SWR measurements) and pyrgeometers (for LWR measurements), allowing the evaluation of global and reflected radiation, and thus the calculation of albedo, as one of the important parameters affecting snowmelt dynamics.

3.2.2 Modeling approaches

With the development of technology, modeling techniques are now becoming a widely used method in catchment hydrology studies. Hydrological modeling has become an essential tool for understanding, predicting, and managing the complex dynamics of water systems, including snow processes. By integrating diverse data sources and establishing relations, hydrological models can contribute to a better understanding of hydrological variables and their interactions. Snow hydrological models simulate snow accumulation, snowmelt processes, and runoff generation, providing important insights for water resource management, flood forecasting, drought prevention, or more specific hydrological events such as RoS situations. Using climate data and possible future scenarios, snow hydrology models can improve our understanding of how changing climatic conditions affect snow dynamics.

For RoS quantification and the evaluation of RoS changes, modeling techniques are even more important because RoS events generally occur at higher elevations and higher latitudes, which typically have sparse observation networks (Pall *et al.*, 2019). Therefore, many studies have recently employed modeling approaches to detect RoS events or predict climate change-driven RoS changes (Table 2). Individual models use different numbers of inputs and influencing factors that are included in the model calculation, while an increasing model complexity (more parameters included) leads to

increasing uncertainty in the model simulation. Therefore, model calibration and validation procedures are being assessed for their ability to achieve as much agreement as possible between observed and simulated values (Section 3.2.3).

Table 2: List of hydrological and meteorological models frequently used in RoS-related studies.

Study	Model used
Paper II-IV	HBV (Hydrologiska Byråns Vattenavdelning)
Schirmer <i>et al.</i> (2022)	AWE-GEN-2d
Mooney and Li (2021; Yang <i>et al.</i> (2022)	Noah-MP
Sezen <i>et al.</i> (2020)	GR6J (Génie Rural à 6 paramètres Journalier), CemaNeige snow modul
Li <i>et al.</i> (2019)	VIC (Variable Infiltration Capacity)
Corripio and López-Moreno (2017)	WRD-ARW
Wever <i>et al.</i> (2016); Würzer and Jonas (2018)	SNOWPACK
Pomeroy <i>et al.</i> (2016)	CRHM (Cold Regions Hydrological Modelling)
Beniston and Stoffel (2016)	snowMAUS
Wayand <i>et al.</i> (2015)	DHSVM (Distributed Hydrology Soil Vegetation Model)
Rössler <i>et al.</i> (2014)	WaSiM-ETH (Water Flow and Balance Simulation Model)
Pradhanang <i>et al.</i> (2013)	SNODAS (Snow Data Assimilation System)
Mazurkiewicz <i>et al.</i> (2008)	SNOBAL

A modeling approach was used in all three RoS-related studies ([Papers II-IV](#)). For the model simulations, a time series of meteorological (air temperature, precipitation) and hydrological data (discharge, SWE, snow depth) were collected for individual catchments. These datasets were provided by national institutes based on the location of the study.

3.2.3 HBV model

In order to derive individual components of the rainfall-runoff process, and subsequently to detect RoS days/events and assess the hydrological response, a semi-distributed bucket-type HBV model (Lindström *et al.*, 1997; Seibert and Bergström, 2022) in its software implementation “HBV-light” (Seibert and Vis, 2012) was used in [Papers II-IV](#).

The HBV model is composed of four routines (Fig. 8), including a snow routine that simulates snow accumulation and snowmelt using a degree-day approach (Section 2.2.2), taking the potential refreezing of meltwater and snow water holding capacity into account. In addition to the snow routine, a soil moisture routine calculates groundwater recharge and actual evapotranspiration (AET) as a function of the soil moisture. For this, the input data of potential evapotranspiration (PET) was calculated based on air temperature data using the method presented by Oudin *et al.* (2005). Runoff from two groundwater boxes is simulated by a groundwater routine, from which baseflow is calculated directly by the model. A routing routine calculates the propagation of runoff through the catchment using a triangular function.

Each catchment was split into elevation zones of 100 m. This enables some characteristics to be simulated separately for these elevation zones, specifically precipitation, air temperature (using calibrated lapse rates), SWE, snowmelt, soil moisture, AET and groundwater recharge. For details of the model structure and routines, see Seibert and Vis (2012). This approach was applied in all studies where the HBV model was used ([Papers II-IV](#)).

In [Papers II-IV](#), the HBV model was automatically calibrated against the observed mean daily runoff and SWE for each study catchment using a genetic algorithm in 100 independent calibration trials.

Since the genetic algorithm contains stochastic elements, each calibration trial will result in different optimized parameter sets, especially if there is significant parameter uncertainty (equifinality) (Beven, 2021). Following a split-sample approach, the period was divided into calibration and validation windows. Table 3 shows calibration and validation periods for individual studies. As an objective function, a weighted mean of the NSE (the Nash-Sutcliffe model efficiency coefficient) based on the logarithmic runoff series, the volume error and the NSE based on the logarithmic SWE were used for the evaluation of the goodness of fit of the model separately in [Papers II-IV](#).

Table 3: Calibration and validation periods used in the modeling procedures.

Study	Calibration	Validation
Paper II	2004-2009	2010-2014
Paper III	1980-1997	1998-2014
Paper IV (Czech catchments)	1981-1997	1998-2014
Paper IV (Swiss catchments)	1981-2000	2001-2020

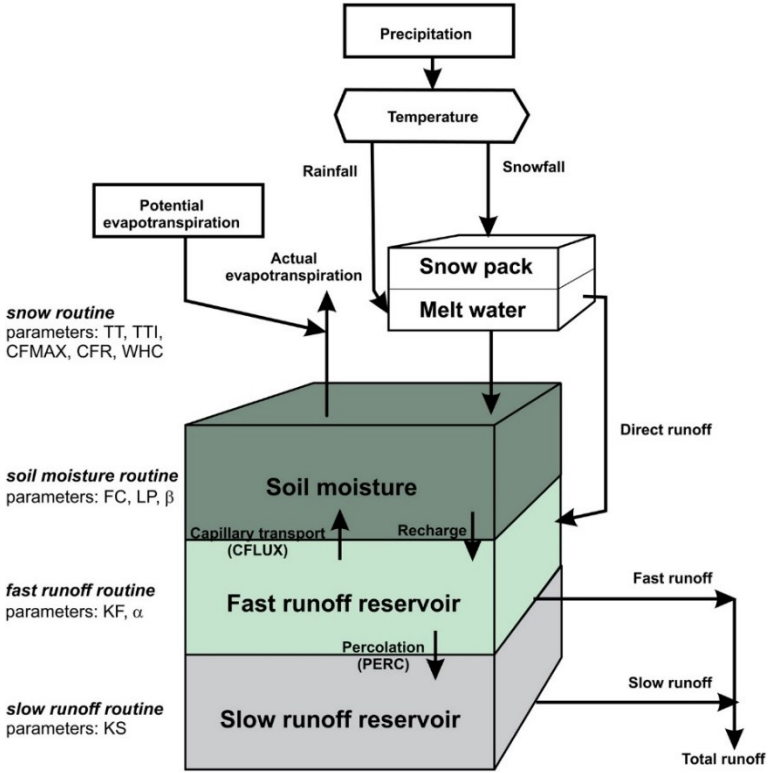


Figure 8: Structure and parameters of the HBV model (Wawrzyniak *et al.*, 2017).

3.3 Identification of RoS events

Although the RoS topic has been a focus for hydrologists over the last several decades, the physical complexity and associated impacts of RoS have led to different definitions and methods used in their assessments (Pall *et al.*, 2019). While variations in the threshold values set to identify individual RoS days/events may significantly affect the total number of recognized situations, a unified RoS definition does not exist in the literature. Different authors use different parameters and thresholds in their studies (Table 4).

For air temperature, several studies (Bieniek *et al.*, 2018; Crawford *et al.*, 2020; Surfleet and Tullos, 2013, [Paper III](#)) used the threshold of 0°C for the daily mean air temperature, while numerous recent studies did not specify the temperature threshold for RoS detection (Mooney and Li, 2021; Pall *et al.*, 2019; Schirmer *et al.*, 2022; Yang *et al.*, 2022). In [Papers II](#) and [IV](#), the air temperature threshold was calibrated by the model to obtain specific values for each study catchment. Despite the variations in definition, Jennings *et al.* (2018) suggested the temperature range between -0.4 and 2.4°C is valid for 95% of the stations across the Northern Hemisphere.

Table 4: RoS situations defined in selected studies based on several criteria, including air temperature (T), rainfall intensity (P), snow depth (SCE) or snow water equivalent (SWE), snowmelt (M, indicated by a decrease of SCE/SWE) and runoff response (Q_{change}). Q₁ represents 1-year return peak flow, DP is dew point temperature, P_{eq} is a sum of daily rainfall and snowmelt during the RoS event, T_t represents calibrated threshold temperature, +/- indicates whether the value is not defined (-) or defined and not specified (+).

Study	T	P	SCE / SWE	M	Q _{change}
Paper IV	> T _t	≥ 5mm/d	SWE ≥ 10 mm	-	-
Paper III	> 0	> 5 mm/d	SWE > 10 mm	-	-
Schirmer <i>et al.</i> (2022)	-	> 10 mm/d	SWE > 10 mm	+	-
Yang <i>et al.</i> (2022)	-	≥ 5 mm/d	-	≥ 3 mm/d	-
Paper II	> T _t	> 0 mm	SWE ≥ 10 mm	-	-
Mooney and Li (2021)	-	≥ 5 mm/d	-	≥ 3 mm/d	-
Sezen <i>et al.</i> (2020)	-	-	-	> 0.1 mm/d	+
Crawford <i>et al.</i> (2020)	≥ 0°C	≥ 2.54 mm	SCE > 2.54 mm	-	-
Ohba and Kawase (2020)	-	> 10 mm/d	SCE > 10 cm	-	-
Pall <i>et al.</i> (2019)	-	≥ 5 mm/d	-	≥ 3 mm/d	-
Bieniek <i>et al.</i> (2018)	> 0°C	≥ 0.254 mm/d	SCE > 0 cm	-	-
Würzer and Jonas (2018)	-	≥ 20 mm/d	SCE ≥ 25 cm	-	+
Il Jeong and Sushama (2017)	-	> 1 mm	SWE > 1 mm	-	+
Trubilowicz and Moore (2017)	-	> 0.1 mm/3h; 5 mm/d	SWE > 10 mm	+	-
Guan <i>et al.</i> (2016)	-	≥ 10 mm/d	SWE > 0 mm	+	-
Würzer <i>et al.</i> (2016)	0.7-1.7°C	≥ 20 mm	SCE ≥ 25 cm	-	+
Cohen <i>et al.</i> (2015)	-	≥ 10 mm/d	SCE > 0 cm	-	-
Freudiger <i>et al.</i> (2014)	-	≥ 3 mm	SWE ≥ 10 mm	+	20% P _{eq}
Surfleet and Tullos (2013)	> 0°C	> 0 mm	SCE > 0 cm	+	≥ Q ₁
Mazurkiewicz <i>et al.</i> (2008)	> 0.5°C DP	> 0.1 mm/3h	SCE > 0 cm	-	-
McCabe <i>et al.</i> (2007)	-	> 0 mm	SCE > 0 cm	+	-

Following the relevant definition of RoS days/events, these hydrological situations were comprehensively analyzed from various points of view (Fig. 1), including interannual variability of RoS ([Paper II](#)), RoS trends and climate-driven changes ([Papers III](#) and [IV](#)), and their effect on runoff ([Papers II-IV](#)).

4 Published research overview

This chapter summarizes the results and scopes of all four research papers compiled within the dissertation thesis.

4.1 Paper I

Hotovy O, Jenicek M. 2020. The impact of changing subcanopy radiation on snowmelt in a disturbed coniferous forest. *Hydrological Processes* 34 (26): 5298–5314 <https://doi.org/10.1002/hyp.13936>

This experimental study was performed in a mountainous catchment of the Ptaci Brook in the Bohemian Forest, southwestern Czechia, aiming to understand snowmelt processes in different canopy structures. Investigating the effects of forest cover on the sub-canopy energy balance is important for improving snowmelt models for accurate prediction of catchment runoff from forested mountain catchments (Hock, 2003), especially in the context of land cover changes due to either human activities or climate change.

This study quantified the changes and temporal variations in shortwave (SWR) and longwave (LWR) radiation and their effects on snowmelt at three sites with different canopy structures, including a treeless open area, a forested environment and a site covered by a coniferous forest disturbed by the bark beetle (*Ips typographus*). We benefited from detailed measurements from radiometers placed at all three experimental sites. The sampling design adopted in this study enabled the main components of the energy balance to be analyzed in hourly, daily and seasonal resolution. This research added to earlier studies by focusing on the evolution of both main radiation fluxes (SWR and LWR) during 3 years with gradual forest decay and also by detailed quantification of the relative contribution of other energy fluxes, such as sensible heat, latent heat, ground heat and energy supplied by liquid precipitation (Fig. 9).

Rain contributed from 13 to 29% during the days with heavy rainfall (RoS days) which supported the fact that energy from rain can be very important when assessing the snowpack energy balance at daily and shorter temporal resolutions. Therefore, the topic was further investigated in [Papers II-IV](#). This study concluded that coniferous forest significantly modifies the snowpack energy balance by reducing the total amount of solar SWR and increasing the role of tree-emitted LWR. The results showed that net SWR at the healthy forest site represented only 7% of the amount at the open site due to the shading effect of trees. In contrast, net LWR represented a positive component of the snowpack energy balance at the healthy forest site and thus contributed the most to the snowmelt. The progressive decay of disturbed forest caused decreased LWR and increased SWR, resulting in accelerated snowmelt rates by 50%.

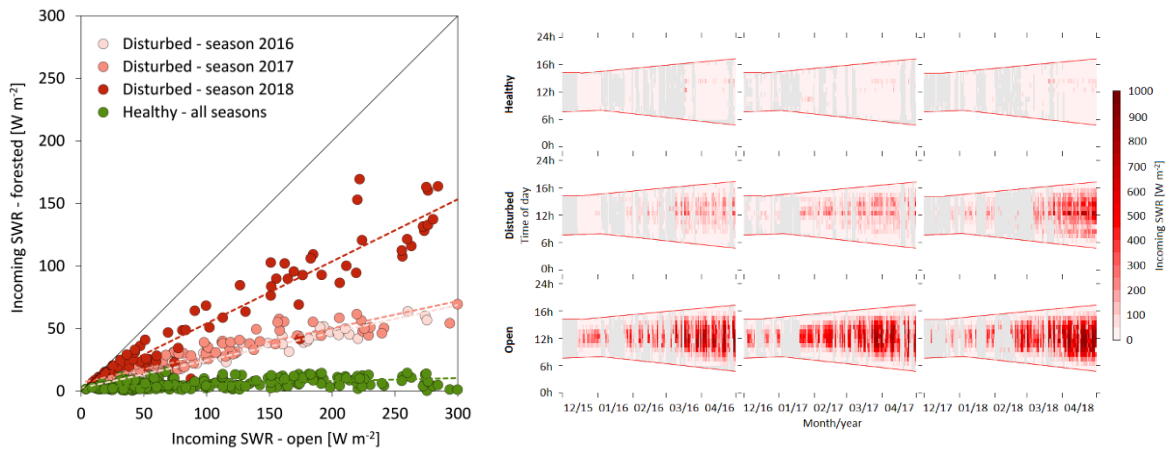


Figure 9: Sample figure from Paper I. Mean daily incoming shortwave radiation (SWR) at the open site compared to forested sites during seasons 2016, 2017 and 2018 (left panel). Mean hourly incoming SWR at the healthy spruce forest site, disturbed forest site and open site during seasons 2016, 2017 and 2018. Red lines represent time of sunrise and sunset. Grey color represents missing data (right panel).

4.2 Paper II

Juras R, Blöcher JR, Jenicek M, Hotovy O, Markonis Y. 2021. What affects the hydrological response of rain-on-snow events in low-altitude mountain ranges in Central Europe? *Journal of Hydrology* 603: 127002 <https://doi.org/10.1016/j.jhydrol.2021.127002>

The RoS-related hydrological response was comprehensively analyzed in this study. Although several studies have focused on modeled runoff response or on single events, empirical analyses of the extended RoS events dataset using measured streamflow at an hourly resolution are rather rare or are even missing in many regions with seasonal snow cover, including European regions outside of the Alps. RoS events are thought to cause severe winter/spring floods, but in most cases, they do not trigger elevated runoff as the snowpack can store a considerable amount of incoming rainwater (Juras *et al.*, 2017). Understanding the hydrological regime of RoS is becoming even more important with the ongoing decline of the snowfall fraction and subsequent changes in snow storage. This study contributed to knowledge of the role of individual climate and snowpack characteristics which control the dynamics of runoff response.

We identified 611 RoS situations which were further analyzed and classified using selected meteorological, snow and runoff indices, based on the observed data and data simulated by the hydrological HBV model. This study benefited from 11 years (10 cold seasons from 2004 to 2014) of hourly climatological and hydrological data for 15 near-natural catchments at different elevations within the highest Czech mountain ranges (Krkonosé and Jeseníky mountains). The focus on elevation was essentially important in this study (Fig. 10). Our methods accounted for the fact that only a part of the catchment contributes to runoff during the specific RoS events due to the strong dependence of snowmelt on air temperature at specific elevations. The analysis of the runoff response revealed that only 5% of RoS events resulted in high runoff exceeding the 1-year return period, but most of the events (82%) did not cause a significant runoff increase. Moreover, we classified these events according to the major driver controlling runoff response using self-organizing maps. This method

enabled us to categorize the events and better understand what combination of hydrometeorological characteristics led to various runoff responses. Low snow depth together with high volumes of rain were identified as important factors in the generating of high runoffs. In contrast, higher snow depths affected by rain under lower air temperatures usually resulted in lower runoffs. The results proved the importance of the snowpack in preventing extreme runoff even when a large amount of rainfall occurs.

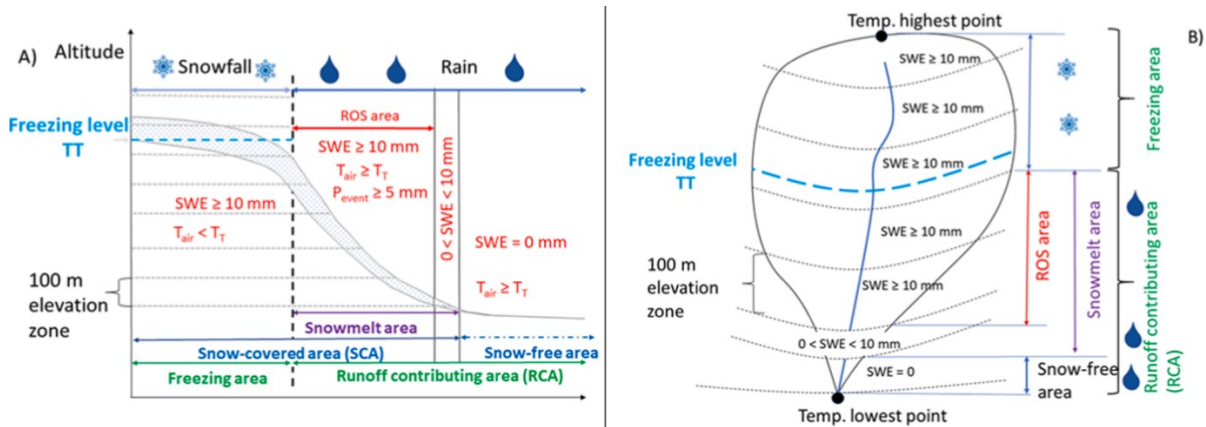


Figure 10: Sample figure from [Paper II](#). The concept of catchment division by elevation zones and area related to snow cover, RoS event, rain-affected area, snow-free area, and runoff area depicted as a) side and b) plan view. Symbol P_{event} represents hourly rainfall and T_T is the threshold temperature [$^{\circ}\text{C}$] calibrated for each catchment.

4.3 Paper III

Hotovy O, Nedelcev O, Jenicek M. 2023. Changes in rain-on-snow events in mountain catchments in the rain-snow transition zone. *Hydrological Sciences Journal* 68 (4): 572–584
<https://doi.org/10.1080/02626667.2023.2177544>

With regards to an expected shift from snowfall to rain and subsequent changes in snow storage and RoS event occurrence due to warming climate in the future, this study was our first attempt to evaluate the frequency, ongoing trends in RoS events and their runoff responses with a focus on RoS behavior at different elevations and the effect of changes in climate variable. Although changes in RoS frequency and intensity have been studied recently, trend analysis of both RoS occurrence and related runoff response was rather scarce, with limited focus on the specifics of different elevations. Similarly to [Papers II](#) and [IV](#), this study was unique for its interest in trends in non-Alpine regions within central Europe. We were particularly focused on lower-elevation mountain ranges since they represent rain-snow transition areas with large changes in snow storage affecting ROS occurrence.

The study was performed for 40 near-natural catchments located in five mountain ranges in Czechia. This study benefited from long time series (1965-2019, 55 cold seasons) of daily meteorological and hydrological variables, which enabled us to simulate several components of the water cycle for different elevations using a semi-distributed conceptual HBV model. Using this methodology setup, we identified almost 16,000 RoS days at a catchment scale during the study period. We recognized a typical mean air temperature during the RoS days (2°C), mean daily precipitation (12 mm), mean snowmelt (9 mm) and the mean SWE (111 mm). Generally, values of all four variables increased with elevation. The results showed statistically significant, yet small and not consistent, changes in the

number of RoS days in multiple catchments. In contrast, strong, significant trends in RoS days were identified for specific months (March and April) at different elevations (from 700 to 1200 m a.s. l.) (Fig. 11). Regarding the runoff response evaluation, we identified nearly 12,000 RoS events at a catchment scale, showing large temporal and spatial differences. According to our results, RoS event runoff contributed 3-32% to the total direct catchment runoff during the snow season, with the largest relative contribution in January. The long-term changes in RoS event runoff volume were mostly weak and not consistent across individual catchments. The detected trends reflected the changes in climate and snow variables, with an increase in air temperature resulting in the decrease in snowfall fraction and shorter snow cover period. Only about 10% of all assessed RoS events had flood-generation potential and these events occurred mostly in March.

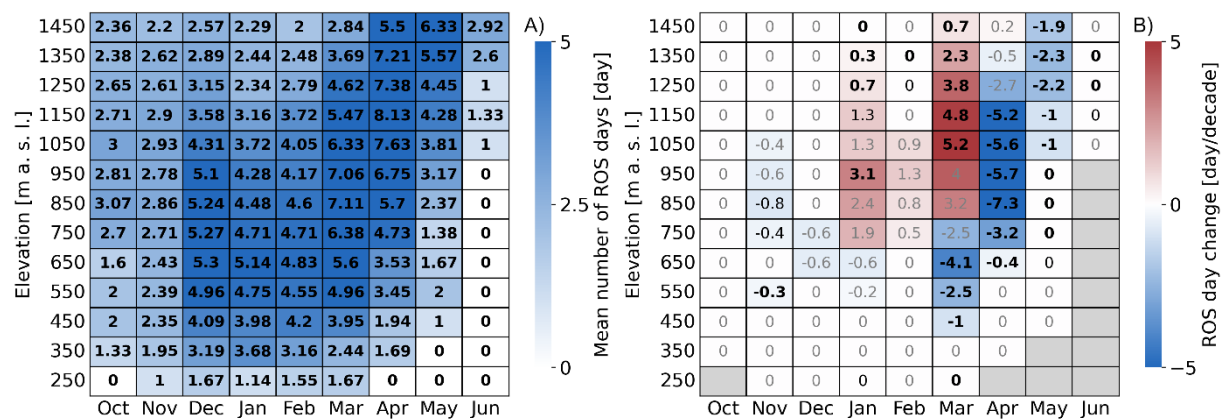


Figure 11: Sample figure from Paper III. Mean number of RoS days (a), decadal trends in RoS days (b) from October to June at different elevations for the period 1965-2019. The cell values in panel (a) represent absolute values of RoS days. The cell values in panel (b) represent Theil-Sen's slopes of the regression line. Significant Mann-Kendall trends are highlighted in black bold ($p < .05$) and in black ($p < .1$), decreasing trends in shades of blue and increasing trends in shades of red. Grey indicates no trends due to no RoS days.

4.4 Paper IV

Hotovy O, Nedelcev O, Seiber J, Jenicek M. 2024. Rain-on-snow events in mountainous catchments under climate change. *Hydrology and Earth System Sciences* (under review)

In this study, we attributed changes in selected climate variables, particularly air temperature and precipitation, to simulated variations in RoS events, using a sensitivity analysis approach. The occurrence and intensity of RoS events are expected to change in response to climate variations. Changes in precipitation, increase in air temperature and subsequent changes in the snow occurrence will likely affect future RoS behavior and dynamics. However, the real impact of climate change on RoS events and related hydrologic implications remains unclear, mainly due to their complex nature (Sezen *et al.*, 2020; Mooney and Li, 2021; Myers *et al.*, 2023, Papers II and III). Subsequent changes in runoff responses driven by RoS events were also evaluated in this study since there is a lack of studies analyzing both changes in RoS and the related runoff responses. Moreover, most European studies have had a limited focus on elevation, which significantly influences the precipitation phase and snow cover and consequently affects RoS occurrence. Analyzing runoff responses driven by

extreme meteorological events within these rain-snow transition zones is a valuable contribution of this paper.

In this study, we present differences between commonly analyzed catchments within the Alpine region and relatively scarce low-elevation locations outside of this mountain range that represent the areas within the transition zones where the largest changes in snow storage typically occur. A selection of 93 mountainous catchments across Central Europe, located in Czechia, Switzerland and Germany, was a substantial extension of the number of catchments analyzed in the previous studies from the same region (Girons Lopez *et al.*, 2020; Nedelcev and Jenicek, 2021; [Paper III](#)). Similarly to [Papers II](#) and [III](#), a conceptual hydrological HBV model was used to simulate runoff components for 24 climate projections relative to the reference period 1980-2010, along with model testing included in the study.

Results showed that climate change-driven RoS changes were highly variable over regions, across elevations, and during the cold season. The warmest projections (up to 4°C) suggested a significant decrease in RoS days by about 75% for some locations (Fig. 12). An increase in the number of RoS days was limited to higher elevations and the coldest winter months. Our projections also suggested that the RoS contribution to annual runoff will be considerably reduced. However, the RoS contribution to runoff may even increase in winter months, especially for projections leading to an increase in precipitation, demonstrating the joint importance of air temperature and precipitation for future hydrological behavior in snow-dominated catchments.

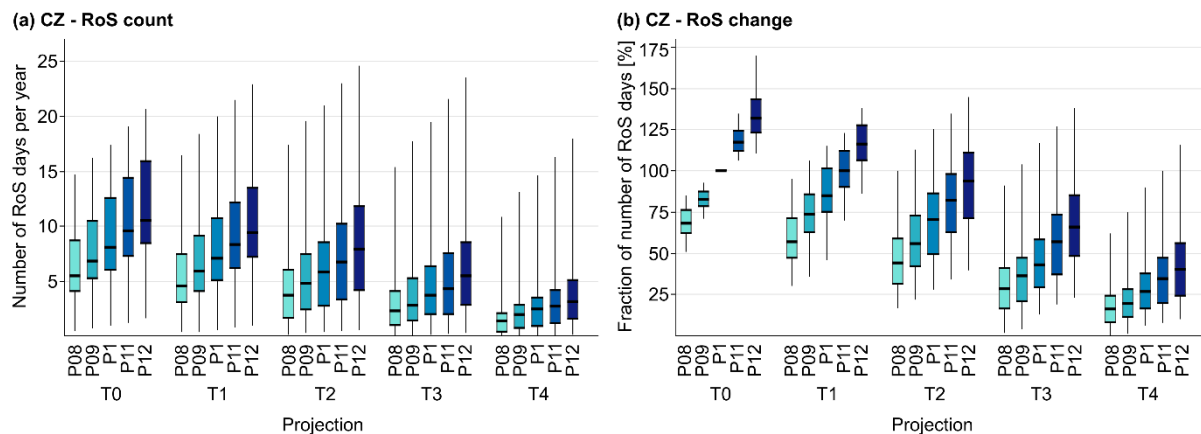


Figure 12: Sample figure from [Paper IV](#). Number of RoS days per year (a) and a fraction of the number of RoS days relative to reference conditions (b) in Czech catchments. Boxplots represent the variation among catchments, with the 25th and 75th percentiles represented by each box, the median as a thick line and the whiskers showing the maximum and minimum values. Boxes are grouped and colored according to the temperature (T) and precipitation (P) projections.

5 Discussion

5.1 Hydrological implications

All papers presented within the dissertation thesis aimed to contribute to the scientific knowledge on the hydrological implications of snowmelt in different environments ([Paper I](#)) and RoS-driven runoff ([Papers II-IV](#)). Although the model testing showed satisfactory results also for parameters related to runoff (Section 3.2.3), we found some inconsistencies between observed and simulated variables. These uncertainties are likely due to the interaction of different influencing factors which made it difficult to accurately simulate the effect of snow cover on runoff formation during RoS events (Würzer *et al.*, 2016). Several studies (Garvelmann *et al.*, 2015; Juras *et al.*, 2017; Würzer *et al.*, 2017; Brandt *et al.*, 2022) pointed out the strong influence of the initial snowpack properties. Therefore, the behavior of rainwater within the snowpack is one of the important issues to be properly understood.

As a general remark of [Paper II](#), rainfall was the main driver of maximum runoff and runoff in general. However, individual events associated with heavy rainfall were categorized into different runoff groups (based on the self-organizing map method) which supported the expected combined effect of other influencing factors. The temperature was found to play a secondary role, enhancing or attenuating the runoff response depending on the initial snow water equivalent. Apart from the aforementioned hydrometeorological predictors, RoS-related runoff is driven and affected by other individual catchment characteristics such as the type of forest, bedrock, aspect or slope (Li *et al.*, 2019, [Paper I](#)). [Paper I](#) pointed out that some uncertainties may arise from the calculation of total heat as the energy balance approach requires specific datasets with limited availability (Section 2.2.1). This resulted in high absolute errors between simulated and observed snowmelt rates and consequently runoff responses. [Paper I](#) discussed possible errors related to sensor location or the effect of tree composition affecting shading. This study showed that forest disturbance led to important changes in snowmelt processes and runoff conditions, similar to Schelker *et al.* (2013) or Holko *et al.* (2022). Ongoing climate change may further accentuate the effect of these land cover changes on runoff (Langhammer *et al.*, 2015; Blahusiakova *et al.*, 2020). However, faster snowmelt does not necessarily mean that total runoff or flood peaks would be higher, as documented by (Pomeroy *et al.*, 2012).

Our results showed that the majority of RoS events (82% in [Paper II](#), 72% in [Paper III](#)) did not cause significant runoff increase which is consistent with previous studies (Merz and Blöschl, 2003; Wayand *et al.*, 2015). Furthermore, the model testing in [Paper III](#) showed that 27% of RoS events were overestimated in terms of hydrological response. As the analyses were focused mainly on the relative differences and trends in RoS rather than on absolute values, we still believe that the model provided sufficiently good simulations. Most of the high runoff events were projected to occur in March, probably due to the generally higher air temperature, more intensive spring rainfall and high SWE. Elevated runoff responses during the winter season (December-February) were probably related to the non-ripe snowpack with generally lower snow densities and prevailing preferential flow paths that allowed rainwater to efficiently propagate through the snowpack and thus causing faster and higher runoff (Juras *et al.*, 2017).

5.2 Uncertain climate impacts

In order to limit the uncertainties related to the climatological modeling, a sensitivity analysis was used in [Paper IV](#) instead of the complex climatological modeling approach to assess how changes in air temperature and precipitation affect the occurrence and extremity of RoS. In this study, climate

variables were altered with respect to the expected future climate variations presented by respected sources (Gutiérrez *et al.*, 2021). Different sources of uncertainty resulting from the modeling approach have been considered in several RoS studies, with natural climate variability being seen as the primary source of uncertainty in RoS projections (Schirmer *et al.*, 2022). A sensitivity analysis approach for RoS-related research was performed by (López-Moreno *et al.*, 2021) who used this method to demonstrate the effects of the warming climate and argued that the hydrological importance of RoS is not expected to decrease, although the overall frequency of RoS will drop.

Our results are consistent with the conclusions presented by Schirmer *et al.* (2022) or Mooney and Li (2021) who found climate change signals towards more intense and frequent RoS events for an RCP 8.5 scenario at high elevations. Many recent studies (Il Jeong and Sushama, 2017; Trubilowicz and Moore, 2017; Musselman *et al.*, 2018; Li *et al.*, 2019; Sezen *et al.*, 2020; Mooney and Li, 2021) evaluating and modeling RoS events for different climate scenarios predict an increase in RoS events, particularly at higher elevations (usually valid for catchments above 1500 m a.s.l.). In contrast, their results showed a general decrease in RoS with lower hydrological extremes at lower elevations (usually for catchments below 1000 m a.s.l.). These broader elevation-based behaviors were investigated in [Papers II-IV](#) and appeared to be more pronounced in the Czech catchments. The results also showed seasonal changes in RoS occurrence. Most of the projections in [Paper IV](#) suggested a decrease in the number of RoS days towards the end of winter (particularly April and May) which supports the findings presented by Sezen *et al.* (2020). The signals towards more frequent RoS events, which were more pronounced in the Swiss catchments, were detected in the middle of the snow season. The increase in RoS is likely to be driven by changes in precipitation as more precipitation is expected to fall as rain rather than snow (Nedelcev and Jenicek, 2021). Mann-Kendall trend tests performed in [Paper III](#) showed a statistically significant change in RoS days in 21 out of 40 Czech catchments. However, the identified trends were rather weak and not consistent across catchments, although some regional patterns can be identified.

The RoS-driven hydrological impacts presented in [Papers III](#) and [IV](#) are in agreement with the findings by Sikorska-Senoner and Seibert (2020) who found an overall decreasing trend in RoS-related flooding for 27 Swiss catchments between 1980 and 2014, which is consistent with our general results for the Swiss study catchments ([Paper IV](#)). In our study, we found that these general trends may not be present for the winter months (January, February and March) due to expected changes in air temperature and precipitation patterns. Beniston and Stoffel (2016) concluded that the frequency of floods triggered by RoS may increase by 50% in Switzerland with a temperature increase of 2-4°C. However, an air temperature increase of more than 4 °C may lead to a decrease in RoS-driven floods due to a decline in snowpack duration.

5.3 RoS identification

In [Paper II-IV](#), we emphasized that variations in the thresholds used to identify RoS days/events can significantly affect the total number of recognized RoS situations identified. However, a unified RoS definition does not exist in the literature which makes the results of different studies hardly comparable (Brandt *et al.*, 2022). Therefore, comparing the occurrence of RoS between different regions can be challenging. This was demonstrated in [Paper II](#) where two mountain ranges (Krkonoše and Jeseníky) showed different RoS frequencies despite their close proximity, proving the statement that RoS occurrence is usually limited to specific regions (Li *et al.*, 2019; Yang *et al.*, 2022) since the

spatial and temporal distribution of RoS days and events is controlled by current and local weather conditions.

Average temperature, duration of snow cover, and the dominant phase of precipitation are expected to be the main factors explaining the variation in RoS sensitivity to climate warming (López-Moreno *et al.*, 2021).

For air temperature, several studies (Surfleet and Tullos, 2013; Bieniek *et al.*, 2018; Crawford *et al.*, 2020, [Paper III](#)) used the threshold of 0°C for the daily mean air temperature, while many recent studies did not specify the temperature threshold for RoS detection (Pall *et al.*, 2019; Mooney and Li, 2021; Schirmer *et al.*, 2022; Yang *et al.*, 2022). In [Paper IV](#), we determined the air temperature threshold as one of the RoS-defining parameters, which was calibrated separately for each of the study catchments. This approach appeared to be a valuable addition to the previous definition used in [Paper III](#) where zero was used as the temperature threshold. The varying threshold temperature can buffer local climatic conditions influenced by different catchment characteristics such as elevation range, topography or vegetation, and thus reducing one of the potential sources of error when identifying RoS days and events.

The derived threshold temperatures applied in [Paper IV](#) varied from -1.9 to 1.6°C within all study catchments. The mean threshold temperature reached -0.4°C for the study catchments in [Paper III](#). These values were comparable to those presented by Jennings *et al.* (2018), who identified a temperature range between -0.4 and 2.4°C to be valid for 95% of the stations across the Northern Hemisphere, indicating the air temperature at which rain and snowfall occur with equal frequency. Lower temperature thresholds occurred particularly in high-elevation catchments where snowfall is more common than rainfall. The temperature threshold is a challenging criterion used in the model to distinguish the phase of precipitation (Section 3.3). This can be particularly challenging on days when the air temperature fluctuates around the freezing point, making the snowfall fraction even more sensitive to changes in air temperature.

Thresholds defined for rainfall intensity and SWE appear to be less sensitive. A sensitivity analysis conducted partly in the same study area within [Paper II](#) showed that RoS characteristics remain similar when different limits for minimum rainfall and SWE are applied.

Regarding the general occurrence of RoS, most of the events analyzed in [Papers II-IV](#) occurred between November and May (with rather rare events in October and June at the highest elevations) which is in good agreement with the findings by Freudiger *et al.* (2014). In [Paper III](#), we defined a typical RoS day as a day with a daily mean air temperature ranging from 1.5°C at the lowest elevations to 2.9°C at the highest elevations. This temperature range, as well as typical rainfall intensities and SWEs, do not differ from those reported in other European regions with similar climate (Garvelmann *et al.*, 2015; Würzer *et al.*, 2016; Trubilowicz and Moore, 2017).

5.4 Data complexity in snow hydrology

Discussions about research complexity and level of detail were present throughout the PhD research. These discussions raised further questions about data complexity which is highly dependent on the spatial scale of the research. Mountainous snow hydrology and topics related to RoS events both represent a unique set of challenges and complexities in data collection, analysis, and interpretation,

resulting from their complex nature (Sezen *et al.*, 2020). Understanding and managing these complexities is critical for accurate and high quality snow hydrology research.

The scale of observation has a significant impact on the complexity of data in snow hydrology. Data collected at the local scale need to be integrated with macro-scale observations. Bridging the gap between these scales requires multi-scale modeling approaches and downscaling techniques. This dissertation thesis introduces both approaches commonly used in hydrology. An experimental study ([Paper I](#)) required various datasets, usually with a higher temporal resolution. This study used site-level energy balance calculations and such approaches are not easily transferable to larger regions. The remaining studies ([Paper II-IV](#)) represented large-sample hydrology that generally uses limited data sources with a lower level of detail. The RoS analyses in these studies were performed at a multi-catchment level, using input data from climate stations limited to air temperature and precipitation data, which did not allow the use of the energy balance approach.

Further uncertainties may arise from the fact that the snow cover is inherently heterogeneous, both spatially and temporally. Variations in snow depth, density, and water content at different scales add to the uncertainty. In addition, snow distribution is influenced by numerous factors. Most of these are well-recognized (e.g. air temperature or precipitation), but some can not be easily assessed without appropriate additional data. Several studies have pointed out that the initial properties of the snowpack and its retention capacity are both important factors with a strong influence on snowmelt and runoff formation (Garvelmann *et al.*, 2015; Würzer *et al.*, 2016), as investigated in [Paper II](#). The actual storage potential for the rainwater is controlled by the snow ripeness and the physical properties of the snowpack such as grain size, grain shape (Singh and Singh, 2001), and layering, especially the presence of capillary barriers (Avanzi *et al.*, 2016).

Snow water equivalent (SWE) data appeared to be one of the most important and also challenging parameters for assessing snowmelt processes across scales. The availability of SWE data was crucial for all studies presented within the PhD research. Since the number of stations with long-term daily monitoring of SWE was limited (not the case for the Swiss catchments in [Paper IV](#)), the ability of the model to accurately simulate SWE values was repeatedly addressed and discussed (Section 3.2.3). Differences between observed and modeled values may result from the lack of SWE measurements and the representativeness of the measurement location, particularly across the Czech catchments. Furthermore, detailed snowpack data (snow depth, snow water equivalent, etc.) are usually provided at a point scale, which is not necessarily representative of the catchment scale (Würzer and Jonas, 2018).

Although air temperature and precipitation data series are usually available for different temporal and spatial scales, there were some issues in analyzing and processing these primary data. As discussed in all papers where the modeling approach was used ([Papers II-IV](#)), the definition of the threshold temperature (T_T), as one of the parameters for RoS identification (Section 3.3) can be difficult using daily data, especially for days with high daily temperature amplitude (warm days and cold nights) resulting in a mean daily temperature around zero despite the fact that precipitation phase may change during the day, or for days with air temperature oscillating near the freezing point. Moreover, T_T can significantly differ among individual catchments with specific influencing factors. Therefore, we addressed this uncertainty by using different methods in [Papers III](#) and [IV](#) (fixed T_T vs. moving T_T calibrated for individual study catchments).

In addition to the data commonly used to evaluate snow dynamics, we introduced some other complementary methods to increase the complexity of our research. In [Paper I](#), we assessed canopy structure and forest density by calculating Leaf Area Indexes (LAI) for individual study sites from the hemispherical images. We were aware of potential errors from our radiation measurements as these data represented point information and might be affected by the specific fixed position of the sensor.

5.5 Uncertainty in modeling approach

Hydrological models used for the simulations of individual components of the rainfall-runoff process are subject to various uncertainties. These uncertainties stem from model structure, parameter setting and input data quality. In [Papers II-IV](#), a semi-distributed bucket-type HBV model (Lindström *et al.*, 1997; Seibert and Bergström, 2022) in its software implementation “HBV-light” (Seibert and Vis, 2012) was used (Section 3.2.3).

The HBV model uses the modified degree-day approach (Section 2.2.2) within its snow routine (Section 3.2.3) which may raise questions about model simplification. According to Seibert and Bergström (2022), more sophisticated models that use the entire energy balance in their structure perform better at a catchment scale. However, several studies have demonstrated that the degree-day approach is adequately used for snow storage simulation at a catchment scale under a changing climate (Addor *et al.*, 2014; Etter *et al.*, 2017; Jenicek *et al.*, 2021). Although these bucket-type models can generate some limitations, testing of 64 modifications of the HBV snow routine done by Girons Lopez *et al.* (2020) showed that the current snow routine within the HBV model provides satisfactory results at a catchment scale and confirmed that model procedures, setup and derived parameters acceptably represent the actual natural processes, including specifics of RoS events (Freudiger *et al.*, 2014). Authors of this study admitted that some modifications of the routine might represent an interesting alternative. Nevertheless, increased model complexity does not necessarily result in a better model ability to simulate SWE and runoff.

Since the results related to RoS events, as well as RoS identification (presented in [Papers II-IV](#)) were both based on modeled SWE, uncertainties arising from the model parametrization needed to be addressed in all three studies. Model calibration, validation and testing were performed in several recent studies using similar datasets (Jenicek and Ledvinka, 2020; Jenicek *et al.*, 2021; Sipek *et al.*, 2021). Consistently with these studies, multi-criteria model calibration and reiterated calibration runs were performed in [Paper II-IV](#) to reduce the overall parameter uncertainty. Nash-Sutcliffe efficiency values over 0.7 were reached in [Papers II](#) and [III](#), and also for the extended dataset in [Paper IV](#) (Fig. 13). This represented one of the acceptable test criteria (Moriassi *et al.*, 2015). However, it might be difficult to agree on specific efficiency benchmarks signaling a good model performance (Seibert *et al.*, 2018). Thus, model justification required multiple model testing.

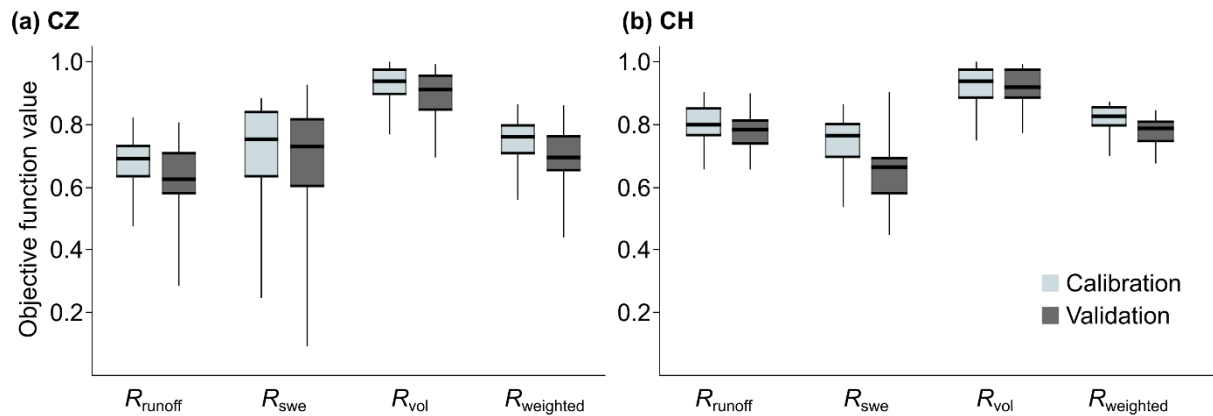


Figure 13: Model performance for all 93 study catchments within both Czech (a) and Swiss (b) regions evaluated by the combination of selected objective criteria, including the logarithmic Nash-Sutcliffe efficiency for runoff (R_{runoff}), Nash-Sutcliffe efficiency for SWE (R_{swe}), and volume error (R_{vol}). These criteria were weighted (R_{weighted}) to calculate the overall objective function of the model. Boxplots represent the variation among catchments, with the 25th and 75th percentiles within a box, the median as a thick line and the whiskers represent maximum and minimum values ([Paper IV](#)).

The assessment of the model’s ability to simulate SWE and thus detect RoS days correctly was investigated in [Paper III](#) where we compared counts of observed and simulated RoS days, as well as simulated runoff and SWE during RoS events. We did not find major inconsistencies in the model runs and assumed that the model provided sufficiently good simulations. More detailed testing of SWE simulations for the Czech catchments was carried out by (Jenicek *et al.*, 2021; Nedelcev and Jenicek, 2021). For example, Nedelcev and Jenicek (2021) compared simulated and observed trends in air temperature, precipitation, and SWE, concluding that the model can provide overall reliable simulations of the above variables, which are temporally and spatially consistent with observed data.

6 Outlook and conclusions

This thesis aims to assess the changes in mountain snowmelt and rain-on-snow (RoS) runoff across scales, primarily in the context of climate and landscape changes within the region of central Europe. This research resolves some of the uncertainties associated with the complex snowmelt processes and contributes to the understanding of snowmelt dynamics and their changes during hazardous events in the context of climate change. This cross-scale research is beneficial for a better estimating of snow storages, contributing to a higher accuracy of hydrological modeling, and thus mitigating the risk of drought and flood towards effective water resource management in the future. We performed various types of research at different spatial and temporal scales, from the experimental site study to regional and international multi-catchment research. We were particularly focused on the changes across elevations that include the areas within the rain-snow transition zones where large changes in snow storage, snow dynamics and RoS occurrence typically occur due to climate warming. Individual studies applied various methodological approaches and addressed different topics related to snowmelt and subsequent hydrological implications, with the specific focus on changes of the frequency and intensity of RoS events.

The effects of forest cover on the sub-canopy energy balance and snowmelt processes were explored in [Paper I](#). This study helped to understand the detailed mechanisms of snowmelt dynamics related to the heat fluxes within the snowpack energy balance and demonstrated what are the differences between the sites with different canopy structures. This study supported the fact that energy from rain can be important when assessing snowmelt at daily and shorter temporal resolutions, which initiated research questions for subsequent studies ([Papers II-IV](#)). [Paper I](#) highlighted the role of shortwave radiation (SWR), which was the major energy contributor to snowmelt at the open (treeless) site. In the healthy forested site, SWR represented only 7% of the amount at the open site due to tree shading. In contrast, longwave radiation (LWR) was the dominant energy component, representing 41% of all energy fluxes, and thus contributed most to snowmelt. Notable effects of gradual forest decay on snowmelt processes were also shown in [Paper I](#).

Changes in the occurrence of RoS days/events and the associated hydrological implications were the main topics of the dissertation thesis and were investigated in [Papers II-IV](#), primarily in the context of climate change. At the multi-catchment scale, we assessed thousands of RoS days/events, and contributed to the understanding of the temporal and spatial variability of this hydrological phenomenon. We found the most frequent RoS occurrences in the elevation range from 1000 to 2000 m a.s.l. Distinct catchments saw the average RoS occurrence at different times of the year from mid-January to mid-May ([Paper IV](#)). The results showed that climate change-driven RoS changes are highly variable across regions and sub-regions, across elevations, and within the cold season ([Papers II-IV](#)). These changes were rather small and inconsistent at the catchment scale but were more pronounced (strong and significant trends) at higher resolution - for specific months at different elevations ([Paper III](#)). The largest decrease was detected at elevations between 700 and 1200 m a.s.l. during April, most likely caused by a shortening of the period with existing snow cover on the ground due to increasing air temperature. The largest increase was recorded at elevations above 1000 m a.s.l. in March which was associated with more frequent rainfall.

In general, RoS days are expected to occur less frequently with further warming, particularly at lower elevations ([Paper III](#) and [IV](#)). The warmest projections defined in [Paper IV](#) suggested a significant decrease in RoS days by about 75% for some locations. An increase in the number of RoS days was

limited to higher elevations and the coldest winter months. Our projections also suggested that the RoS contribution to annual runoff is likely to decrease significantly. However, the RoS contribution to runoff may even increase in the winter months, especially for projections that lead to an increase in precipitation, demonstrating the joint importance of air temperature and precipitation for future hydrological behavior in snow-dominated catchments.

Moreover, the effect of various seasonal climate and snow characteristics that may control RoS behavior was investigated in [Paper IV](#), concluding that the RoS occurrence was identified as more sensitive to changes in snowfall in the Czech catchments, whereas seasonal precipitation totals (regardless of snowfall or rainfall) appeared to be the primary driver in Switzerland. Surprisingly, the correlation between RoS and air temperature was relatively weak in both regions.

Focusing on the hydrological implications of changes in snowmelt processes and RoS events is important and our findings ([Papers I-IV](#)) contribute to improve the process understanding, which is further important for improving snowmelt and catchment runoff models. Although the methods of experimental study presented in [Paper I](#) are rather limited to the specific study area and may not be easily generalized, the results proved that changes in individual energy balance components after forest disturbance have important consequences on snowmelt rates which may further affect the seasonal distribution of spring runoff. The highest simulated snowmelt rates were observed at the open site (median snowmelt rate 13.5 mm.d⁻¹). The modeled snowmelt was significantly slower at the disturbed forest site (5.9 mm/d⁻¹) and at the healthy forest site (3.3 mm/d⁻¹).

Analyzing runoff responses driven by extreme meteorological events such as RoS within transition zones is a valuable contribution of [Papers II-IV](#). We concluded that only about 10% of all RoS events have flood-generation potential and most of the events (up to 82%) did not cause a significant runoff increase. Within the catchments in Czechia, RoS event runoff contributed 3-32% to the total direct catchment runoff during the snow season, with the largest relative contribution in January ([Paper III](#)). [Paper IV](#) suggested that RoS contribution to annual runoff is likely to decrease due to changes in climate variables from the current 10% to 2-4% for the warmest projections in Czechia, and from 18% to 5-9% in Switzerland. However, the RoS contribution to runoff may increase in winter months in Switzerland, for almost all projections with the same or higher amount of precipitation, regardless of air temperature increase. With more frequent RoS events expected during these months, Swiss catchments, particularly those at higher elevations, may face more extreme RoS-related flood events in the future. For Czech catchments, the increase in winter runoff is expected only for wet projections with a relatively small air temperature increase. Despite the expectations that the overall RoS impact on runoff will be lower in the future, extreme hydrological response and flooding triggered by RoS events may still represent a significant flood risk.

7 References

- Addor N, Rössler O, Köplin N, Huss M, Weingartner R, Seibert J. 2014. Robust changes and sources of uncertainty in the projected hydrological regimes of Swiss catchments. *Water Resources Research* **50** (10): 7541–7562 DOI: 10.1002/2014WR015549
- Assaf H. 2007. Development of an Energy-budget Snowmelt Updating Model for Incorporating Feedback from Snow Course Survey Measurements. *Journal of Engineering, Computing and Architecture* **1** (1)
- Avanzi F, Hirashima H, Yamaguchi S, Katsushima T, De Michele C. 2016. Observations of capillary barriers and preferential flow in layered snow during cold laboratory experiments. *Cryosphere* **10** (5): 2013–2026 DOI: 10.5194/tc-10-2013-2016
- Bartik M, Holko L, Janco M, Skvarenina J, Danko M, Kostka Z. 2019. Influence of mountain spruce forest dieback on snow accumulation and melt. *Journal of Hydrology and Hydromechanics* **67** (1): 59–69 DOI: 10.2478/johh-2018-0022
- Bartsch A, Bergstedt H, Pointner G, Muri X, Rautiainen K, Leppänen L, Joly K, Sokolov A, Orekhov P, Ehrich D, et al. 2023. Towards long-term records of rain-on-snow events across the Arctic from satellite data. *Cryosphere* **17** (2): 889–915 DOI: 10.5194/TC-17-889-2023
- Bartsch A, Kumpula T, Forbes BC, Stammer F. 2010. Detection of snow surface thawing and refreezing in the Eurasian arctic with QuikSCAT: Implications for reindeer herding. *Ecological Applications* **20** (8): 2346–2358 DOI: 10.1890/09-1927.1
- Beniston M, Stoffel M. 2016. Rain-on-snow events, floods and climate change in the Alps: Events may increase with warming up to 4 °C and decrease thereafter. *Science of the Total Environment* **571**: 228–236 DOI: 10.1016/j.scitotenv.2016.07.146
- Berghuijs WR, Harrigan S, Molnar P, Slater LJ, Kirchner JW. 2019. The Relative Importance of Different Flood-Generating Mechanisms Across Europe. *Water Resources Research* **55** (6): 4582–4593 DOI: 10.1029/2019WR024841
- Beven K. 2021. An epistemically uncertain walk through the rather fuzzy subject of observation and model uncertainties I. *Hydrological Processes* **35** (1): 1–9 DOI: 10.1002/hyp.14012
- Bieniek PA, Bhatt US, Walsh JE, Lader R, Griffith B, Roach JK, Thoman RL. 2018. Assessment of Alaska rain-on-snow events using dynamical downscaling. *Journal of Applied Meteorology and Climatology* **57** (8): 1847–1863 DOI: 10.1175/JAMC-D-17-0276.1
- Blahusiakova A, Matouskova M, Jenicek M, Ledvinka O, Kliment Z, Podolinska J, Snopkova Z. 2020. Snow and climate trends and their impact on seasonal runoff and hydrological drought types in selected mountain catchments in Central Europe. *Hydrological Sciences Journal*: 1–14 DOI: 10.1080/02626667.2020.1784900
- Blöschl G, Bierkens MFP, Chambel A, Cudennec C, Destouni G, Fiori A, Kirchner JW, McDonnell JJ, Savenije HHG, Sivapalan M, et al. 2019. Twenty-three unsolved problems in hydrology (UPH)—a community perspective. *Hydrological Sciences Journal* **64** (10): 1141–1158 DOI: 10.1080/02626667.2019.1620507
- Brandt WT, Haleakala K, Hatchett BJ, Pan M. 2022. A Review of the Hydrologic Response Mechanisms During Mountain Rain-on-Snow. *Frontiers in Earth Science* **10**: 791760 DOI: 10.3389/FEART.2022.791760
- Broxton PD, Harpold AA, Biederman JA, Troch PA, Molotch NP, Brooks PD. 2015. Quantifying the effects of vegetation structure on snow accumulation and ablation in mixed-conifer forests. *Ecohydrology* **8** (6): 1073–1094 DOI: 10.1002/eco.1565

- Brunner MI, Fischer S. 2022. Snow-influenced floods are more strongly connected in space than purely rainfall-driven floods. *Environmental Research Letters* **17** (10): 104038 DOI: 10.1088/1748-9326/ac948f
- Cohen J, Ye H, Jones J. 2015. Trends and variability in rain-on-snow events. *Geophysical Research Letters* **42** (17): 7115–7122 DOI: 10.1002/2015GL065320
- Corripio JG, López-Moreno JI. 2017. Analysis and predictability of the hydrological response of mountain catchments to heavy rain on snow events: A case study in the Spanish Pyrenees. *Hydrology* **4** (2): 20 DOI: 10.3390/hydrology4020020
- Courbaud B, De Coligny F, Cordonnier T. 2003. Simulating radiation distribution in a heterogeneous Norway spruce forest on a slope. *Agricultural and Forest Meteorology* **116** (1–2): 1–18 DOI: 10.1016/S0168-1923(02)00254-X
- Crawford AD, Alley KE, Cooke AM, Serreze MC. 2020. Synoptic climatology of rain-on-snow events in Alaska. *Monthly Weather Review* **148** (3): 1275–1295 DOI: 10.1175/MWR-D-19-0311.1
- DeWalle DR, Rango A. 2008. *Principles of Snow Hydrology*. Cambridge University Press.
- Earman S, Campbell AR, Phillips FM, Newman BD. 2006. Isotopic exchange between snow and atmospheric water vapor: Estimation of the snowmelt component of groundwater recharge in the southwestern United States. *Journal of Geophysical Research* **111**: D09302 DOI: 10.1029/2005JD006470
- Ellis, Pomeroy JW, Essery RLH, Link TE. 2011. Effects of needleleaf forest cover on radiation and snowmelt dynamics in the Canadian Rocky Mountains. *Canadian Journal of Forest Research* **41** (3): 608–620 DOI: 10.1139/X10-227
- Essery R, Pomeroy J, Ellis C, Link T. 2008. Modelling longwave radiation to snow beneath forest canopies using hemispherical photography or linear regression. *Hydrological Processes* **22** (15): 2788–2800 DOI: 10.1002/hyp.6930
- Etter S, Addor N, Huss M, Finger D. 2017. Climate change impacts on future snow, ice and rain runoff in a Swiss mountain catchment using multi-dataset calibration. *Journal of Hydrology: Regional Studies* **13**: 222–239 DOI: 10.1016/j.ejrh.2017.08.005
- Förster K, Garvelmann J, Meißl G, Strasser U. 2018. Modelling forest snow processes with a new version of WaSiM. *Hydrological Sciences Journal* **63** (10): 1540–1557 DOI: 10.1080/02626667.2018.1518626
- Freudiger D, Kohn I, Stahl K, Weiler M. 2014. Large-scale analysis of changing frequencies of rain-on-snow events with flood-generation potential. *Hydrology and Earth System Sciences* **18** (7): 2695–2709 DOI: 10.5194/hess-18-2695-2014
- Garvelmann J, Pohl S, Weiler M. 2014. Variability of Observed Energy Fluxes during Rain-on-Snow and Clear Sky Snowmelt in a Midlatitude Mountain Environment. *Journal of Hydrometeorology* **15** (3): 1220–1237 DOI: 10.1175/JHM-D-13-0187.1
- Garvelmann J, Pohl S, Weiler M. 2015. Spatio-temporal controls of snowmelt and runoff generation during rain-on-snow events in a mid-latitude mountain catchment. *Hydrological Processes* **29** (17): 3649–3664 DOI: 10.1002/hyp.10460
- Girons Lopez M, Vis MJP, Jenicek M, Griessinger N, Seibert J. 2020. Assessing the degree of detail of temperature-based snow routines for runoff modelling in mountainous areas in central Europe. *Hydrology and Earth System Sciences* **24** (9): 4441–4461 DOI: 10.5194/hess-24-4441-2020
- Gouttevin I, Lehning M, Jonas T, Gustafsson D, Mölder M. 2015. A two-layer canopy model with thermal inertia for an improved snowpack energy balance below needleleaf forest (model

- SNOWPACK, version 3.2.1, revision 741). *Geoscientific Model Development* **8** (8): 2379–2398 DOI: 10.5194/gmd-8-2379-2015
- Grenfell TC, Putkonen J. 2008. A method for the detection of the severe rain-on-snow event on Banks Island, October 2003, using passive microwave remote sensing. *Water Resources Research* **44** (3): 3425 DOI: 10.1029/2007WR005929
- Guan B, Waliser DE, Ralph FM, Fetzer EJ, Neiman PJ. 2016. Hydrometeorological characteristics of rain-on-snow events associated with atmospheric rivers. *Geophysical Research Letters* **43** (6): 2964–2973 DOI: 10.1002/2016GL067978
- Gutiérrez JM, Jones RG, Narisma GT, Alves LM, Amjad M, Gorodetskaya I V., Grose M, Klutse NAB, Krakovska S, Li J, et al. 2021. Atlas. In *Climate Change 2021 – The Physical Science Basis* Cambridge University Press; 1927–2058. DOI: 10.1017/9781009157896.021
- Hale KE, Jennings KS, Musselman KN, Livneh B, Molotch NP. 2023. Recent decreases in snow water storage in western North America. *Communications Earth and Environment* **4** (1): 1–11 DOI: 10.1038/s43247-023-00751-3
- Hammond JC, Saavedra FA, Kampf SK. 2018. How Does Snow Persistence Relate to Annual Streamflow in Mountain Watersheds of the Western U.S. With Wet Maritime and Dry Continental Climates? *Water Resources Research* **54** (4): 2605–2623 DOI: 10.1002/2017WR021899
- Helbig N, Moeser D, Teich M, Vincent L, Lejeune Y, Sicart J-E, Monnet J-M. 2019. Snow processes in mountain forests: Interception modeling for coarse-scale applications. *Hydrology and Earth System Sciences Discussions*: 1–24 DOI: 10.5194/hess-2019-348
- Helgason W, Pomeroy JW. 2012. Problems Closing the Energy Balance over a Homogeneous Snow Cover during Midwinter. *Journal of Hydrometeorology* **13** (2): 557–572 DOI: 10.1175/JHM-D-11-0135.1
- Hock R. 2003. Temperature index melt modelling in mountain areas. *Journal of Hydrology* **282** (1–4): 104–115 DOI: 10.1016/S0022-1694(03)00257-9
- Holko L, Jančo M, Danko M, Sleziak P. 2022. Influence of forest dieback on the overland flow and isotopic composition of precipitation. *Acta Hydrologica Slovaca* **23** (1): 82–88 DOI: 10.31577/ahs-2022-0023.01.0009
- Hotovy O, Jenicek M. 2020. The impact of changing subcanopy radiation on snowmelt in a disturbed coniferous forest. *Hydrological Processes* **34** (26): 5298–5314 DOI: 10.1002/hyp.13936
- Hotovy O, Nedelcev O, Jenicek M. 2023. Changes in rain-on-snow events in mountain catchments in the rain–snow transition zone. *Hydrological Sciences Journal* **68** (4): 572–584 DOI: 10.1080/02626667.2023.2177544
- Hundecha Y, Parajka J, Viglione A. 2017. Flood type classification and assessment of their past changes across Europe. *Hydrology and Earth System Sciences Discussions*: 1–29
- Iziomon MG, Mayer H, Matzarakis A. 2003. Downward atmospheric longwave irradiance under clear and cloudy skies: Measurement and parameterization. *Journal of Atmospheric and Solar-Terrestrial Physics* **65** (10): 1107–1116 DOI: 10.1016/j.jastp.2003.07.007
- Jenicek M, Ledvinka O. 2020. Importance of snowmelt contribution to seasonal runoff and summer low flows in Czechia. *Hydrology and Earth System Sciences* **24** (7): 3475–3491 DOI: 10.5194/hess-24-3475-2020

- Jenicek M, Hnilica J, Nedelcev O, Sipek V. 2021. Future changes in snowpack will impact seasonal runoff and low flows in Czechia. *Journal of Hydrology: Regional Studies* **37**: 100899 DOI: 10.1016/j.ejrh.2021.100899
- Jenicek M, Hotovy O, Matejka O. 2017. Snow accumulation and ablation in different canopy structures at a plot scale: Using degree-day approach and measured shortwave radiation. *Acta Universitatis Carolinae, Geographica* **52** (1): 61–72 DOI: 10.14712/23361980.2017.5
- Jenicek M, Pevna H, Matejka O. 2018. Canopy structure and topography effects on snow distribution at a catchment scale: Application of multivariate approaches. *Journal of Hydrology and Hydromechanics* **66** (1): 43–54 DOI: 10.1515/johh-2017-0027
- Jennings K, Jones JA. 2015. Precipitation-snowmelt timing and snowmelt augmentation of large peak flow events, western Cascades, Oregon. *Water Resources Research* **51** (9): 7649–7661 DOI: 10.1002/2014WR016877
- Jennings KS, Winchell TS, Livneh B, Molotch NP. 2018. Spatial variation of the rain-snow temperature threshold across the Northern Hemisphere. *Nature Communications* **9** (1): 1–9 DOI: 10.1038/s41467-018-03629-7
- Il Jeong D, Sushama L. 2017. Rain-on-snow events over North America based on two Canadian regional climate models. *Climate Dynamics* **50** (1–2): 303–316 DOI: 10.1007/s00382-017-3609-x
- Juras R, Blöcher JR, Jenicek M, Hotovy O, Markonis Y. 2021. What affects the hydrological response of rain-on-snow events in low-altitude mountain ranges in Central Europe? *Journal of Hydrology* **603**: 127002 DOI: 10.1016/j.jhydrol.2021.127002
- Juras R, Würzer S, Pavlasek J, Vitvar T, Jonas T. 2017. Rainwater propagation through snowpack during rain-on-snow sprinkling experiments under different snow conditions. *Hydrology and Earth System Sciences* **21** (9): 4973–4987 DOI: 10.5194/hess-21-4973-2017
- Langhammer J, Su Y, Bernsteinova J. 2015. Runoff response to climate warming and forest disturbance in a mid-mountain basin. *Water* **7** (7): 3320–3342 DOI: 10.3390/w7073320
- Lendziocch T, Langhammer J, Jenicek M. 2019. Estimating Snow Depth and Leaf Area Index Based on UAV Digital Photogrammetry. *Sensors* **19** (5): 1027 DOI: 10.3390/S19051027
- Li D, Lettenmaier DP, Margulis SA, Andreadis K. 2019. The Role of Rain-on-Snow in Flooding Over the Conterminous United States. *Water Resources Research* **55** (11): 8492–8513 DOI: 10.1029/2019WR024950
- Li Z, Chen Y, Li Y, Wang Y. 2020. Declining snowfall fraction in the alpine regions, Central Asia. *Scientific Reports* **10** (1): 1–12 DOI: 10.1038/s41598-020-60303-z
- Lindström G, Johansson B, Persson M, Gardelin M, Bergström S. 1997. Development and test of the distributed HBV-96 hydrological model. *Journal of Hydrology* **201** (1–4): 272–288 DOI: 10.1016/S0022-1694(97)00041-3
- López-Moreno JI, Pomeroy JW, Morán-Tejeda E, Revuelto J, Navarro-Serrano FM, Vidaller I, Alonso-González E. 2021. Changes in the frequency of global high mountain rain-on-snow events due to climate warming. *Environmental Research Letters* **16** (9): 094021 DOI: 10.1088/1748-9326/ac0dde
- Lundquist JD, Dickerson-Lange SE, Lutz JA, Cristea NC. 2013. Lower forest density enhances snow retention in regions with warmer winters: A global framework developed from plot-scale observations and modeling. *Water Resources Research* **49** (10): 6356–6370 DOI: 10.1002/wrcr.20504

- Maina FZ, Kumar S V. 2023. Diverging Trends in Rain-On-Snow Over High Mountain Asia. *Earth's Future* **11** (3) DOI: 10.1029/2022EF003009
- Malle J, Rutter N, Mazzotti G, Jonas T. 2019. Shading by trees and fractional snow cover control the sub-canopy radiation budget. *Journal of Geophysical Research: Atmospheres* **124**: 3195–3207 DOI: 10.1029/2018jd029908
- Marks D, Kimball J, Tingey D, Link T. 1998. The sensitivity of snowmelt processes to climate conditions and forest cover during rain-on-snow: a case study of the 1996 Pacific Northwest flood. *Hydrological Processes* **12**: 1569–1587 Available at: http://www.hydro.washington.edu/pub/shrad/dew_files/Snowhydrology/Rain_on_snow/Marks_rainonsnow.pdf [Accessed 25 October 2018]
- Marty C, Schlögl S, Bavay M, Lehning M. 2017. How much can we save? Impact of different emission scenarios on future snow cover in the Alps. *Cryosphere* **11** (1): 517–529 DOI: 10.5194/tc-11-517-2017
- Mazurkiewicz AB, Callery DG, McDonnell JJ. 2008. Assessing the controls of the snow energy balance and water available for runoff in a rain-on-snow environment. *Journal of Hydrology* **354** (1–4): 1–14 DOI: 10.1016/j.jhydrol.2007.12.027
- Mccabe GJ, Clark MP, Hay LE. 2007. Rain-on-snow events in the western United states. *American meteorological society* **88**: 319–328 DOI: 10.1175/BAMS-88-3-319
- Meriö LJ, Rauhala A, Ala-Aho P, Kuzmin A, Korpelainen P, Kumpula T, Kløve B, Marttila H. 2023. Measuring the spatiotemporal variability in snow depth in subarctic environments using UASs - Part 2: Snow processes and snow-canopy interactions. *Cryosphere* **17** (10): 4363–4380 DOI: 10.5194/tc-17-4363-2023
- Merz R, Blöschl G. 2003. A process typology of regional floods. *Water Resources Research* **39** (12): 1340 DOI: 10.1029/2002WR001952
- Moeser D, Mazzotti G, Helbig N, Jonas T. 2016. Representing spatial variability of forest snow: Implementation of a new interception model. *Water Resources Research* **52** (2): 1208–1226 DOI: 10.1002/2015WR017961
- Mooney PA, Li L. 2021. Near future changes to rain-on-snow events in Norway. *Environmental Research Letters* **16** (6): 064039 DOI: 10.1088/1748-9326/abfdeb
- Morán-Tejeda E, López-Moreno JJ, Stoffel M, Beniston M. 2016. Rain-on-snow events in Switzerland: Recent observations and projections for the 21st century. *Climate Research* **71** (2): 111–125 DOI: 10.3354/cr01435
- Moriasi DN, Gitau MW, Pai N, Daggupati P. 2015. Hydrologic and water quality models: Performance measures and evaluation criteria. *Transactions of the ASABE* **58** (6): 1763–1785 DOI: 10.13031/trans.58.10715
- Musselman KN, Pomeroy JW. 2017. Estimation of Needleleaf Canopy and Trunk Temperatures and Longwave Contribution to Melting Snow. *Journal of Hydrometeorology* **18** (2): 555–572 DOI: 10.1175/jhm-d-16-0111.1
- Musselman KN, Lehner F, Ikeda K, Clark MP, Prein AF, Liu C, Barlage M, Rasmussen R. 2018. Projected increases and shifts in rain-on-snow flood risk over western North America. *Nature Climate Change* **8** (9): 808–812 DOI: 10.1038/s41558-018-0236-4
- Musselman KN, Pomeroy JW, Link TE. 2015. Variability in shortwave irradiance caused by forest gaps: Measurements, modelling, and implications for snow energetics. *Agricultural and Forest Meteorology* **207**: 69–82 DOI: 10.1016/j.agrformet.2015.03.014

- Myers DT, Ficklin DL, Robeson SM. 2023. Hydrologic implications of projected changes in rain-on-snow melt for Great Lakes Basin watersheds. *Hydrology and Earth System Sciences* **27** (9): 1755–1770 DOI: 10.5194/hess-27-1755-2023
- Nedelcev O, Jenicek M. 2021. Trends in seasonal snowpack and their relation to climate variables in mountain catchments in Czechia. *Hydrological Sciences Journal* **66** (16): 2340–2356 DOI: 10.1080/02626667.2021.1990298
- Notarnicola C. 2020. Hotspots of snow cover changes in global mountain regions over 2000–2018. *Remote Sensing of Environment* **243**: 111781 DOI: 10.1016/j.rse.2020.111781
- Ohba M, Kawase H. 2020. Rain-on-Snow events in Japan as projected by a large ensemble of regional climate simulations. *Climate Dynamics* **55** (9–10): 2785–2800 DOI: 10.1007/s00382-020-05419-8
- Oudin L, Hervieu F, Michel C, Perrin C, Andréassian V, Anctil F, Loumagne C. 2005. Which potential evapotranspiration input for a lumped rainfall-runoff model? Part 2 - Towards a simple and efficient potential evapotranspiration model for rainfall-runoff modelling. *Journal of Hydrology* **303** (1–4): 290–306 DOI: 10.1016/j.jhydrol.2004.08.026
- Pall P, Tallaksen LM, Stordal F. 2019. A climatology of rain-on-snow events for Norway. *Journal of Climate* **32** (20): 6995–7016 DOI: 10.1175/JCLI-D-18-0529.1
- Pomeroy J, Fang X, Ellis C. 2012. Sensitivity of snowmelt hydrology in Marmot Creek, Alberta, to forest cover disturbance. *Hydrological Processes* **26** (12): 1892–1905 DOI: 10.1002/hyp.9248
- Pomeroy JW, Fang X, Marks DG. 2016. The cold rain-on-snow event of June 2013 in the Canadian Rockies — characteristics and diagnosis. *Hydrological Processes* **30** (17): 2899–2914 DOI: 10.1002/hyp.10905
- Poschlod B, Zscheischler J, Sillmann J, Wood RR, Ludwig R. 2020. Climate change effects on hydrometeorological compound events over southern Norway. *Weather and Climate Extremes* **28**: 100253 DOI: 10.1016/j.wace.2020.100253
- Pradhanang SM, Frei A, Zion M, Schneiderman EM, Steenhuis TS, Pierson D. 2013. Rain-on-snow runoff events in New York. *Hydrological Processes* **27**: 3035–3049 DOI: 10.1002/hyp.9864
- Reid TD, Essery RLH, Rutter N, King M. 2014. Data-driven modelling of shortwave radiation transfer to snow through boreal birch and conifer canopies. *Hydrological Processes* **28** (6): 2987–3007 DOI: 10.1002/hyp.9849
- Rennert KJ, Roe G, Putkonen J, Bitz CM. 2009. Soil thermal and ecological impacts of rain on snow events in the circumpolar arctic. *Journal of Climate* **22** (9): 2302–2315 DOI: 10.1175/2008JCLI2117.1
- Rössler O, Froidevaux P, Börst U, Rickli R, Martius O, Weingartner R. 2014. Retrospective analysis of a nonforecasted rain-on-snow flood in the Alps-A matter of model limitations or unpredictable nature? *Hydrology and Earth System Sciences* **18** (6): 2265–2285 DOI: 10.5194/hess-18-2265-2014
- Roth TR, Nolin AW. 2017. Forest impacts on snow accumulation and ablation across an elevation gradient in a temperate montane environment. *Hydrology and Earth System Sciences* **21** (11): 5427–5442 DOI: 10.5194/hess-21-5427-2017
- Schelker J, Kuglerova L, Eklöf K, Bishop K, Laudon H. 2013. Hydrological effects of clear-cutting in a boreal forest - Snowpack dynamics, snowmelt and streamflow responses. *Journal of Hydrology* **484**: 105–114 DOI: 10.1016/j.jhydrol.2013.01.015

- Schirmer M, Winstral A, Jonas T, Burlando P, Peleg N. 2022. Natural climate variability is an important aspect of future projections of snow water resources and rain-on-snow events. *The Cryosphere* **16** (9): 3469–3488 DOI: 10.5194/tc-16-3469-2022
- Seibert J, Bergström S. 2022. A retrospective on hydrological catchment modelling based on half a century with the HBV model. *Hydrology and Earth System Sciences* **26** (5): 1371–1388 DOI: 10.5194/HESS-26-1371-2022
- Seibert J, Vis MJP. 2012. Teaching hydrological modeling with a user-friendly catchment-runoff-model software package. *Hydrology and Earth System Sciences* **16**: 3315–3325 DOI: 10.5194/hess-16-3315-2012
- Seibert J, Vis MJP, Lewis E, van Meerveld HJ. 2018. Upper and lower benchmarks in hydrological modelling. *Hydrological Processes* **32** (8): 1120–1125 DOI: 10.1002/hyp.11476
- Serquet G, Marty C, Dulex JP, Rebetez M. 2011. Seasonal trends and temperature dependence of the snowfall/precipitation- day ratio in Switzerland. *Geophysical Research Letters* **38** (7): L07703 DOI: 10.1029/2011GL046976
- Sezen C, Sraj M, Medved A, Bezak N. 2020. Investigation of rain-on-snow floods under climate change. *Applied Sciences (Switzerland)* **10** (4) DOI: 10.3390/app10041242
- Sikorska-Senoner AE, Seibert J. 2020. Flood-type trend analysis for alpine catchments. *Hydrological Sciences Journal* **65** (8): 1281–1299 DOI: 10.1080/02626667.2020.1749761
- Singh P, Singh VP. 2001. *Snow and glacier hydrology*. Springer Science & Business Media. DOI: 10.1029/01EO00355
- Sipek V, Jenicek M, Hnilica J, Zelikova N. 2021. Catchment Storage and its Influence on Summer Low Flows in Central European Mountainous Catchments. *Water Resources Management* **35** (9): 2829–2843 DOI: 10.1007/s11269-021-02871-x
- Su Y, Langhammer J, Jarsjö J. 2017. Geochemical responses of forested catchments to bark beetle infestation: Evidence from high frequency in-stream electrical conductivity monitoring. *Journal of Hydrology* **550**: 635–649 DOI: 10.1016/j.jhydrol.2017.05.035
- Surfleet CG, Tullos D. 2013. Variability in effect of climate change on rain-on-snow peak flow events in a temperate climate. *Journal of Hydrology* **479**: 24–34 DOI: 10.1016/j.jhydrol.2012.11.021
- Suriano ZJ. 2022. North American rain-on-snow ablation climatology. *Climate Research* **87**: 133–145 DOI: 10.3354/cr01687
- Trubilowicz JW, Moore RD. 2017. Quantifying the role of the snowpack in generating water available for run-off during rain-on-snow events from snow pillow records. *Hydrological Processes* **31** (23): 4136–4150 DOI: 10.1002/hyp.11310
- Urban G, Richterová D, Kliegrová S, Zusková I. 2023. Reasons for shortening snow cover duration in the Western Sudetes in light of global climate change. *International Journal of Climatology* **43** (12): 5485–5511 DOI: 10.1002/joc.8157
- Vlach V, Ledvinka O, Matouskova M. 2020. Changing Low Flow and Streamflow Drought Seasonality in Central European Headwaters. *Water* **12** (12): 3575 DOI: 10.3390/w12123575
- Wawrzyniak T, Osuch M, Nawrot A, Napiorkowski JJ. 2017. Run-off modelling in an Arctic unglaciated catchment (Fuglebekken, Spitsbergen). *Annals of Glaciology* **58** (75): 36–46 DOI: 10.1017/aog.2017.8
- Wayand NE, Lundquist JD, Clark MP. 2015. Modeling the influence of hypsometry, vegetation, and storm energy on snowmelt contributions to basins during rain-on-snow floods. *Water Resources Research* **51** (10): 8551–8569 DOI: 10.1002/2014WR016576

- Webster C, Rutter N, Zahner F, Jonas T. 2016. Modeling subcanopy incoming longwave radiation to seasonal snow using air and tree trunk temperatures. *Journal of Geophysical Research: Atmospheres* **121**: 1220–1235 DOI: 10.1002/2015JD024099
- Welch CM, Stoy PC, Rains FA, Johnson A V, Mcglynn BL. 2016. The impacts of mountain pine beetle disturbance on the energy balance of snow during the melt period. *Hydrological Processes* **30** (4): 588–602 DOI: 10.1002/hyp.10638
- Wever N, Würzer S, Fierz C, Lehning M. 2016. Simulating ice layer formation under the presence of preferential flow in layered snowpacks. *Cryosphere* **10** (6): 2731–2744 DOI: 10.5194/tc-10-2731-2016
- Würzer S, Jonas T. 2018. Spatio-temporal aspects of snowpack runoff formation during rain on snow. *Hydrological Processes* **32** (23): 3434–3445 DOI: 10.1002/hyp.13240
- Würzer S, Jonas T, Wever N, Lehning M. 2016. Influence of Initial Snowpack Properties on Runoff Formation during Rain-on-Snow Events. *Journal of Hydrometeorology* **17** (6): 1801–1815 DOI: 10.1175/JHM-D-15-0181.1
- Würzer S, Wever N, Juras R, Lehning M, Jonas T. 2017. Modelling liquid water transport in snow under rain-on-snow conditions - Considering preferential flow. *Hydrology and Earth System Sciences* **21** (3): 1741–1756 DOI: 10.5194/hess-21-1741-2017
- Yang T, Li Q, Hamdi R, Chen X, Zou Q, Cui F, De Maeyer P, Li L. 2022. Trends and spatial variations of rain-on-snow events over the high Mountain Asia. *Journal of Hydrology* **614** (PB): 128593 DOI: 10.1016/j.jhydrol.2022.128593
- Yang Z, Chen R, Liu Y, Zhao Y, Liu Z, Liu J. 2023. The impact of rain-on-snow events on the snowmelt process: A field study. *Hydrological Processes* **37** (11): e15019 DOI: 10.1002/hyp.15019
- Zheng Z, Kirchner PB, Bales RC. 2016. Topographic and vegetation effects on snow accumulation in the southern Sierra Nevada: a statistical summary from lidar data. *Cryosphere* **10** (1): 257–269 DOI: 10.5194/tc-10-257-2016

8 Supplements

See all published papers in the original journal form attached.

RESEARCH ARTICLE

The impact of changing subcanopy radiation on snowmelt in a disturbed coniferous forest

Ondrej Hotovy  | Michal Jenicek 

Department of Physical Geography and Geoecology, Charles University, Prague, Czechia

Correspondence
Ondrej Hotovy, Department of Physical Geography and Geoecology, Charles University, Prague, Czechia.
Email: ondrej.hotovy@natur.cuni.cz

Funding information
Grantová Agentura České Republiky, Grant/Award Number: 18-06217Y; Grantová Agentura, Univerzita Karlova, Grant/Award Number: 272119

Abstract

Understanding the role of forests on snowmelt processes enables better estimates of snow storages at a catchment scale and contributes to a higher accuracy of spring flood forecasting. A coniferous forest modifies the snowpack energy balance by reducing the total amount of solar shortwave radiation (SWR) and enhancing the role of longwave radiation (LWR) emitted by trees. This study focuses on changes in SWR and LWR at three sites with different canopy structure (Bohemian Forest, Czechia), including one site affected by the bark beetle (*Ips typographus*). Measurements of incoming and outgoing SWR and LWR were performed at all sites equipped with CNR4 Net Radiometers for three cold seasons. In addition to SWR and LWR, sensible and latent heat, and ground heat and energy supplied by liquid precipitation were calculated. The results showed that net SWR at the healthy forest site represented only 7% of the amount at the open site due to the shading effect of trees. In contrast, net LWR represented a positive component of the snowpack energy balance at the healthy forest site and thus contributed the most to snowmelt. However, the modelled snowmelt rates were significantly lower in the forest than in the open area since the higher LWR in the forest did not compensate for the lower SWR. The progressive decay of disturbed forest caused the decrease in mean net LWR from -3.1 W/m^2 to -12.9 W/m^2 and the increase in mean net SWR from 31.6 W/m^2 to 96.2 W/m^2 during the study period. These changes caused an increase in modelled snowmelt rates by 50% in the disturbed forest, compared to the healthy forest site, during the study period. Our findings have important implications for runoff from areas affected by land cover changes due to either human activity or climate change.

KEYWORDS

disturbance, longwave radiation, shortwave radiation, snowmelt, snowpack energy balance

1 | INTRODUCTION

Snowpack represents an important component of the hydrological cycle in mountainous regions in humid climates, because it stores a substantial amount of precipitation during the winter season. If this water is released suddenly during warmer or rainy days, intense runoff may occur, resulting in higher flood risk. Therefore, understanding the role of forests on snowmelt processes enables better estimates of

snow storages, and contributes to a higher accuracy of spring flood forecasting (Hock, 2003). At local scales, snow accumulation and ablation are controlled dominantly by local topography (Zheng, Kirchner, & Bales, 2016), canopy structure (Jenicek, Pevna, & Matejka, 2018; Lendzioch, Langhammer, & Jenicek, 2019) and by meteorological conditions (Assaf, 2007). Forest significantly affects the amount and distribution of individual energy fluxes and influences physical properties of snowpack (Broxton et al., 2015; Lundquist, Dickerson-Lange,

Lutz, & Cristea, 2013; Pomeroy, Fang, & Ellis, 2012). For the snowpack energy balance, the species composition is crucial, as it affects canopy structure and consequently local meteorological conditions and distribution of radiation fluxes (Musselman & Pomeroy, 2017; Roth & Nolin, 2017), resulting in differences in physical snowpack properties and water volume stored in the snowpack in forests compared to open areas.

Potential changes in forest structure, such as forest disturbances, lead to significant changes in snowmelt and runoff conditions (Bartik et al., 2019; Su, Langhammer, & Jarsjö, 2017). These changes also include changes in energy exchange after forest disturbance, with expected higher snow storages due to lower snow interception and faster snowmelt (Förster, Garvelmann, Meißl, & Strasser, 2018; Moeser, Mazzotti, Helbig, & Jonas, 2016; Pugh & Small, 2013; Stähli, Jonas, & Gustafsson, 2009). The latter may be explained mainly by (a) the increase in incoming shortwave radiation (SWR) due to a lower shading effect of trees after forest disturbance (Malle, Rutter, Mazzotti, & Jonas, 2019; Pomeroy et al., 2012) and (b) the decrease in both incoming and net longwave radiation (LWR; net LWR is the difference between incoming and outgoing LWR) emitted by trees, which contributes significantly to the snowpack energy balance (Essery, Pomeroy, Ellis, & Link, 2008; Webster, Rutter, Zahner, & Jonas, 2016).

Many studies have focused on the temporal variability of the main components of the energy balance (Garvelmann, Pohl, & Weiler, 2015; Welch, Stoy, Rains, Johnson, & Mcglynn, 2016). Several approaches were used in these studies to calculate the components, resulting in a variety of models simulating the snow ablation and snowmelt runoff (Ellis, Essery, & Link, 2011; Gouttevin, Lehning, Jonas, Gustafsson, & Mölder, 2015; Helgason & Pomeroy, 2012). Several authors have focused primarily on the role of SWR (Courbaud, De Coligny, & Cordonnier, 2003; Musselman, Pomeroy, & Link, 2015; Reid, Essery, Rutter, & King, 2014), while others have focused specifically on the role of LWR (Essery et al., 2008; Iziomon, Mayer, & Matzarakis, 2003; Webster et al., 2016).

The decrease in snowmelt rates in forested sites cannot be explained only by the decrease in incoming solar radiation, but the role of LWR is also very important (Assaf, 2007; Malle et al., 2019; Webster et al., 2016). The differences in energy fluxes between forested and open environments cause, in connection with other influencing factors, different snowmelt rates and snow cover duration in open areas compared to forests (Helgason & Pomeroy, 2012; Jenicek, Hotovy, & Matejka, 2017; Lundquist et al., 2013). Canopy structure also determines the interception rate which controls the subcanopy snow accumulation. Through interception, up to 60% of the cumulative snowfall may be captured by tree crowns in coniferous forests during winter (Helbig et al., 2019). Together with reduced snow redistribution by wind at forested sites, the amount of accumulated snow in coniferous forests may differ significantly compared to open areas.

The spatial and temporal variability in SWR and LWR is important for the timing and intensity of spring runoff. Both radiation components together can represent up to 80% of the total energy used for

snowmelt (Cline, 1997), although the contribution is highly variable based on actual meteorological conditions. For example, during rain-on-snow events, turbulent fluxes (sensible and latent heats) are dominant (Würzer, Jonas, Wever, & Lehning, 2016). Such processes are important when assessing the snowmelt on a daily (event) scale. At longer (seasonal) scales, radiation components (SWR and LWR) become more important. Therefore, an effective forecast of the timing and magnitude of mountain snowmelt runoff requires accurate estimates of SWR and LWR (Ellis & Pomeroy, 2007). Accurate LWR data are, however, usually not available in a forest environment and are often substituted by modelled values or not considered at all.

The above studies show that the effects of forests on both snow accumulation and snowmelt, and the resulting catchment runoff, have been widely studied. However, there is still limited knowledge about the specific contribution of individual energy balance components, namely SWR and LWR, to the snowpack energy balance and snowmelt rates in forested areas with different canopy structure, and how this contribution changes during forest disturbance. Understanding the effects of forest cover on the sub-canopy energy balance is important to improve snowmelt models for accurate prediction of catchment runoff from forested mountain catchments. For example, many models use a degree-day approach for snowmelt calculations where the accurate representation of the energy balance is more challenging. Therefore, the objective of this study was (a) to quantify temporal variations in SWR and LWR at sites with different canopy structure, (b) to assess how the contribution of SWR and LWR to the energy balance changed due to forest disturbance caused by the bark beetle (*Ips typographus*) and (c) to assess how the changes in individual energy balance components affected snowmelt. We benefit from measured data of SWR and LWR from radiometers placed at three selected sites with different canopy structure. Our study adds to earlier studies by focusing on the evolution of both SWR and LWR during a 3-year period with gradual forest decay at our study plots and by quantification of the relative contribution of individual energy fluxes to snowmelt rates. Exploring the changing energy balance is important especially in the context of land cover changes, which are occurring either due to human activity or climate change.

2 | MATERIAL AND METHODS

2.1 | Study area and data monitoring

The study was performed at three sites with different forest structure located on a flat terrain at 1,140 m a.s.l. We used data measured over three consecutive cold seasons (December 1–April 30) between 2015 and 2018; 2015/2016 (hereafter referred to as season 2016), 2016/2017 (season 2017) and 2017/2018 (season 2018). The sites are located in the Ptaci Brook catchment (an experimental catchment of the Charles University, Prague) in the Bohemian Forest (Sumava National park) in the southwest part of Czechia (Figure 1). The canopy structure was described by the leaf area index (LAI) integrated over the zenith angles 0–60° and calculated from digital hemispherical

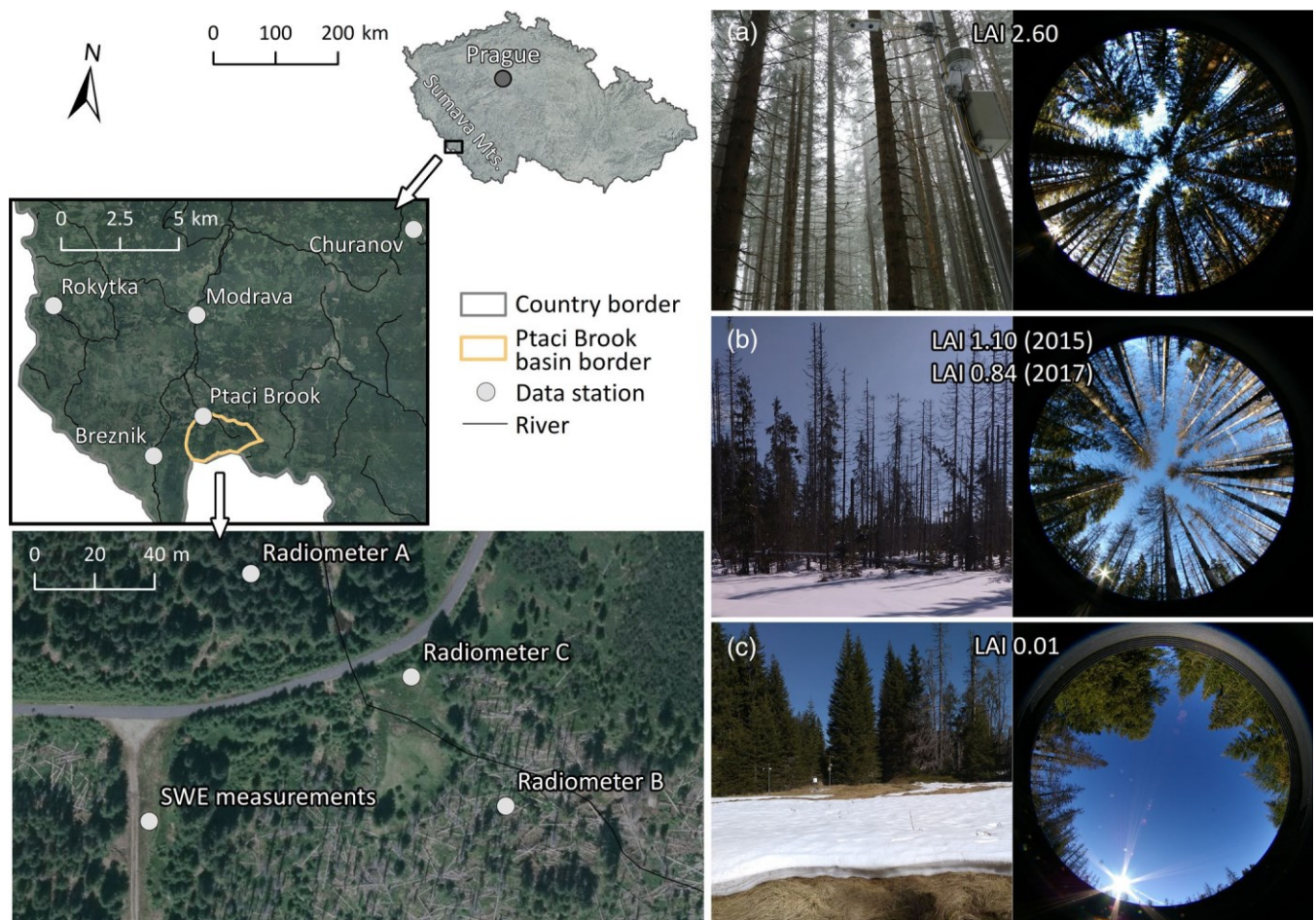


FIGURE 1 Geographical location of the Ptaci Brook catchment and the position of all data stations used in the study. Each sampling site with radiometers represents specific vegetation structure described by leaf area index (LAI); healthy dense spruce forest (a), disturbed spruce forest (b) and open meadow (c) (Data: Czech Office for Surveying, Mapping and Cadastre ČÚZK; photos by the authors)

photographs of the sky and canopy (Figure 1) and analysed using Gap Light Analyzer software (Frazer, Canham, & Lertzman, 1999; Varhola, Coops, Alila, & Weiler, 2014). The first experimental site (A) was covered by healthy dense spruce forest (LAI = 2.6). The second site (B) was covered by disturbed spruce forest affected by the bark beetle (*I. typographus*), where LAI was equal to 1.1 at the start of our study (2015) and decreased to 0.84 at the beginning of the last season 2018. The third site (C) was a reference site situated in an open meadow (LAI = 0.01).

The annual mean air temperature at the study plots is 4°C and -2°C during cold season, varying from -5°C in January and February to 3°C in April. The annual precipitation is approximately 1,100 mm, with mean 400 mm during cold season, usually falling as a snow. The snow accumulation season usually starts in November, maximum snow water equivalent (SWE) reaches 500 mm and snowmelt runoff occurs approximately from late March to mid-May, forming from 30 to 40% of the total annual runoff from the catchment. A bark beetle disturbance that occurred intermittently over the last three decades, caused significant vegetation changes over the whole region, affecting individual components of the water cycle, including

interception, evaporation and runoff (Langhammer, Su, & Bernsteinova, 2015; Su et al., 2017). In addition to these changes, the character of irradiation below the forest canopy changed.

An experimental catchment is equipped to measure precipitation (without a heating module), snow and air temperature, snow depth, SWE, SWR and LWR. The measurements of SWR and LWR were performed at all three sites equipped with CNR4 Net Radiometers (Kipp & Zonen, Figure 1). These devices consist of two pyranometers (one oriented upward and one oriented downward) and two pyrgeometers (with the same configuration as the pyranometers). This configuration enabled measurements of both global (incoming) and reflected (outgoing) radiation. All radiometers were additionally equipped with sensors to measure air temperature and snow depth.

Since the radiometer sensors lack heating, the identification of days when sensors were covered with snow was necessary. These days were identified as days when SWR from the downward oriented sensor was higher than SWR from the upward oriented sensor. This would result in albedo higher than one, which is physically impossible and thus it indicated that the upward oriented sensor was covered with snow causing the attenuation of incoming SWR. Based on the

above procedure, both SWR and LWR data for the specific day have been removed from the analysis. In total, 25–32% of the data have been removed for individual years.

Snowpack Analyser SPA (Sommer Messtechnik) was used for continuous measurements of SWE (based on measurements of the dielectric constant of the ice, water and gas in the snowpack; Heggli, 2013; Jenicek et al., 2017) and snow depth (using an ultrasonic sensor) at the open site (Figure 1). The liquid water content (L_{wc}), measured as the mass of liquid water per unit mass of the snowpack, was calculated for each time step from SPA data. All data were measured in 10-min temporal resolution, but were aggregated to hourly and daily values for analysis.

Data available for the study area were supplemented with data from other nearby stations (Figure 1); winter precipitation (with a heated rain gauge) and wind speed were measured at the Modrava station (4 km from the study site; 982 m a.s.l.), atmospheric pressure and wind speed were measured at the Churanov station (10 km from the study site; 1,118 m a.s.l.), air humidity was measured at the Breznik station (3 km from the study site; 1,140 m a.s.l.), and soil temperature from two soil depths (20 and 60 cm) was measured at the Rokytkka station (8 km from the study site; 1,100 m a.s.l.).

2.2 | Calculation of snowpack energy balance

A physically based energy balance approach was used to calculate main energy fluxes driving the snowmelt process. This method quantifies heat fluxes on atmosphere-snow-soil ground interfaces and heat exchange inside the snowpack (Singh & Singh, 2001). The total heat Q_m (W/m^2) accessible for snowmelt was calculated for days with snow on the ground as a sum of six components (Equation (1)),

$$Q_m = Q_{ns} + Q_{nl} + Q_h + Q_e + Q_p + Q_g, \quad (1)$$

where Q_{ns} is net SWR and Q_{nl} is net LWR, Q_h is sensible heat, Q_e is latent heat, Q_p is heat supplied by liquid precipitation and Q_g is ground heat flux. Positive values of Q_m represent snowpack energy gain (when snowpack temperature is 0°C, snowmelt occurs), negative Q_m represents energy losses with no snowmelt.

The net SWR and LWR were calculated as a difference between values from upward- and downward-oriented sensors. Since changes in SWR and LWR are more important during forest decay compared to changes in other energy balance components, we were mostly focused on changes in these components in the study.

The Q_h represents a convective transfer of sensible heat, which occurs when there is a difference between air and snowpack surface temperatures (Equation (2); DeWalle & Rango, 2008).

$$Q_h = \rho_a c_p C_h u_a (T_a - T_s), \quad (2)$$

where ρ_a is density of air (1.27 kg/m^3 for air temperature of 5°C), c_p is specific heat of air ($1.005 \times 10^3 \text{ J kg}^{-1} \text{ K}^{-1}$), C_h is bulk transfer coefficient for sensible heat (2.01×10^{-3} , dimensionless), u_a is wind speed

(m/s), T_a is air temperature (K) and T_s is snow surface temperature (K). Since only wind speed data from the open area were available, the wind speed values at the forested sites were adjusted according to procedure presented in Tarboton and Luce (1996) who related the wind speed attenuation under forest canopy to LAI. Based on this procedure, the wind speed at the healthy forest site was assumed to be 0.2 times the wind speed at the open site, and 0.7 times the wind speed at the disturbed forest site.

The snow surface temperature was estimated from measurements of the snow temperature at different heights above bare ground (0.3, 0.6, 0.9 and 1.2 m). For each day, the snow surface temperature was assumed to be equal to the snow temperature measured by the highest snow-covered thermometer.

The Q_e represents latent heat flux, which is the heat loss or gain due to water phase changes (Equation (3); DeWalle & Rango, 2008).

$$Q_e = (\rho_a 0.622L/P_a) C_e u_a (e_a - e_0), \quad (3)$$

where L is latent heat of vaporization or sublimation ($2.496 \times 10^6 \text{ J/kg}$), P_a is atmospheric pressure (hPa), C_e is the bulk transfer coefficient for vapour exchange (2.01×10^{-3} , dimensionless), e_a is atmospheric vapour pressure (hPa), which is the product of saturation vapour pressure for a given air temperature and relative humidity, and e_0 is vapour pressure at the snowpack surface, which is generally assumed to be the saturation vapour pressure at the snowpack temperature. This means that e_0 is changing with the snow surface temperature and reaches a maximum of 6.1078 hPa during melting at 0°C.

The Q_p indicates heat input supplied by liquid precipitation (Equation (4); DeWalle & Rango, 2008).

$$Q_p = P_r \rho_w c_w (T_r - T_s), \quad (4)$$

where P_r is rainfall intensity (m/s), ρ_w is the density of liquid water ($1 \times 10^3 \text{ kg/m}^3$), c_w is specific heat of liquid water ($4.1876 \times 10^3 \text{ J kg}^{-1} \text{ C}^{-1}$), T_r is the temperature of rain (assumed to be equal to air temperature during the rain event) (°C).

The Q_g represents ground heat flux (Equation (5); DeWalle & Rango, 2008).

$$Q_g = k_g \delta T_g / \delta z, \quad (5)$$

where k_g is the soil thermal conductivity ($0.5 \text{ W m}^{-1} \text{ C}^{-1}$) for saturated gleysols, podzols and organosols (McKenzie, Siegel, Rosenberry, Glaser, & Voss, 2007) typically occurring at our study sites, T_g is the soil temperature (°C) at depth z (m). We used T_g measured at the nearby Rokytkka station, where $z_1 = -0.2 \text{ m}$ and $z_2 = -0.6 \text{ m}$.

2.3 | Calculation of snowmelt rates

The energy balance Q_m was used to calculate snowmelt rates M_{sim} (mm/day) at individual study sites using Equation (6) (DeWalle & Rango, 2008). To assess the accuracy of the model, simulated

snowmelt rates were compared with observed snowmelt rates M_{obs} (mm/day) at the open site, calculated for days with existing snow cover based on Equation (7).

$$M_{sim} = \begin{cases} \frac{Q_m}{\rho_w L_f B}, & Q_m > 0 \\ 0, & Q_m \leq 0 \end{cases} \quad (6)$$

$$M_{obs} = \begin{cases} SWE_{d-1} - SWE_d + P_d, & SWE_{d-1} > SWE_d \\ 0, & SWE_{d-1} \leq SWE_d \end{cases} \quad (7)$$

where L_f is the latent heat of fusion (0.334×10^6 J/kg at 0°C), B (-) is the thermal quality of the snowpack as shown in Equation (8) (DeWalle & Rango, 2008). SWE_d (mm) is the daily average SWE for a given day, SWE_{d-1} (mm) represents the daily average SWE of a previous day and P_d is the daily precipitation (mm).

$$B = [(1 - L_{wc})L_f + c_i T]/L_f, \quad (8)$$

where L_{wc} is liquid water content, c_i is specific heat of ice (2.1×10^3 J kg⁻¹C⁻¹) and T is the snowpack temperature depression below 0°C (the absolute value of the snow temperature).

The calculated M_{sim} at individual study sites were used for the snowmelt simulation (Equation (9)) to assess how different snowmelt rates influenced melt-out days at individual sites. We selected periods of the main spring snowmelt after peak SWE, which roughly corresponds to the period from late March to early April (depending on the specific study year).

$$SWE_d = SWE_{d-1} - M_{sim} + P_d. \quad (9)$$

The initial SWE for the open site was set from continuous SWE measurements. For forested sites, initial SWE values were calculated using snow depth (measured at the same position as the individual radiometers) and snow density (assumed to be the same as snow density at the open site).

3 | RESULTS

3.1 | Variability in SWR

Canopy structure affected the snowpack energy balance at individual sites because forest shading reduced the total amount of SWR. The amount of SWR varied significantly during the study period according to the canopy structure and meteorological conditions (Figures 2-4). The net SWR at the healthy forest site represented only 7% of the amount at the open site (Figure 2). At the disturbed forest site, the mean net SWR increased from 31.6 W/m² in season 2016 to 39.7 W/m² in season 2017, and to 96.2 W/m² in season 2018. This represented 28% of the net SWR amount at the open site in season 2016, 34% in season 2017, and 66% in season 2018, respectively. The increased SWR was caused mainly by the gradual forest decay after the bark beetle infestation. The relatively larger increase in incoming, outgoing and net SWR between the second and third year of the monitoring compared to the first and second years was affected by a strong windstorm, which occurred in the study area in October 2017.

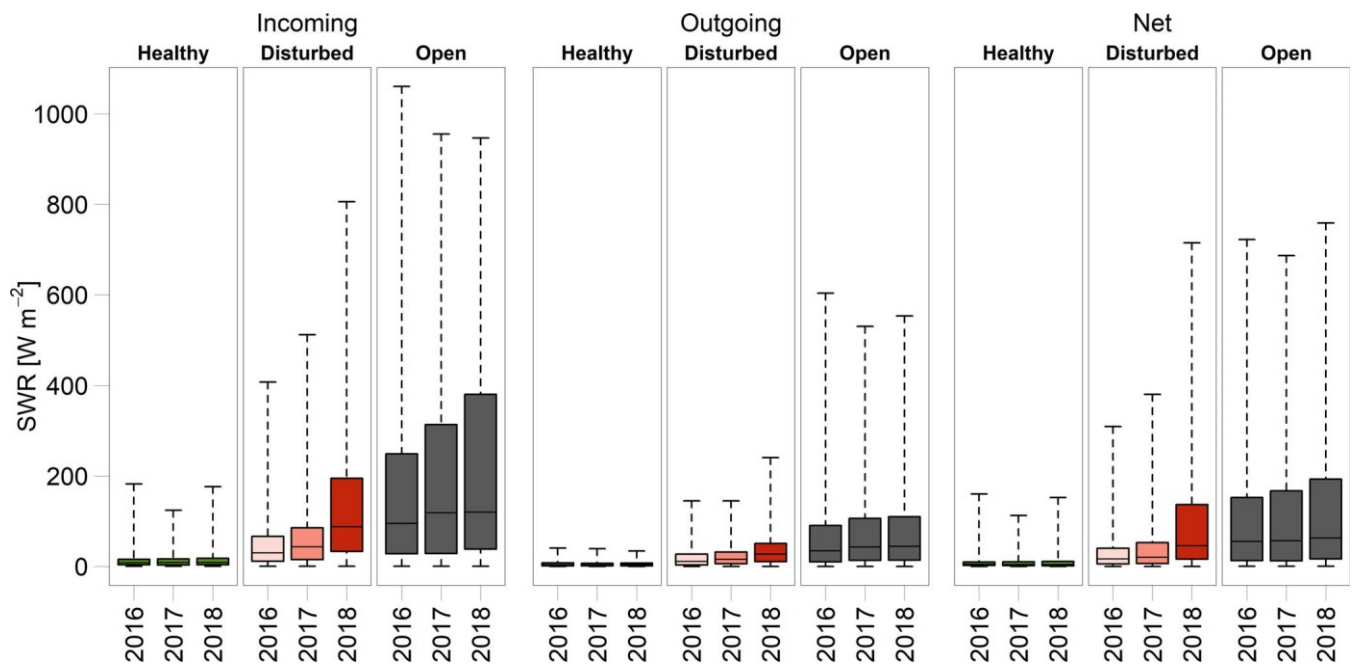


FIGURE 2 Variability in mean hourly incoming, outgoing and net shortwave radiation (SWR) during seasons 2016, 2017 and 2018 at individual study sites. Boxes represent 25 and 75% percentile (with median as a black line) and whiskers represent interquartile ranges

This windstorm caused many windthrows of decayed trees and thus the site became more open to SWR.

Although the incoming and net SWR increased relatively at the disturbed forest, the relative SWR attenuation at the forest site compared to the open site did not change significantly (Figure 2). This provided evidence that the increase in SWR at the disturbed forest site was caused by the gradual, windstorm-based forest decay rather than changes in meteorological conditions over these 3 years. The above result is supported by Figure 3, which shows the relation between daily mean SWR at the open site compared to forested sites in individual years. The increase in SWR in disturbed forest between individual seasons is clearly visible in Figure 3, especially between seasons 2017 and 2018.

The hourly distribution in intensity of incoming SWR was determined by the sun position, with positive values occurring between sunrise and sunset, and peak values at solar noon (Figure 4). As the solar elevation angle increased during the cold season towards spring, the intensity of SWR gradually increased as well. Maximum values were reached during late April mid-afternoons at the open site (about $1,000 \text{ W/m}^2$ on hourly average, Figure 4, bottom panels). Lower values were measured at healthy and disturbed spruce forest sites due to the shading effect of trees (Figure 4, top and middle panels).

Changes in both incoming and outgoing SWR controlled surface albedo (net SWR) at individual sites (Figure 5). Albedo at the open site reached 0.47 (average over all three seasons), 0.42 at the disturbed forest site, and 0.39 at the healthy forest site. The absolute values of albedo were much lower than expected for the snow surface, which could be explained by the fact that the view angle of both upward and downward oriented radiometers is about 170° , which causes the albedo of surrounding surfaces, with generally lower albedo, such as

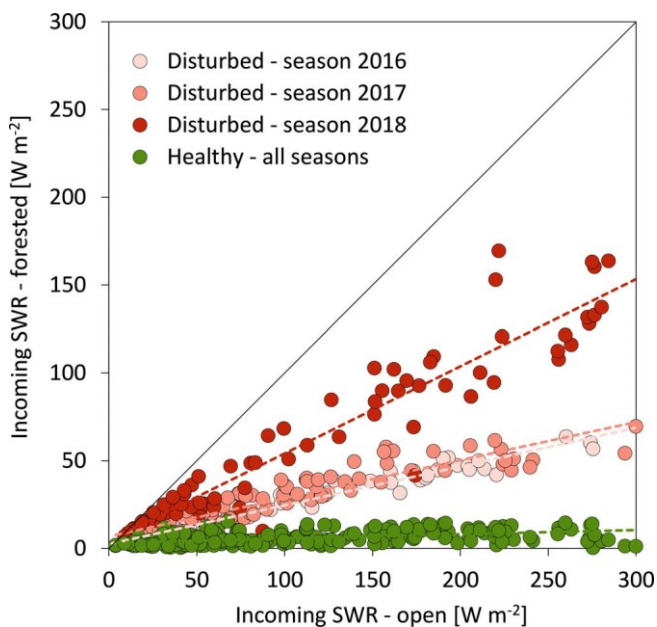


FIGURE 3 Mean daily incoming shortwave radiation (SWR) at the open site compared to forested sites during seasons 2016, 2017 and 2018

trees, to influence the absolute values. Absolute albedo values were also affected by days with partial snow cover. The relatively lower albedo in both forested sites compared to the open site was probably caused by a dirty snow surface under the trees, with needles and wood lying on it, and by the fact that snow melted earlier in the forest than in the open area (due to generally lower SWE before melting), and thus albedo decreased. Overall, changes in albedo at individual sites during the study period can be related to changes in snow and meteorological conditions. However, our results did not prove any changes in albedo due to changes in canopy structure at the disturbed forest site during the study period (Figure 5).

3.2 | Variability in LWR

While the only natural source for SWR is the sun, LWR is produced by any object with a non-zero absolute temperature ($T > 0 \text{ K}$). Therefore, net snowpack LWR may be either positive (snowpack energy gain) or negative (snowpack energy loss).

In general, the incoming LWR at the open site reached 350 W/m^2 at its maximum during midday in late April compared to values over 400 W/m^2 at the forest site (Figure 6). The mean incoming LWR decreased at the disturbed forest site during the 3-year study period due to gradual forest decay after the bark beetle infestation and related event-based windstorms. The amount and temporal variations in incoming LWR at the disturbed forest site were similar to LWR at the healthy forest site in the first season while it became more closely related to the open site during the last season (Figure 6). The progressive decrease in incoming LWR at the disturbed forest site is shown in Figure 7a where the most distanced points below the one-to-one line are those representing the season 2018 (dark red points).

Individual study sites showed substantial differences in net LWR (Figures 6–8). The net LWR represented mostly a negative component of the snowpack energy balance at the open site (daily mean -20.5 W/m^2). In contrast, net LWR was mostly positive at the healthy forest site with a daily average of 3.3 W/m^2 . Negative values rarely occurred. The forest decay caused the significant decrease in net LWR at the disturbed forest site from -3.1 W/m^2 in season 2016 to -12.9 W/m^2 in season 2018. The reason for this decrease was mainly due to reduced forest density caused by the bark beetle. Therefore, the site became more open and the LWR emitted by trees decreased over the study period. This is shown in Figure 7b, where values from the first season are located mostly in the top right quadrant, while values from the last season are located mostly in the bottom right quadrant. Similar to incoming LWR, as shown in Figure 7a, the change in net LWR indicated an increasing difference between both forested sites.

The net LWR at individual sites varied throughout the cold season reflecting meteorological conditions, especially air temperature and radiation conditions (clear sky or cloudy). The difference between day- and night-time LWR, and between sites, decreased during advective weather conditions (cloudy days) because clouds scatter and absorb solar SWR on their particles which causes higher emission of

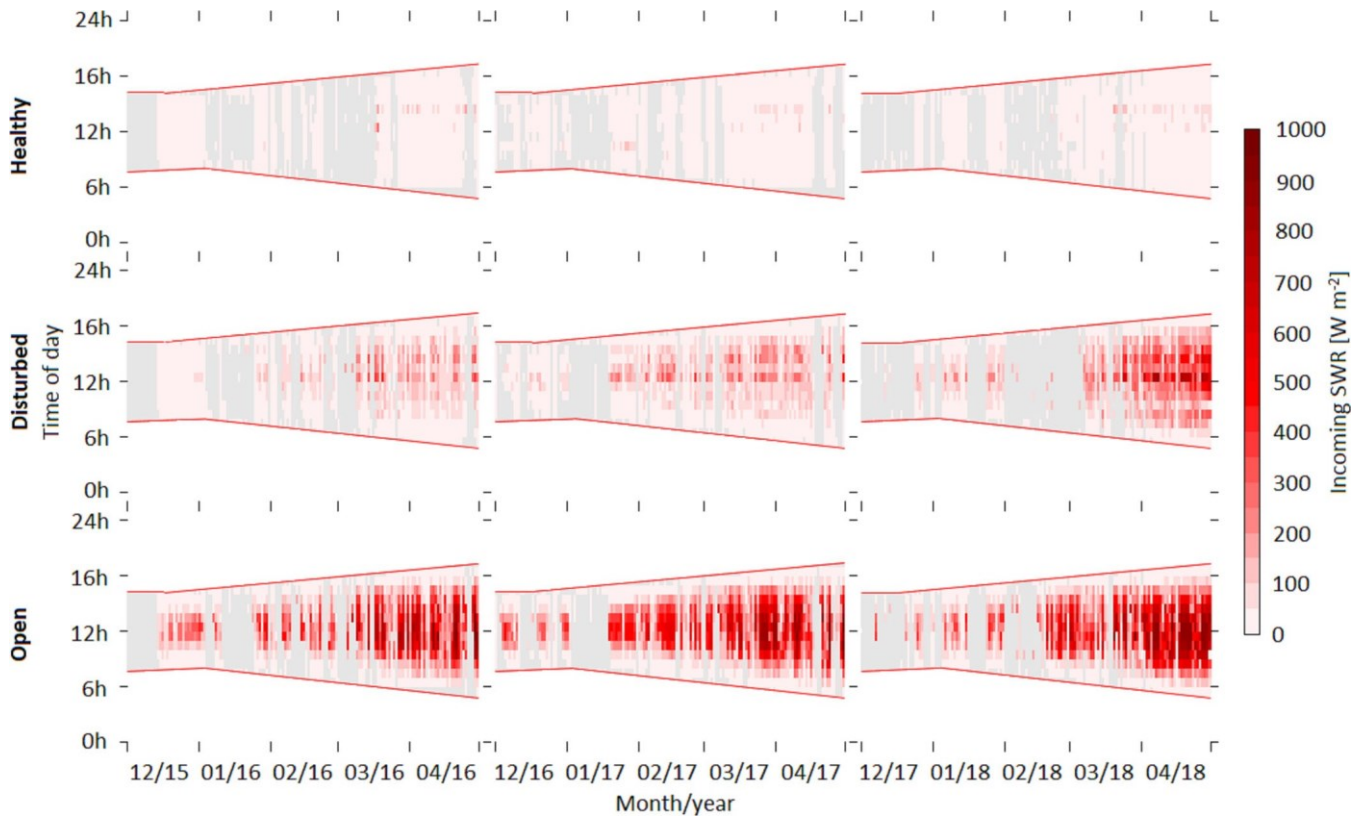


FIGURE 4 Mean hourly incoming shortwave radiation (SWR) at the healthy spruce forest site (top panels), disturbed forest site (middle panels) and open site (bottom panels) during seasons 2016, 2017 and 2018. Red lines represent time of sunrise and sunset. Grey colour represents missing data

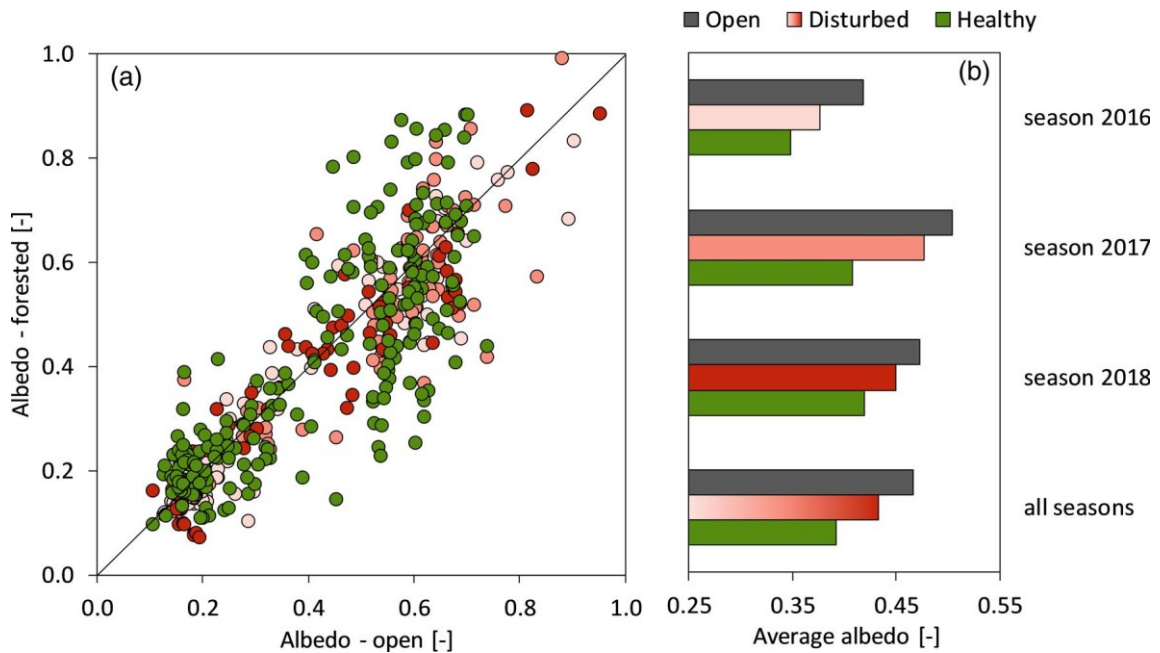


FIGURE 5 Mean daily albedo (panel (a)) and mean seasonal albedo (panel (b)) during seasons 2016, 2017 and 2018 at study sites

LWR. Additionally, total incoming LWR was generally higher for cloudy days compared to clear sky conditions (results not shown). Therefore, the LWR emitted by the atmosphere became a relatively more

important component of the snowpack energy balance during these cloudy days. In contrast, the difference between day-time and night-time net LWR, and between sites, increased for clear sky conditions.

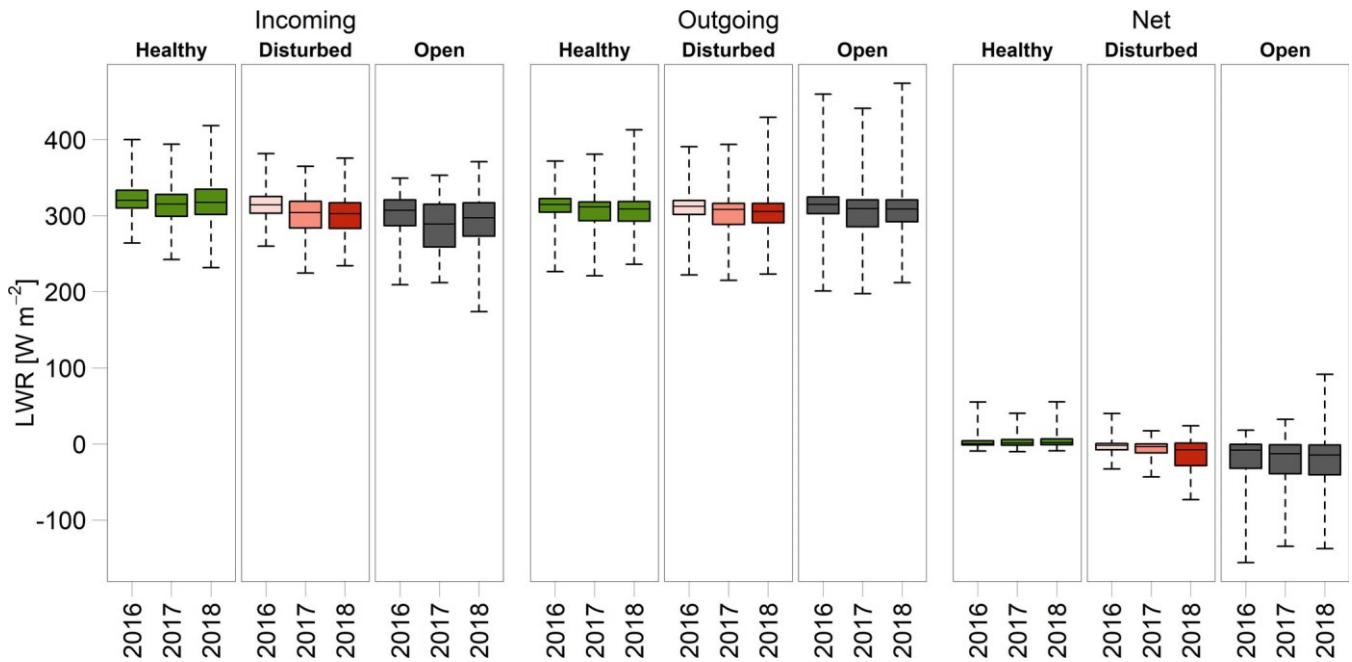


FIGURE 6 Variability in mean hourly incoming, outgoing and net longwave radiation (LWR) during seasons 2016, 2017 and 2018 at individual study sites. Boxes represent 25 and 75% percentile (with median as a black line) and whiskers represent interquartile ranges

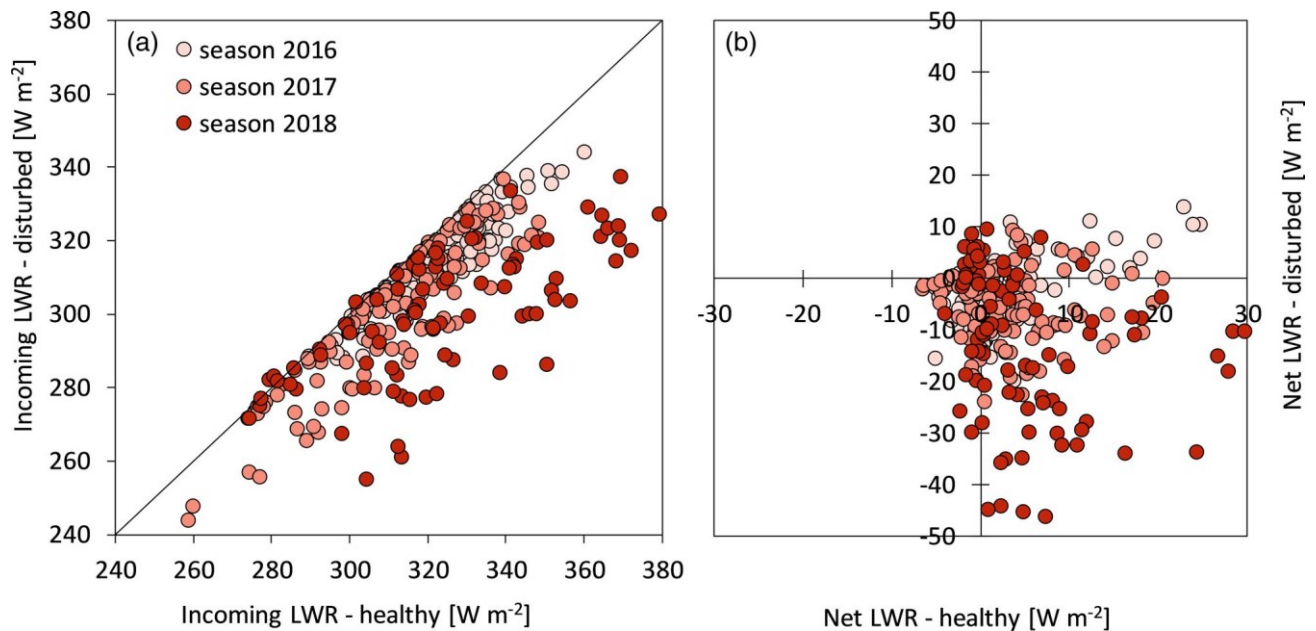


FIGURE 7 Mean daily incoming longwave radiation (LWR) (panel (a)) and mean daily net LWR (panel (b)) at the healthy forest and disturbed sites during seasons 2016, 2017 and 2018

Clear sky emission was considerably lower in this case and thus LWR emitted by vegetation was dominant. The positive values of net LWR in forested sites show only small differences between day and night with somewhat higher emission during the day (Figure 8). In contrast, diurnal variations can be seen for negative values of net LWR at the open site with minimum values from early morning (before sunrise) to approximately early afternoon.

3.3 | Relative contribution of energy fluxes to the snowpack energy balance

The measured SWR, LWR and other meteorological variables were used to calculate the snowpack energy balance at individual sites using equations described in Section 2.2. The individual bar plots in Figure 9 summarize mean daily contribution of SWR, LWR, sensible

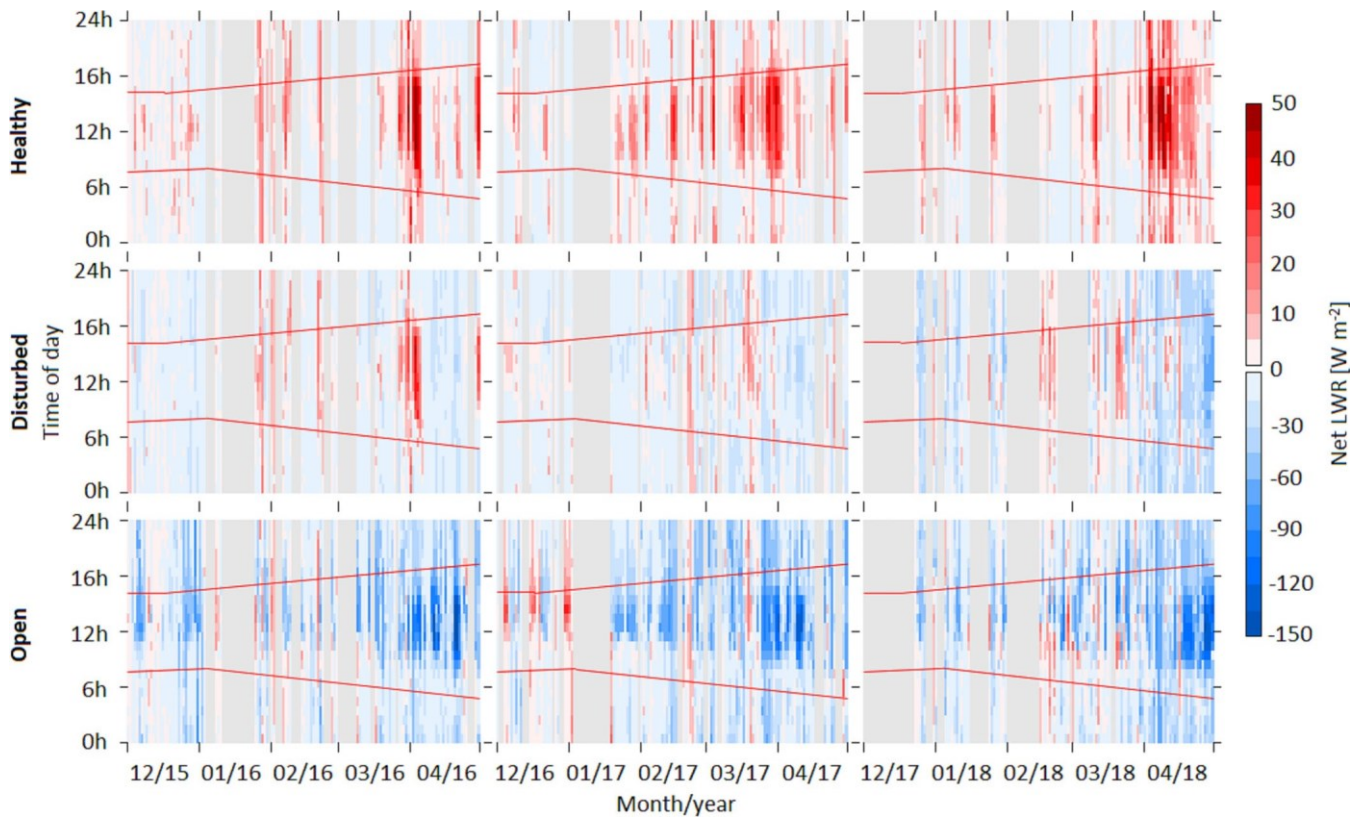


FIGURE 8 Variability in net longwave radiation (LWR) at the healthy forest site (top panels), disturbed forest site (middle panels) and open site (bottom panels), during seasons 2016, 2017 and 2018. Red lines represent time of sunrise and sunset. Grey colour represents missing data. Please note different scales for positive and negative legends

heat flux, latent heat flux, heat supplied by liquid precipitation on the snowpack, and ground heat flux.

The results showed that SWR was a major source of energy at the open site (55% of a sum of absolute values of all energy fluxes) and its intensity depended on the amount of solar radiation (Figure 9). Energy gained by the snowpack from SWR outweighed energy losses from LWR and latent heat during March and April. The total energy exchange at the open site reached higher values in absolute terms compared to healthy and disturbed forest sites, which led to faster snowmelt (see Section 3.4). The SWR at the healthy forest site was largely reduced by the shading effect of trees and represented only 23% of all energy fluxes for the study period. Therefore, LWR was the primary source of energy at the healthy forest site (41% of all energy fluxes on average during the study period, and up to 58% during warm and sunny April 2018) and thus significantly contributed to snowmelt.

The SWR increased both absolutely and relatively (from 49% in season 2017 to 59% of all energy fluxes in season 2018) at the disturbed forest site. In contrast, LWR contributed either positive or slightly negative component of the energy balance in season 2016 (only 7% of all energy fluxes) and then changed to a mostly negative contribution in season 2018 (27%) due to the gradual decay of trees at this plot.

The sensible heat flux represented a positive energy input for snowpack at all three sites (Figure 9). Larger energy gains occurred mainly in March and April, when air temperature differences between air and snowpack exceeded 10°C . The sensible heat flux represented from 8 to 12% of the snowpack energy balance at all three sites for the study period. The relative contribution of sensible heat decreased from 17% in season 2016 to 5% in season 2018 at the disturbed forest site.

The latent heat represented a negative energy output for snowpack at all three sites during the study period as it contributed on average from 10 to 16% of all energy fluxes (Figure 9). However, February 2018 showed even more than 50% contribution to the snowpack energy balance. Compared to other energy fluxes, any significant changes in relative values of latent heat at the disturbed forest site was not evident.

The heat from liquid precipitation represented a relatively small energy source for snowmelt as it contributed on average from 1 to 3% of the energy, with more than 8% during relatively rainy months with rain-on-snow events, for example, February 2016 (Figure 9). Similarly, ground heat flux formed on average 3% of snowpack energy balance at the open and disturbed forest sites, with a larger relative contribution at the healthy forest site (9%).

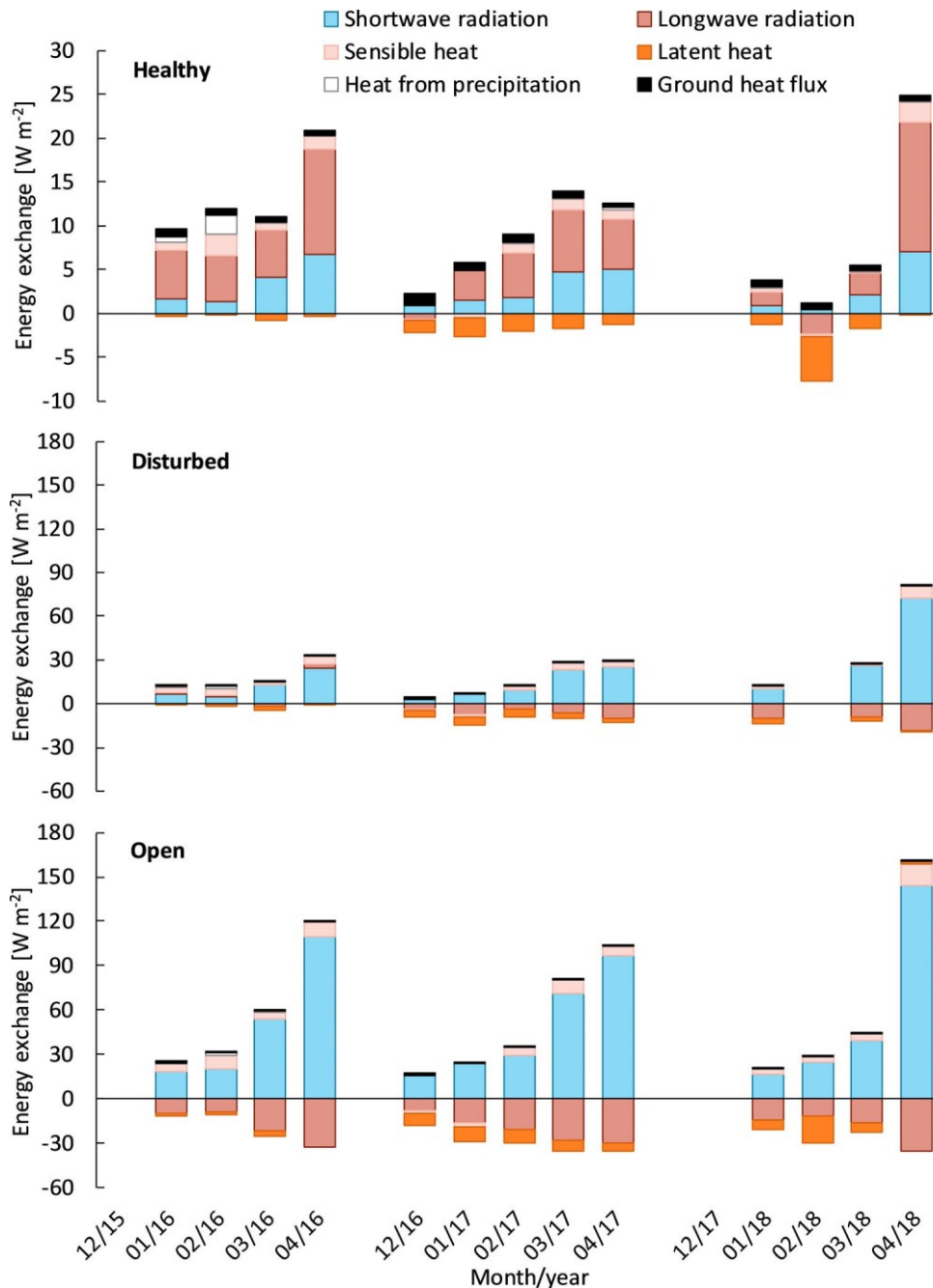


FIGURE 9 Mean daily energy fluxes to snowpack (positive fluxes) and from snowpack (negative fluxes) for individual months and seasons at the healthy forest site (top panel), disturbed forest site (middle panel) and open site (bottom panel). The energy fluxes cannot be calculated for 02/18 (disturbed forest) and for 12/15 and 12/17 (all sites) due to missing data. Note the different y-axis of the top panel

3.4 | Impact of changes in energy fluxes on snowmelt rates

Total heat Q_m calculated using Equation (1) was used to simulate snowmelt (Equation (6)) for the three study sites. The simulated snowmelt rates were compared with snowmelt rates calculated from observed SWE data (Equation (7)) measured at a small meadow 50 m from the open site. Simulated snowmelt rates overestimated the observed one by 67% (simulated median snowmelt rate reached 13.5 mm/day compared to the observed one which reached 8.1 mm/day) which was caused by different height and proximity of trees at both locations. At location with measured SWE, the surrounding trees

are higher and closer to the SWE sensor causing larger shading effects and thus slower snowmelt compared to the open site for which the snowmelt rates were simulated. Therefore, any direct comparison of the measured and simulated data is limited due to different energy balance. Nevertheless, the Spearman rank correlation r_s between simulated and observed snowmelt rates showed significant correlation ($r_s = 0.56$; p value $< .001$). Comparison of both observed and simulated SWE for main snowmelt periods is shown in Figure 11.

The largest snowmelt rates were calculated at the open site (Figure 10) where the median snowmelt rate reached 13.5 mm/day, while slower snowmelt was simulated at the disturbed forest site (median snowmelt rate 5.9 mm/day) and at the healthy forest site

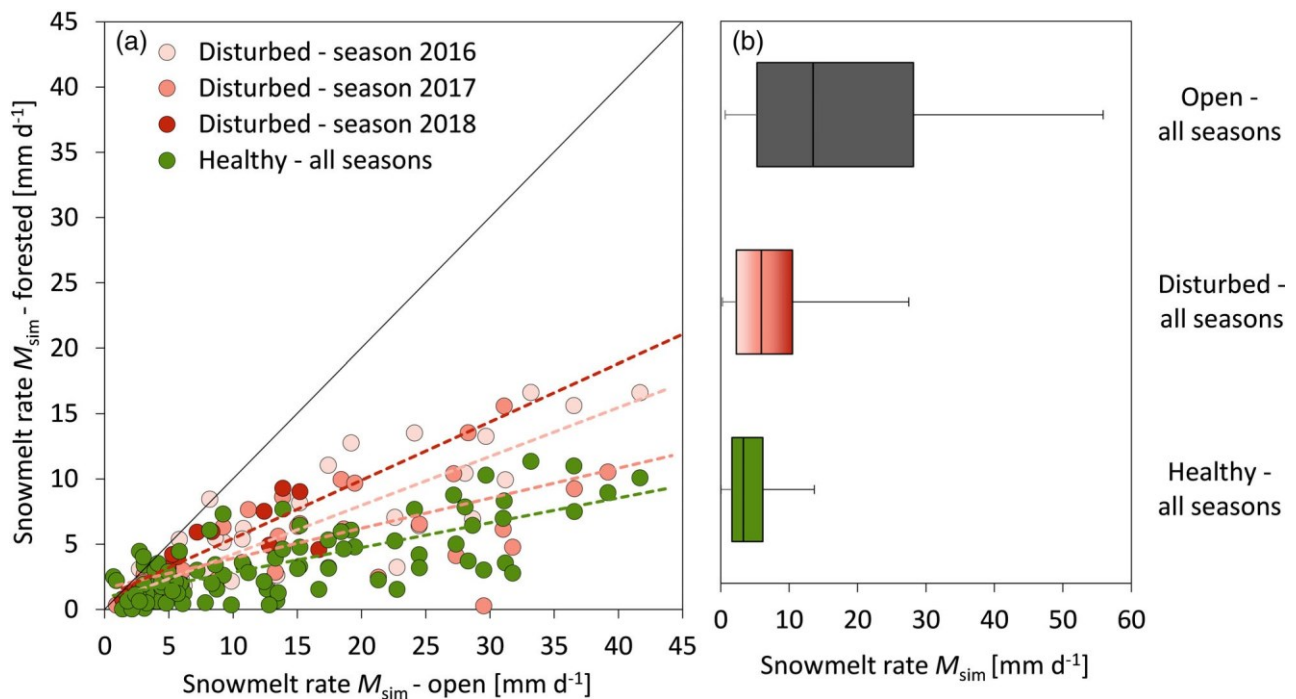


FIGURE 10 (a) Daily simulated snowmelt rates (M_{sim}) at forested sites compared to the open site during seasons 2016, 2017 and 2018. (b) Daily simulated snowmelt rates at individual study sites. Boxes represent 25 and 75% percentile (with the median shown as a black line in the box) and whiskers represent interquartile ranges

(median snowmelt rate 3.3 mm/day). The snowmelt rates at the disturbed forest site did not increase between the first and second year, but a significant increase occurred between the second and third year of the study period (Figure 10). Simulated snowmelt at the disturbed forest site was 1.6 times faster compared to snowmelt at the healthy forest site during the first season 2016 and 2.4 times faster than in the healthy forest site in the third season 2018 (which represents a relative increase by 50%). In general, the increase in snowmelt rates at the disturbed forest site during the study period was most likely caused by the increase in SWR due to forest decay (see Section 3.1) which was not compensated by increasing energy losses from LWR and latent heats. However, the missing consistent increase in snowmelt rates between the first and second year of the study period indicated the potentially important role of the meteorological conditions causing snowmelt at different years.

Simulated SWE during the main spring snowmelt periods in individual seasons illustrated how differently the snowpack energy balance influenced snowmelt dynamics and melt-out days at individual sites (Figure 11, top panels). Simulated SWE reflected generally lower snow storages in forested sites compared to the open area at the beginning of the snowmelt period which was caused mainly by snow interception. These different initial snow storages caused relatively small differences in simulated melt-out days for the study periods. The results showed that snow melted earlier at the open site due to higher snowmelt rates, despite the fact that the initial SWE was higher compared to the forested sites. Snow melted later at the disturbed forest site compared to the open site which indicates slower

snowmelt at the disturbed forest site due to still having some shading effect from decayed trees. Snowmelt at the disturbed forest site accelerated in season 2018 due to further forest decline.

Figure 11 shows the relative contribution of the individual energy fluxes to snowmelt rates during the main snowmelt periods (whereby only positive fluxes which contributed to snowmelt were considered). On average, SWR and turbulent fluxes together represented 99% of the total contribution to snowmelt at the open site (SWR contributed by 87%, turbulent fluxes by 12%). LWR contributed only 1% to snowmelt as it mostly represented a negative component of the snowpack energy balance. In contrast, SWR and LWR represented 37 and 48% of the total snowmelt contribution at the healthy forest site during the three snowmelt periods and other turbulent fluxes contributed on average by 15% to snowmelt. At the disturbed forest site, SWR represented 80% of the snowmelt rates, with an increase from 67% in season 2016 to 87% in season 2018, as the trees decayed and the site became more open to SWR. LWR represented only a minor contribution (4%) to snowmelt rates, with a decrease from 11% in season 2016 to 3% in seasons 2017 and 2018.

The ground heat flux and heat supplied by rain contributed together 2% and thus represented rather minor contributions to snowmelt rates. For the rain heat input, however, the contribution was much larger during rainy days. For example, on March 18, 2017, the rain contributed from 13 to 29% to the total snowmelt indicating that this heat input is important for snowmelt generation at lower temporal resolutions.

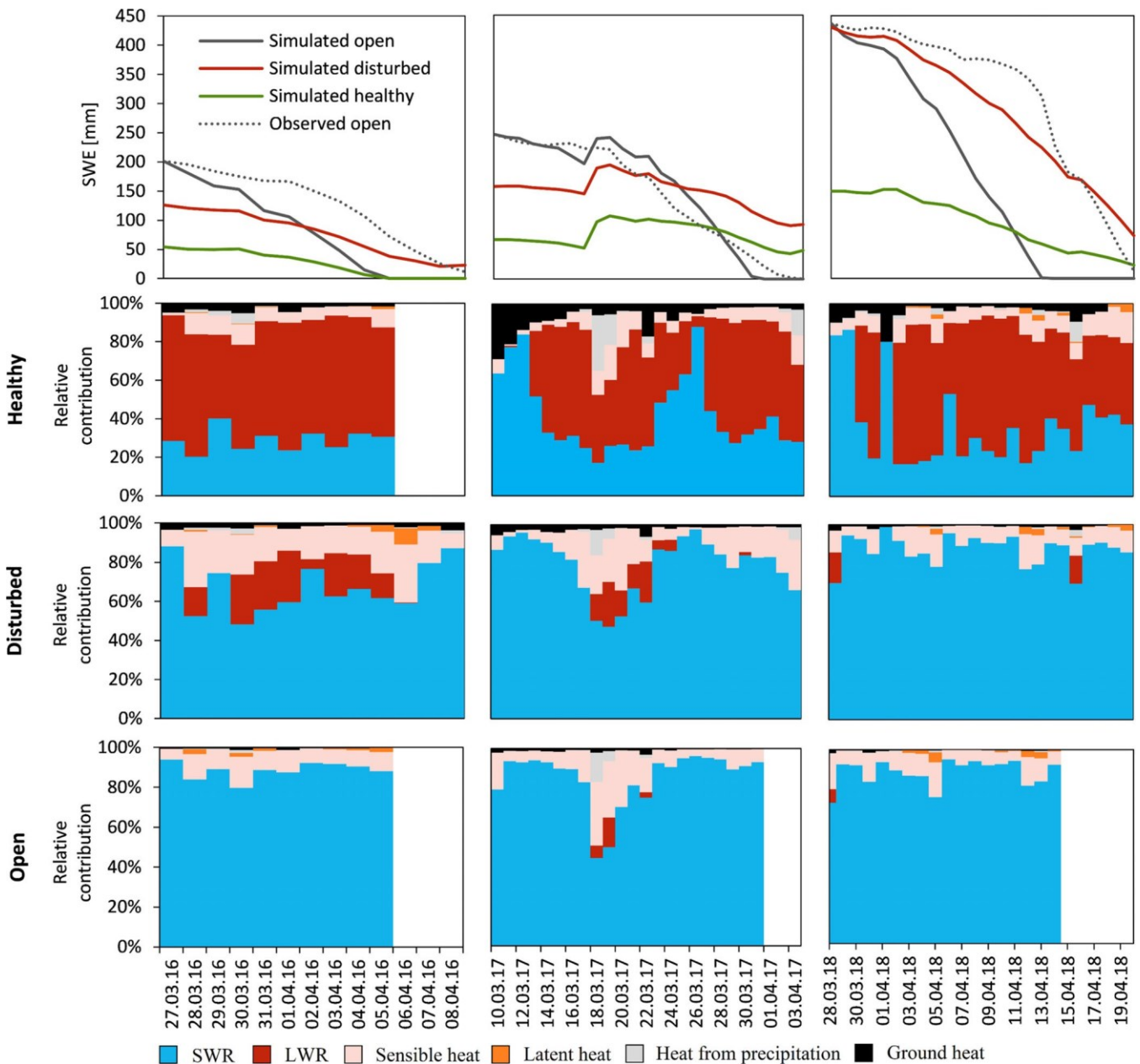


FIGURE 11 Simulated SWE at individual study sites and observed SWE at a nearby open meadow during the main spring snowmelt periods in seasons 2016, 2017 and 2018 (first line panels). Relative daily contribution of individual energy fluxes to snowmelt rates at the healthy forest site (second line panels), disturbed forest site (third line panels) and open site (fourth line panels)

4 | DISCUSSION

4.1 | Contribution of radiation fluxes to the snowpack energy balance

The sampling design adopted in this study enabled the most important energy balance components in hourly, daily and seasonal resolution to be analysed. The attenuation of incoming SWR due to tree shading, on average by 93%, corresponded to results of a previous study performed for the same study area over a partly different time period

(Jenicek et al., 2017). Although several studies reported lower SWR reduction (by around 80% in coniferous forest compared to open areas; Courbaud et al., 2003; Ellis et al., 2011), any comparison is always difficult due to the unique character of vegetation at individual locations, especially at forested environment, where the variability in SWR and snow is usually larger than in open areas (Ellis & Pomeroy, 2007; Musselman et al., 2015). At our study sites, we described the canopy structure by calculating LAI for 25 × 25 m rectangle around the radiometers. The LAI values ranged from 0.71 to 5.0 (mean 2.6) for the healthy forest site and from 0.21 to 1.86 (mean 1.1

in 2015 and 0.84 in 2017) for the disturbed forest site. This indicates that the site variability in individual radiative fluxes can be large and any generalization is always difficult.

The incoming and net LWR showed significant diurnal, seasonal, and year-to-year variations because the amount of LWR is primarily driven by meteorological conditions and the density of canopy structure. While the only source of SWR is the sun, LWR is emitted by the atmosphere, snowpack, snow-free ground and surrounding vegetation. In our sampling design, it was not possible to fully separate LWR emitted by the atmosphere and LWR emitted by vegetation since our reference measurement at the open site also captured a little LWR from surrounding vegetation (mainly small trees up to 5 m height, located around 10–15 m from the radiometer). However, we consider this effect as rather negligible. Therefore, all differences between LWR at both forest sites compared to the open site may be related to changes in vegetation structure.

Net LWR at the healthy forest site reached comparable values to those found by Webster et al. (2016). At the open site, negative net LWR was measured which corresponds to results presented by Helgason and Pomeroy (2012). In general, results clearly showed that denser forest is connected with higher LWR as a source of the energy, which is in line with findings of previous studies (Klos & Link, 2018; Malle et al., 2019).

The diurnal and seasonal variability in SWR and LWR at study sites was affected by actual meteorological conditions during individual days, which made interpretation of SWR changes between the three study seasons more difficult. This was especially important when separating the effect of changing canopy from changing weather conditions at the disturbed forest site during the study period. However, since weather conditions above the canopy were constant for all sites on a specific day (all selected sites are located close to each other on a flat terrain of the same elevation), any temporal changes in energy balance components during the study period may be related to vegetation changes in those locations. Therefore, the canopy structure was considered to be the main control driving the sub-canopy SWR budget, as also documented by several related studies (Malle et al., 2019; Marks, Domingo, Susong, Link, & Garen, 1999).

The measured radiation data represent point information reflecting the canopy structure above the radiometers (see Section 2.1). This was important at both forested sites with relatively higher variability of the canopy structure compared to the open site. Therefore, measured data may be affected by the specific position of the sensor. Thus, although our results represent the study area, the upscaling to the catchment scale is rather limited. Uncertainty resulting from the fixed position of the radiometers may be reduced by measuring at even more locations with different forest structure or by using a moving sensor as used by Stähli et al. (2009) or by Malle et al. (2019). However, such an experimental set-up usually requires large and costly construction, which was not possible in our study area situated in the most protected zone of the Sumava National Park. Nevertheless, since we were focused mainly on relative changes in individual energy balance components between study sites, we

believe that using point measurements for our analysis is still an acceptable simplification.

4.2 | Contribution of turbulent fluxes to the snowpack energy balance

The calculation of sensible and latent heat fluxes partly reflected different meteorological conditions at individual sites since air temperature was measured separately at all sites. Thus, the resulting energy budget reflected different sub-canopy air temperatures. However, the wind speed and air humidity were measured at nearby meteorological stations placed in an open area and thus they do not account for vegetation. Therefore, attenuation coefficients were applied for wind speed to reflect sub-canopy wind conditions, based on their relation to LAI as presented in Tarboton and Luce (1996). The attenuation coefficients were also compared with earlier tests performed at the study sites (Matejka & Jenicek, 2015). Therefore, both sensible and latent heat fluxes need to be considered as additional information for the entire snowpack energy balance, with limited applicability in different areas. Nevertheless, relative proportions of individual energy balance components are comparable with values presented in other studies (Andreadis, Storck, & Lettenmaier, 2009; Koivusalo & Kokkonen, 2002).

Heat from liquid precipitation added rather negligible additional energy to the snowpack at seasonal level, as also reported by other studies (Mazurkiewicz, Callery, & McDonnell, 2008). This was because there was no extreme rain-on-snow event which would supply a significant amount of liquid water into the snowpack. However, this heat exchange might be important when assessing the energy balance at daily and shorter temporal resolutions (Juras, Würzer, Pavlasek, Vitvar, & Jonas, 2017; Würzer et al., 2016). In general, rain input might be a significant heat flux for basins with air temperature fluctuating near the freezing point during winter months and thus rain events occur more often. However, we can expect an increasing importance of rain input for the future in a warming climate when more precipitation will fall as rain rather than snow (Jenicek, Seibert, & Staudinger, 2018; Musselman et al., 2018; Sezen, Sraj, Medved, & Bezak, 2020).

Ground heat flux generally represented a relatively minor energy source for snowmelt during snow accumulation due to relatively low heat conductivity of soils (Li et al., 2019). Nevertheless, ground heat flux can become relatively more important at the end of the snow season when SWR transmission to the soil is enabled due to only partial snow cover (Lund et al., 2017). Our results showed only a small effect of ground heat flux on snowmelt which, in absolute terms, does not differ between study sites due to applying the same soil temperatures for all study sites.

Although all simplifications made in turbulent fluxes calculations might affect the absolute values of the individual energy balance components, they did not affect the overall day-by-day variability at the specific location and site-by-site variability between locations which was the main focus of our study.

4.3 | Consequences for snowmelt

Spatiotemporal changes in the snowpack energy balance under the forest canopy are further important to govern snowmelt both at local and catchments scales (Burles & Boon, 2011; Ellis et al., 2011; Jenicek, Pevna, & Matejka, 2018). Consequently, changes in snowmelt dynamics and timing may directly affect runoff from the catchment (Pomeroy et al., 2012; Schelker, Kuglerova, Eklöf, Bishop, & Laudon, 2013). Our study showed that differences in snowmelt dynamics between individual plots may be mostly linked to differences in SWR, LWR and, with minor importance, to the sensible and latent heat fluxes. Higher simulated snowmelt rates occurred at the open site compared to the forested sites, largely due to a higher SWR. However, the difference may seem to be more significant than presented in other studies (Gelfan, Pomeroy, & Kuchment, 2004; Lundquist et al., 2013). Some uncertainties may result from a calculation of total heat for the individual sites, as the presented energy balance approach requires specific datasets which have limited availability. This resulted in high absolute error between observed and simulated snowmelt rates, which was caused by different location of sensor used to measure SWE and sensors used to calculate the snowpack energy balance (see Figure 1 for locations). The mentioned different position resulted in different SWR and LWR balance since both open sites are affected by surrounding trees resulting in different shading effects.

The results of snowmelt also rely on the accuracy of parameter B (Equation (8)), representing the snowpack thermal quality. This parameter was calculated from measured L_{wc} and ranged from 0.75 to 1.06 according to the state of the snow ripening process (DeWalle & Rango, 2008). At the disturbed forest site, the contribution of individual components to the entire energy balance changed significantly both relatively and absolutely during the study period due to the gradual forest decay and event-based windstorms after the bark beetle infestation. The major change was the increase in SWR during the study period which substantially increased the contribution of this flux to the snowpack energy balance. In contrast, net LWR decreased during the study period and became mainly a negative flux in the last study season. Nevertheless, the increase in net SWR was more important than a decrease in net LWR and thus the snowmelt accelerated over the study period, as also reported by (Burles & Boon, 2011).

Forest disturbance led to important changes in snowmelt processes which might further affect runoff conditions, especially spring runoff (Schelker et al., 2013). Additionally to all these changes, ongoing climate change might further underline the effect of land cover changes on runoff (Blahusiakova et al., 2020; Langhammer et al., 2015). However, the faster snowmelt does not necessarily mean that total runoff or flood peaks would be higher as documented, for example, by Pomeroy et al. (2012) in their study sites affected by the pine beetle infestation.

Dense forest also delays seasonal snowmelt and melt-out, which usually occurs from one, up to 3 weeks later compared to more open areas such as large meadows and clearings (Link & Marks, 1999;

Lundquist et al., 2013), which is in agreement with our simulated SWE decrease in season 2017 and 2018. In contrast, melt-out day occurred earlier at the healthy forest site in season 2016. This was caused by generally lower snow storages at the forest site than at the open site. In general, our results showed rather small differences in melt-out days at individual sites (up to several days), which corresponds to findings presented by Bartik et al. (2019).

5 | CONCLUSION

We analysed temporal variability in SWR and LWR based on data from radiometers located at three sites with different canopy structure in a mountain catchment in the Bohemian Forest, Czechia. We were particularly interested in changes in SWR and LWR during forest disturbance due to the bark beetle and windstorms. Based on the results, we can draw the following conclusions:

The SWR was the major source of energy at the open site, especially by the end of the winter season. In the dense coniferous forest, the measured net SWR represented only 7% of the amount at the open site due to tree shading. In contrast, net LWR was the dominant source of energy at the healthy forest site (on average 41% of all energy fluxes) and thus contributed most to snowmelt. However, the resulting snowmelt rates were lower in the forest than in the open area since the higher LWR in the forest did not compensate for the lower SWR.

The results showed significant differences in the relative LWR contribution to the entire snowpack energy balance. LWR was generally positive at the forest site (representing an energy gain) and mostly negative at the open site (representing an energy loss). Therefore, using snow energy balance models to enable accounting for LWR is advisable for snowmelt runoff simulations especially in small forested catchments.

The differences in energy balance at the study sites resulted in different snowmelt rates. The largest simulated snowmelt rates occurred at the open site (median snowmelt rate 13.5 mm/day). The modelled snowmelt was significantly slower at the disturbed forest site (median snowmelt rate 5.9 mm/day) and at the healthy forest site (median snowmelt rate 3.3 mm/day).

The progressive decay of disturbed forest caused a significant change in both SWR and LWR during the study period. The mean net LWR decreased from -3.1 W/m^2 to -12.9 W/m^2 and the mean net SWR increased from 31.6 W/m^2 to 96.2 W/m^2 during the study period as the site became more open to solar radiation. The changes in the energy balance at the disturbed forest site caused the increase in snowmelt rates by 50% relative to the healthy forest site during the study period. This might have important implications for runoff from catchments affected by land cover changes due to either human activity or climate change.

Our results showed that changes in individual energy balance components after forest disturbance led to important consequences in snowmelt rates which might further affect the seasonal distribution of runoff in spring. However, our results are rather limited to the

specific study area and may not be easily generalized. Nevertheless, our findings may contribute to improve the process understanding, which is further important to improve snowmelt and catchment runoff models.

ACKNOWLEDGEMENTS

Meteorological data for this study were measured at stations operated by the Charles University, Department of Physical Geography and Geoecology and are available from the corresponding author upon request. Support from the Czech Science Foundation (project no. 18-06217Y, Influence of seasonal snowpack on summer low flows: Climate change implications on hydrological drought) and from the Charles University Grant Agency (project no. GAUK 272119, Modelling of future effects of changes in snow storages on occurrence and extremity of runoff caused by rain-on-snow events) is gratefully acknowledged. Many thanks are due to Tracy Ewen for improving the language.

AUTHOR CONTRIBUTIONS

Both authors together have contributed to conception and design, or acquisition of data, or analysis and interpretation of data, been involved in drafting the manuscript or revising it critically for important intellectual content, given final approval of the version to be published. Both authors have participated sufficiently in the work to take public responsibility for appropriate portions of the content and agreed to be accountable for all aspects of the work.

DATA AVAILABILITY STATEMENT

Meteorological data for this study were measured at stations operated by the Charles University, Department of Physical Geography and Geoecology. These data that support the findings of this study are available from the corresponding author upon reasonable request.

ORCID

Ondrej Hotovy  <https://orcid.org/0000-0002-3587-1725>

Michal Jenicek  <https://orcid.org/0000-0002-1103-0403>

REFERENCES

- Andreadis, K. M., Storck, P., & Lettenmaier, D. P. (2009). Modeling snow accumulation and ablation processes in forested environments. *Water Resources Research*, 45(5), W05429. <https://doi.org/10.1029/2008WR007042>
- Assaf, H. (2007). Development of an energy-budget snowmelt updating model for incorporating feedback from snow course survey measurements. *Journal of Engineering, Computing and Architecture*, 1(1), 1-25.
- Bartik, M., Holko, L., Janco, M., Skvarenina, J., Danko, M., & Kostka, Z. (2019). Influence of mountain spruce forest dieback on snow accumulation and melt. *Journal of Hydrology and Hydromechanics*, 67(1), 59-69. <https://doi.org/10.2478/johh-2018-0022>
- Blahusiakova, A., Matouskova, M., Jenicek, M., Ledvinka, O., Kliment, Z., Podolinska, J., & Snopkova, Z. (2020). Snow and climate trends and their impact on seasonal runoff and hydrological drought types in selected mountain catchments in Central Europe. *Hydrological Sciences Journal*, 65(12), 2083-2096. <https://doi.org/10.1080/02626667.2020.1784900>
- Broxton, P. D., Harpold, A. A., Biederman, J. A., Troch, P. A., Molotch, N. P., & Brooks, P. D. (2015). Quantifying the effects of vegetation structure on snow accumulation and ablation in mixed-conifer forests. *Ecohydrology*, 8(6), 1073-1094. <https://doi.org/10.1002/eco.1565>
- Burles, K., & Boon, S. (2011). Snowmelt energy balance in a burned forest plot, Crownsnest Pass, Alberta, Canada. *Hydrological Processes*, 25(19), 3012-3029. <https://doi.org/10.1002/hyp.8067>
- Cline, D. W. (1997). Snow surface energy exchanges and snowmelt at a continental, midlatitude Alpine site. *Water Resources Research*, 33(4), 689-701. <https://doi.org/10.1029/97WR00026>
- Courbaud, B., De Coligny, F., & Cordonnier, T. (2003). Simulating radiation distribution in a heterogeneous Norway spruce forest on a slope. *Agricultural and Forest Meteorology*, 116(1-2), 1-18. [https://doi.org/10.1016/S0168-1923\(02\)00254-X](https://doi.org/10.1016/S0168-1923(02)00254-X)
- DeWalle, D. R., & Rango, A. (2008). *Principles of snow hydrology*. Cambridge: Cambridge University Press.
- Ellis, P. J. W., Essery, R. L. H., & Link, T. E. (2011). Effects of needleleaf forest cover on radiation and snowmelt dynamics in the Canadian Rocky Mountains. *Canadian Journal of Forest Research*, 41(3), 608-620. <https://doi.org/10.1139/X10-227>
- Ellis, C. R., & Pomeroy, J. W. (2007). Estimating sub-canopy shortwave irradiance to melting snow on forested slopes. *Hydrological Processes*, 21, 2581-2593. <https://doi.org/10.1002/hyp.6794>
- Essery, R., Pomeroy, J., Ellis, C., & Link, T. (2008). Modelling longwave radiation to snow beneath forest canopies using hemispherical photography or linear regression. *Hydrological Processes*, 22(15), 2788-2800. <https://doi.org/10.1002/hyp.6930>
- Förster, K., Garvelmann, J., Meißl, G., & Strasser, U. (2018). Modelling forest snow processes with a new version of WaSiM. *Hydrological Sciences Journal*, 63(10), 1540-1557. <https://doi.org/10.1080/02626667.2018.1518626>
- Frazer, G., Canham, C., & Lertzman, K. (1999). Gap Light Analyzer (GLA): Version 2.0: Imaging software to extract canopy structure and gap light transmission indices from true-colour fisheye photographs, users manual and program documentation. 4887176.
- Garvelmann, J., Pohl, S., & Weiler, M. (2015). Spatio-temporal controls of snowmelt and runoff generation during rain-on-snow events in a mid-latitude mountain catchment. *Hydrological Processes*, 29(17), 3649-3664. <https://doi.org/10.1002/hyp.10460>
- Gelfan, A. N., Pomeroy, J. W., & Kuchment, L. S. (2004). Modeling forest cover influences on snow accumulation, sublimation, and melt. *Journal of Hydrometeorology*, 5(5), 785-803. [https://doi.org/10.1175/1525-7541\(2004\)005<0785:MFCIOS>2.0.CO;2](https://doi.org/10.1175/1525-7541(2004)005<0785:MFCIOS>2.0.CO;2)
- Gouttevin, I., Lehning, M., Jonas, T., Gustafsson, D., & Mölder, M. (2015). A two-layer canopy model with thermal inertia for an improved snowpack energy balance below needleleaf forest (model SNOWPACK, version 3.2.1, revision 741). *Geoscientific Model Development*, 8(8), 2379-2398. <https://doi.org/10.5194/gmd-8-2379-2015>
- Heggli, A. (2013). Data Analysis of the Snow Pack Analysing System Tested by UCAR. Western Snow Conference, pp. 842-845.
- Helbig, N., Moeser, D., Teich, M., Vincent, L., Lejeune, Y., Sicart, J.-E., & Monnet, J.-M. (2019). Snow processes in mountain forests: Interception modeling for coarse-scale applications. *Hydrology and Earth System Sciences Discussions*, 24, 1-24. <https://doi.org/10.5194/hess-2019-348>
- Helgason, W., & Pomeroy, J. W. (2012). Problems closing the energy balance over a homogeneous snow cover during midwinter. *Journal of Hydrometeorology*, 13(2), 557-572. <https://doi.org/10.1175/JHM-D-11-0135.1>
- Hock, R. (2003). Temperature index melt modelling in mountain areas. *Journal of Hydrology*, 282(1-4), 104-115. [https://doi.org/10.1016/S0022-1694\(03\)00257-9](https://doi.org/10.1016/S0022-1694(03)00257-9)
- Iziomon, M. G., Mayer, H., & Matzarakis, A. (2003). Downward atmospheric longwave irradiance under clear and cloudy skies: Measurement and parameterization. *Journal of Atmospheric and Solar-Terrestrial*

- Physics*, 65(10), 1107-1116. <https://doi.org/10.1016/j.jastp.2003.07.007>
- Jenicek, M., Hotovy, O., & Matejka, O. (2017). Snow accumulation and ablation in different canopy structures at a plot scale: Using degree-day approach and measured shortwave radiation. *Acta Universitatis Carolinae, Geographica*, 52(1), 61-72. <https://doi.org/10.14712/23361980.2017.5>
- Jenicek, M., Pevna, H., & Matejka, O. (2018). Canopy structure and topography effects on snow distribution at a catchment scale: Application of multivariate approaches. *Journal of Hydrology and Hydromechanics*, 66(1), 43-54. <https://doi.org/10.1515/johh-2017-0027>
- Jenicek, M., Seibert, J., & Staudinger, M. (2018). Modeling of future changes in seasonal snowpack and impacts on summer low flows in Alpine catchments. *Water Resources Research*, 54(1), 538-556. <https://doi.org/10.1002/2017WR021648>
- Juras, R., Würzler, S., Pavlasek, J., Vitvar, T., & Jonas, T. (2017). Rainwater propagation through snowpack during rain-on-snow sprinkling experiments under different snow conditions. *Hydrology and Earth System Sciences*, 21(9), 4973-4987. <https://doi.org/10.5194/hess-21-4973-2017>
- Klos, P. Z., & Link, T. E. (2018). Quantifying shortwave and longwave radiation inputs to headwater streams under differing canopy structures. *Forest Ecology and Management*, 407, 116-124. <https://doi.org/10.1016/j.foreco.2017.10.046>
- Koivusalo, H., & Kokkonen, T. (2002). Snow processes in a forest clearing and in a coniferous forest. *Journal of Hydrology*, 262(1-4), 145-164. [https://doi.org/10.1016/S0022-1694\(02\)00031-8](https://doi.org/10.1016/S0022-1694(02)00031-8)
- Langhammer, J., Su, Y., & Bernsteinova, J. (2015). Runoff response to climate warming and forest disturbance in a mid-mountain basin. *Water*, 7(7), 3320-3342. <https://doi.org/10.3390/w7073320>
- Lendziach, T., Langhammer, J., & Jenicek, M. (2019). Estimating snow depth and leaf area index based on UAV digital photogrammetry. *Sensors*, 19(5), 1027. <https://doi.org/10.3390/S19051027>
- Li, R., Zhao, L., Wu, T., Wang, Q., Ding, Y., Yao, J., et al. (2019). Soil thermal conductivity and its influencing factors at the Tanggula permafrost region on the Qinghai-Tibet Plateau. *Agricultural and Forest Meteorology*, 264, 235-246. <https://doi.org/10.1016/j.agrformet.2018.10.011>
- Link, T. E., & Marks, D. (1999). Distributed simulation of snowcover mass and energy balance in the boreal forest. *Hydrological Processes*, 13, 2439-2452. [https://doi.org/10.1002/\(SICI\)1099-1085\(199910\)13:14/15<2439::AID-HYP866>3.0.CO;2-1](https://doi.org/10.1002/(SICI)1099-1085(199910)13:14/15<2439::AID-HYP866>3.0.CO;2-1)
- Lund, M., Stiegler, C., Abermann, J., Citterio, M., Hansen, B. U., & van As, D. (2017). Spatiotemporal variability in surface energy balance across tundra, snow and ice in Greenland. *Ambio*, 46(1), 81-93. <https://doi.org/10.1007/s13280-016-0867-5>
- Lundquist, J. D., Dickerson-Lange, S. E., Lutz, J. A., & Cristea, N. C. (2013). Lower forest density enhances snow retention in regions with warmer winters: A global framework developed from plot-scale observations and modeling. *Water Resources Research*, 49(10), 6356-6370. <https://doi.org/10.1002/wrcr.20504>
- Malle, J., Rutter, N., Mazzotti, G., & Jonas, T. (2019). Shading by trees and fractional snow cover control the sub-canopy radiation budget. *Journal of Geophysical Research: Atmospheres*, 124, 3195-3207. <https://doi.org/10.1029/2018jd029908>
- Marks, D., Domingo, J., Susong, D., Link, T. E., & Garen, D. (1999). A spatially distributed energy balance snowmelt model for application in mountain basins. *Hydrological Processes*, 13(12-13), 1935-1959. [https://doi.org/10.1002/\(SICI\)1099-1085\(199909\)13:12/13<1935::AID-HYP868>3.0.CO;2-C](https://doi.org/10.1002/(SICI)1099-1085(199909)13:12/13<1935::AID-HYP868>3.0.CO;2-C)
- Matejka, O., & Jenicek, M. (2015). An energy-based model accounting for snow accumulation and snowmelt in a coniferous forest and in an open area. In *Voda a Krajina*, pp. 67-80. Available from <http://storm.fsv.cvut.cz>
- Mazurkiewicz, A. B., Callery, D. G., & McDonnell, J. J. (2008). Assessing the controls of the snow energy balance and water available for runoff in a rain-on-snow environment. *Journal of Hydrology*, 354(1-4), 1-14. <https://doi.org/10.1016/j.jhydrol.2007.12.027>
- McKenzie, J. M., Siegel, D. I., Rosenberry, D. O., Glaser, P. H., & Voss, C. I. (2007). Heat transport in the Red Lake Bog, Glacial Lake Agassiz Peatlands. *Hydrological Processes*, 21(3), 369-378. <https://doi.org/10.1002/hyp.6239>
- Moeser, D., Mazzotti, G., Helbig, N., & Jonas, T. (2016). Representing spatial variability of forest snow: Implementation of a new interception model. *Water Resources Research*, 52(2), 1208-1226. <https://doi.org/10.1002/2015WR017961>
- Musselman, K. N., Lehner, F., Ikeda, K., Clark, M. P., Prein, A. F., Liu, C., ... Rasmussen, R. (2018). Projected increases and shifts in rain-on-snow flood risk over western North America. *Nature Climate Change*, 8(9), 808-812. <https://doi.org/10.1038/s41558-018-0236-4>
- Musselman, K. N., & Pomeroy, J. W. (2017). Estimation of needleleaf canopy and trunk temperatures and longwave contribution to melting snow. *Journal of Hydrometeorology*, 18(2), 555-572. <https://doi.org/10.1175/jhm-d-16-0111.1>
- Musselman, K. N., Pomeroy, J. W., & Link, T. E. (2015). Variability in shortwave irradiance caused by forest gaps: Measurements, modelling, and implications for snow energetics. *Agricultural and Forest Meteorology*, 207, 69-82. <https://doi.org/10.1016/j.agrformet.2015.03.014>
- Pomeroy, J., Fang, X., & Ellis, C. (2012). Sensitivity of snowmelt hydrology in Marmot Creek, Alberta, to forest cover disturbance. *Hydrological Processes*, 26(12), 1892-1905. <https://doi.org/10.1002/hyp.9248>
- Pugh, E. T., & Small, E. E. (2013). The impact of beetle-induced conifer death on stand-scale canopy snow interception. *Hydrology Research*, 44(4), 644-657. <https://doi.org/10.2166/nh.2013.097>
- Reid, T. D., Essery, R. L. H., Rutter, N., & King, M. (2014). Data-driven modelling of shortwave radiation transfer to snow through boreal birch and conifer canopies. *Hydrological Processes*, 28(6), 2987-3007. <https://doi.org/10.1002/hyp.9849>
- Roth, T. R., & Nolin, A. W. (2017). Forest impacts on snow accumulation and ablation across an elevation gradient in a temperate montane environment. *Hydrology and Earth System Sciences*, 21(11), 5427-5442. <https://doi.org/10.5194/hess-21-5427-2017>
- Schelker, J., Kuglerova, L., Eklöf, K., Bishop, K., & Laudon, H. (2013). Hydrological effects of clear-cutting in a boreal forest—Snowpack dynamics, snowmelt and streamflow responses. *Journal of Hydrology*, 484, 105-114. <https://doi.org/10.1016/j.jhydrol.2013.01.015>
- Sezen, C., Sraj, M., Medved, A., & Bezak, N. (2020). Investigation of rain-on-snow floods under climate change. *Applied Sciences (Switzerland)*, 10(4), 1242. <https://doi.org/10.3390/app10041242>
- Singh, P., & Singh, V. P. (2001). *Snow and glacier hydrology*. London: Springer Science & Business Media. <https://doi.org/10.1029/01EO00355>
- Stähli, M., Jonas, T., & Gustafsson, D. (2009). The role of snow interception in winter-time radiation processes of a coniferous sub-alpine forest. *Hydrological Processes*, 23, 2498-2512. <https://doi.org/10.1002/hyp.7180>
- Su, Y., Langhammer, J., & Jarsjö, J. (2017). Geochemical responses of forested catchments to bark beetle infestation: Evidence from high frequency in-stream electrical conductivity monitoring. *Journal of Hydrology*, 550, 635-649. <https://doi.org/10.1016/j.jhydrol.2017.05.035>
- Tarboton, D. G., & Luce, C. H. (1996). Utah energy balance snow accumulation and melt model (UEB). Available from <http://www.engineering.usu.edu/dtarb/>
- Varhola, A., Coops, N. C., Alila, Y., & Weiler, M. (2014). Exploration of remotely sensed forest structure and ultrasonic range sensor metrics to improve empirical snow models. *Hydrological Processes*, 28(15), 4433-4448. <https://doi.org/10.1002/hyp.9952>
- Webster, C., Rutter, N., Zahner, F., & Jonas, T. (2016). Modeling subcanopy incoming longwave radiation to seasonal snow using air and tree trunk

- temperatures. *Journal of Geophysical Research: Atmospheres*, 121, 1220-1235. <https://doi.org/10.1002/2015JD024099>
- Welch, C. M., Stoy, P. C., Rains, F. A., Johnson, A. V., & McGlynn, B. L. (2016). The impacts of mountain pine beetle disturbance on the energy balance of snow during the melt period. *Hydrological Processes*, 30(4), 588-602. <https://doi.org/10.1002/hyp.10638>
- Würzer, S., Jonas, T., Wever, N., & Lehning, M. (2016). Influence of initial snowpack properties on runoff formation during rain-on-snow events. *Journal of Hydrometeorology*, 17(6), 1801-1815. <https://doi.org/10.1175/JHM-D-15-0181.1>
- Zheng, Z., Kirchner, P. B., & Bales, R. C. (2016). Topographic and vegetation effects on snow accumulation in the southern Sierra Nevada: A statistical summary from lidar data. *The Cryosphere*, 10(1), 257-269. <https://doi.org/10.5194/tc-10-257-2016>

How to cite this article: Hotovy O, Jenicek M. The impact of changing subcanopy radiation on snowmelt in a disturbed coniferous forest. *Hydrological Processes*. 2020;1-17. <https://doi.org/10.1002/hyp.13936>



Research papers

What affects the hydrological response of rain-on-snow events in low-altitude mountain ranges in Central Europe?

Roman Juras^{a,*}, Johanna R. Blöcher^a, Michal Jenicek^b, Ondrej Hotovy^b, Yannis Markonis^a

^a Faculty of Environmental Sciences, Czech University of Life Sciences Prague, Kamýcká 129, 165 00 Prague, Czechia

^b Department of Physical Geography and Geoecology, Charles University, Albertov 6, 128 43 Prague, Czechia



ARTICLE INFO

This manuscript was handled by Marco Borga, Editor-in-Chief, with the assistance of Francesco Avanzi, Associate Editor

Keywords:

Snow hydrology
Snowmelt
Runoff generation
Rain-on-snow
Self-organising maps

ABSTRACT

Rain-on-snow (ROS) events influence the hydrological regime of rivers in regions with seasonal snow cover. Although ROS events are often related to floods, they do not always cause severe runoff. During ROS, the snowpack has an ambiguous effect on runoff generation; it can either store a significant portion of rain or amplify runoff by additional snowmelt. There is a need to understand under what circumstances ROS events produce runoff. We analysed eleven years of hourly meteorological, snow water equivalent and streamflow data from 15 catchments located in two mountain ranges in Czechia. We identified 611 ROS events which were further analysed and classified using selected meteorological, snow and runoff indices. The analysis of the runoff response of all ROS events revealed that only 5% of them resulted in high runoff exceeding the 1-year return period, but most of the events (82%) did not cause any significant runoff increase. Employing self-organising maps enabled us to categorise the events and better understand what combination of hydrometeorological characteristics leads to various runoff responses. High volumes of rain together with low snow cover were identified as important factors in the generation of high runoffs. In contrast, a deep and extended snowpack affected by rain under low air temperatures usually caused lower runoffs. The results of this study showed the importance of the snowpack, which can often prevent extreme runoff even when a large amount of rainfall occurs. Understanding the hydrological regime of ROS is becoming even more important with the ongoing decline of the snowfall fraction and subsequent changes in snow storage.

1. Introduction

Rain-on-snow (ROS) events have been in the focus of hydrologists in recent decades, and Blöschl et al. (2019) addressed ROS as one of the twenty-three unsolved hydrological problems in the context of complex water management. ROS events are often associated with natural hazards such as floods (Badoux et al., 2013; McCabe et al., 2007; Pomeroy et al., 2016; Rössler et al., 2014), avalanches (Baggi and Schweizer, 2008; Conway and Raymond, 1993; Haywood, 1988), or slushflows (Clark et al., 2009; Decaulne and Saemundsson, 2006), often with severe consequences for human lives, health, and property. For instance, floods in the Bernese Alps (Switzerland) in 2011 (Rössler et al., 2014) or large floods in Alberta (Canada) in 2013 cost millions of dollars and caused the evacuation of thousands of inhabitants (Pomeroy et al., 2016).

Since global precipitation patterns are changing (Markonis et al., 2019) the frequency of ROS is changing as well. This is mainly because of rising air temperatures at high elevations (Dong and Menzel, 2019;

Marty et al., 2017; Pepin et al., 2015) and changes in global atmospheric circulation (Cassou and Cattiaux, 2016). These changes impact snow cover and precipitation and, therefore, ROS events. Snow cover depth and the number of days with snow on the ground (Beniston et al., 2018; Dong and Menzel, 2019; Marty et al., 2017), snow density (Zhong et al., 2014), as well as snowfall fraction (Li et al., 2020) are decreasing in many regions of the world (Notarnicola, 2020). In the Main River catchment in Germany, ROS events were found to be an important factor for runoff generation above the elevation of 400 m (Sui et al., 2010). However, changes in elevation and temporal distribution of ROS can be expected in the future. Musselman et al. (2018) predicted that ROS in the USA will be more frequent at higher elevations and will shift from spring to winter. Many historical floods in the USA are associated with ROS events originating at elevations of 1000–1500 m above sea level (a.s.l.); moreover, ROS are predicted to originate even above 2000 m (Li et al., 2019). This is mainly because increasing temperatures result in more frequent liquid, rather than solid, precipitation at higher

* Corresponding author.

E-mail address: Juras@fzp.czu.cz (R. Juras).

elevations (Musselman et al., 2018). Additionally, a similar trend in the change in precipitation can be observed in the Arctic (Bintanja, 2018) and in Europe (Jacob et al., 2014).

The most severe floods from ROS events are usually associated with simultaneous snowmelt, which can contribute considerably to runoff. Sui et al. (2010) reported that in the Main River watershed, snowmelt contributed between 23% and 64% of an equivalent precipitation depth during ROS. Another study from north-western USA reports that maximum snowmelt contribution during ROS varied between 2% and 47% (Wayand et al., 2015). Trubilowicz and Moore (2017) showed that snowmelt enhanced snowpack runoff from a lysimeter by about 25%. Nevertheless, the contribution of heat energy from rain to the total melt is usually only up to 10% at daily and longer temporal resolutions (Hotovy and Jenicek, 2020; Li et al., 2019; Trubilowicz and Moore, 2017). Also, the main contributor to melt production usually differs, depending on the locality and meteorological conditions during the ROS event. Li et al. (2019) reported that the dominant factor in western USA was net radiation, but in eastern USA both net radiation and turbulent heat flux contributed equally to snowmelt production during ROS. This supports a study from Germany where, during ROS, snowmelt was mostly initiated by the turbulent exchange of latent and sensible heat in open sites, whereas longwave radiation and turbulent fluxes contributed equally to snowmelt in forested sites (Garvelmann et al., 2014). Dominance of turbulent heat exchange as a main contributor for snowmelt during ROS was also reported in Würzler et al. (2016) in the Swiss Alps.

Although ROS events can cause an increase in runoff, not all ROS events do so. The snowpack can store a considerable amount of incoming rainwater and, thus, may generate reduced or even zero runoff. Previous field experiments conducted by Juras et al. (2017) showed that snowpack temporarily stored up to 70% of incoming rainwater volume (about 40 mm). The actual storage potential for the rainwater is controlled by the snow ripeness and snowpack physical properties, such as grain shape, grain size (Singh and Singh, 2001), and layering – especially the presence of capillary barriers (Avanzi et al., 2016). Wayand et al. (2015) showed that half of the largest investigated ROS events in north-western USA did not cause floods. Kattelmann (1987b) reported that forested catchments even stored all rainwater during ROS and generated no additional snowpack outflow. Snow also insulates the ground and prevents it from freezing. More water is able to infiltrate into unfrozen soil compared to frozen soil (Seibert et al., 2014). Previous studies showed that runoff can often be generated faster and with higher magnitude from snow-free areas (Seibert et al., 2014). These facts emphasize the ambiguous effect and importance of snowpack on the hydrological regime during ROS, and the need to understand why and when ROS events produce exceptional runoff (Blöschl et al. 2019).

Although several studies have focused on modelled runoff response (Würzler et al., 2016; Würzler and Jonas, 2018) or on single events (Garvelmann et al., 2015; Rössler et al., 2014), empirical analyses of the extended ROS events dataset using measured streamflow at an hourly resolution are rather rare (Merz et al., 2006) or even missing in many regions with seasonal snow cover. Additionally, there is still limited knowledge of the role of individual climate and snowpack characteristics which control the dynamics of runoff response. Many of the studies were performed in the USA or the European Alps. To fill this knowledge gap, we set the main objectives of our study to 1) identify past ROS events in low-altitude Central European mountain ranges and analyse their characteristics in terms of seasonal variability and runoff response, and 2) classify the ROS events according to major drivers controlling runoff response. Our methods also account for the fact that only a part of the catchment contributes to runoff during the specific ROS event due to strong dependence of snowmelt on air temperature at specific elevation. Explaining the causes leading to high runoff during ROS events is one of the unsolved scientific problems in hydrology recently defined by the hydrological community (Blöschl et al., 2019). Our study benefits from 11 years of hourly climatological and hydrological data from 15 catchments at different elevations. The focus on elevation is important

because ROS events highly depend on air temperature influencing the phase of precipitation, which also influences the fraction of the catchment contributing to runoff.

2. Material and methods

2.1. Study area

The hydrological response of ROS events was analysed for 15 catchments (Fig. 1, Table 1) in the two highest Czech mountain ranges (or in very close proximity to them), Krkonoše (or Giant Mountains) and Jeseníky in the Sudetes region (Czechia) for 10 cold seasons 2004–2014 (Nov. 1st to May 31st). Two catchments (Kr-CS, Jes-BP) only covered 2005 to 2014, due to data gaps. The catchments were selected based on large snow storage during winter (and, thus, the potential of ROS occurrences) and the availability of adequate data. The catchments were chosen to be as natural as possible without dams or water transfers. Even though the catchments are partly urbanised and include some ski resorts, the total extent of such areas is minor or negligible. The location and basic characteristics of catchments are depicted in Fig. 1 and summarized in Table 1.

The elevation range of all catchments is from 438 m to 1602 m a.s.l. and the area varies in size between 2.6 and 181.3 km². The land cover of the catchments is characterized by coniferous forests (prevailing European spruce – *Picea abies*), while the highest parts of the catchments are usually above the tree line, partially covered by mountain pine (*Pinus mugo*) shrubs. The forest coverage ranges between 26% and 93% and areas above 1 400 m a.s.l. are mountain tundra.

2.2. Rain-on-snow events

2.2.1. Rain-on-snow event definition

A ROS event was defined as the period of rain occurring simultaneously with snow laying on the ground. Specifically, when snow water equivalent (SWE) ≥ 10 mm, air temperature \geq threshold temperature (T_T), and rainfall > 0 mm.

2.2.2. Input data and modelling approaches

Meteorological and runoff data were acquired from the Czech Hydrometeorological Institute (CHMI). Air temperature, streamflow, and precipitation were provided in an hourly time step. Observed snow water equivalent (SWE) data were only available in a weekly time step (measured every Monday).

Rain-on-snow can vary with elevation and may differ across the catchment. In order to include elevation in the analysis, we used the semi-distributed bucket-type HBV model in its software implementation HBV-light (Lindström et al., 1997; Seibert and Vis, 2012) to obtain spatial distribution of precipitation, air temperature, snowmelt and SWE and to estimate the precipitation phase across elevations. Note, that runoff used in this study was not modelled, but measured. The model was chosen for its comprehensive snow accumulation and snowmelt routine and the robust way of model calibration. The snow routine included in the model uses a degree-day approach which calculates snow accumulation and snowmelt, including snow water holding capacity and potential refreezing of meltwater. The main inputs of the model form time series of daily mean air temperature, daily precipitation, and monthly mean potential evapotranspiration (PET). The PET values were calculated by the temperature-based method presented by Oudin et al. (2005). Additionally, daily lapse rates for air temperature were calculated from observed data received from two neighbouring stations located at different elevations. Precipitation phase partitioning was performed using a single threshold temperature (T_T) approach. The value of T_T was calibrated separately for each catchment. Details regarding model structure can be found in several studies (Girons Lopez et al., 2020; Seibert and Vis, 2012).

The HBV-light model was calibrated automatically for each study

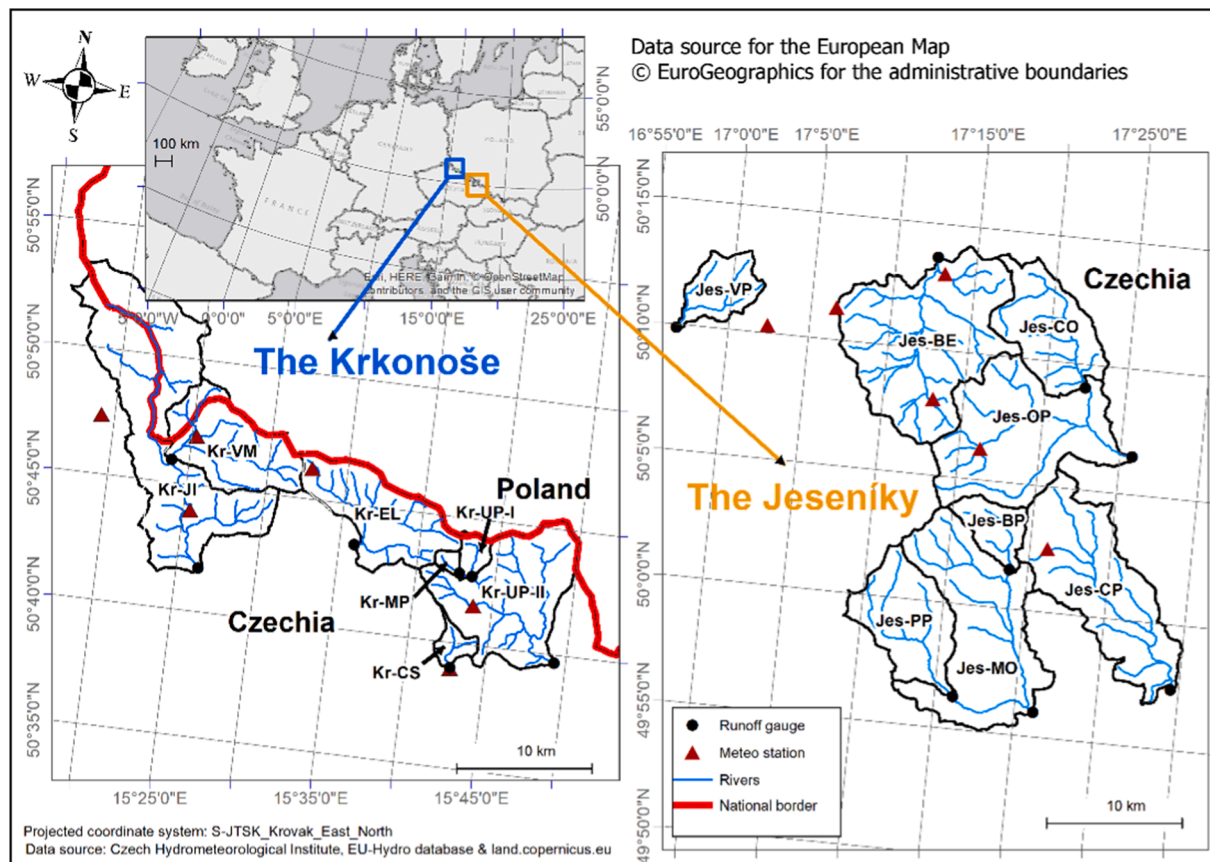


Fig. 1. Maps of the catchments with locations of runoff gauges and meteorological stations.

Table 1

Selected characteristics of the study catchments. Mean snowfall fraction, and maximum snow water equivalent (SWE-max) covering cold seasons 2004–2014 (Nov. 1st to May 31st). Catchments abbreviated with Kr-* and Jes-* belong to Krkonoše and Jeseníky, respectively. *Snowfall fraction and SWE_{max} are catchments means calculated from the snow accumulation and snowmelt model (see Section 2.2.2 for details).

Catchment name	Code	Outlet profile	Elevation [m a.s.l.]		Area [km ²]	*Snowfall fraction [-]	*SWE _{max} [mm]
			Min	Max			
Modrý potok	Kr-MP	Modrý Důl	1016	1552	2.6	0.38	368
Čistá	Kr-CS	Černý Důl	736	1350	6.5	0.28	287
Úpa-I	Kr-UP-I	Obrů Důl	903	1597	8.9	0.35	384
Velká Mumlava	Kr-VM	Janov-Harrachov	595	1434	51.3	0.38	357
Elbe	Kr-EL	Špindlerův Mlýn	699	1553	53.1	0.3	368
Úpa-II	Kr-UP-II	Horní Maršov	574	1602	82.0	0.33	315
Jizera	Kr-JI	Jablonec nad Jizerou	438	1434	181.3	0.33	420
Bělokamenný potok	Jes-BP	Malá Morávka	674	1420	17.9	0.28	130
Vrbenský potok	Jes-VP	Staré Město pod Sněžníkem	523	1118	21.9	0.23	158
Černá Opava	Jes-CO	Mnichov	568	1218	50.5	0.27	131
Podolský potok	Jes-PP	Rýmařov	593	1356	50.7	0.27	161
Černý potok	Jes-CP	Mezina	500	1026	92.1	0.24	114
Bělá	Jes-BE	Jeseník	438	1417	118.0	0.25	167
Opava	Jes-OP	Karlovice	484	1492	150.8	0.31	141
Moravice	Jes-MO	Velká Štáhle	542	1465	168.6	0.28	172

catchment against observed runoff and SWE using a genetic optimization algorithm (Seibert, 2000) for the hydrological years 2004–2009 (2006–2010 for two catchments with shorter time series). A combination of three objective criteria was used to evaluate goodness-of-fit of the model: 1) logarithmic Nash-Sutcliffe efficiency for runoff (Nash and Sutcliffe, 1970); 2) Nash-Sutcliffe efficiency for SWE; and 3) volume error for runoff. The main emphasis was put on model ability to reproduce the observed SWE. The model was validated for 2010–2014. Ten different optimized parameter sets resulting from ten calibration runs were used to create ten simulations. The median simulation was used for further analysis. The results of model calibration and validation are

shown in supplement (Table S1, Fig. S1). A similar approach for model calibration was also used by Jenicek and Ledvinka (2020) for partly the same study region.

Simulated daily snowmelt was downscaled to an hourly step considering its diurnal cycle using the method of Tobin et al. (2013), as follows:

$$M(x, t) = \begin{cases} \frac{a_r(T(x, t) - T_r)}{n} & T(x, t) > T_r \\ 0 & T(x, t) \leq T_r \end{cases} \quad (1)$$

where $T(x,t)$ is the air temperature at a given elevation zone x at a given hour t . Parameter a_r represents a constant degree-day factor [$\text{mm } ^\circ\text{C day}^{-1}$] and T_T is a threshold temperature above which snowmelt can occur. Both a_r and T_T were calibrated by the HBV model, as described above, and particular values are presented in Table. S1 in the supplement.

2.2.3. Catchment division – semi distributed approach

Catchment division enables detailed spatial assessment of runoff response, which depends on the fraction of the catchment area involved in the runoff generation process. Since the meteorological input data were not available in gridded form, the semi distributed approach was used as the best available method to estimate area portion contributing to ROS or runoff.

Each catchment was divided into 100 m high elevation zones between 450 m and 1650 m a.s.l. In these zones, snow water equivalent (SWE), snowmelt, and ROS occurrence were modelled (see Section 2.2.2). Total SWE and snowmelt per catchment were calculated as a weighted mean and a weighted sum, respectively, where the area of a given zone represented the weight.

The area of each elevation zone was calculated according to the hypsographic curve for each catchment. These curves were constructed based on a digital elevation model with a resolution of 1 arcsec (lat. 50°) ≈ 20 m (Farr et al., 2007), using a modified ‘hypsometric’ function included in the ‘hydroTSM’ package (Zambrano-Bigiarini, 2020) in the R language (R Core Team, 2019). Mean air temperature was then calculated as an average of the highest and lowest point temperature of the catchment. The snow-covered elevation zone was determined when $\text{SWE} > 0$ mm, otherwise the zone was considered snow-free. Runoff contributing area (RCA) represents the sum of elevation zone areas where runoff occurred either by snowmelt or by rain. In other words, RCA represents the area located below the freezing level (defined by threshold temperature – T_T) (Fig. 2). Finally, we calculated the relative fraction of each specific zone described above to the entire catchment area. A graphical interpretation of the concept is depicted in Fig. 2.

2.2.4. Rain-on-snow event selection

ROS events were identified for every hour and each elevation zone to be able to estimate the fraction of catchment affected by ROS (hereafter ROS area). Total ROS area was calculated as a sum of elevation zones affected by ROS. Next, we defined ROS runoff duration (RRD) as a period of a ROS event extended by the subsequent runoff response (Fig. 3).

From the initial selection above, we further created a subset of

events, when at least 5 mm of cumulative rain was recorded, the RRD was shorter than 144 h, and runoff increase was detected.

Multiple events were characterised by two or more ROS events in one RRD with a time gap between rain onsets shorter than 96 h. For longer time gaps, the events were classified as two separate events.

2.3. Hydrograph analysis

For streamflow analysis, the original discharge data were recalculated to runoff depth [mm].

Rainfall and streamflow parameters used in this study are defined in the following. Fig. 3 is a graphic conceptualization of the main hydrograph parameters.

The following parameters were estimated:

- **Event start** corresponds to rain onset of the ROS event.
- **Event end** was calculated from the falling limb of the hydrograph based on the constant- k method according to Blume et al. (2007):

$$k = \frac{dQ_{obs}}{dt} \cdot \frac{1}{Q_{obs}(t)}, \quad (2)$$

where Q_{obs} [mm] represents observed runoff at a specific hour (t). After visual validation of the method, parameter k was smoothed to avoid discrepancies caused by occasional high volatility in runoff data. Event end was set when the absolute value of k 3-hour moving average reached the limit $1e^{-2}$.

- **Event rainfall (P_{event})** represents total amount of rain [mm] recorded at the closest meteorological station during an ROS event (Fig. 1).
- **Event runoff (Q_{event})** represents total runoff volume caused by ROS [mm]. Event runoff was distinguished from base flow (Q_{base}) by the linear separation method depicted in Fig. 3 (Dingman 2015). We assume that the observed runoff only consists of base flow during the first and last hour of the event. Linear interpolation between these two points gives us a separation line between two runoff components, where event runoff is above this line and base flow below it. Event runoff can be thus calculated as:

$$Q_{event}(t) = \sum_{t=1}^N Q_{obs}(t) - Q_{base}(t), \quad (3)$$

where Q_{obs} [mm] is observed runoff and Q_{base} [mm] is base flow runoff linearly interpolated between the first and last hour of observed runoff

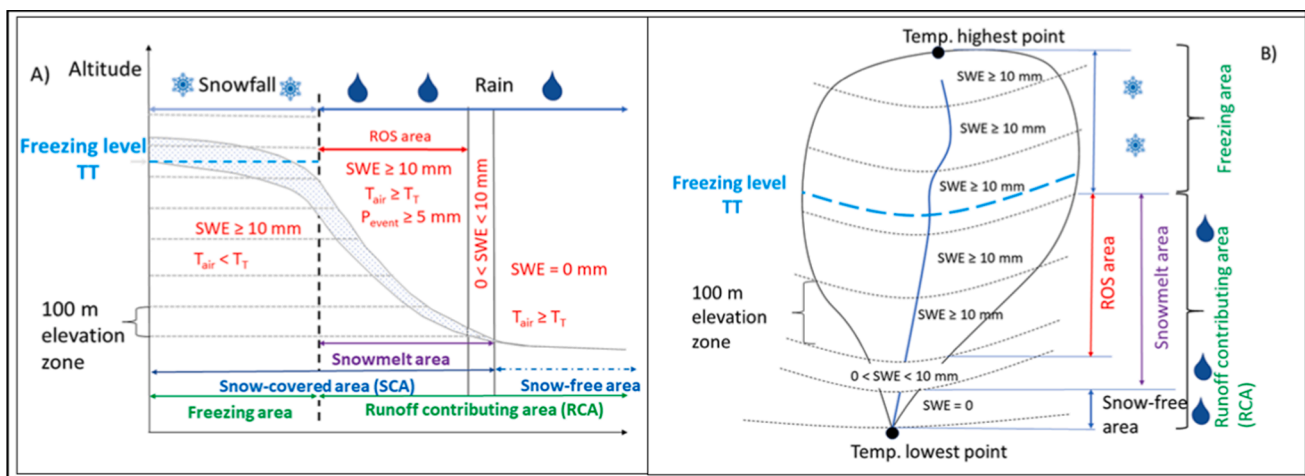


Fig. 2. The concept of catchment division by elevation zones and area related to snow cover, ROS event, rain-affected area, snow-free area, and runoff area depicted as a) side and b) plan view. Symbol P_{event} represents hourly rainfall and T_T is threshold temperature [$^\circ\text{C}$] calibrated for each catchment.

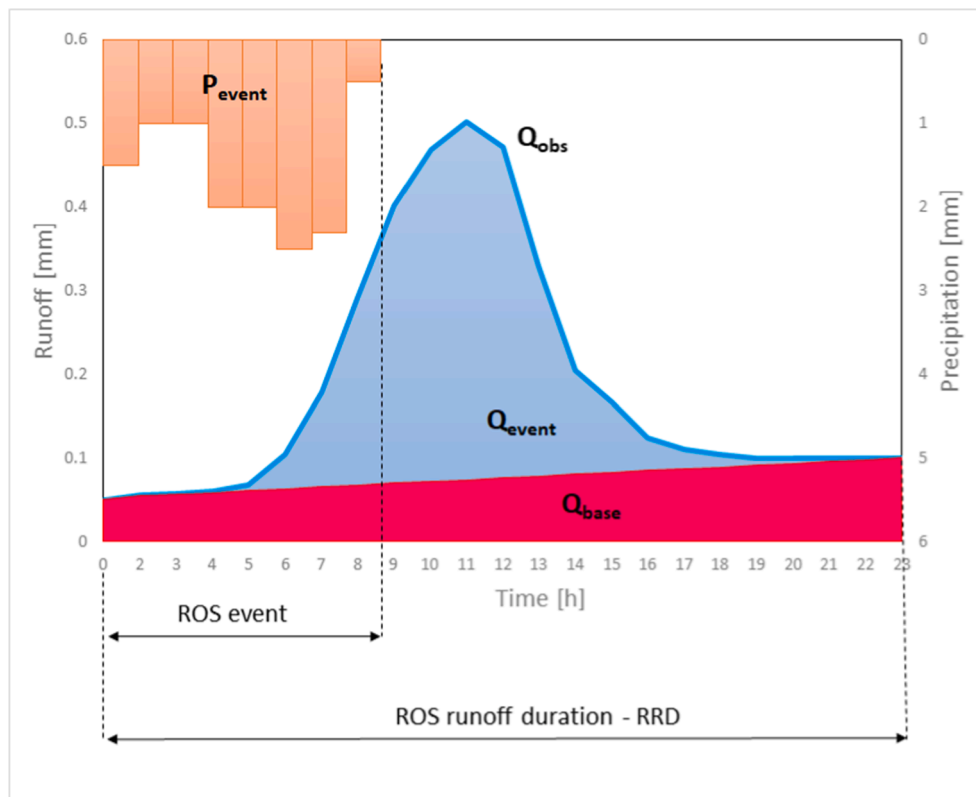


Fig. 3. Graphic conceptualization of hydrograph parameters, depicting ROS event, ROS runoff duration (RRD), event rainfall (P_{event}) and separated event runoff (Q_{event}) and base flow (Q_{base}) from the observed stream flow (Q_{obs}).

in a single RRD. N represents the number of hours of the event and t represents iteration for a given hour.

- **Runoff coefficient (C)** is the ratio of event runoff (Q_{event}) to event rainfall (P_{event}).
- **Water budget (WB)** defines the difference between Q_{event} and P_{event} [mm]. A negative WB represents water storage in the catchment, whereas a positive WB indicates runoff excess. We neglected other physical processes such as evapotranspiration, sublimation, or condensation in the WB calculation.

2.3.1. Runoff types

The resulting ROS events were divided into four types according to event runoff, named “Negligible runoff”, “Low runoff”, “Medium runoff”, and “High runoff” (Table 2). This categorisation helps to better describe precursors of different hydrological responses to ROS. The ROS event was classified as type 1 (negligible runoff) if cumulative event runoff did not exceed 25% of cumulative baseflow. The ROS event was classified as type 2 (low runoff) if cumulative event runoff exceeded 25% but not 75% of cumulative baseflow. The ROS event was classified as type 3 (medium runoff) if cumulative event runoff exceeded 75% of cumulative baseflow anytime during the course of the RRD. And ROS

Table 2

Definition of runoff types. Q_{event} and Q_{base} represent cumulative event runoff and baseflow, respectively. Q_1 represents the given limit for the particular catchment of the 1-y runoff return period.

Type	Runoff	Definition
1	Negligible runoff	$Q_{event} \leq 0.25 Q_{base}$
2	Low runoff	$0.25 Q_{base} < Q_{event}$ less than $0.75 Q_{base}$
3	Medium runoff	$Q_{event} \geq 0.75 Q_{base}$
4	High runoff	$Q_{obs}(t) > Q_1$

events of runoff type 4 (high runoff) were selected from the previously defined types if observed runoff (Q_{obs}) exceeded the 1-y return period (Q_1).

2.4. Events clustering – self-organizing maps

One of the key questions is how to detect which hydrometeorological conditions lead to increased runoff or even to floods, and which do not. A possible approach is classification of the conditions related to specific ROS events with some data-driven clustering technique. To further categorize ROS events and detect some patterns in their characteristics, the Self-Organizing Map (SOM) technique was applied. It is based on a data-driven, iterative algorithm used to classify the original, multivariate dataset into some representative categories. The algorithm is presented in detail by Kohonen (1990) while numerous applications of SOMs in water resources can be found in the work of Kalteh et al. (2008).

The basic principle of the method is to create a two-dimensional output layer of nodes, where each node attracts members of the original dataset with common features. In our case, these are ROS events. The next step is to decide which properties will be used as descriptors or classifiers, i.e., event rainfall and initial SWE. In this example, with each iteration of the algorithm, events with similar rainfall and SWE will move closer to each other. This procedure is repeated until there is no change in the number of events per node. Finally, all events that have similar descriptors will cluster over different nodes and each node can then be regarded as an individual group.

An advantage of the SOM algorithm lies in the fact that there is no need for preselecting the constraints of each group. The number of nodes must be predefined though; however, there is no standard approach to determine the number of nodes. In most studies, various experiments are performed with SOMs of different sizes. There is a significant amount of subjectivity in the selection of node number. Usually, it is based on a balance between the homogeneity of different clusters and

comprehensibility of the classification scheme (Chang et al., 2010; Ley et al., 2011; Markonis et al., 2018; Markonis et al., 2021; Rousi et al., 2017).

In this study, a range of SOM sizes between 9 and 36 was examined for symmetrical topologies, i.e., 3×3 to 6×6 , using the *kohonen* package in R language (Wehrens and Kruisselbrink, 2018). To select the most representative one, we used the node variance minimization approach (Markonis and Strnad, 2020). The SOM with the minimum variance between its nodes has dimensions of 4×4 nodes, which corresponds to a theoretical average of 38 events per node. Clustering ROS events into 16 groups brings the best solution based on node variance minimization. This number allows statistical inference from the sample of each node. However, in practice, some nodes are expected to be quite higher and others lower or even zero. It should be noted that SOMs reveal patterns of similarity with no causal attribution and therefore their interpretation should be performed with caution.

3. Results

3.1. Rain-on-snow occurrence

We identified 611 ROS events in the study area during 2004–2014. ROS events were more frequent in Krkonoše (479) compared to Jeseníky (132) (Fig. 4a). The highest occurrence of ROS was identified during November (17.8%) and the lowest during February (6.2%). The seasonal distribution of ROS events differed between the mountain ranges. ROS in Krkonoše mostly occurred during May (15.9%) and in Jeseníky during March (6.2%). In contrast, February saw the fewest ROS events in both mountain ranges (6.2%). Since a single ROS event can start in one month and end in the next one, the occurrences are related to event start. From the annual perspective, the richest year in ROS events was 2007, when 71 events occurred in Krkonoše and 29 in Jeseníky. Note that ROS events can occur simultaneously in several individual catchments, while only event start or event end can differ.

Table 3 summarises the number of events from the runoff response perspective, where almost half of all events caused negligible runoff (59%). This means that most of the rain was retained in the catchment. More ROS events caused low runoff (23%) than medium runoff (13%), and only 5% of ROS events resulted in high runoff. The longest exceedance of Q1 for a single event lasted for 28 h in the Opava catchment - Jes-OP (Jeseníky). Nevertheless, in regard to events causing high runoff, none exceeded a 5-year return period or higher. Most high runoff events were identified in the Modrý potok catchment - Kr-MP (Krkonoše). The time distribution of runoff types over the season is depicted in Fig. 4b, which shows that ROS events causing high runoff

Table 3

Number of ROS events in particular catchments according to runoff types.

Catchment	Runoff type				No. events
	Negligible - 1	Low - 2	Medium - 3	High - 4	
Kr-MP	45	20	10	9	84
Kr-CS	55	17	12	3	87
Kr-UP-I	19	6	3	5	33
Kr-VM	23	14	11	3	51
Kr-EL	73	23	20	4	120
Kr-UP-II	36	11	0	1	48
Kr-JI	26	17	13	0	56
Jes-BP	5	2	3	0	10
Jes-VP	1	0	0	0	1
Jes-CO	18	0	0	0	18
Jes-PP	16	8	3	0	27
Jes-CP	12	2	0	1	15
Jes-BE	8	4	0	0	12
Jes-OP	7	4	0	2	13
Jes-MO	18	13	4	1	36
Krkonoše	277	108	69	25	479
Jeseníky	85	33	10	4	132
Total	362	141	79	29	611

were mostly generated during November, March, and May.

3.2. Seasonal variability of rain-on-snow descriptors

Since the definition of ROS events is based on meteorological inputs such as air temperature (distinguishing between solid and liquid precipitation), SWE and rainfall, the analysis of seasonal distribution of these descriptors over ROS events was performed.

Mean air temperatures in the catchments over the course of ROS ranged between -2.2 °C to 13.9 °C. The results showed that ROS featured similar mean air temperature in Krkonoše (2.8 °C) and in Jeseníky (2.9 °C). Temporal monthly distribution of the mean air temperature for individual ROS events shows a similar pattern for both mountain ranges (Fig. 5a). Although, in our study, ROS events were defined for air temperatures above T_T (which is unique for each catchment), lower mean temperatures could occur as well. This is because mean air temperature is calculated for the entire catchment and in some cases ROS events do not occur in the higher parts, where the air temperature is below T_T .

Snow storage demonstrated the largest seasonal differences among the investigated ROS descriptors. Analysis of initial SWE shows that ROS events are associated with considerably higher SWE in Krkonoše (Fig. 5b). Here, the highest mean values of initial SWE were observed in

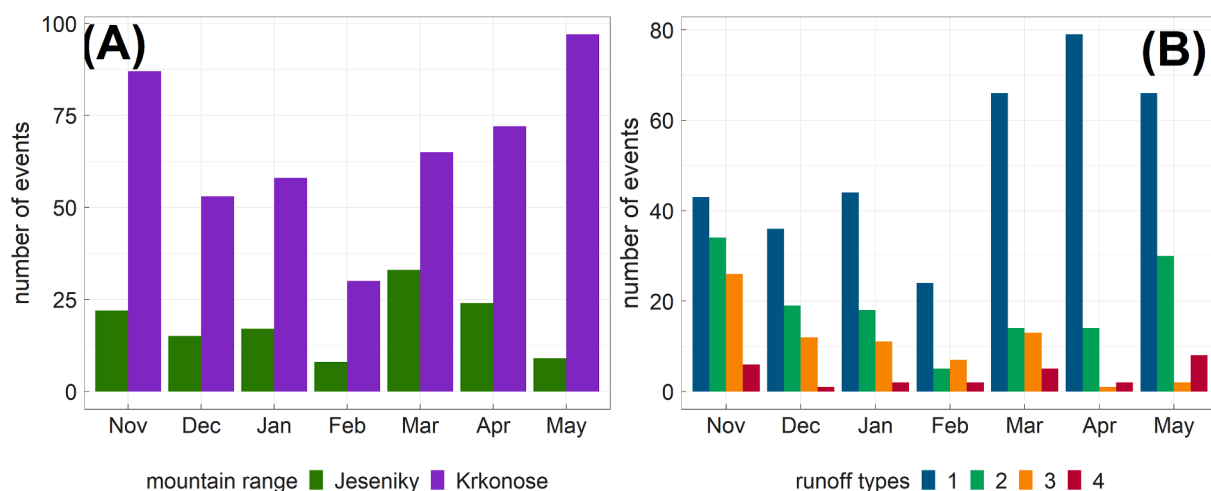


Fig. 4. Total number of ROS events over the study period covering cold seasons 2004–2014 (Nov. 1st to May 31st); A) in Krkonoše and in Jeseníky, and B) for four runoff types.

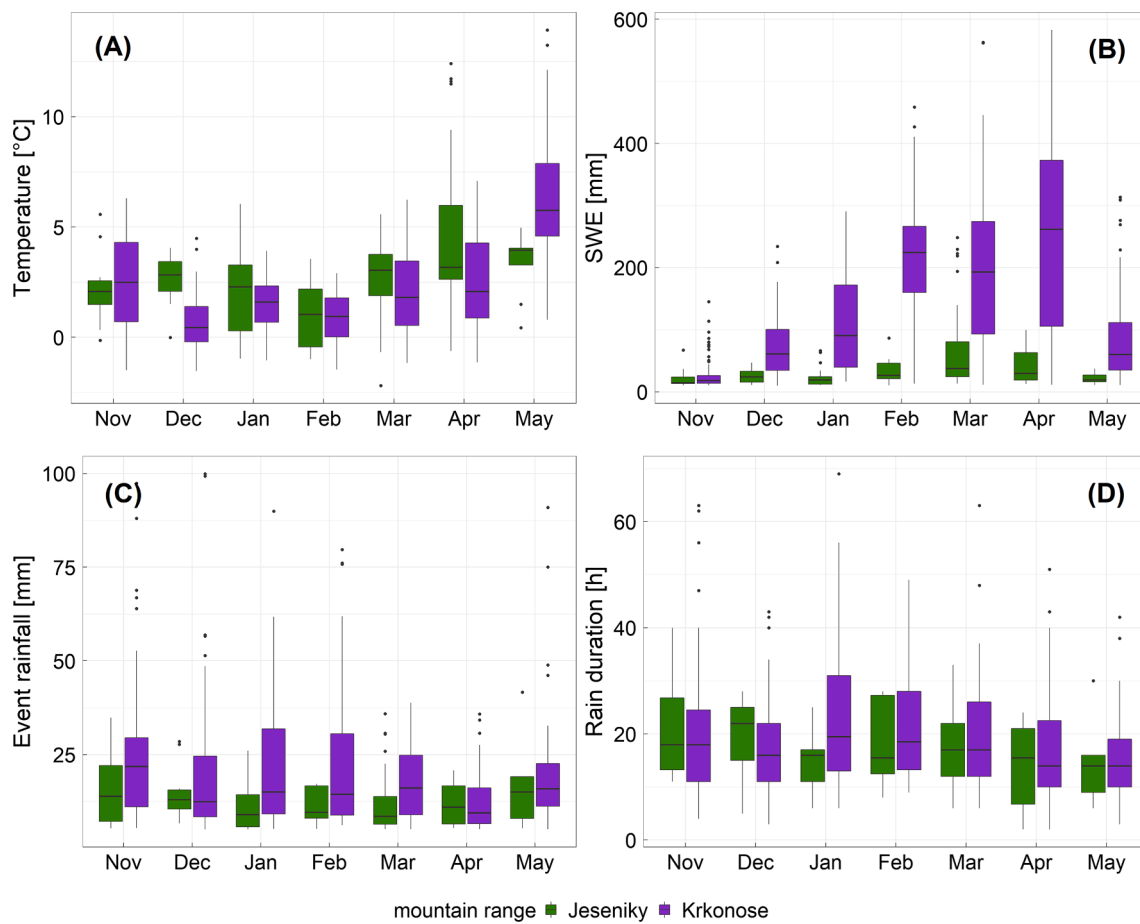


Fig. 5. Seasonal distribution of selected meteorological parameters during the RRD; A) mean air temperature in the catchment, B) initial SWE over the ROS area, C) event rainfall over the ROS area, and D) rain duration.

April (229 mm) and the lowest in November (35 mm). In contrast, the highest SWE values in Jeseníky were reached in March (72 mm), with the lowest in November (20 mm).

Event rainfall showed similar patterns in both mountain ranges for event rainfall and duration (Fig. 5c, d). ROS events are, on average, associated with more rain and longer rain durations (20.0 mm, 19 h) in Krkonoše compared to Jeseníky (13.2 mm, 17.6 h). ROS events associated with the highest mean of rainfall amounts occurred in November in Krkonoše (33.2 mm) and in May in Jeseníky (18.1 mm). Nonetheless, total maximum rainfall (99.9 mm) during one ROS event was observed in the Elbe catchment (Krkonoše) in December 2007.

3.3. Hydrometeorological characteristics of runoff types

Several hydrometeorological descriptors for each **runoff response** type were analysed (1- negligible runoff, 2 – low runoff, 3 – medium runoff, 4 – high runoff). These descriptors included snowmelt, rainfall, initial SWE, runoff and rainfall intensity, and runoff coefficient (Fig. 6). These analysis revealed different patterns among the runoff types and also between the two mountain ranges. Whereas snowmelt and rainfall increased with runoff type in Krkonoše, in Jeseníky the event rainfall was lowest for runoff type 4. The greatest difference in Jeseníky could be seen between types 3 and 4, while type 3 was mostly associated with higher rainfall compared to snowmelt. Mean values of water input in type 3 in Krkonoše reached 38.5 mm (30 mm of rain/8.5 mm of snowmelt), while Jeseníky experienced only 26.7 mm (23.3 mm/3.4 mm). As expected, type 4 was initiated by the largest snowmelt and rainfall, with mean water inputs of 62.0 mm (48.9 mm/13.1 mm) in Krkonoše and 26.9 mm (15.3 mm/11.6 mm) in Jeseníky. Details on water inputs for

each runoff type are presented in Fig. 6a,b.

Since runoff response depends on initial catchment conditions, initial SWE within the ROS area was analysed. Interestingly, few differences were documented between runoff types. Initial SWE values were mostly higher in Krkonoše than in Jeseníky, which is depicted in Fig. 6c. In Krkonoše, initial SWE slightly decreased with runoff type, while the lowest values were recorded for type 4 and highest for type 1, when the median reached 32 mm and 93 mm, respectively. In Jeseníky, the lowest initial SWE values were recorded for type 2 (21 mm) and the highest for type 4 (115 mm). High snow cover in combination with high temperatures (median = 3.9 °C) clearly released a significant amount of meltwater resulting in high runoff in Jeseníky. Comparing the input characteristics for Krkonoše type 1 and Jeseníky type 4, we found that mean initial SWE (Krkonoše = 133 mm, Jeseníky = 119 mm) and event rainfall (Krkonoše = 14.0 mm, Jeseníky = 15.3 mm) were comparable. The significant difference was identified within the mean snowmelt volumes (Krkonoše = 5.7 mm, Jeseníky = 11.6 mm).

Runoff intensity represents how fast event runoff volume can be transported within a stream over ROS runoff duration (event runoff divided by RRD). Runoff intensity increases with runoff type in both mountain ranges, but Krkonoše shows higher runoff intensities compared to Jeseníky (Fig. 6d).

High runoff intensities were also associated with high rainfall intensity (Fig. 6e), although this effect was clear only in Krkonoše. High runoff in Krkonoše was related not only to high volumes of rainfall, but also to high rainfall intensity (mean = 1.8 mm.h⁻¹). In contrast, high runoff in Jeseníky was associated with the lowest rainfall intensity (mean = 0.75 mm.h⁻¹). Maximum rainfall intensity (4.8 mm.h⁻¹) was recorded in Krkonoše, which resulted in low runoff.

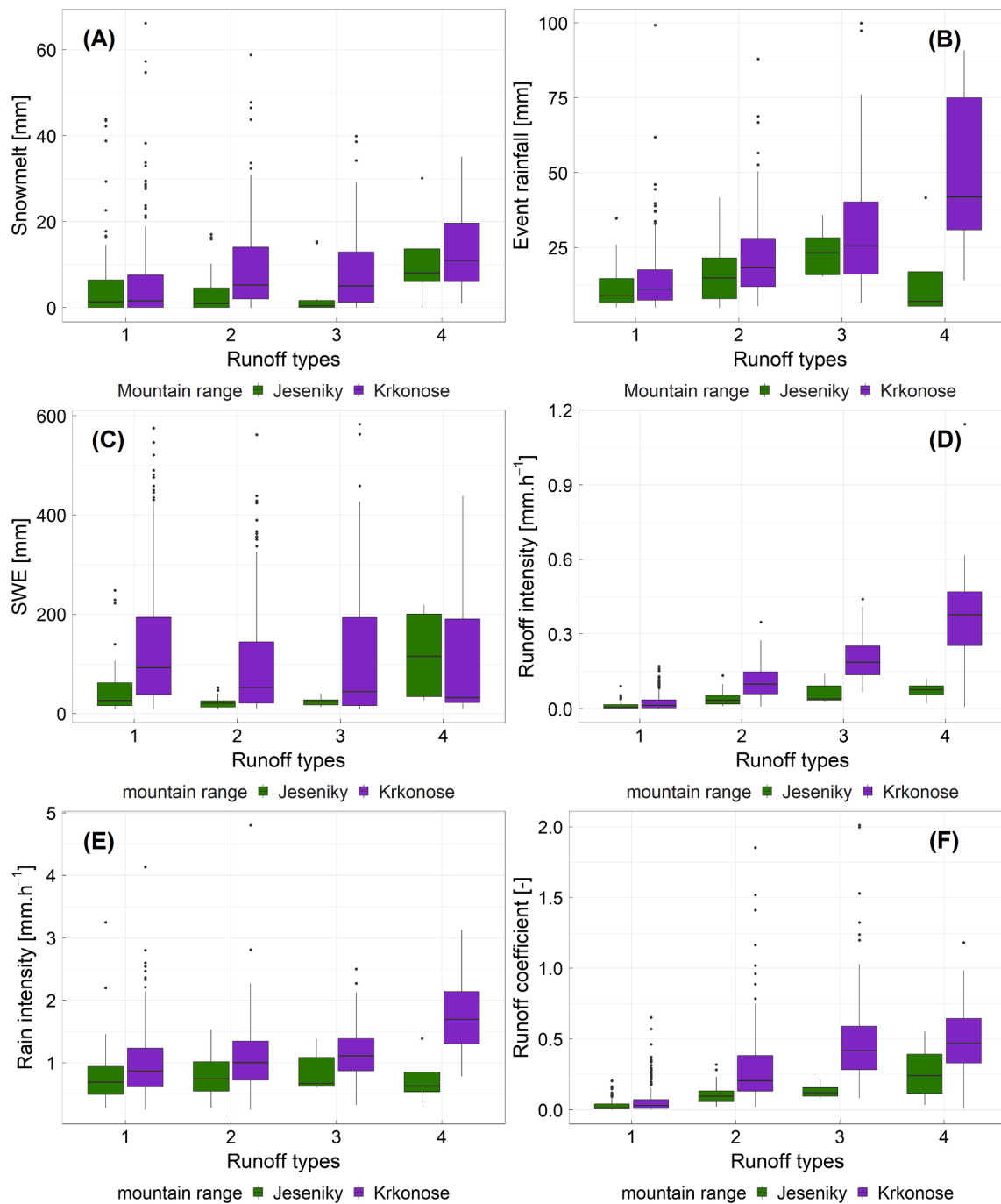


Fig. 6. Hydrometeorological parameters for all runoff types; A) Snowmelt, B) event rainfall, C) initial SWE over the ROS area, D) runoff intensity, E) rain intensity, and F) runoff coefficient.

As expected, runoff coefficient (C) increased with runoff type in both mountain ranges. The runoff coefficient also rarely exceeded 1, indicating higher runoff volume than incoming rainfall. Such high values of runoff coefficient were only documented in Krkonoše, and only for runoff types 2, 3 and 4 (Fig. 6f). Interestingly, the highest runoff coefficient for Jeseníky was identified within runoff type 4, although median rainfall was the lowest among all runoff types. This means that high runoff in Jeseníky was mainly driven mainly by snowmelt and only slightly by rainfall. However, runoff type 4 only contains four ROS events; therefore, we have to interpret such results with caution.

We also investigated if the catchment fraction effected by ROS influenced runoff response. Moreover, we analysed the effect on event runoff of the snow-covered area (SCA) and runoff contributing area

(RCA) (Fig. 7). Runoff was not generated from the entire catchment in many cases, since ROS events only occurred in part of the catchment (i. e., only below the freezing level and with sufficient snow cover). The extent of the SCA also matters because it represents the source of snowmelt during non-ROS conditions and potential for possible storage of rainwater. These parameters can significantly influence runoff response.

The analysis revealed that the mentioned areal fractions differed between all runoff types and mountain ranges. Median RCA fraction is >50% (except runoff type 3 in Jeseníky) (Fig. 7a). In contrast, median ROS area fraction was less than 56% of the catchment area for all runoff types (Fig. 7b). In addition, the highest snow area fractions were associated with medium runoff in Krkonoše (median = 98%), but highest

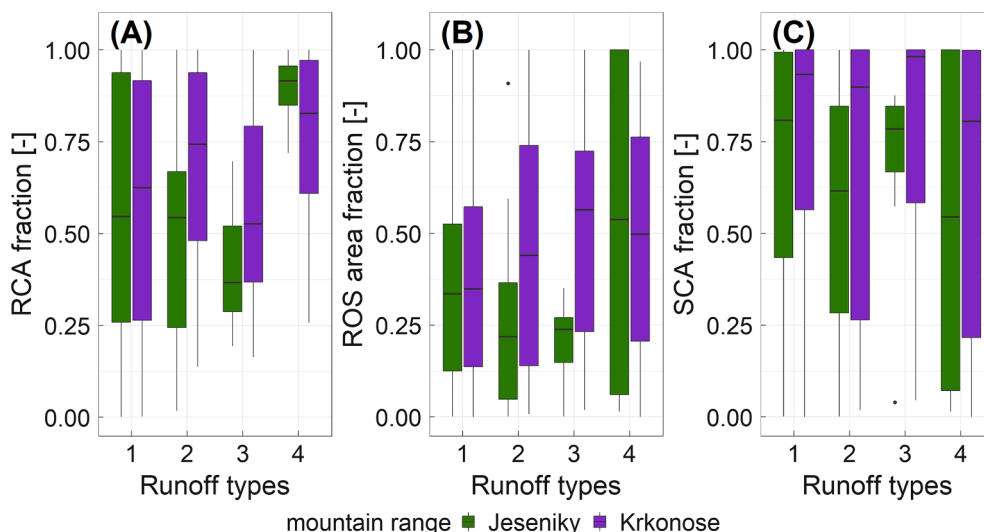


Fig. 7. Different mean fractions of catchment affecting runoff generation; A) RCA (Runoff contributing area), B) ROS area, and C) SCA (snow-covered area).

SCA resulted in negligible runoff in Jeseníky (median = 81%) (Fig. 7c). On the other hand, SCA within types 1 and 3 showed very similar coverage per mountain range. ROS responded in both mountain ranges with high runoff, when snowpack extended over the smallest part of the

catchment. In contrast, runoff type 4 was generated from the largest part of the catchments in both mountain ranges, which documented high medians of RCA fraction (Krkonose = 0.83, Jeseníky = 0.92) (Fig. 7a). High runoff was characterised in Jeseníky by higher RCA compared to

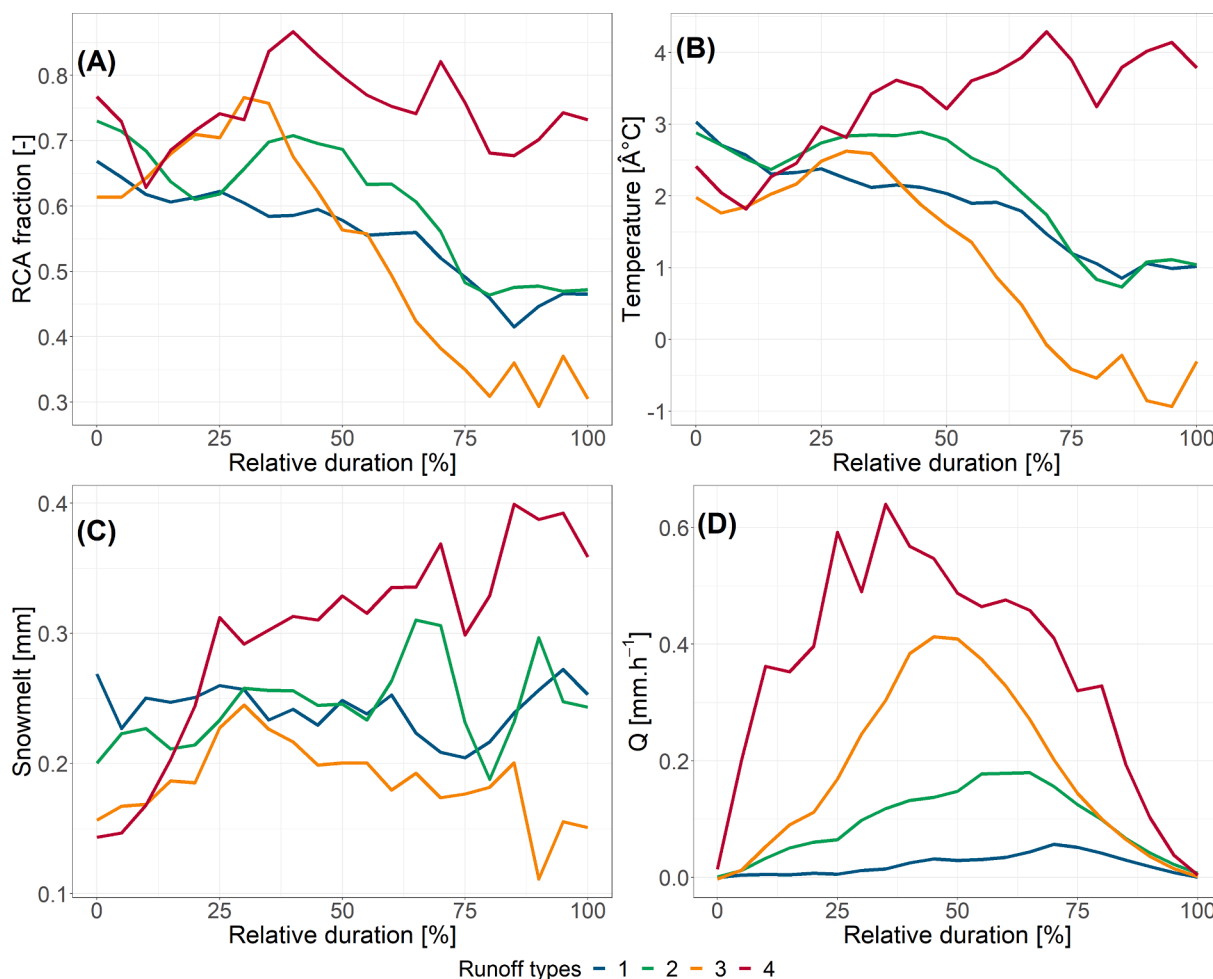


Fig. 8. Mean temporal dynamics over the relative ROS-runoff duration of selected hydrometeorological parameters related to runoff type. Individual lines represent means obtained from all events for individual runoff types. A) Runoff contributing area (RCA) fraction, B) mean catchment air temperature, C) snowmelt rate, and D) event runoff.

the SCA, which means that runoff was also generated from snow-free areas.

3.4. Temporal dynamics of rain-on-snow events

Better understanding of ROS events requires analysis of the dynamics of hydrometeorological parameters over the course of the events. Fig. 8 shows mean temporal evolution of the RCA, air temperature, snowmelt volume, and event runoff over the RRD. To compare events of different duration from different catchments, the RRD of all events was normalised, where 0 % is the start and 100 % the end of an event. First, RCA shrank over the course of the events for runoff types 1 and 2 (Fig. 8a). Similar behaviour showed that mean air temperature decreased over time for runoff types 1, 2, and 3 (Fig. 8b). The lowest temperatures were found during runoff type 3 and, in contrast, the highest temperatures were recorded for runoff type 4. For runoff type 3, temperature decreased over the course of the event, which was consistent with decreasing snowmelt production shown in Fig. 8c. In contrast, a temperature increase was only identified for type 4. Snowmelt fraction increased at the beginning for all runoff types. During medium runoff events, snowmelt only contributed a little to runoff (Fig. 8c), despite the event runoff constantly being second highest (Fig. 8d). This shows that

medium runoff was mostly driven by rainfall, with snowmelt as a secondary factor.

Event runoff expectedly differed according to runoff type, with the steepest increasing and decreasing limb in the hydrograph for runoff type 4 and the flattest curve for runoff type 1.

3.5. Classification of rain-on-snow events with self-organizing maps

For the detection of any meaningful classes between the ROS events, four variables were used as classifiers. These were P_{event} , initial SWE, runoff coefficient (C), and snowmelt. They were chosen after considering two factors. The first was maintaining representability of the processes involved in maximum runoff generation, and second was to use the least correlated variables. The resulting 16 groups of the SOM have a range between 8 and 118 events per node, with a median of 25.5, which is quite close to the theoretical mean of 38.2 (Fig. 9).

Each radar plot represents the standardized mean value of each variable per node/group and are ordered regarding to event rainfall. For instance, in Group 1 we have the 14 events with the highest rainfall, low snowmelt and runoff coefficient, and minimal initial SWE. These are the events in which rainfall is the key driver resulting mainly in high runoff (runoff type 4). In contrast, the 14 ROS events within Group 16 are

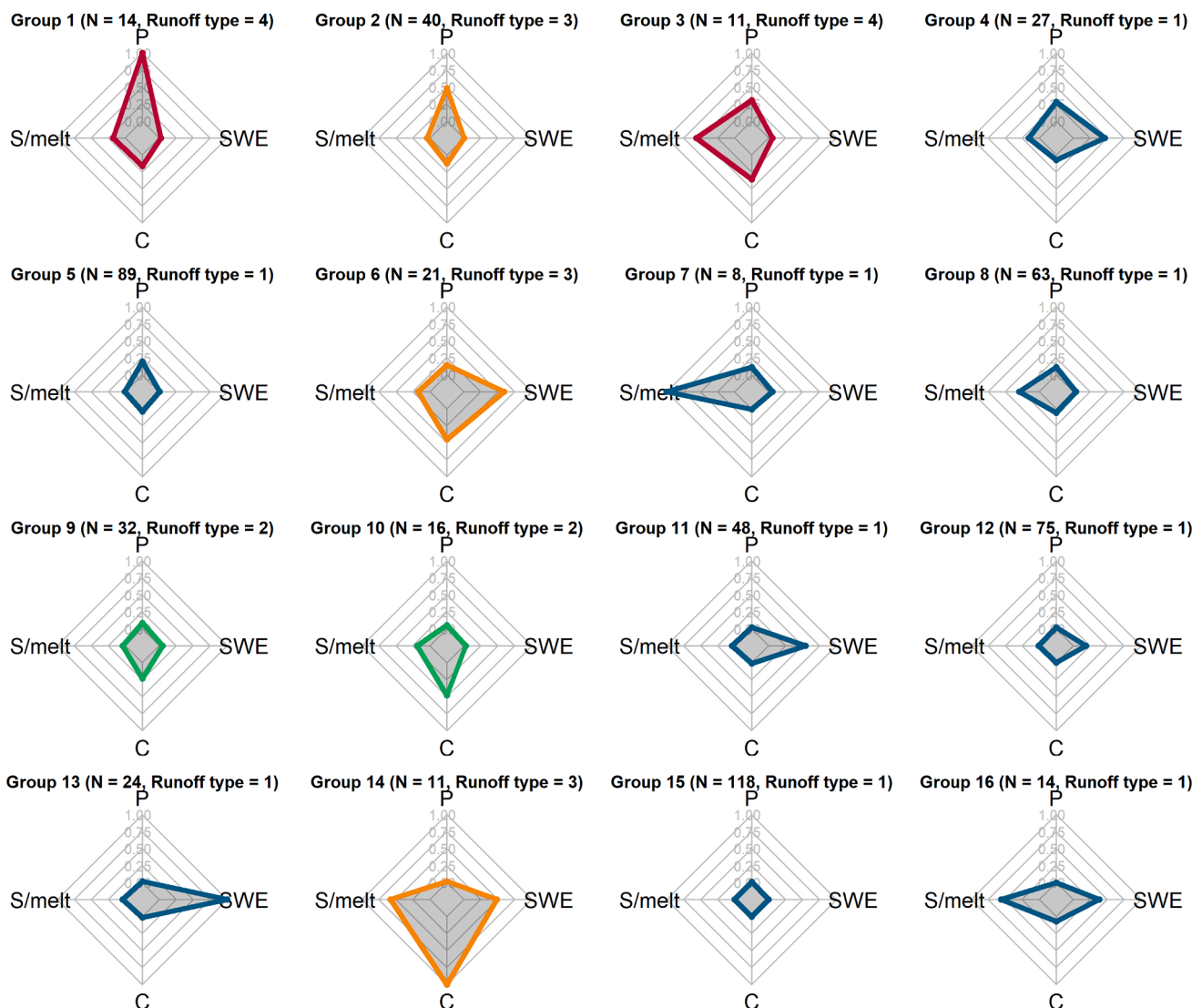


Fig. 9. Self-organizing map groups and their classification variables: P (Event rainfall), SWE (Initial Snow Water Equivalent), C (Runoff coefficient), and S/melt (Snowmelt). In the parentheses, the number of ROS events per group (N) and the most frequent runoff type are presented.

classified by minimum rainfall, but high runoff coefficient, snowmelt, and SWE generating minimal event runoff (runoff type 1). The rest of the nodes represent other combinations of the four classifying variables, providing a rich mosaic of various ROS event categories that can help us understand the relationship between climatic and hydrological variables. To do so, we further examined four additional key variables (mean air temperature, maximum runoff, mean runoff contributing area, and mean snow-covered area) that are linearly correlated to the four classifiers and see whether any nonlinear relationships appear (Fig. 10).

As expected, the groups dominated by high or medium runoff types (3 and 4) are linked to high rainfall (Groups 1, 2), temperature (Group 14), or both (Group 3). These are groups with a small number of events, except for Group 2 (40 events), which consists of events with extremely low air temperature, and thus snowmelt, low initial snow water equivalent and RCA, and varying SCA. Its main difference from Group 1 is the amount of rainfall, which in the latter case is quite high. On the other

hand, Group 14 is driven solely by temperature. It represents a small number of events that occurred in spring and generated rather high maximum runoff. It is interesting to compare it with Group 16, which mainly represents late spring events, has similar rainfall and snowmelt behaviour, but results in negligible runoff. Perhaps the answer may lie in the difference in initial snow conditions (higher SWE/SCA for Group 14). Group 3 consists of events with high Q_{max} and C that are driven by high temperature and medium rainfall. These are events that occurred exclusively in autumn and spring, and even though the snow-covered area is smaller, their runoff contributing area is larger. The last medium runoff group, Group 6, has a broad rainfall range under low temperature conditions. The maximum runoff and runoff coefficient are high, as well as initial snow amount and coverage. The regime seems to be similar to Group 14, but with the values of climatic variables reversed (high rainfall/low temperature).

Among the groups with low or negligible runoff, Group 5 (89 events

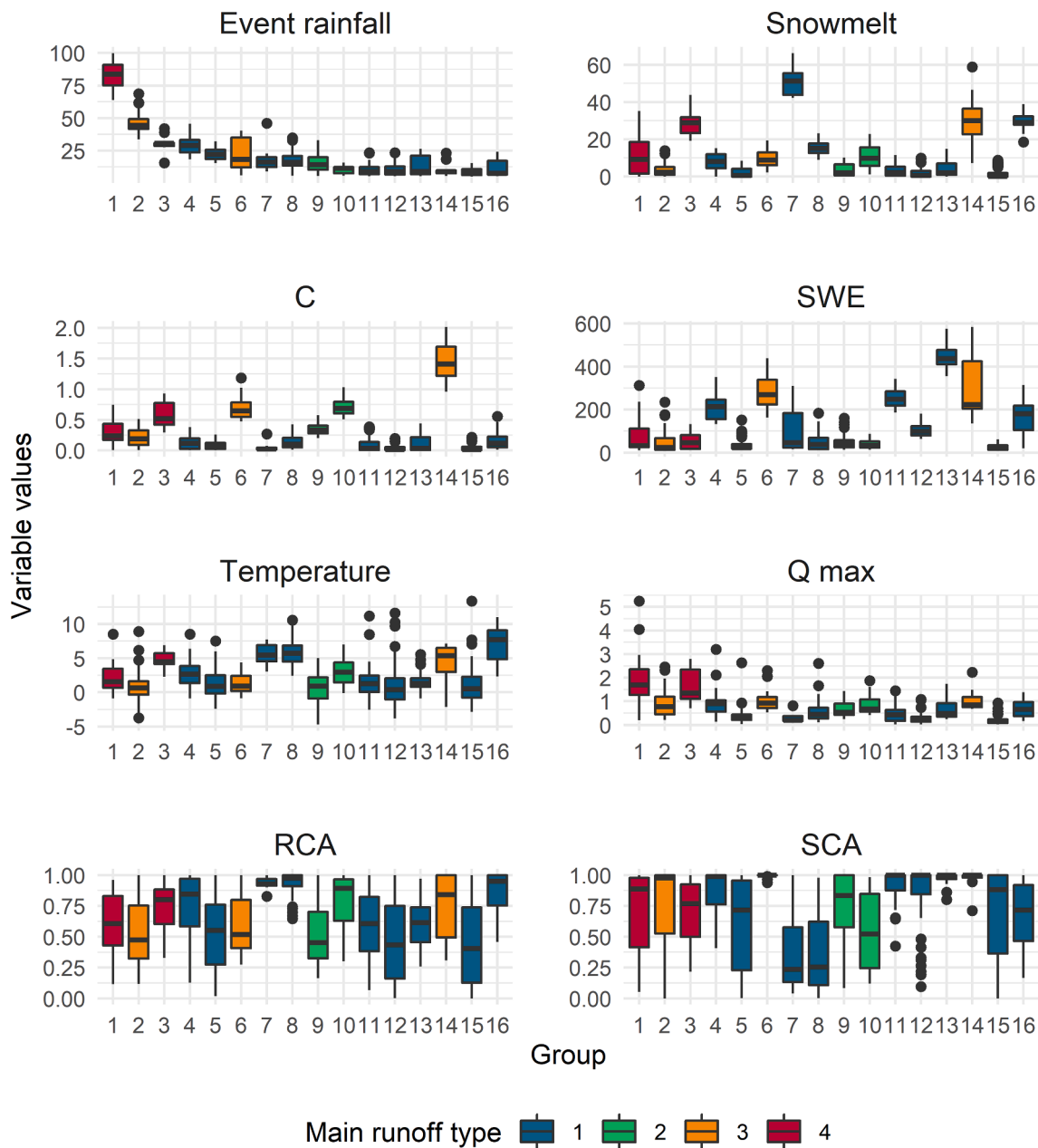


Fig. 10. ROS groups ordered by event rainfall amount (P_{event} in mm). Other variables presented are mean air temperature (T in °C), initial snow water equivalent (SWE in mm), runoff coefficient (C; dimensionless), total snowmelt (in mm), maximum runoff (Q_{max} in mm), mean runoff contributing area (RCA; fraction of catchment area), and mean snow-covered area (SCA; fraction of catchment area).

from October to May) is a reasonable candidate for the most representative group of ROS events. Even though Group 15 has a higher number of events (119), rainfall is minimal and offers no real insight into the processes involved. In contrast, Group 5 is characterized by medium rainfall under cold air temperature, low snowmelt and snow water equivalent, and medium runoff contribution and snow-covered areas. Group 5 events generate low maximum runoff and have one of the lowest runoff coefficients, as expected from runoff type 1.

This is not the case, though, for the 27 events of Group 4. In these events, approximately 30% more rainfall and a two-degree increase in air temperature result in maximum runoff that is comparable to medium and high runoff (types 3 and 4). Further comparison with the high runoff events, and Group 3 in particular, reveals that, even though both groups have similar rainfall, Group 4 presents high initial snow amount and coverage, which could restrain total runoff at lower temperatures. Another noteworthy comparison between runoff type 1 is between Group 7 and Group 8. These groups have identical climatic conditions and very similar snow water equivalent and coverage but result in extremely different snowmelt. Further investigation showed that Group 7 consists of events that occurred solely in the Krkonoše mountains, providing some insight into the importance of catchment properties in snowmelt. The rest of the groups contain a reasonable number of events from both mountain ranges, although Group 10 and Group 13 are dominated by events over the Jeseníky mountains. Summary of the major groups (1, 2, 3, 5, 14) of ROS events according to SOM is depicted in Table 4.

4. Discussion

4.1. Rain-on-snow events characteristics

The absolute number of identified events can depend, beside other things, on the ROS definition and subsequent selection criteria. In particular, thresholds for SWE and rain can affect the number of identified ROS events. However, a preliminary sensitivity analysis revealed that the presented patterns of ROS characteristics remain similar, even if the limits for minimum cumulative rainfall and SWE are changed (SWE = 20 mm, rainfall = 10 mm). Nonetheless, a unified international definition of ROS is needed to make results of different studies comparable. In addition, estimation of the exact amount of liquid precipitation and spatial distribution of snow is also challenging. Rain intensity is usually not constant over a catchment at a given moment. Furthermore, snow cover is distributed unevenly in the catchment because of changing topography and related snow transport. These issues introduce uncertainty into the computation of water inputs and rain-affected area.

In general, weather conditions govern the temporal distribution of ROS over the cold season. Low occurrence of ROS during February was usually caused by lower frequency of liquid precipitation due to low temperatures. In contrast, high numbers of ROS events were observed during months when rainfall is more probable, and the snowpack featured sufficient SWE. During November, catchments usually experience the first snow with low SWE which often melts. May is typified by high temperatures, frequent rain, and a ripped snowpack with shallow snow depths but high densities. Our results thus partially agree with study of Freudiger et al. (2014), who reported ROS occurrence in the

uplands of German catchments from December to April. In contrast, other studies from the European region describing floods initiated by ROS in October (Rössler et al., 2014), December (Garvelmann et al., 2015), or January to March (Freudiger et al., 2014). Thus, we can assume that ROS occurrence varies with regional conditions. Despite their close proximity, even the two mountain ranges analysed here showed different ROS frequencies (Fig. 4). We argue that this can be caused by slightly different synoptic and climate patterns combined with local peculiarities. Jeseníky is more influenced by ombic continentality causing lower precipitation during the winter season. On the other hand, the Krkonoše mountains received more precipitation in the snow seasons (mean = 672 mm) over the study period compared to Jeseníky (mean = 387 mm) due to frequent W and SW winds bringing humidity from the Atlantic (Tolasz, 2007; Žák, 2021). Lower precipitation in Jeseníky can also be caused by their lower mean elevation compared to Krkonoše (Table 1). Different patterns in ROS related to climate were also found by Li et al., (2019) who pointed out that the western mountain ranges of the USA are affected by ROS more frequently than the eastern mountain ranges.

Important aspects within the ROS analysis are the meteorological conditions, which can be used as a proxy for further hydrological modelling and forecasting of hydrological consequences.

Moreover, we can directly compare these meteorological conditions during ROS with other studies. Our results show that identified ROS events were characterised by similar mean air temperatures compared to other European regions. Würzer et al. (2016) found that 90% of 1063 ROS in the Swiss Alps exceeded 1.7 °C and Garvelmann et al. (2015) reported 1.9 °C and 4.4 °C respectively for two ROS events in the Black Forest (Germany). As expected, the high runoffs were associated with the high air temperatures initializing intensive snowmelt (Fig. 8b, c), which also reported Würzer and Jonas (2018). The importance of snowmelt contribution to high runoff generation or even floods is also emphasized by other studies (Garvelmann et al., 2015; Li et al., 2019; Wayand et al., 2015; Würzer and Jonas, 2018). In most cases, snowmelt production at the end of the ROS event is higher than event runoff (compare Fig. 8c and d). This can be explained by the snowmelt runoff process, when not all produced snowmelt appears in a stream, but can be stored in the soil underneath or in the snowpack (Kattelmann, 1987a; Woelber et al., 2018). Furthermore, snowmelt volume is not only dependent on air temperature, but also on snow volume (i.e. SWE and SCA). This is probably the case in the Modrý potok catchment, which showed the most ROS events resulting in high runoff. This catchment is located on the leeward part of the mountain and thus accumulates high amounts of snow, which can often reach about 10 m (Hejzman et al., 2006). This in combination with southern aspects enables high snowmelt rates and prolonged the snow (and thus ROS) season. Nevertheless, the reported typical maximum values of SWE during the identified ROS events are comparable with Garvelmann et al. (2015), who reported the highest SWE of 289 mm during ROS in December in the Black Forrest.

Studies from other regions refer to even higher maximum precipitation values. For instance, during mid-winter, an ROS event in the British Columbia (Canada) saw 343 mm of rain (Trubilowicz and Moore, 2017), and 613 mm in the Swiss Alps (Würzer et al., 2016). Additionally, the recorded maximum rainfall intensity during ROS over Czech catchments was about half compared to another study conducted in the Swiss Alps (Würzer et al., 2016). On the other hand, Würzer et al. (2016) reported a mean rain duration of about 18 h ranging from 3 to 96 h, which is comparable to our study.

Runoff coefficient varied with the runoff group and in some cases runoff volume even exceeded incoming rainfall. High runoff coefficient for ROS events already described in Merz et al. (2006) for the Austrian catchments. We assume that values over 1 can be caused mainly by a combination of two factors: 1) during ROS a substantial amount of snowmelt can be induced due to positive air temperature and additional heat energy from rain and wind; 2) a wet snowpack starts to release pre-event water stored in its pores (liquid water content), while this water is

Table 4

Major groups of rain-on-snow events according to self-organising maps (SOM) classification.

SOM Group	Event rainfall	Air temperature	Runoff type	Number of events
1	Very heavy	Low	High	14
2	Heavy	Low	Medium	40
3	Medium	High	High	11
5	Medium	Low	Low	89
14	Low	High	Medium	11

pushed by the incoming rainwater. This mechanism can be described as a piston flow effect (Feng et al., 2001; Juras et al., 2017; Unnikrishna et al., 2002). Previous physical experiments showed that rainwater contributed about 20–50% to snowpack runoff (Juras et al., 2017).

The SOM classification highlighted that ROS events present very rich patterns, with various combinations between climatic conditions, initial snow regime, and runoff behaviour. As a general remark, rainfall is the main driver of maximum runoff and runoff in general. However, the events that are associated with the high rainfall can result to either high (Group 1) or medium runoff (Groups 2) types, with events in Group 2 appearing three times more often compared to the events of Group 1 (Table 4). Temperature is found to have a secondary role, amplifying, or weakening runoff response depending on initial snow water equivalent. It is likely that there might be some temperature threshold, controlling the role of existing snow amount to enhance or constrain the intensity of ROS events. This is a plausible interpretation of the comparison between Group 3 and Group 4, but a clear relationship remains inconclusive. It might seem counter-intuitive, but the representation of the enhanced variety in the ROS event features is one of the main benefits of using SOM, or any other classification algorithm, because it reveals the underlying complexity of the phenomenon.

4.2. The role of snowpack in runoff generation during rain-on-snow

The effect of snow cover on runoff generation is ambiguous; on the one hand, snowpack holds rainwater and, on the other, snowmelt strengthens runoff. The results show that not only SWE but also SCA plays an important role in generating ROS event runoff. The vast majority of the analysed ROS events (82%) caused only negligible or low event runoff. This means that most of the incoming rainfall during ROS was held by the snow-covered catchment, which involves retention in the snowpack, soil, or canopy. The snowpack itself can also store a significant amount of rainwater, but the holding capacity of snowpack changes during the season and depends on snow properties like micro-structure (Fierz, 2009; Singh and Singh, 2001). Self-organizing maps revealed that during the 27 ROS events (Group 4), snow cover most significantly prevented extensive runoff. This is because high rainfall (median = 29.1 mm) over a sufficient snowpack (medians; SWE = 214 mm, SCA = 99%) caused only 3.8 mm (median) of the event runoff. Although relatively high Q_{\max} ($0.9 \text{ mm}\cdot\text{h}^{-1}$) was also reached during these events, this was probably caused by high baseflow and not by event runoff. High rainwater storage by snow-covered catchments can be also seen within the 54 ROS events (Groups 1, 2) which received the highest amount of rainfall, but about 76–81% was stored in the catchment and only a little portion appeared in runoff. This fact is documented by the lowest water budget and relatively low runoff coefficient (Fig. 10). Groups 1 and 2 are also related to low SWE and shallow snowpack, which can only store a limited amount of liquid water. Therefore, within these groups it was most likely that the rainwater was also stored in the soil or retained by the vegetation cover, because SWE was often insufficient to hold such amounts of water. Although a significant amount of rainwater was stored during ROS events within Groups 1 and 2, total water input was so significant that stream runoff reacted with a massive increase.

The highest runoffs (Groups 1 and 3) were associated with high inputs of meltwater in combination with high rainfall (Fig. 6), but also with the lower SWE and SCA (Fig. 10). This is in agreement with other studies (e.g. Rücker et al., 2019; Würzer and Jonas, 2018). On the other hand, significant runoff response occurred also during 21 ROS events (Group 6), when sufficient snow cover (SCA = 100%, SWE = 269 mm; median) was hit by a considerable amount of rain (median = 18.3 mm). Runoff responded with high Q_{\max} and C, which could be explained by two effects. First, the combination of high baseflow and event runoff. Second, the higher amount of discharged water can also be generated due to the piston flow effect, when incoming rainwater pushes out less mobile meltwater. The piston flow effect is closely discussed in Section

4.1. Both effects can also explain the runoff reaction of Group 14 (Fig. 10), when mostly lower amounts of rainfall resulted in the highest runoff coefficients and even in runoff excess within group 14 (positive water budget). Surprisingly, we do not see similar runoff reactions within ROS events of Group 7, featured by the highest snowmelt and rainfall comparable to Group 6. Nevertheless, the most significant difference between Group 7 and Groups 6 and 14 is lower SWE, SCA, and ROS affected area.

The highest Q_{\max} (Groups 1–4, 6, 14) were rarely generated from the entire catchment area. In particular, when RCA is smaller than SCA (Fig. 7 and Fig. 10), then runoff is generated mostly within the snowpack. Würzer and Jonas (2018) reported that, in Swiss catchments, high runoff was connected to snow cover together with high air temperatures. Moreover, they emphasize the significance of SCA, while snow-free parts of the catchment caused higher runoff earlier compared to snow-covered parts. Our results are ambiguous regarding this issue and therefore cannot support their conclusions about high runoff timing. Surprisingly, most of the ROS events resulting in high runoff supported by high snowmelt (Group 1, 3), occurring during early winter (Nov–Dec, $n = 14$) and only few ($n = 6$) occurred during spring (Apr - May). This finding differs from the study of Würzer and Jonas (2018), which reported most of highest runoffs during spring months.

However, snowmelt water does not necessarily have to propagate to streamflow. Some part of snowmelt is usually stored in the snowpack or infiltrates into the soil (Woelber et al., 2018). This can be clearly seen in Group 7, and partially in Group 16, where a significant amount of snowmelt appeared over the course of ROS, but apparently only a fraction appeared in the runoff. The importance of snowmelt during runoff generation can also be documented by comparison of Groups 5 and 10. Eventhough both groups are characterised by similar snowpack and water input (median = 24.1 mm and 24.9 mm, respectively), Group 10 caused double the Q_{\max} and Q_{event} . This can be explained by different snowmelt volumes, where in Group 5 only 8% of the water input was snowmelt, compared to 54% within Group 10.

4.3. Uncertainties of modelling and analysis

A potential uncertainty in simulating SWE data may be the threshold temperature for precipitation phase partition and snowmelt. Threshold temperature controls the amount of snowfall and thus snow storage, and it was calibrated by the HBV model separately for each catchment. Testing of different HBV model structures, which was recently done partly over the same study area, did not show a considerable improvement of use, i.e., two threshold temperatures with linear or exponential functions for precipitation phase partition between these two threshold temperatures (Girons Lopez et al., 2020). Overall, the study by Girons Lopez et al. (2020) tested 64 modifications of the HBV model snow routine and showed that the original snow routine (also used in our study) included in the HBV model provided relatively good results, although some modifications might represent an interesting alternative, such as using an exponential snowmelt function or seasonally-variable melt factor. Nevertheless, increased model complexity does not necessarily mean better model ability to reproduce SWE and runoff.

Uncertainty issues resulting from SWE data used for ROS analysis might be overcome by using an energy balance approach, which would better reflect the physical nature of the snowmelt process. However, our analysis was done at a multi-catchment level over a broader region, which did not allow for the use of energy balance approaches since sufficiently dense input data from climate stations are only available for precipitation and air temperature. Other necessary meteorological data do not sufficiently cover the whole region and elevation extent, or they are even missing. In general, energy balance calculations are usually employed at a site level (see i.e., Hotovy and Jenicek, 2020; Moeser et al., 2020) and such approaches are not easily transferable to larger regions, for which the degree-day approach is widely used (Freudiger et al., 2014) or they even rely on observed SWE data (McCabe et al.,

2007). However, we introduced a downscaling approach of daily snowmelt data to hourly step to reflect its diurnal cycle (Eq. 1). The limitation of this approach is clearly the fact that, the diurnal cycle has been considered only for days when snowmelt was simulated by the HBV model.

Due to a lack of data, we ignored snow microstructure in the analysis, although this factor plays a crucial role in water movement, storage, and release (Juras et al., 2017; Würzer et al., 2017). Moreover, detailed snowpack data are usually provided at a point scale, which is not necessarily representative for the catchment scale (Würzer and Jonas, 2018). Waldner et al. (2004) reported that a heterogeneous snowpack is more often connected to preferential flow, contrary to matrix flow which appears more likely in homogenous snow. Although rainwater can be transported faster through preferential flow paths (Hirashima et al., 2010; Juras et al., 2017; Waldner et al., 2004), a considerable amount of liquid water can also be stored above capillary barriers (Avanzi et al., 2016).

Beside the above-mentioned hydrometeorological descriptors, runoff generation during the ROS is also driven by individual catchment characteristics, such as the presence and type of forest, bedrock, aspect or slope (Kattelmann, 1987b; Li et al., 2019). For instance, we can assume that forested catchments would respond differently to the given ROS event, compared to catchments with less or no portion of forest. First, precipitation is usually reduced in forested catchments due to canopy interception (Beria et al., 2018). Second, snowmelt production is usually lower compared to open sites due to less snow and reduction of solar radiation and turbulent heat exchange (Garvelmann et al., 2014). However, more studies relating to catchment characteristics and runoff response would be beneficial to even better understand runoff generation during ROS.

5. Conclusions

Employing HBV model and geomorphological catchment characteristics, we identified 611 ROS events over the study period of 10 winter seasons (2004–2014). Most ROS events did not cause a significant runoff increase. Identified ROS events were sorted into four types according to runoff response. Furthermore, with self-organising maps, 16 groups of ROS events with similar characteristics were classified that helped us shed some light on the links between hydrometeorological descriptors and runoff response. Our results revealed that snowpack is an important element protecting catchments against floods, because 82% of ROS events resulted in low or negligible runoff. We argue that this is probably a consequence of high storage potential of snow-covered catchment, while a sufficient volume of incoming rainfall did not appear directly in runoff.

In contrast, when heavy rainfall met shallow and sparsely distributed snow cover, supported by intense snowmelt, streamflow responded mostly with high runoffs. High rainfall or snowmelt alone were usually not strong enough to initiate high runoffs. Nevertheless, the highest runoffs were not extreme, while only 29 ROS events exceeded a 1-year return period, but not higher. Seasonal distribution of ROS also plays its role in runoff response. Medium or high runoffs were mostly observed during late autumn or spring, when snowpack is usually low and high air temperatures support intense snowmelt.

Despite the spatial proximity of investigated mountain ranges, we found that the frequency and magnitude of the main drivers governing runoff response differ significantly. ROS events were more frequent in the Krkonoše Mts., where they also caused higher runoffs. This dissimilarity is likely because of less precipitation in the Jeseníky Mts. due to different climatic patterns.

We hope that our study may contribute to better forecasting of ROS runoff response over low and medium mountain ranges in central Europe. Further research should be oriented to the implementation of catchment characteristics and snowpack structure, which can bring even better insights necessary for the understanding of ROS events and

subsequent runoff response.

CRediT authorship contribution statement

Roman Juras: Conceptualization, Formal analysis, Supervision, Methodology, Data curation, Writing – original draft, Visualization. **Johanna R. Blöcher:** Methodology, Data curation, Visualization, Funding acquisition, Formal analysis, Writing – original draft. **Michal Jenicek:** Methodology, Data curation, Formal analysis, Writing – original draft, Visualization. **Ondrej Hotovy:** Formal analysis, Writing – review & editing. **Yannis Markonis:** Methodology, Writing – original draft, Visualization, Formal analysis.

Declaration of Competing Interest

The authors declare that they have no known competing financial interests or personal relationships that could have appeared to influence the work reported in this paper.

Acknowledgements

We would like to thank the Internal Grant Agency of Faculty of Environmental Sciences, Czech University of Life Sciences, Prague (project no. 20184236) and the Charles University Grant Agency (project no. GAUK 272119) for financial support of this research. We are also grateful to the Czech Hydrometeorological Institute that provided hydrological and climatic data. Thanks are due to Mark Sixsmith, who carefully proofread the manuscript, and Ondřej Ledvinka from CHMI for providing hydrological data and valuable comments.

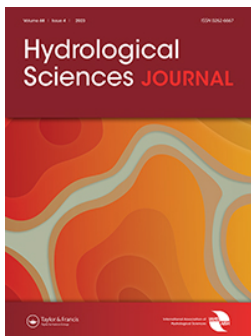
Appendix A. Supplementary data

Supplementary data to this article can be found online at <https://doi.org/10.1016/j.jhydrol.2021.127002>.

References

- Avanzi, F., Hirashima, H., Yamaguchi, S., Katsushima, T., Michele, C.D., 2016. Observations of capillary barriers and preferential flow in layered snow during cold laboratory experiments. *Cryosphere* 10, 2013–2026. <https://doi.org/10.5194/tcd-9-6627-2015>.
- Badoux, A., Hofer, M., Jonas, T., 2013. Hydrometeorologische Analyse des Hochwasserereignisses vom 10. Oktober 2011. Birmensdorf, Eidg. Forschungsanstalt für Wald, Schnee und Landschaft WSL; Davos, WSL-Institut für Schnee- und Lawinenforschung SLF 92.
- Baggi, S., Schweizer, J., 2008. Characteristics of wet-snow avalanche activity: 20 years of observations from a high alpine valley (Dischma, Switzerland). *Nat. Hazards* 50 (1), 97–108. <https://doi.org/10.1007/s11069-008-9322-7>.
- Beniston, M., Farinotti, D., Stoffel, M., Andreassen, L.M., Coppola, E., Eckert, N., Fantini, A., Giacomoni, F., Hauck, C., Huss, M., Huwald, H., Lehning, M., López-Moreno, J.-I., Magnusson, J., Marty, C., Morán-Tejeda, E., Morin, S., Naaïm, M., Provenzale, A., Rabatel, A., Six, D., Stötter, J., Strasser, U., Terzago, S., Vincent, C., 2018. The European mountain cryosphere: a review of its current state, trends, and future challenges. *Cryosphere* 12 (2), 759–794. <https://doi.org/10.5194/tc-12-759-2018>.
- Beria, H., Larsen, J.R., Ceperley, N.C., Michelon, A., Vennemann, T., Schaeffli, B., 2018. Understanding snow hydrological processes through the lens of stable water isotopes. *WIREs Water* 5 (6). <https://doi.org/10.1002/wat2.1311>.
- Bintanja, R., 2018. The impact of Arctic warming on increased rainfall. *Sci. Rep.* 8, 1–6. <https://doi.org/10.1038/s41598-018-34450-3>.
- Blöschl, G., Bierkens, M.F.P., Chambel, A., Cudennec, C., Destouni, G., Fiori, A., Kirchner, J.W., McDonnell, J.J., Savenijje, H.H.G., Sivapalan, M., Stumpff, C., Toth, E., Volpi, E., Carr, G., Lupton, C., Salinas, J., Széles, B., Viglione, A., Aksoy, H., Allen, S.T., Amin, A., Andréassian, V., Arheimer, B., Aryal, S.K., Baker, V., Bardsley, E., Barendrecht, M.H., Bartosova, A., Batelaan, O., Berghuijs, W.R., Beven, K., Blume, T., Bogaard, T., Borges de Amorim, P., Böttcher, M.E., Boulet, G., Breinl, K., Brilly, M., Brocca, L., Buytaert, W., Castellarin, A., Castelletti, A., Chen, X., Chen, Y., Chen, Y., Chiffard, P., Claps, P., Clark, M.P., Collins, A.L., Croke, B., Dathe, A., David, P.C., de Barros, F.P.J., de Rooij, G., Di Baldassarre, G., Driscoll, J. M., Duethmann, D., Dwivedi, R., Eris, E., Farmer, W.H., Feiccabrino, J., Ferguson, G., Ferrari, E., Ferraris, S., Fersch, B., Finger, D., Foglia, L., Fowler, K., Gartsmann, B., Gascoin, S., Gaume, E., Gelfan, A., Geris, J., Gharari, S., Gleeson, T., Glendell, M., Gonzalez Bevacqua, A., González-Dugo, M.P., Grimaldi, S., Gupta, A.B., Guse, B., Han, D., Hannah, D., Harpold, A., Haun, S., Heal, K., Helfricht, K., Herrnegger, M., Hipsey, M., Hlaváčiková, H., Hohmann, C., Holko, L., Hopkinson, C.,

- Rousi, E., Ulbrich, U., Rust, H.W., Anagnostopoulou, C., 2017. An NAO climatology in reanalysis data with the use of self-organizing maps. In: *Perspectives on Atmospheric Sciences*. Springer, pp. 719–724.
- Rücker, A., Boss, S., Kirchner, J.W., Freyberg, J.V., 2019. Monitoring snowpack outflow volumes and their isotopic composition to better understand streamflow generation during rain-on-snow events. *Hydrol. Earth Syst. Sci.* 23 (January), 2983–3005. <https://doi.org/10.5194/hess-23-2983-2019>.
- Seibert, J., 2000. Multi-criteria calibration of a conceptual runoff model using a genetic algorithm. *Hydrol. Earth Syst. Sci.* 4 (2), 215–224.
- Seibert, J., Vis, M.J.P., 2012. Teaching hydrological modeling with a user-friendly catchment-runoff-model software package. *Hydrol. Earth Syst. Sci.* 16 (9), 3315–3325. <https://doi.org/10.5194/hess-16-3315-2012>.
- Seibert, J., Jenicek, M., Huss, M., Ewen, T., 2014. Snow and Ice in the Hydrosphere. In: Haeberli, W., Whiteman, C. (Eds.), *Snow and Ice-Related Hazards, Risks, and Disasters*. Elsevier, Amsterdam, pp. 99–137.
- Singh, P., Singh, V.P., 2001. *Snow and Glacier Hydrology*, first ed. Kluwer Academic Publishers, Boston.
- Sui, J., Koehler, G., Krol, F., 2010. Characteristics of rainfall, snowmelt and runoff in the headwater region of the main river watershed in Germany. *Water Resour. Manag.* 24 (10), 2167–2186. <https://doi.org/10.1007/s11269-009-9545-8>.
- Tobin, C., Schaeffli, B., Nicótina, L., Simoni, S., Barrenetxea, G., Smith, R., Parlange, M., Rinaldo, A., 2013. Improving the degree-day method for sub-daily melt simulations with physically-based diurnal variations. *Adv. Water Resour.* 55, 149–164. <https://doi.org/10.1016/j.advwatres.2012.08.008>.
- Tolasz, R., 2007. *Climate Atlas of Czechia*. Czech Hydrometeorological Institute, Prague.
- Trubilowicz, J.W., Moore, R.D., 2017. Quantifying the role of the snowpack in generating water available for run-off during rain-on-snow events from snow pillow records. *Hydrol. Process.* 31 (23), 4136–4150. <https://doi.org/10.1002/hyp.11310>.
- Unnikrishna, P.V., McDonnell, J.J., Kendall, C., 2002. Isotope variations in a Sierra Nevada snowpack and their relation to meltwater. *J. Hydrol.* 260 (1-4), 38–57. [https://doi.org/10.1016/S0022-1694\(01\)00596-0](https://doi.org/10.1016/S0022-1694(01)00596-0).
- Waldner, P.A., Schneebeli, M., Schultze-Zimmermann, U., Flüeler, H., 2004. Effect of snow structure on water flow and solute transport. *Hydrol. Process.* 18 (7), 1271–1290. <https://doi.org/10.1002/hyp.1401>.
- Wayand, N.E., Lundquist, J.D., Clark, M.P., 2015. Modeling the influence of hypsometry, vegetation, and storm energy on snowmelt contributions to basins during rain-on-snow floods. *Water Resour. Res.* 51 (10), 8551–8569. <https://doi.org/10.1002/2014WR016576>.
- Wehrens, R., Krusselbrink, J., 2018. *Flexible Self-Organizing Maps in kohonen 3.0*. J. Stat. Software.
- Woelber, B., Maneta, M.P., Harper, J., Jencso, K.G., Payton Gardner, W., Wilcox, A.C., López-Moreno, I., 2018. The influence of diurnal snowmelt and transpiration on hillslope throughflow and stream response. *Hydrol. Earth Syst. Sci.* 22 (8), 4295–4310. <https://doi.org/10.5194/hess-22-4295-2018>.
- Würzer, S., Jonas, T., 2018. Spatio-temporal aspects of snowpack runoff formation during rain on snow. *Hydrol. Process.* 32 (23), 3434–3445. <https://doi.org/10.1002/hyp.13240>.
- Würzer, S., Jonas, T., Wever, N., Lehning, M., 2016. Influence of initial snowpack properties on runoff formation during rain-on-snow events. *J. Hydrometeorol.* 17 (6), 1801–1815. <https://doi.org/10.1175/JHM-D-15-0181.1>.
- Würzer, S., Wever, N., Juras, R., Lehning, M., Jonas, T., 2017. Modeling liquid water transport in snow under rain-on-snow conditions considering preferential flow. *Hydrol. Earth Syst. Sci.* 21 (August), 1741–1756. <https://doi.org/10.5194/hess-2016-351>.
- Žák, M., 2021. Email message to author (in Czech).
- Zambrano-Bigiarini, 2020. hydroTSM: Time Series Management, Analysis and Interpolation for Hydrological Modelling. R package version 0.6-0. <https://doi.org/10.5281/zenodo.3706912>.
- Zhong, X., Zhang, T., Wang, K., 2014. Snow density climatology across the former USSR. *Cryosphere* 8 (2), 785–799. <https://doi.org/10.5194/tc-8-785-2014>.



Changes in rain-on-snow events in mountain catchments in the rain-snow transition zone

Ondrej Hotovy, Ondrej Nedelcev & Michal Jenicek

To cite this article: Ondrej Hotovy, Ondrej Nedelcev & Michal Jenicek (2023) Changes in rain-on-snow events in mountain catchments in the rain-snow transition zone, Hydrological Sciences Journal, 68:4, 572-584, DOI: [10.1080/02626667.2023.2177544](https://doi.org/10.1080/02626667.2023.2177544)

To link to this article: <https://doi.org/10.1080/02626667.2023.2177544>



© 2023 The Author(s). Published by Informa UK Limited, trading as Taylor & Francis Group.



[View supplementary material](#)



Published online: 10 Mar 2023.



[Submit your article to this journal](#)



Article views: 1935



[View related articles](#)



[View Crossmark data](#)



Citing articles: 6 [View citing articles](#)

Changes in rain-on-snow events in mountain catchments in the rain–snow transition zone

Ondrej Hotovy , Ondrej Nedelcev  and Michal Jenicek 

Department of Physical Geography and Geoecology, Charles University, Prague, Czechia

ABSTRACT

A shift from snowfall to rain affecting snow storage is expected in future. Consequently, changes in rain-on-snow (ROS) events may occur. We evaluated the frequency and trends in ROS events and their runoff responses at different elevations related to changes in climate variables. We selected 40 central European mountain catchments located in the rain–snow transition zone, and used a conceptual catchment model to simulate runoff components for the period 1965–2019. The results showed large temporal and spatial differences in ROS events and their respective runoff responses across individual study catchments and elevations, with primarily an ROS increase at highest elevations and a decrease at lower elevations during spring. ROS events contributed 3–32% to the total seasonal direct runoff. The detected trends reflect changes in climate and snow variables, with an increase in air temperature resulting in the decrease in snowfall fraction and shorter snow cover period.

ARTICLE HISTORY

Received 26 July 2022
Accepted 13 January 2023

EDITOR

A. Castellarin

ASSOCIATE EDITOR

S. Kampf

KEYWORDS

rain-on-snow events; rain-on-snow variability; rain-on-snow trends; rain–snow transition zone; climate change

1 Introduction

Seasonal snowpack significantly influences catchment runoff and thus represents an important component of the hydrological cycle. Moreover, snowpack accumulated during the cold season affects groundwater recharge and thus influences spring runoff and summer low flows (Hammond *et al.* 2018, Jenicek and Ledvinka 2020, Vlach *et al.* 2020). Predicted changes in climate variables will have a strong impact on hydrometeorological processes including snow storage and snowmelt dynamics (Jennings *et al.* 2018, Sezen *et al.* 2020). Additionally, changes in precipitation intensity and distribution, as well as a shift from snowfall to rain, are expected (Serquet *et al.* 2011, Musselman *et al.* 2018, Blahusiakova *et al.* 2020, Li *et al.* 2020). These changes, among others, affect rain-on-snow (ROS) events, which are considered to be one of the major causes of winter floods in many regions (Pradhanang *et al.* 2013, Würzer *et al.* 2017, Brunner *et al.* 2019) and which may occur more frequently in the future (Freudiger *et al.* 2014, Jennings *et al.* 2018, Musselman *et al.* 2018). Due to their complex and still not fully understood behaviour, ROS events are considered to be one of the major unsolved problems in hydrology (Blöschl *et al.* 2019). According to Il Jeong and Sushama (2017), 80% of the annual January to May maximum daily runoff is associated with ROS for large parts of Northern America. Moreover, it is still not clear how climate change will affect ROS occurrence due to its complex nature (Sezen *et al.* 2020). Changes in the frequency and intensity of ROS events in a warming climate may vary temporally and spatially, reflecting changes in snow cover and the amount of rain, while projections reveal a decrease in snow

storage for all elevations, time periods and emission scenarios (Marty *et al.* 2017, Notarnicola 2020, Jenicek *et al.* 2021).

There is still considerable uncertainty regarding how the frequency of ROS events will change with temperature increase, while peak streamflow caused by ROS is predicted to increase due to more rapid melting from enhanced energy inputs, and a warmer snowpack during future ROS (López-Moreno *et al.* 2021). Potential ROS changes can be also attributed to changes in the occurrence of dominant weather patterns leading to ROS events, or to variations of the freezing point line (Krug *et al.* 2020, Ohba and Kawase 2020). Beniston and Stoffel (2016) revealed that the number of ROS events could increase by 50% as an initial response to a temperature increase of 2–4°C compared to the present, but decline thereafter when the air temperature increase exceeds 4°C. The same study showed that the temperature increase observed in north-eastern Switzerland for the 1960–2015 period has contributed directly to the increase in the number of ROS events by about 40% at low elevations, and by 200% at high elevations. Results of other recent studies, however, showed that the number of ROS events is expected to decrease in low- and mid-latitude regions by reducing the number of days with snow cover on the ground (McCabe *et al.* 2007, Surfleet and Tullos 2013, Musselman *et al.* 2018, Li *et al.* 2019, López-Moreno *et al.* 2021). In contrast, ROS events are predicted to occur more frequently in the future due to an increase in the number of days with rain in both high-elevation and high-latitude regions (Surfleet and Tullos 2013, Il Jeong and Sushama 2017, Trubilowicz and Moore 2017, Musselman *et al.* 2018, Li *et al.*

CONTACT Ondrej Hotovy  ondrej.hotovy@natur.cuni.cz  Department of Physical Geography and Geoecology, Charles University, Albertov 6, Prague 128 00, Czechia

 Supplemental data for this article can be accessed online at <https://doi.org/10.1080/02626667.2023.2177544>

© 2023 The Author(s). Published by Informa UK Limited, trading as Taylor & Francis Group.

This is an Open Access article distributed under the terms of the Creative Commons Attribution-NonCommercial-NoDerivatives License (<http://creativecommons.org/licenses/by-nc-nd/4.0/>), which permits non-commercial re-use, distribution, and reproduction in any medium, provided the original work is properly cited, and is not altered, transformed, or built upon in any way.

2019). Future projections for the humid mountain regions suggest an overall ROS increase in the middle of the winter season (from November to March) since more precipitation will fall as rain rather than snow (Il Jeong and Sushama 2017). In contrast, a decrease in ROS is expected for early and late winter due to the shortening of the period with existing snow cover on the ground (Sezen *et al.* 2020). Similar changes may occur in many regions that experience both snow and rain during winter months (Cohen *et al.* 2015). A broader area is expected to become vulnerable to changes in ROS in the future, as future climate projections show an increase in the frequency and areal extent of ROS, including many parts of the Arctic over the next 50 years (Rennert *et al.* 2009).

An assessment of changes in ROS events for large areas should be preceded by a detailed analysis of all processes and influencing factors affecting ROS situations. Several recent studies have attempted to better understand these processes and factors for larger areas. The results of Würzer *et al.* (2016) for the Swiss Alps demonstrated the strong influence of initial snowpack properties on runoff formation during ROS, indicating that the retention capacity of the snowpack is crucial during ROS events (Garvelmann *et al.* 2015, Brandt *et al.* 2022). Nevertheless, not all ROS events generate direct runoff, since the snowpack can store a large amount of incoming rainwater (Wayand *et al.* 2015, Juras *et al.* 2021). Therefore, one important issue is to properly understand rainwater behaviour in the snowpack (Surfleet and Tullos 2013, Juras *et al.* 2017, Würzer *et al.* 2017). Another important issue is to consider ROS events in the context of the entire snowpack energy balance, which controls overall snowmelt amount and dynamics (Brandt *et al.* 2022). Although the heat supplied by the rain during ROS usually contributes rather a minor energy source for snowmelt – usually up to 10% of the total energy balance at longer temporal resolutions (Mazurkiewicz *et al.* 2008, Trubilowicz and Moore 2017, Li *et al.* 2019) – rain heat input is more important for snowmelt generation at shorter temporal resolutions (Hotovy and Jenicek 2020). The heat from rain may contribute more than 25% of the total energy accessible for melt during days with heavy rain (Jennings and Jones 2015, Hotovy and Jenicek 2020), resulting in faster snowmelt and consequently related to a higher flood risk. Furthermore, rainfall events are often associated with additional turbulent (sensible and latent) heat input (Marks *et al.* 1998, Garvelmann *et al.* 2014), and longwave radiation that can speed up snowmelt as well (Sezen *et al.* 2020).

The interaction of different influencing factors makes it difficult to accurately predict the effect of snow cover on runoff formation for an upcoming ROS event (Würzer *et al.* 2016). Most ROS studies use similar approaches, for example they are event based and region specific (Li *et al.* 2019). Although ROS events have been a focus for hydrologists over the last several decades, the physical complexity and associated impacts of ROS has led to varying definitions and methods applied in their assessments (Pall *et al.* 2019). For example, various threshold values for air temperature, total precipitation, snowpack and runoff characteristics are used for ROS event definition (Freudiger *et al.* 2014, Würzer *et al.* 2016, Bieniek *et al.* 2018, Crawford *et al.* 2020, Brandt *et al.* 2022). Studies performed in different regions around the world have reported a

wide range (4–75%) of snowmelt contribution to runoff during ROS (Li *et al.* 2019), thus, any regional comparison is complicated. The quantification of ROS, and the assessment of their changes, is also made difficult because ROS events generally occur at higher elevations and/or latitudes, which typically have sparse observation networks (Pall *et al.* 2019). Therefore, several studies employed modelling approaches as suitable tools to detect ROS events (Mazurkiewicz *et al.* 2008, Wayand *et al.* 2015, Beniston and Stoffel 2016, Wever *et al.* 2016, Würzer and Jonas 2018), or to predict changes in the ROS occurrence reflecting existing climate projections implemented into hydrological models (Bieniek *et al.* 2018, Ohba and Kawase 2020).

Although several studies have focused on changes in ROS frequency and intensity, trend analysis of both ROS occurrence and related runoff response is rather scarce. Most of these studies, furthermore, were done at a catchment scale with limited focus on elevation, which highly influences precipitation phase and snow cover. Additionally, most of the central European studies were done in the region of the Alps, while studies performed in other, usually lower elevation mountain ranges are rare. The focus on lower elevation mountain ranges is, however, important since they represent areas in rain–snow transition zones with typically large changes in snow storage, affecting ROS occurrence (Freudiger *et al.* 2014, Juras *et al.* 2021, Nedelcev and Jenicek 2021). Understanding the spatial distribution, temporal variability, and influencing drivers causing ROS in a changing climate is critically important to better predict these events and to create strategies to mitigate their effects on the terrestrial ecosystems and society (Bieniek *et al.* 2018, Brandt *et al.* 2022).

To fill this research gap, the objectives of this study were (1) to evaluate the frequency and ongoing trends in ROS events at different elevations and to relate them to changes in climate variables, and (2) to analyse changes in runoff responses related to ROS events. We selected 40 near-natural central European mountain catchments located in rain–snow transition zones with significant snow influence on runoff. Our study benefits from long time series (1965–2019) of daily meteorological and hydrological variables, which enabled us to simulate several components of the water cycle for different elevations using a semi-distributed conceptual model.

2 Material and methods

2.1 Study area and data monitoring

The study was performed for 40 catchments located in five mountain ranges in Czechia (Fig. 1). The same set of study catchments was used in Nedelcev and Jenicek (2021). Selected characteristics of all study catchments are listed in Table S1 in the Supplementary material. Mountain catchments with near-natural streamflow, with snow influence on runoff and with no major human influences were selected. Additionally, the availability of long-term time series of hydrological and meteorological data were an important criterion for the selection. We used time series of daily precipitation and daily mean air temperature, both for the period 1965–2019, and mean daily discharge and weekly snow water equivalent (SWE), both for

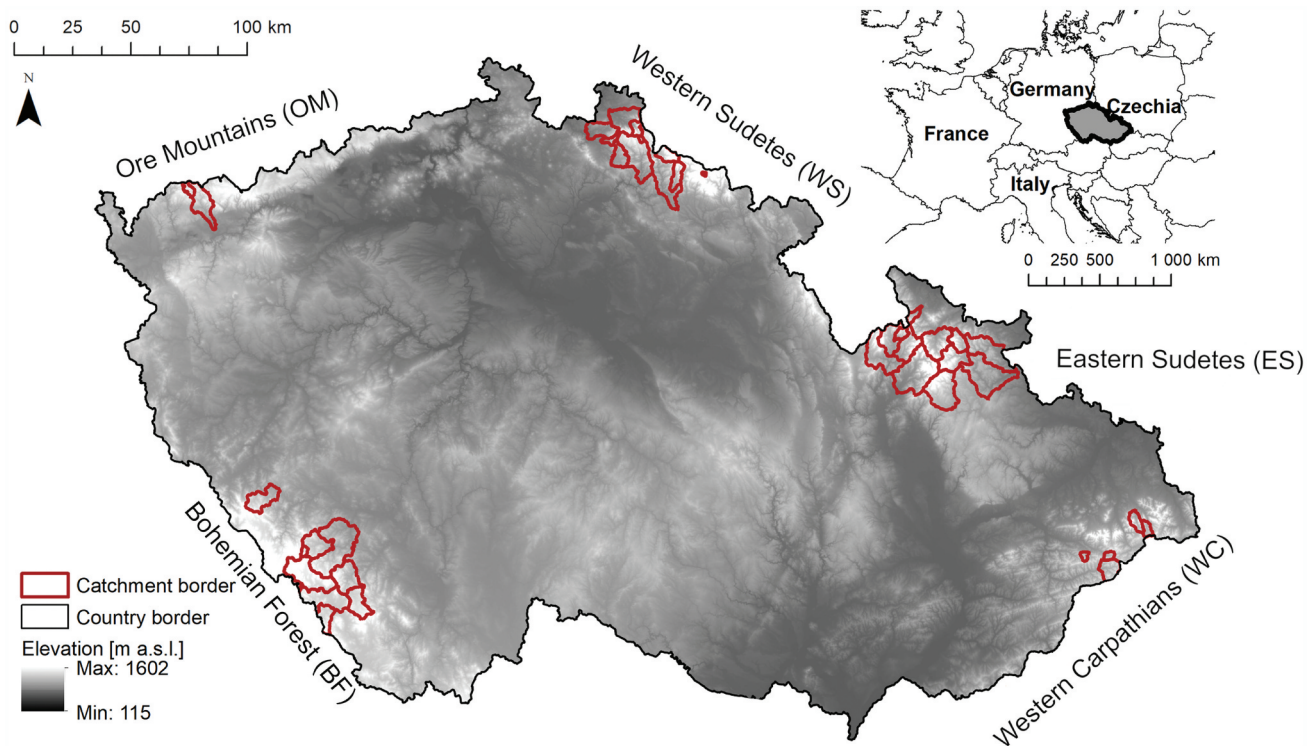


Figure 1. Location of the 40 study catchments, located in five mountain ranges in Czechia (Nedelcev and Jenicek 2021).

the period 1980–2014. All data were available from 22 meteorological stations and 40 hydrological stations operated by the Czech Hydrometeorological Institute (CHMI) and were further used in a hydrological model, described in the next section. Station and modelled data together enabled the analysis of 55 seasons from 1965 to 2019, where one season represents a hydrological year (1 November–31 October).

2.2 HBV-light model

A semi-distributed bucket-type Hydrologiska Byråns Vattenbalansavdelning model (Lindström *et al.* 1997) in its software implementation “HBV-light” (Seibert and Vis 2012) was used to simulate individual components of the rainfall–runoff process, including direct runoff and baseflow. Each study catchment was divided into elevation zones at intervals of 100 m, for which all input data at a daily resolution were distributed using calibrated lapse rates for both air temperature and precipitation. The HBV model consists of four basic routines – a snow routine, soil routine, groundwater routine, and routing function to simulate catchment runoff – based on time series of observed daily mean air temperature, daily precipitation and monthly potential evapotranspiration calculated using the temperature-based method defined by Oudin *et al.* (2005). The details of the model structure can be found in Seibert and Vis (2012) or Giron Lopez *et al.* (2020).

The calibration and validation of the model were originally done for previous studies which share the same set of study catchments (Jenicek and Ledvinka 2020, Jenicek *et al.* 2021). We thus provide the basic description here and refer readers to the above studies for a more detailed description of the procedure. The HBV model was calibrated automatically for each

of the study catchments against observed daily runoff and weekly SWE for the calibration period 1980–1997, using a genetic optimization algorithm (Seibert 2000). One hundred optimized parameter sets resulting from 100 calibration trials were derived and further used to create 100 simulations for each catchment. Finally, a median simulation for each catchment was calculated and used for the following analyses. The model was validated for the period 1998–2014.

A combination of several objective criteria was used to evaluate the goodness of fit of the model: (1) logarithmic Nash-Sutcliffe efficiency for runoff (Nash and Sutcliffe 1970) with 60% weight, (2) Nash-Sutcliffe efficiency for SWE with 20% weight, and (3) volume error with 20% weight. These three criteria were weighted to calculate the resulting objective function of the model.

The results of model calibration and testing were detailed in Jenicek *et al.* (2021) and Nedelcev and Jenicek (2021). These studies showed the model’s ability to correctly simulate SWE and runoff including existing trends in time series. In this new study, we additionally provide throughout an assessment of the model’s ability to simulate SWE and snowmelt related to ROS events (Section 3.1 and Supplementary material, Figs S1–S5).

2.3 Definition of ROS days and events

Several selection criteria were defined to identify individual ROS days and ROS events that may occur during periods with snow cover and rainfall occurrence. Here, we distinguished between an ROS day and an ROS event as follows.

An ROS day was identified when the three following threshold conditions were fulfilled: (1) the daily mean air temperature was higher than 0°C, determining whether precipitation falls as rain or

snowfall; (2) SWE was higher than 10 mm, ensuring that a sufficiently thick snowpack layer is on the ground; and (3) the rainfall intensity exceeded 5 mm d to avoid negligible amounts of rain or drizzle. The HBV model simulates the three above variables both at a catchment scale and for individual elevation zones, which enabled an analysis of the occurrence of ROS days for each elevation zone across the whole study area.

Unlike the ROS day, the ROS event may include both ROS days and non-ROS days. The duration of the ROS event is calculated from the initial ROS day (Q_1 ; the first day when all three of the above threshold criteria were fulfilled) to the last day (Q_{last}), the day when the maximum simulated runoff was reached. We set the maximum response time to six days, similar to Freudiger *et al.* (2014), to avoid multiple runoff events or long runoff responses caused by multiple interactions (e.g. first rain and then long periods of above-zero temperatures causing snowmelt). Since an ROS event was defined based on the simulated runoff, the related analysis of runoff responses was performed at a catchment scale only.

2.4 Runoff classes and hydrological response calculation

Detected ROS events were divided into four runoff classes (Table 1) based on the change of simulated runoff between the day preceding the first ROS day (Q_0 , zero day) and the day with the maximum event runoff (Q_{last}), to assess the intensity of individual hydrological responses. A similar runoff classification was used in Juras *et al.* (2021).

Here, we assigned an ROS event as class 1 (negligible runoff) if simulated runoff on the last day did not exceed 125% of simulated runoff on the zero day; as class 2 (low runoff) if simulated runoff on the last day exceeded 125% but did not exceed 250% of simulated runoff on the zero day; as class 3 (medium runoff) if simulated runoff on the last day exceeded 250% but did not exceed 500% of simulated runoff on the zero day; and as class 4 (high runoff) if simulated runoff on the last day was higher than 500% of simulated runoff on the zero day.

Additionally, total direct (event) runoff Q_{event} (mm) was calculated for each ROS event to assess the change of the hydrological response to ROS (Equation (1)).

$$Q_{event} = \sum_{t=1}^N (Q(t) - Q_{base}(t)) \quad (1)$$

where Q (mm d^{-1}) is simulated runoff on day t and Q_{base} (mm d^{-1}) is baseflow runoff simulated by the HBV model as an outflow from the lowest groundwater box. N represents the number of days of the ROS event and t is iterated over the first to the last day of the ROS event.

Table 1. Classification of ROS event runoff response. Q_0 represents daily runoff on the day preceding the first ROS day of the specific ROS event, and Q_{last} represents simulated daily runoff on the last day of the specific ROS event (defined as the day with maximum runoff).

Runoff class	Hydrological response	Definition
1	Negligible runoff	$Q_{last} \leq 125\% Q_0$
2	Low runoff	$125\% Q_0 < Q_{last} \leq 250\% Q_0$
3	Medium runoff	$250\% Q_0 < Q_{last} \leq 500\% Q_0$
4	High runoff	$Q_{last} > 500\% Q_0$

2.5 Trend analysis

The Mann-Kendall test (Mann 1945, Kendall 1975) was used to analyse the univariate time series for the presence of statistically significant trends of various ROS-related variables for the study period 1965–2019. The presence of a consistently decreasing or increasing temporal trend was tested using the Mann-Kendall test p value. The p value was calculated based on the 55-year data series (1965–2019) with two different trend significance threshold levels, of .1 and .05. The Theil-Sen's slope estimator was used to assess the monotonic trend slope (Sen 1968), expressing the change in variables per defined time period (decade).

3 Results

3.1 Model calibration and testing

For model calibration and validation, it was important to ensure that the model correctly simulates both SWE and runoff during ROS events. All results from this analysis are shown in the Supplementary material (Figs S1–S5).

Overall model performance was assessed using several objective functions, showing the median model efficiency for runoff using a logarithmic Nash-Sutcliffe criterion equal to 0.67 for model calibration and 0.61 for model validation (Fig. S1). The median runoff volume error reached 1.0 for calibration (i.e. perfect fit) and 0.90 for validation. The median model efficiency for SWE was 0.70 for model calibration and 0.72 for model validation (Fig. S1). We also assessed how 100 model parameterizations impacted the results (Fig. S2). Results showed that median simulations resulted in close-to-median numbers of ROS days in individual catchments. In addition, the accuracy of the SWE simulations was further assessed for both ROS and non-ROS days (Fig. S3), which did not show any major inconsistencies in the SWE simulations. More detailed testing of SWE simulations was carried out by Jenicek *et al.* (2021) and Nedelcev and Jenicek (2021), who worked with the same set of catchments as used in our study.

The model slightly underestimated the number of ROS days in individual catchments; however, the differences were not large (Fig. S4). Comparison of simulated and observed ROS event classification, defined in Section 2.4, showed that 4180 out of 7428 ROS events (54%) were assigned the same class, 27% were overestimated (simulated runoff class was higher than observed), and 19% were underestimated (simulated runoff class was lower than observed) (Fig. S5).

3.2 ROS day occurrence

At a catchment scale, we identified a total of 15 894 ROS days in all 40 catchments during the study period, 1965–2019. It is worth noting that ROS days usually occurred at the same time at multiple catchments and elevation zones, but ROS days were analysed separately.

Rainfall–runoff variables simulated by the HBV model enabled us to analyse the number of ROS days in relation to climate conditions occurring during the specific ROS day at different elevations (Fig. 2). Results showed that mean snowmelt during ROS days was 9 mm, ranging from 5.8 mm to

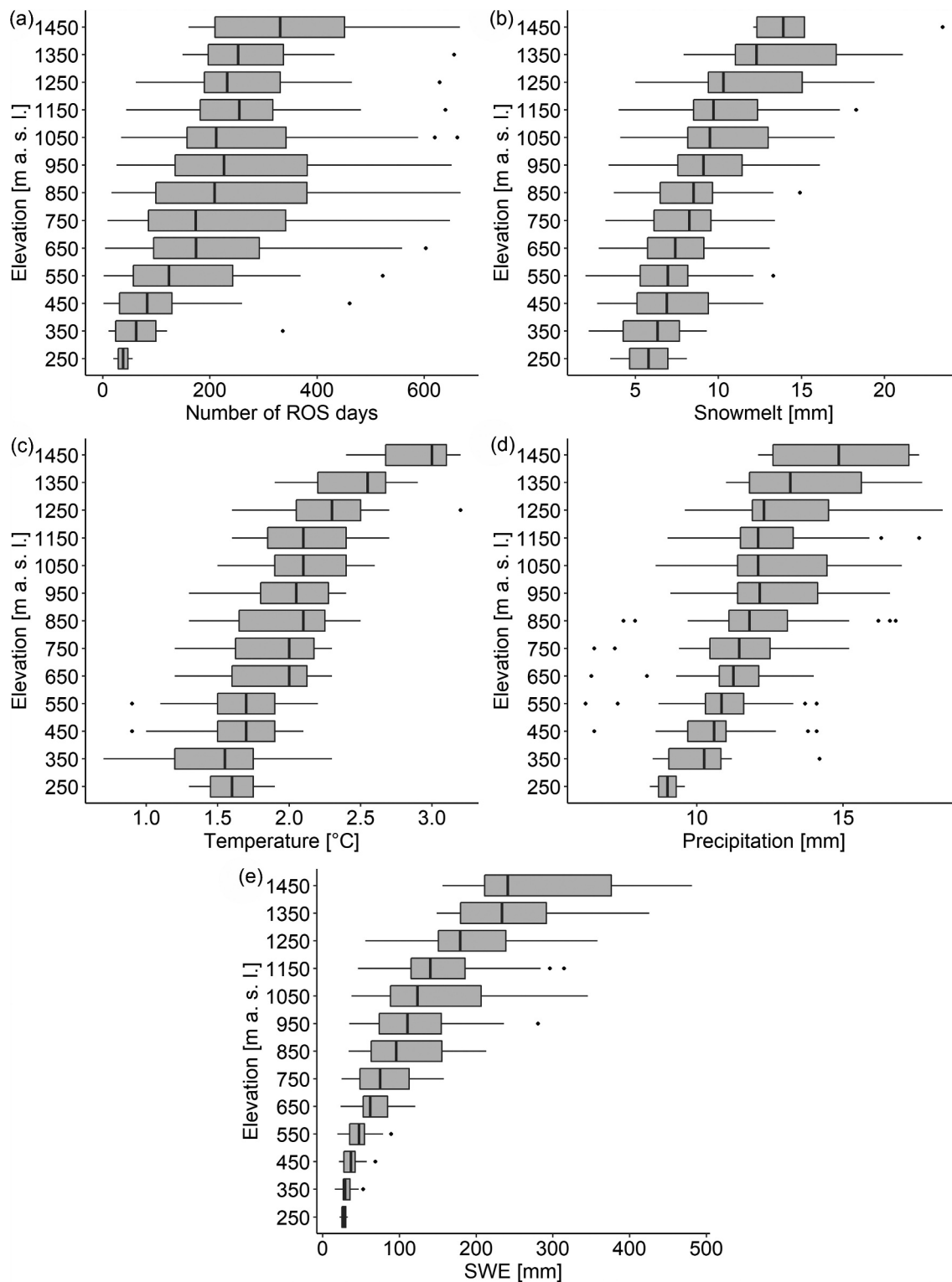


Figure 2. Variability in (a) number of ROS days, (b) snowmelt, (c) daily air temperature, (d) daily precipitation, and (e) SWE in ROS days for all study catchments and elevation zones. Note that individual study catchments differ in the number of defined elevation zones. Boxes represent the 25th and 75th percentiles (with the median as a thick line), whiskers represent interquartile ranges and points represent outliers.

15.1 mm from lowest to highest elevations; mean air temperature was 2°C, ranging from 1.5°C at lower elevations to 2.9°C at higher elevations; mean daily precipitation was 12 mm, ranging from 9 mm to 14.9 mm; and mean SWE was 111 mm, ranging from 27.7 mm to 290 mm.

3.3 Long-term trends in ROS-related variables

3.3.1 Long-term trends at a catchment scale

The Mann-Kendall test was performed to detect changes in the number of ROS days for each catchment, and to assess potential changes in climate conditions occurring during either an

individual ROS day or an entire snow season (a period with typical snow cover occurring in the study catchments, usually from October to May or June). Results showed a statistically significant change in the number of ROS days in multiple

catchments. The above rather small and inconsistent changes are indicated by lower Theil-Sen's slope values with often opposite signs (Fig. 3), denoting rather weak trends in the number of ROS days, although some regionalization patterns were obvious.

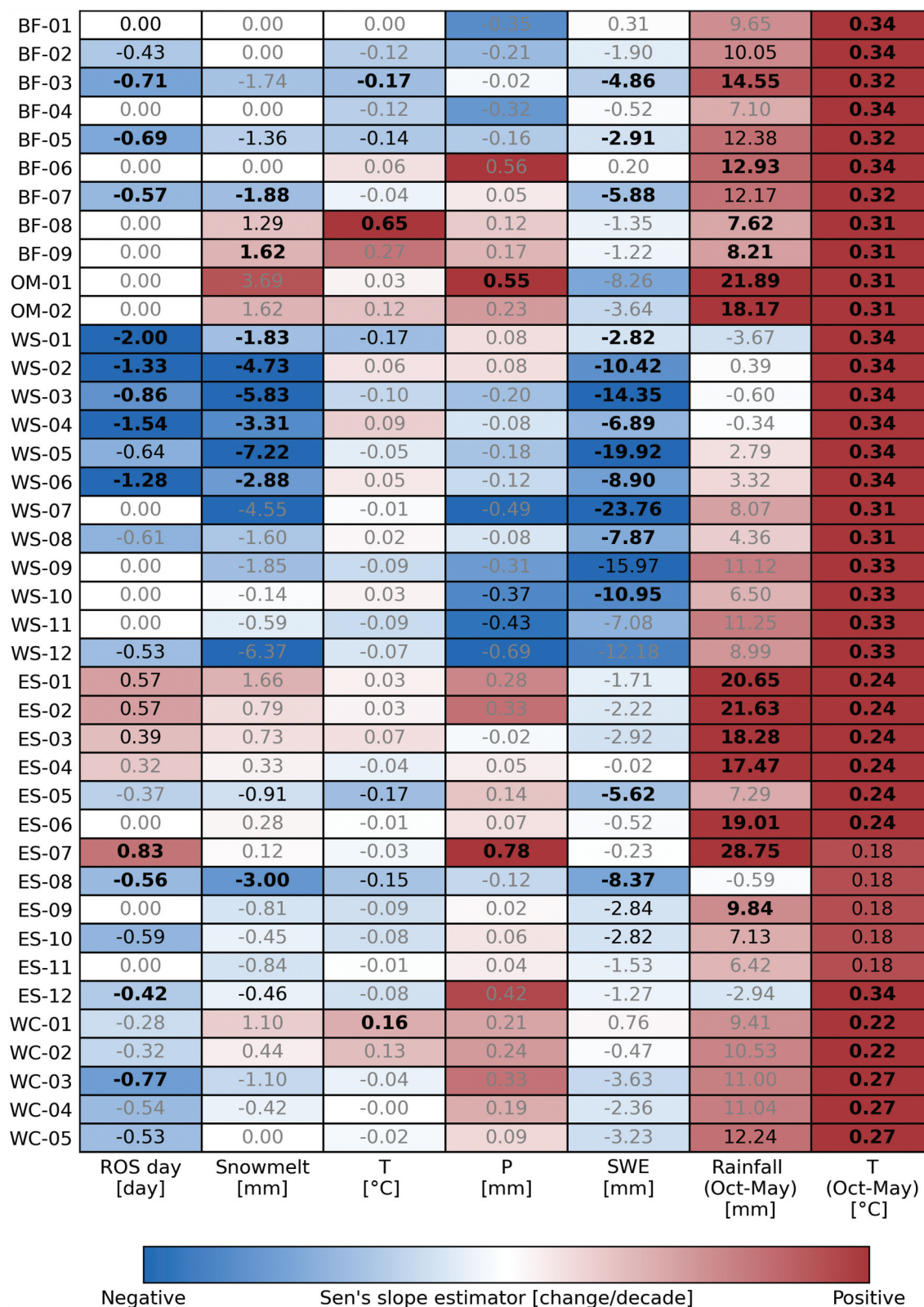


Figure 3. Decadal changes in number of ROS days, snowmelt, mean air temperature, mean daily precipitation and mean SWE occurring in ROS days, and changes in seasonal (October–May) rainfall and air temperature for all study catchments in the period 1965–2019. Cell values represent Theil-Sen's slopes of linear trends. Significant Mann-Kendall trends are highlighted in black bold ($p < .05$) and in black ($p < .1$), decreasing trends in shades of blue and increasing trends in shades of red.

The number of ROS days increased slightly in the Eastern Sudetes region, while a slight decrease was detected mainly in the Western Sudetes region where ROS occurrence was more frequent compared to other regions (Table S1). The biggest change was detected in the Jerice catchment (WS-01), where the annual number of ROS days decreased by two each decade, and at Bela catchment (ES-07), where an increase by 0.8 each decade was detected (Fig. 3).

Changes in air temperature and precipitation occurring in individual ROS days were not significant, which indicates that meteorological conditions during ROS days did not change (Fig. 3). This does not correspond to seasonal (October–May) changes in air temperature, where significant increasing trends were detected for all study catchments. This air temperature increase caused the change in precipitation phase resulting in a significant liquid precipitation increase in 17 out of 40 catchments. This shift in precipitation phase towards more rain rather than snowfall may enhance the ROS potential. A strong significant decreasing snowmelt and SWE trends during ROS days were found in multiple catchments, mostly in the Western Sudetes and partially in the Bohemian Forest, both situated in the western parts of the study area.

3.3.2 Monthly and elevation distribution of trends

While the above results obtained at a catchment scale often showed no consistent (although regionally different) trends in ROS days, analysis done for different elevations on a monthly basis enabled a much closer look at the ROS distribution. Figure 4 summarizes trends in ROS days and trends in total rainfall for individual months of the snow season at different elevations (Fig. 4(b) and (d)), together with monthly and elevation distribution of the absolute values for both characteristics (Fig. 4(a) and (c)). Results clearly show that ROS day trends in individual months of the snow season differ across elevation zones. A statistically significant decrease in the number of ROS days during the study period was detected at the end of the snow season in March, at elevations below 700 m a.s.l.; a large decrease was detected at elevations 700–1200 m a.s.l. during April, and a small decrease was detected at elevations above 1200 m a.s.l. in May. The above monthly and elevation-dependent decreases in ROS days were caused by the shortening of the period with existing snow cover on the ground (results not shown) as a response to increasing air temperature, since no corresponding significant changes in rainfall were detected (Fig. 4(d)). The largest decrease in ROS days (Theil-Sen slope equals to -7.3) was detected at elevations of

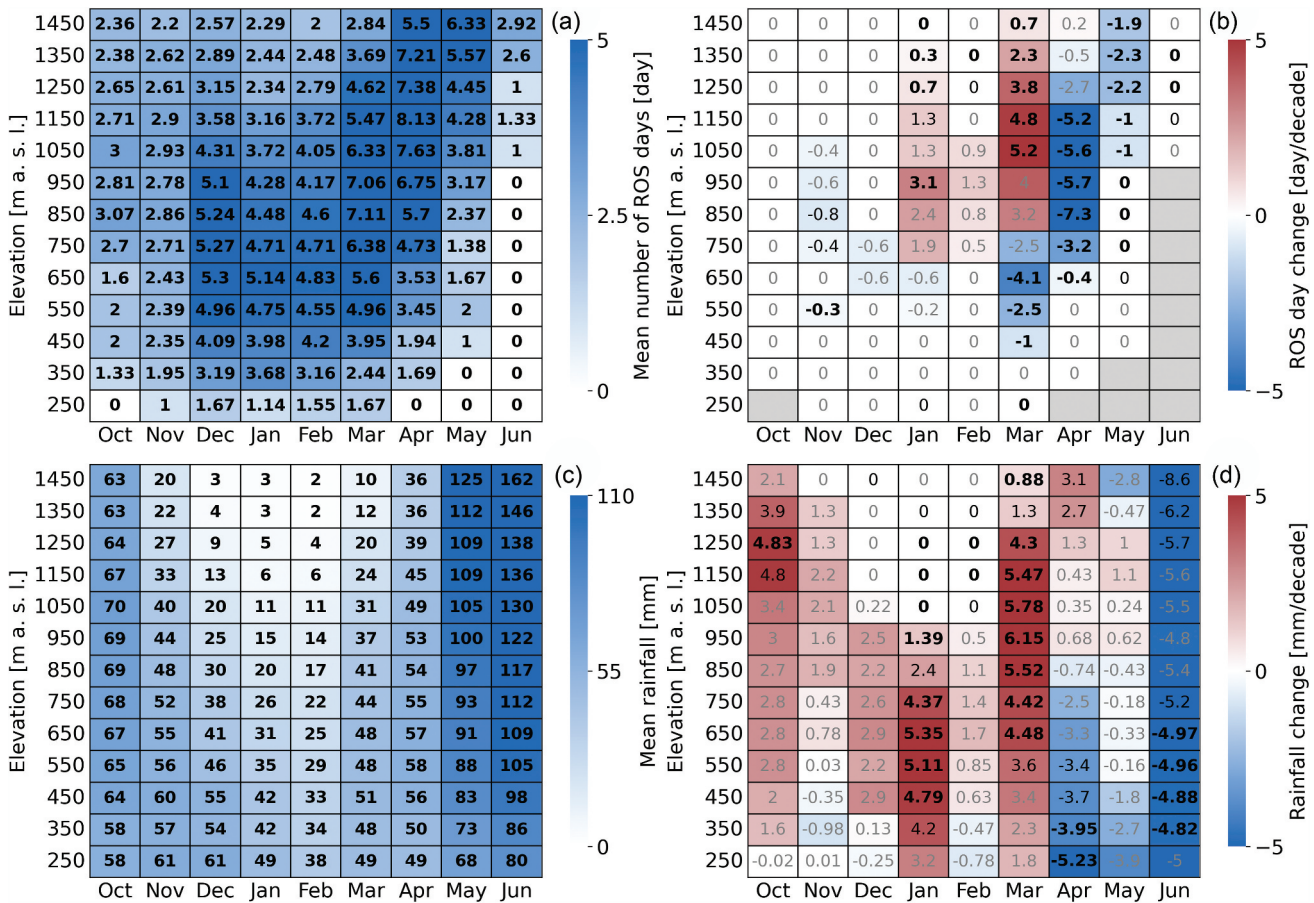


Figure 4. (a) Mean number of ROS days, (b) decadal trends in ROS days, (c) mean rainfall and (d) decadal trends in rainfall from October to June at different elevations for the period 1965–2019. The cell values in panels (a) and (c) represent absolute values of ROS days and rainfall, respectively. The cell values in panels (b) and (d) represent Theil-Sen’s slopes of the regression line. Significant Mann-Kendall trends are highlighted in black bold ($p < .05$) and in black ($p < .1$), decreasing trends in shades of blue and increasing trends in shades of red (panels B and D). Grey indicates no trends due to no ROS days.

800–900 m a.s.l. in April, indicating the reduction in number of ROS days by roughly seven days per decade.

In contrast, a statistically significant increase in ROS days was detected in January at elevations of 900–1000 m a.s.l. An increasing trend was also found at elevations above 1000 m a.s.l. in March, with an increase in the number of ROS days by up to five days per decade. An increase in ROS days found in the middle of the winter season was associated with the fact that more precipitation occurred as rainfall (Fig. 4(d)).

3.4 Hydrological response of ROS events

Using our definition provided in Section 2.3, we identified a total number of 11 852 ROS events at a catchment scale that were analysed for their hydrological response. All ROS events were classified into four groups based on their hydrological response (see Section 2.4). The results showed that 29% (3379 ROS events) caused only negligible runoff (class 1), 43% (5121 ROS events) resulted in low runoff (class 2), 18% (2148 ROS events) caused medium runoff (class 3), and 10% (1204 ROS events) caused high runoff (class 4) (Fig. 5(a)).

Most of the ROS events, regardless of their runoff class, occurred in March and April, including the most dangerous situations accompanied by high runoffs and enhanced flood risk. Events categorized into classes 2, 3 and 4 were more equally distributed across the main winter season (December–April) compared to class 1 runoff responses.

ROS event runoff (Q_{event}) contributed 1–30% to the total direct catchment runoff during the individual months of the snow season, with the largest ROS event contribution in January. Classes 3 and 4 were the main contributors from November to February (4–12%), and class 2 was the main contributor from March to the end of the snow season (3–9%) (Fig. 5(b)). ROS event runoff contributed 3–32% to the total direct runoff within individual study catchments, with a mean ROS event contribution of 17% (results not shown).

Calculation of ROS event runoff volumes enabled us to assess their changes over time (Fig. 6). Results showed that the statistically significant decreases in ROS event runoff volumes were detected only for classes 2 and 3 in April, which can be explained by an overall decrease in snow storage (result not shown). Other identified trends are rather weak and not significant, although a certain increase in runoff volumes was detected particularly for classes 2 and 3 for January to March and for the most extreme class 4 in March.

The analysis of trends in ROS event runoff volume was also carried out for individual catchments. However, detected trends were rather weak and no regional dependencies were found (results not shown). A statistically significant increase in runoff volume was detected only in six catchments (out of 40) in March, and a significant volume decrease was found in eight catchments in April.

Besides trends in ROS event runoff responses, an interesting question is also how inter-annual changes in driving climatic variables control the annual volume of ROS event runoff. To answer this question, annual anomalies in two key ROS drivers – the seasonal sum of positive air temperature and seasonal precipitation – were related to anomalies in ROS event runoff volume in individual years (Fig. 7). Results expectedly showed that the largest ROS event runoff volume anomalies occurred in both wet and warm years (top right quadrant in Fig. 7), although seasonal precipitation seems to be more important. An increasing number of years with positive anomalies in the sum of positive air temperatures occurring in the second half of the study period (1992–2019; solid circle margins in Fig. 7) did not lead to more positive anomalies of ROS runoff volumes in this period compared to the first half of the study period. This partial result corresponds to mostly missing trends in ROS runoff volumes in individual catchments, as described above.

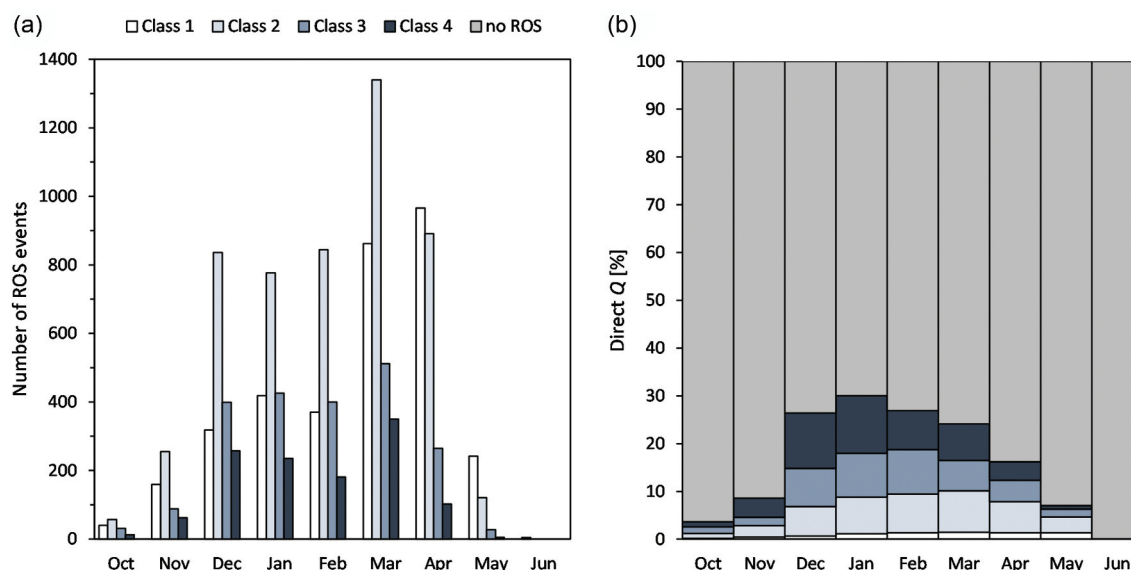


Figure 5. (a) Number of ROS events classified according to runoff responses from October to June in the period 1965–2019. (b) Relative contribution of direct ROS event runoff to total monthly direct runoff.

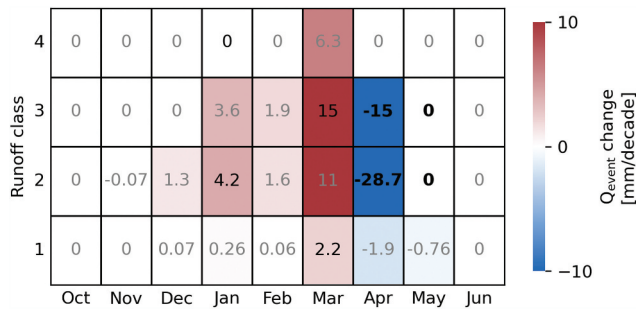


Figure 6. Trends in runoff volume classes of ROS events (Q_{event}) during the period 1965–2019. The cell values represent Theil-Sen's slopes of the regression line. Significant Mann-Kendall trends are highlighted in black bold ($p < .05$) and in black ($p < .1$), decreasing trends in shades of blue and increasing trends in shades of red.

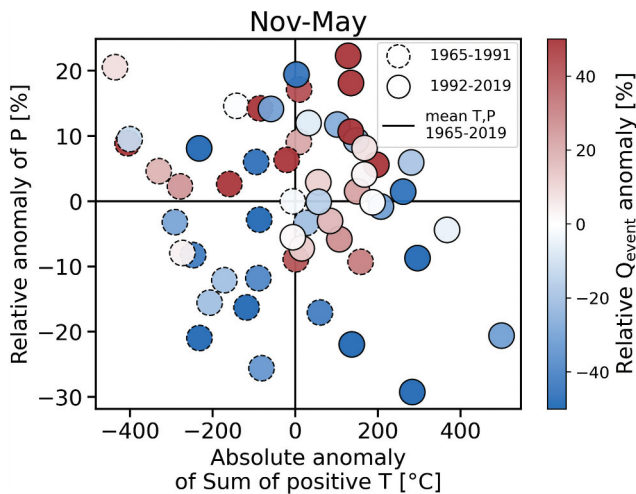


Figure 7. Relationship between relative anomaly in November to May precipitation (y-axis), absolute anomaly in November to May sum of positive air temperatures (x-axis), and relative anomaly in ROS event runoff volume (colour scale) in two different periods, 1965–1991 and 1992–2019.

4 Discussion

4.1 Uncertainty in modelling approach

In this study, we used a semi-distributed hydrological model to derive individual components of the rainfall–runoff process and to assess the occurrence and selected characteristics of ROS, similar to Freudiger *et al.* (2014) who assessed ROS frequencies of ROS events in Germany. Our modelling approach may raise questions related to model parameterization and structure, specifically how individual model parameters and procedures represent real natural processes, such as ROS events. The uncertainty arising from the model parameterization needs to be addressed, since the results presented are based on runoff simulations, and primarily on modelled SWE, as one of the parameters that defines ROS occurrence in this study. The HBV model was calibrated automatically against both SWE and observed runoff. Calibration results were evaluated using a combination of three objective functions (see Section 2.2) originally for study by Jenicek and Ledvinka (2020) and further used by Nedelcev and Jenicek (2021) and Sipek *et al.* (2021). One hundred calibration runs were performed to lower the overall parameter uncertainty,

and multi-criteria model calibration enabled us to better control the simulation of the SWE in individual catchments. ROS analyses were performed at a multi-catchment level, using input data from climate stations limited to air temperature and precipitation data, which did not allow the use of the energy balance approach. Therefore, we used the modified degree-day approach implemented in the HBV model. While we are aware of the limitations of bucket-type approaches in general and the degree-day approach specifically, model inter-comparisons in the literature have demonstrated repeatedly that simple model approaches can provide results at least as good as those produced by more complex, physically-based models in practice, despite the latter being superior in theory (Seibert and Bergström 2022). Despite the limitations of degree-day approaches, several studies proved to be sufficient for simulating snow storage at a catchment scale under climate change (Addor *et al.* 2014, Etter *et al.* 2017, Jenicek *et al.* 2021) or even ROS runoff (Freudiger *et al.* 2014, Juras *et al.* 2021). This is especially the case for the variation of the degree-day approach we are using because it also accounts for liquid water content stored in the snow and refreezing. Additionally, the recent study by Girons Lopez *et al.* (2020) largely confirmed that the current HBV snow routine provides results at a catchment scale that are hard to improve despite increasing physical realism.

Since the air temperature and precipitation data were adjusted for individual elevation zones using lapse rates calibrated separately for each catchment, we assume a high level of accuracy to correctly define ROS and non-ROS days, related trends and hydrological responses related to ROS. This was recently shown by Nedelcev and Jenicek (2021), who tested long-term trends in simulated and observed seasonal precipitation, air temperature and SWE in the same study domain and found no major differences.

Model calibration showed mostly satisfactory results (Fig. S1), with Nash-Sutcliffe efficiency values higher than 0.7. For example, Moriasi *et al.* (2015) argued that Nash-Sutcliffe efficiency values above 0.5 using the daily time step can be regarded as a satisfactory modelling result. Nevertheless, it might be difficult to agree on specific efficiency benchmarks, or on how to define the lower benchmark for good model performance (Seibert *et al.* 2018). Thus, model justification required further model testing, presented in the Supplementary material (Figs S2–S5).

We assessed how 100 model parameterizations resulting in 100 simulations for each catchment impacted the variability of the investigated parameters, such as the number of ROS days (Fig. S2). Results showed that simulated numbers of ROS days do not vary significantly in five selected catchments, except one in the Western Carpathians (WC-04). Nevertheless, results showed that median simulations resulted also in close-to-median numbers of ROS days, which reduces the sensitivity of our results to individual model parameterizations and thus increases the overall reliability of the model.

Since the number of stations with long-term monitoring of SWE was limited, we used only 15 stations with weekly SWE observations. Because of the shorter time series and weekly data, we obtained a reduced number of cases, which were compared with simulated ROS days from the same elevation

zone as observed data (Figs S3 and S4). However, the potential disagreement of the modelled values with observed ones does not necessarily mean that the model is incorrect. Observed data are also uncertain, especially due to the representativeness (or lack thereof) of the measurement location (wind influence, forest effects, slope orientation etc.). Some of the study catchments are relatively larger than others and more diverse and cannot be represented by one SWE time series. Furthermore, the quality of SWE measurements performed by observers decreases back in time.

The comparison of observed and simulated ROS days showed that the simulated number of ROS days was often lower than the observed one (Fig. S4). This was probably due to inaccuracies in simulated SWE at the end of the snow season caused by overestimation of simulated snowmelt rates resulting in earlier snowmelt and thus a lower number of simulated ROS days. Additionally, 27% of ROS events were overestimated in terms of hydrological response, although 54% of all ROS events were assigned to the same runoff class based on simulated and observed data (Fig. S5).

Although the model and observed values partly differ in absolute terms, we did not find any major inconsistencies in model simulations. Since our analysis was focused mainly on the relative differences and trends in ROS days and ROS events rather than on absolute values, we believe that the model provided sufficiently good simulations. More detailed testing of SWE simulations was carried out by Jenicek *et al.* (2021) and Nedelcev and Jenicek (2021), who worked with the same set of catchments as used in our study. Therefore, we refer readers to those studies for further information.

4.2 ROS definition

Defining ROS situations by several selection criteria that are dependent on threshold values may appear arbitrary, since changes in these threshold values can affect the absolute number of identified ROS days and ROS events. Nevertheless, based on the literature review, there is no consistent definition for either an ROS day or an ROS event, which limits the comparison of results across different studies (Brandt *et al.* 2022).

In our study, selection criteria that correspond to previous studies were used; a daily mean air temperature of 0°C to separate snow and rain was also used by Surfleet and Tullos (2013), Bieniek *et al.* (2018), and Crawford *et al.* (2020); an SWE threshold of 10 mm was used by Freudiger *et al.* (2014), Trubilowicz and Moore (2017) and Huang *et al.* (2022); and a daily rainfall intensity threshold of 5 mm was applied by Trubilowicz and Moore (2017) and Pall *et al.* (2019). The air temperature threshold value is apparently the most important criterion because it controls precipitation phase. Definition of the threshold temperature might be difficult using daily data, especially for days with air temperature near the freezing point, or during days with high daily temperature amplitude (cold nights and warmer days in spring) resulting in a mean daily temperature around zero despite the fact that precipitation phase may change during day. Thus, the total number of analysed ROS days and ROS events may differ.

However, the threshold value of 0°C used in this study agrees with the findings of Jennings *et al.* (2018), who argued that air temperature at which rain and snow fall in equal frequency ranges from -0.4 to 2.4°C for 95% of the stations across the Northern Hemisphere. Threshold temperature was one of the calibrated parameters in the HBV model. Based on our results, the mean threshold temperature reached -0.4°C for the study catchments. However, using calibrated values might be inappropriate since they may compensate for other processes or imperfect model structure (precipitation undercatch, temperature or precipitation lapse rates, SWE measurements etc.). Therefore, we decided to use one value for all catchments that is close to the mean of calibrated threshold temperature values. Although we are aware that the threshold value influences the absolute number of ROS days/events, our study rather assessed trends and inter-annual differences, which are less sensitive in terms of the absolute number of events.

Thresholds for rain and SWE seem to be less sensitive. A sensitivity analysis in our previous study performed partly at the same study area revealed that ROS characteristics remain similar when different limits for SWE and minimum rainfall were applied (Juras *et al.* 2021). In addition, threshold parameters for SWE and precipitation may also differ spatially, since snow cover is distributed unevenly and rainfall intensity is usually not constant.

4.3 ROS occurrence

The temporal and spatial distribution of ROS during the winter season is controlled by weather conditions. Accordingly, research studies focusing on ROS are usually area specific (Li *et al.* 2019). Results showed some regional differences in analysed parameters (Fig. 3, Table S1). Despite the relative proximity of the studied regions, climate variables (air temperature, precipitation, snow parameters) affecting ROS occurrence differed considerably during the cold season, probably in relation to increasing continentality from west to east.

In general, ROS occurrence depends on snowpack existence and rainfall occurrence. In the study area, the typical ROS season occurred from November to May (with rather rare events in October and June at the highest elevations), which is in good agreement with findings by Freudiger *et al.* (2014), who analysed ROS events in catchments located in Germany.

We identified a total of 15 894 ROS days in all 40 catchments during the study period, 1965–2019. We found a typical ROS day to be a day with daily mean air temperature ranging from 1.5°C at the lowest elevations to 2.9°C at the highest elevations (Fig. 2). These values as well as typical rainfall intensities and SWEs do not differ from those reported in other European regions with similar climate (Garvelmann *et al.* 2015, Würzer *et al.* 2016, Trubilowicz and Moore 2017). However, comparison of ROS situations across different regions and studies may be difficult, since ROS characteristics are often determined differently across studies and in different temporal resolutions.

Our results showed that air temperature, total rainfall, SWE, and snowmelt during ROS days increased with elevation. The higher mean air temperature and rainfall amount typical

for ROS days at higher elevations may be explained by the fact that most of the ROS occurred in the spring months (even into May and June), with overall higher air temperatures leading to more water vapor in the atmosphere and thus more intensive rainfall compared to winter. Another reason for this elevation dependence might be that ROS days at the highest elevations are usually associated with more intense warm air mass advection typical for low pressures, which brings more intensive rainfall followed by rapid snowmelt, while ROS situations are often distributed throughout the winter season at lower elevations where air temperature often fluctuated around 0°C.

Several studies pointed out that the initial properties of snowpack and its retention capacity are both important factors with a strong influence on runoff formation during ROS (Garvelmann *et al.* 2015, Würzer *et al.* 2016). As a result, not all ROS events generated runoff increase (Merz and Blöschl 2003, Wayand *et al.* 2015, Juras *et al.* 2021). We identified 10% of all ROS events that caused high runoff (according to defined runoff classes), and most of the ROS events (72%) did not cause any significant runoff increase (low or negligible runoff). Our results are consistent with Juras *et al.* (2021) in this respect, who used a similar runoff type classification analysed in a partly overlapping study area.

Most of the negligible- and low-runoff ROS events occurred in March and April, probably due to relatively high snow storage which stores a lot of liquid water coming from rainfall. Dangerous high-runoff situations occurred mainly in March, probably due to more intensive spring rainfall, generally higher air temperature, and high SWE which was often at its seasonal maximum, resulting in faster snowmelt. Earlier medium and high runoff responses during winter season (December–February) might be influenced by the non-ripe snowpack with lower snow densities and prevailing preferential flow paths that allowed rainwater to efficiently propagate through the snowpack, resulting in a faster and higher runoff (Juras *et al.* 2017).

4.4 ROS trends

At a catchment scale, Mann-Kendall trend tests showed a statistically significant change (p value < .1) in ROS days in 21 out of 40 catchments. However, the identified trends are rather weak and not consistent across catchments, although some regional patterns can be identified. Opposite trends in numbers of ROS days were detected in the Eastern Sudetes (increasing trends) and Western Sudetes (decreasing trends), despite their proximity (150 km). We hypothesize that these opposite trends are caused by different synoptic situations that influence precipitation amount and its spatial distribution in individual mountain ranges (Juras *et al.* 2021). For instance, catchments in the Western Sudetes experience high annual precipitation (above 1000 mm) that leads to relatively more ROS days compared to the Eastern Sudetes (results not shown). In contrast, rapid shortening of the period with snow on the ground in the Western Sudetes investigated by Nedelcev and Jenicek (2021) causes ultimately decreasing trends in the number of ROS days.

In general, our results showed that significant change in ROS days related to increasing air temperature is not clear at a

catchment scale. Since both elevation and air temperature are important ROS drivers, there is an ROS decrease due to the shortening of the period with existing snow cover on the ground on the one hand, while there is an increase due to a decrease in snowfall fraction on the other hand. Trends showing elevation-dependent changes and monthly changes are more pronounced and consistent with results of other studies (Li *et al.* 2019, López-Moreno *et al.* 2021), even with those that focus on ROS projections for the future (Sezen *et al.* 2020).

Results clearly showed that ROS trends in individual months of the winter season differ across elevations. We detected a significant ROS decrease at elevations below 700 m a.s.l. (mainly in March) and at elevations from 700 to 1200 m a.s.l. (mainly in April), which supports the findings of Surfleet and Tullos (2013), Musselman *et al.* (2018), and Li *et al.* (2019). In contrast, a predicted increase in the number of ROS days at higher elevations, presented by Il Jeong and Sushama (2017), Trubilowicz and Moore (2017), and Li *et al.* (2019), cannot be suggested uniformly throughout the snow season since trends differ across individual months. At higher elevations, we found a significant ROS decrease in late winter (May) associated with the shorter period with snow cover on the ground, which is in good agreement with the study by Sezen *et al.* (2020). A significant ROS increase was detected only in the middle of the snow season (January and March) since more precipitation occurred as rain rather than snow, as also recently found by Nedelcev and Jenicek (2021) for the same study area. The main reason for these differences in ROS patterns at higher elevations is that different definitions of 'high elevation' were used across the studies. Beniston and Stoffel (2016) showed that the temperature increase observed in Switzerland in the period 1960–2015 has contributed directly to the increase in the number of ROS events by about 40% at low elevations (below 1500 m a.s.l.). This seems to fit well with our results for elevations above 1000 m a.s.l. The offset of roughly 500 m might be caused by the more northern latitude of our study area and its partly different climate.

5 Conclusion

We evaluated the frequency and ongoing trends in ROS days and their runoff responses at different elevations. We were particularly focused on lower elevation mountain ranges since they represent rain–snow transition areas with large changes in snow storage affecting ROS occurrence. Based on the results, we can draw the following conclusions.

We identified a total of 15 894 ROS days at a catchment scale in the period 1965–2019. Mean snowmelt during the ROS days reached 9 mm and the mean SWE was 111 mm. Both parameters showed strong, significant decreasing trends in multiple catchments. Typical mean air temperature during the ROS days was 2°C and mean daily precipitation reached 12 mm. Generally, values of all four variables increased with elevation.

The results showed a statistically significant change in the number of ROS days in multiple catchments. However, these changes were rather small and not consistent at a catchment scale. In contrast, strong, significant trends in ROS days were

identified for specific months at different elevations. The largest decrease was detected at elevations from 700 to 1200 m a.s.l. during April, most likely caused by a shortening of the period with existing snow cover on the ground due to increasing air temperature. The largest increase was detected at elevations above 1000 m a.s.l. in March, which was associated with more frequent rainfall due to the increasing air temperature.

We identified a total of 11 852 ROS events at a catchment scale. About 10% of all ROS events have flood-generation potential (they were classified as high-runoff events) and these events occurred mostly in March.

ROS event runoff contributed 3–32% to the total direct catchment runoff during the snow season, with the largest relative contribution in January. The changes in ROS event runoff volume were mostly weak and not consistent across individual catchments. The largest relative ROS runoff volume anomaly resulted from the combination of a positive anomaly in the sum of positive air temperatures and a positive anomaly in the seasonal precipitation, where the latter seems to be of greater importance.

The results showed that changes in ROS days and their runoff responses differ among individual study catchments, across elevations and for different months during the snow season. Additionally, the impact of increasing air temperature and thus partly decreasing snow storage and shorter snow cover duration clearly affected the ROS spatial and temporal distribution. Overall, our findings contribute to a better understanding of factors leading to ROS events and their runoff responses related to climate variability and projected future climate changes.

Acknowledgements

Many thanks are due to Tracy Ewen for improving the language. We also thank associate editor Stephanie Kampf, reviewer Juraj Parajka and one anonymous reviewer for their valuable feedback.

Disclosure statement

No potential conflict of interest was reported by the authors.

Funding

This work was supported by the Charles University Grant Agency, project no. GAUK 272119 (Modelling of future effects of changes in snow storages on occurrence and extremity of runoff caused by rain-on-snow events) and Technology Agency of the Czech Republic (project SS02030040).

ORCID

Ondrej Hotovy  <http://orcid.org/0000-0002-3587-1725>
 Ondrej Nedelcev  <http://orcid.org/0000-0002-3832-3126>
 Michal Jenicek  <http://orcid.org/0000-0002-1103-0403>

Data availability statement

The data that support the findings of this study are available from the corresponding author, OH, upon reasonable request.

References

- Addor, N., *et al.*, 2014. Robust changes and sources of uncertainty in the projected hydrological regimes of Swiss catchments. *Water Resources Research*, 50 (10), 7541–7562. doi:10.1002/2014WR015549
- Beniston, M. and Stoffel, M., 2016. Rain-on-snow events, floods and climate change in the Alps: events may increase with warming up to 4 °C and decrease thereafter. *Science of the Total Environment*, 571, 228–236. doi:10.1016/j.scitotenv.2016.07.146
- Bieniek, P.A., *et al.*, 2018. Assessment of Alaska rain-on-snow events using dynamical downscaling. *Journal of Applied Meteorology and Climatology*, 57 (8), 1847–1863. doi:10.1175/JAMC-D-17-0276.1
- Blahusiakova, A., *et al.*, 2020. Snow and climate trends and their impact on seasonal runoff and hydrological drought types in selected mountain catchments in Central Europe. *Hydrological Sciences Journal*, 65 (12), 2083–2096. doi:10.1080/02626667.2020.1784900
- Blöschl, G., *et al.*, 2019. Twenty-three unsolved problems in hydrology (UPH)—a community perspective. *Hydrological Sciences Journal*, 64 (10), 1141–1158. doi:10.1080/02626667.2019.1620507
- Brandt, W.T., *et al.*, 2022. A review of the hydrologic response mechanisms during mountain rain-on-snow. *Frontiers in Earth Science*, 10, 791760. doi:10.3389/feart.2022.791760
- Brunner, M.I., *et al.*, 2019. Future shifts in extreme flow regimes in Alpine regions. *Hydrology and Earth System Sciences*, 23 (11), 4471–4489. doi:10.5194/hess-23-4471-2019
- Cohen, J., Ye, H., and Jones, J., 2015. Trends and variability in rain-on-snow events. *Geophysical Research Letters*, 42 (17), 7115–7122. doi:10.1002/2015GL065320
- Crawford, A.D., *et al.*, 2020. Synoptic climatology of rain-on-snow events in Alaska. *Monthly Weather Review*, 148 (3), 1275–1295. doi:10.1175/MWR-D-19-0311.1
- Etter, S., *et al.*, 2017. Climate change impacts on future snow, ice and rain runoff in a Swiss mountain catchment using multi-dataset calibration. *Journal of Hydrology: Regional Studies*, 13, 222–239.
- Freudiger, D., *et al.*, 2014. Large-scale analysis of changing frequencies of rain-on-snow events with flood-generation potential. *Hydrology and Earth System Sciences*, 18 (7), 2695–2709. doi:10.5194/hess-18-2695-2014
- Garvelmann, J., Pohl, S., and Weiler, M., 2014. Variability of observed energy fluxes during rain-on-snow and clear sky snowmelt in a mid-latitude mountain environment. *Journal of Hydrometeorology*, 15 (3), 1220–1237. doi:10.1175/JHM-D-13-0187.1
- Garvelmann, J., Pohl, S., and Weiler, M., 2015. Spatio-temporal controls of snowmelt and runoff generation during rain-on-snow events in a mid-latitude mountain catchment. *Hydrological Processes*, 29 (17), 3649–3664. doi:10.1002/hyp.10460
- Girons Lopez, M., *et al.*, 2020. Assessing the degree of detail of temperature-based snow routines for runoff modelling in mountainous areas in central Europe. *Hydrology and Earth System Sciences*, 24 (9), 4441–4461. doi:10.5194/hess-24-4441-2020
- Hammond, J.C., Saavedra, F.A., and Kampf, S.K., 2018. How does snow persistence relate to annual streamflow in mountain watersheds of the western U.S. with wet maritime and dry continental climates? *Water Resources Research*, 54 (4), 2605–2623. doi:10.1002/2017WR021899
- Hotovy, O. and Jenicek, M., 2020. The impact of changing subcanopy radiation on snowmelt in a disturbed coniferous forest. *Hydrological Processes*, 34 (26), 5298–5314. doi:10.1002/hyp.13936
- Huang, H., *et al.*, 2022. Changes in mechanisms and characteristics of western U.S. floods over the last sixty years. *Geophysical Research Letters*.
- Il Jeong, D. and Sushama, L., 2017. Rain-on-snow events over North America based on two Canadian regional climate models. *Climate Dynamics*, 50 (1–2), 303–316. doi:10.1007/s00382-017-3609-x
- Jenicek, M., *et al.*, 2021. Future changes in snowpack will impact seasonal runoff and low flows in Czechia. *Journal of Hydrology: Regional Studies*, 37, 100899.
- Jenicek, M. and Ledvinka, O., 2020. Importance of snowmelt contribution to seasonal runoff and summer low flows in Czechia. *Hydrology and Earth System Sciences*, 24 (7), 3475–3491. doi:10.5194/hess-24-3475-2020

- Jennings, K.S., *et al.*, 2018. Spatial variation of the rain-snow temperature threshold across the Northern Hemisphere. *Nature Communications*, 9 (1), 1–9. doi:10.1038/s41467-018-03629-7
- Jennings, K. and Jones, J.A., 2015. Precipitation-snowmelt timing and snowmelt augmentation of large peak flow events, western Cascades, Oregon. *Water Resources Research*, 51 (9), 7649–7661. doi:10.1002/2014WR016877
- Juras, R., *et al.*, 2017. Rainwater propagation through snowpack during rain-on-snow sprinkling experiments under different snow conditions. *Hydrology and Earth System Sciences*, 21 (9), 4973–4987. doi:10.5194/hess-21-4973-2017
- Juras, R., *et al.*, 2021. What affects the hydrological response of rain-on-snow events in low-altitude mountain ranges in Central Europe? *Journal of Hydrology*, 603, 127002. doi:10.1016/j.jhydrol.2021.127002
- Kendall, M.G., 1975. Rank correlation measures. London: Charles Griffin.
- Krug, A., *et al.*, 2020. On the temporal variability of widespread rain-on-snow floods. *Meteorologische Zeitschrift*, 29 (2), 147–163. doi:10.1127/metz/2020/0989
- Li, D., *et al.*, 2019. The role of rain-on-snow in flooding over the conterminous United States. *Water Resources Research*, 55 (11), 8492–8513. doi:10.1029/2019WR024950
- Li, Z., *et al.*, 2020. Declining snowfall fraction in the alpine regions, Central Asia. *Scientific Reports*, 10 (1), 1–12. doi:10.1038/s41598-019-56847-4
- Lindström, G., *et al.*, 1997. Development and test of the distributed HBV-96 hydrological model. *Journal of Hydrology*, 201 (1–4), 272–288. doi:10.1016/S0022-1694(97)00041-3
- López-Moreno, I., *et al.*, 2021. Changes in the frequency of global high mountain rain-on-snow events due to climate warming. *Environmental Research Letters*.
- Mann, H.B., 1945. Nonparametric tests against trend. *Econometrica*, 13 (3), 245. doi:10.2307/1907187
- Marks, D., *et al.*, 1998. The sensitivity of snowmelt processes to climate conditions and forest cover during rain-on-snow: a case study of the 1996 Pacific Northwest flood. *Hydrological Processes*, 12 (10–11), 1569–1587. doi:10.1002/(SICI)1099-1085(199808/09)12:10/11<1569::AID-HYP682>3.0.CO;2-L
- Marty, C., *et al.*, 2017. How much can we save? Impact of different emission scenarios on future snow cover in the Alps. *Cryosphere*, 11 (1), 517–529. doi:10.5194/tc-11-517-2017
- Mazurkiewicz, A.B., Callery, D.G., and McDonnell, J.J., 2008. Assessing the controls of the snow energy balance and water available for runoff in a rain-on-snow environment. *Journal of Hydrology*, 354 (1–4), 1–14. doi:10.1016/j.jhydrol.2007.12.027
- Mccabe, G.J., Clark, M.P., and Hay, L.E., 2007. Rain-on-snow events in the western United States. *American Meteorological Society*, 88 (3), 319–328. doi:10.1175/BAMS-88-3-319
- Merz, R. and Blöschl, G., 2003. A process typology of regional floods. *Water Resources Research*, 39 (12), 1340. doi:10.1029/2002WR001952
- Moriasi, D.N., *et al.*, 2015. Hydrologic and water quality models: performance measures and evaluation criteria. *Transactions of the ASABE*, 58 (6), 1763–1785.
- Musselman, K.N., *et al.*, 2018. Projected increases and shifts in rain-on-snow flood risk over western North America. *Nature Climate Change*.
- Nash, J.E. and Sutcliffe, J.V., 1970. River flow forecasting through conceptual models part I - A discussion of principles. *Journal of Hydrology*, 10 (3), 282–290. doi:10.1016/0022-1694(70)90255-6
- Nedelcev, O. and Jenicek, M., 2021. Trends in seasonal snowpack and their relation to climate variables in mountain catchments in Czechia. *Hydrological Sciences Journal*, 66 (16), 2340–2356. doi:10.1080/02626667.2021.1990298
- Notarnicola, C., 2020. Hotspots of snow cover changes in global mountain regions over 2000–2018. *Remote Sensing of Environment*, 243, 111781. doi:10.1016/j.rse.2020.111781
- Ohba, M. and Kawase, H., 2020. Rain-on-snow events in Japan as projected by a large ensemble of regional climate simulations. *Climate Dynamics*, 55 (9–10), 2785–2800. doi:10.1007/s00382-020-05419-8
- Oudin, L., *et al.*, 2005. Which potential evapotranspiration input for a lumped rainfall-runoff model? Part 2 - towards a simple and efficient potential evapotranspiration model for rainfall-runoff modelling. *Journal of Hydrology*, 303 (1–4), 290–306. doi:10.1016/j.jhydrol.2004.08.026
- Pall, P., Tallaksen, L.M., and Stordal, F., 2019. A climatology of rain-on-snow events for Norway. *Journal of Climate*, 32 (20), 6995–7016. doi:10.1175/JCLI-D-18-0529.1
- Pradhanang, S.M., *et al.*, 2013. Rain-on-snow runoff events in New York. *Hydrological Processes*, 27 (21), 3035–3049. doi:10.1002/hyp.9864
- Rennert, K.J., *et al.*, 2009. Soil thermal and ecological impacts of rain on snow events in the circumpolar Arctic. *Journal of Climate*, 22 (9), 2302–2315. doi:10.1175/2008JCLI2117.1
- Seibert, J., 2000. Multi-criteria calibration of a conceptual runoff model using a genetic algorithm. *Hydrology and Earth System Sciences*, 4 (2), 215–224. doi:10.5194/hess-4-215-2000
- Seibert, J., *et al.*, 2018. Upper and lower benchmarks in hydrological modeling. *Hydrological Processes*, 32 (8), 1120–1125. doi:10.1002/hyp.11476
- Seibert, J. and Bergström, S., 2022. A retrospective on hydrological catchment modelling based on half a century with the HBV model. *Hydrology and Earth System Sciences*, 26 (5), 1371–1388. doi:10.5194/hess-26-1371-2022
- Seibert, J. and Vis, M.J.P., 2012. Teaching hydrological modeling with a user-friendly catchment-runoff-model software package. *Hydrology and Earth System Sciences*, 16 (9), 3315–3325. doi:10.5194/hess-16-3315-2012
- Sen, P.K., 1968. Estimates of the regression coefficient based on Kendall's tau. *Journal of the American Statistical Association*, 63 (324), 1379–1389. doi:10.1080/01621459.1968.10480934
- Serquet, G., *et al.*, 2011. Seasonal trends and temperature dependence of the snowfall/precipitation-day ratio in Switzerland. *Geophysical Research Letters*, 38 (7), L07703. doi:10.1029/2011GL046976
- Sezen, C., *et al.*, 2020. Investigation of rain-on-snow floods under climate change. *Applied Sciences (Switzerland)*, 10, 4.
- Sipek, V., *et al.*, 2021. Catchment storage and its influence on summer low flows in central European mountainous catchments. *Water Resources Management*, 35 (9), 2829–2843. doi:10.1007/s11269-021-02871-x
- Surfleet, C.G. and Tullos, D., 2013. Variability in effect of climate change on rain-on-snow peak flow events in a temperate climate. *Journal of Hydrology*, 479, 24–34. doi:10.1016/j.jhydrol.2012.11.021
- Trubilowicz, J.W. and Moore, R.D., 2017. Quantifying the role of the snowpack in generating water available for run-off during rain-on-snow events from snow pillow records. *Hydrological Processes*, 31 (23), 4136–4150. doi:10.1002/hyp.11310
- Vlach, V., Ledvinka, O., and Matouskova, M., 2020. Changing low flow and streamflow drought seasonality in central European headwaters. *Water*, 12 (12), 3575. doi:10.3390/w12123575
- Wayand, N.E., Lundquist, J.D., and Clark, M.P., 2015. Modeling the influence of hypsometry, vegetation, and storm energy on snowmelt contributions to basins during rain-on-snow floods. *Water Resources Research*, 51 (10), 8551–8569. doi:10.1002/2014WR016576
- Wever, N., *et al.*, 2016. Simulating ice layer formation under the presence of preferential flow in layered snowpacks. *Cryosphere*, 10 (6), 2731–2744. doi:10.5194/tc-10-2731-2016
- Würzer, S., *et al.*, 2016. Influence of initial snowpack properties on runoff formation during rain-on-snow events. *Journal of Hydrometeorology*, 17 (6), 1801–1815. doi:10.1175/JHM-D-15-0181.1
- Würzer, S., *et al.*, 2017. Modelling liquid water transport in snow under rain-on-snow conditions - Considering preferential flow. *Hydrology and Earth System Sciences*, 21 (3), 1741–1756. doi:10.5194/hess-21-1741-2017
- Würzer, S. and Jonas, T., 2018. Spatio-temporal aspects of snowpack runoff formation during rain on snow. *Hydrological Processes*, 32 (23), 3434–3445. doi:10.1002/hyp.13240

Rain-on-snow events in mountainous catchments under climate change

Ondrej Hotovy¹, Ondrej Nedelcev¹, Jan Seibert², Michal Jenicek¹

5 ¹Department of Physical Geography and geoecology, Charles University, Prague, Czechia

²Department of Geography, University of Zurich, Zurich, Switzerland

Correspondence to: Ondrej Hotovy (hotovyo@natur.cuni.cz)

Abstract. The frequency and intensity of rain-on-snow events (RoS) are expected to change in response to climate variations due to changes in precipitation, increase in air temperature and subsequent changes in the snow occurrence. In this study, we attributed these changes to the simulated variations in RoS events using a sensitivity analysis of precipitation and air temperature, and subsequent effects on RoS-related runoff responses were evaluated. We selected 93 mountainous catchments located in Central Europe across Czechia (60), Switzerland (26) and Germany (7), and used a conceptual hydrological model to simulate runoff components for 24 climate projections relative to the reference period 1980-2010. Climate change-driven RoS changes were highly variable over regions, across elevations, and within the cold season. The warmest projections suggested a decrease in RoS days by about 75 % for the Czech catchments. In contrast, the Swiss catchments may respond less sensitively, with the number of RoS days even increasing, specifically during the winter months and at higher elevations. Our projections also suggested that the RoS contribution to annual runoff will be considerably reduced from the current 10 % to 2-4 % for the warmest projections in Czechia, and from 18 % to 5-9 % in Switzerland. However, the RoS contribution to runoff may increase in winter months, especially for projections leading to an increase in precipitation, demonstrating the joint importance of air temperature and precipitation for future hydrological behavior in snow-dominated catchments.

1 Introduction

Rain-on-snow (RoS) events threaten society and nature in regions vulnerable to such, often extreme, hydrometeorological events. During RoS events, rain falls on snow and intensifies turbulent, latent, and sensible heat fluxes within the snowpack, which can substantially accelerate snowmelt (Garvelmann et al., 2014; Hotovy and Jenicek, 2020). Although most of these events do not directly lead to severe flooding, since the snowpack, particularly fresh snow, can store large amounts of rainwater (Juras et al., 2021; Wayand et al., 2015), under certain conditions, these events can also trigger excessive runoff and widespread floods (Berghuijs et al., 2019; Brunner and Fischer, 2022). Elevated runoff generated by RoS is often more intense and short-lived than the thermally driven types of snowmelt and related runoff, along with lower groundwater

30 recharge and infiltration (Earman et al., 2006; Parajka et al., 2019). Thus, such events can affect water supplies and lead to snow drought. Moreover, RoS events affect important parameters and mechanisms within the snowpack, including changes in snowpack saturation, an increase in liquid water content, and a decrease in snow albedo, which enhances the energy absorption of the snow. These effects can persist for several days after the rainfall event and further accelerate snowmelt (Yang et al., 2023).

35 The occurrence and intensity of RoS events have been widely studied in recent years, particularly in the Northern Hemisphere. Although the topic is gaining scientific interest, the complex RoS processes are still on the list of unsolved problems in hydrology proposed by Blöschl et al. (2019).

The most vulnerable regions of the world experience more than 10 RoS events per year (Suriano, 2022). Recent studies have mainly addressed catchments in North America (Bieniek et al., 2018; Crawford et al., 2020; Grenfell and Putkonen, 2008; 40 Musselman et al., 2018), where maximum daily runoff is associated with RoS events mainly (80 % of the time) between January and May (Il Jeong and Sushama, 2017). Several studies have been conducted in Siberia (Bartsch et al., 2010), Scandinavia (Mooney and Li, 2021; Pall et al., 2019; Poschlod et al., 2020), Central Europe (Freudiger et al., 2014; Hotovy et al., 2023; Juras et al., 2021; Schirmer et al., 2022), high mountain Asia (Maina and Kumar, 2023; Yang et al., 2022), as well as in the terrestrial Arctic (Bartsch et al., 2023). Much of the current research is focused on highlighting the changes in 45 RoS and snow conditions under ongoing climate change.

Despite the increasing scientific interest, future changes in RoS events are still subject to large uncertainties (López-Moreno et al., 2021; Schirmer et al., 2022). The real impact of climate change on RoS events and related hydrologic implications remains unclear, mainly due to their complex nature (Mooney and Li, 2021; Myers et al., 2023; Sezen et al., 2020). This compound effect makes prediction of future RoS changes in complex climate models highly uncertain.

50 The frequency and intensity of RoS occurrence are expected to change in response to climate variations, including the distribution, intensity, and phase of precipitation (Blahušíaková et al., 2020; Li et al., 2020; Musselman et al., 2018), as well as the expected increase in air temperature and consequent changes in the snow occurrence (Jennings et al., 2018; Sezen et al., 2020). Snow-related changes will likely become the primary driver of interannual variations in RoS events (Suriano, 2022). Many studies predict a significant decrease in snow storage amounts and duration in the future (Hale et al., 2023; 55 Jenicek et al., 2021; Nedelcev and Jenicek, 2021; Notarnicola, 2020), which is confirmed by observed snow cover duration (Urban et al., 2023). These changes are expected to be important factors for future RoS occurrences.

Recent studies have also shown that the behavior and occurrence of RoS can be mainly explained by variations in both spatial and temporal distribution. As Hotovy et al. (2023) investigated, various trends in RoS days were identified for specific months of the winter season at different elevations. The largest decrease was observed at lower elevations towards 60 the end of winter, likely due to a shortening of the period with snow cover on the ground. Similar findings were presented by Beniston and Stoffel (2016); Li et al. (2019); López-Moreno et al. (2021); and Mooney and Li (2021). In contrast, the largest increase was found at higher elevations throughout the winter (Morán-Tejeda et al., 2016; Musselman et al., 2018; Ohba and

Kawase, 2020; Sezen et al., 2020; Trubilowicz and Moore, 2017). These changes can be associated with more frequent rainfall during the cold season, triggered by increasing air temperature (Il Jeong and Sushama, 2017; Mooney and Li, 2021).
65 Although several studies focusing on changes in RoS related to climate change have been carried out, there is still limited knowledge of the role of different climate variables controlling the RoS behavior and dynamics of the RoS-driven runoff responses. There is a lack of studies analyzing both changes in RoS and the related runoff responses. Moreover, most European studies have had a limited focus on elevation, which significantly influences snow cover and precipitation phase and consequently affects RoS occurrence. Analyzing the combined effect of an increase in temperature and changes in
70 precipitation is crucial since some studies have shown that the snow decrease caused by the increase in temperature may be partly offset by the increase in precipitation (Jenicek et al., 2021).

In this study, we present differences between commonly analyzed catchments within the Alpine region and relatively scarce low-elevation locations outside of this mountain range, representing the areas in the rain-snow transition zones where the largest changes in snow storage typically occur. Analyzing runoff responses driven by extreme meteorological events within
75 transition zones is a valuable contribution of this paper, as runoff uncertainty induced by transition elevation is more pronounced during larger precipitation events (Cui et al., 2023). The detailed temporal and spatial analyses of the effect of climate change on RoS behavior are also limited. However, understanding these changes and drivers is crucial to future water management strategies to mitigate risks and impacts associated with RoS events. To address the above research gaps, the objectives of this study are 1) to attribute changes in selected climate variables to simulated changes in RoS events, using
80 a sensitivity analysis of precipitation and air temperature, and 2) to evaluate subsequent changes in RoS-related runoff responses.

2 Material and methods

2.1 Study catchments

The study included 93 mountainous catchments in two regions within central Europe (Fig. 1). All study catchments with
85 selected physical and climate characteristics are listed in Table S1 in the Supplementary material. The first regional dataset (CZ IDs) consists of 60 catchments in six different mountain ranges in Czechia and an additional seven catchments in the eastern German states of Bavaria and Saxony located within the same cross-border mountain ranges. The original dataset of 40 catchments used in Nedelcev and Jenicek (2021) and Hotovy et al. (2023) was extended by 27 catchments in this study. The second regional dataset (CH IDs) includes 26 Swiss catchments in three parts of the Alps. For Switzerland, four
90 catchments were added to the dataset used by Girons Lopez et al. (2020).

These mountainous catchments were selected because they are affected by snow, show near-natural runoff regimes and have no glacierized areas. Catchment areas range from 1.8 to 478 km². The mean catchment elevation ranges from 491 to 2434 m a.s.l. The catchments in Czechia and Germany (CZ) generally represent lower elevations than the Swiss catchments

(CH). Annual mean air temperature varies from -0.9 to 8.9 °C. Annual precipitation totals range from 728 to 2187 mm. See
95 Table S1 for more details at the catchment level.

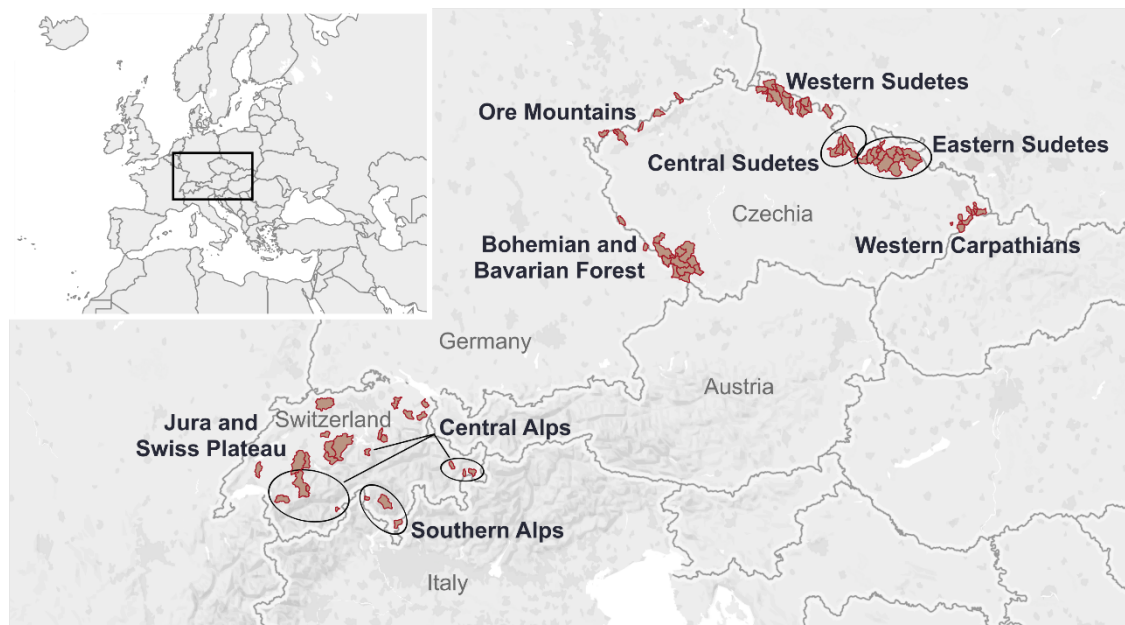


Figure 1: Location of study catchments in Czechia, Germany, and Switzerland.

2.2 Data

For runoff simulations (Sect. 2.3), a time series of daily mean air temperature, precipitation sums, mean discharge, and
100 weekly snow-water equivalent (SWE) estimates were collected. Stational data for the Czech catchments were available from
meteorological and hydrological stations operated by the Czech Hydrometeorological Institute (CHMI). If such a station was
unavailable within a given catchment area, the nearest station representing similar conditions and elevations was used. For
the German catchments, datasets on temperature and precipitation from the open-source database provided by the German
Weather Service (DWD) were used. Discharge data were available from the regional ministries - Landesamt für Umwelt,
105 Landwirtschaft und Geologie (LFULG) for catchments in Saxony (IDs CZ-201, 204-206), and Gewässerkundlicher Dienst
Bayern (GDB) for catchments in Bavaria (IDs CZ-101, 102, 112). Temperature and precipitation data for this dataset covers
the period 1965-2019. Mean daily discharge and weekly SWE data (taken from the nearest Czech stations) were available
for the period 1980-2014.

Data provided by the Swiss Federal Office of Meteorology and Climatology (MeteoSwiss) were used for analyses within the
110 Swiss catchments. The MeteoSwiss gridded data product covers the entire territory of Switzerland and data are available
from 1965. We used this data to calculate the mean daily air temperature and precipitation for each catchment. Hydrological
data used for the analyses were provided by the Swiss Federal Office for the Environment (FOEN). The mean daily SWE for

each catchment was calculated based on a gridded product combining snow depth station data and a snow density model (Magnusson et al., 2014; Mott et al., 2023).

115 2.3 HBV model

To derive individual components of the rainfall-runoff process for the reference period 1980-2010 (30 cold seasons), and to subsequently detect RoS events (Sect. 2.4), a semi-distributed bucket-type HBV model (Lindström et al., 1997; Seibert and Bergström, 2022) in its software implementation “HBV-light” (Seibert and Vis, 2012) was used in this study.

The model is composed of four routines, including a snow routine that simulates snow accumulation and snowmelt using a
120 degree-day approach, taking the potential refreezing of meltwater and snow water holding capacity into account. The precipitation phase is distinguished by a single threshold temperature (T_T) approach, while the T_T values were calibrated separately for each catchment in this study, ranging from -1.66 to 1.16 °C across the Czech catchments and from -1.92 to 1.63 °C for the Swiss catchments. In addition to the snow routine, a soil moisture routine calculates groundwater recharge and actual evapotranspiration (AET) as a function of the soil moisture. For this, the input data of potential evapotranspiration
125 (PET) was calculated based on air temperature data using the method presented by Oudin et al. (2005). Runoff from two groundwater boxes is simulated by a groundwater routine, from which baseflow is directly calculated by the model. A routing routine calculates the propagation of runoff through the catchment using a triangular function.

Each catchment was split into elevation zones of 100 m. This enables the simulation of some of the characteristics separately for these elevation zones, specifically precipitation, air temperature (using calibrated lapse rates), SWE, snowmelt, soil
130 moisture, AET and groundwater recharge. For details of the model structure and routines, see Seibert and Vis (2012).

The HBV model was calibrated automatically against the observed mean daily runoff and SWE for each study catchment using a genetic algorithm in 100 independent calibration trials. Since the genetic algorithm contains stochastic elements, each calibration trial will result in different optimized parameter sets, especially if there is significant parameter uncertainty (equifinality) (Beven, 2021). Following a split-sample approach, the period was divided into calibration and validation
135 windows for both regional datasets (Table 1). As an objective function, a weighted mean of the NSE (the Nash-Sutcliffe model efficiency coefficient) based on the logarithmic runoff series (60 %), the volume error (20 %) and the NSE based on the logarithmic SWE series (20 %) was used along with a combination of several objective criteria, which were used for the evaluation of the goodness of fit of the model.

140 **Table 1: Periods used in the modeling procedure.**

Model simulation periods	CZ dataset	CH dataset
Split-sample periods for model calibration and validation	1981-1997, 1998-2014	1981-2000, 2001-2020
Simulated reference period	1980-2010	1980-2010

This model setup was similar to the approach used in previous studies, e.g. Seibert and Vis (2012) or Girons Lopez et al. (2020), with various model testing studies carried out, including studies evaluating the overall model performance, e.g. Jenicek and Ledvinka (2020), Nedelcev and Jenicek (2021), or more specific studies assessing the RoS occurrence and SWE, based on model simulations, e.g. Hotovy et al. (2023).

2.4 RoS day and RoS event identification

Selection criteria were defined to identify individual RoS days, which happen when rainfall and snow cover occur together. Thus, a RoS day was identified when the following conditions were fulfilled:

1) Precipitation occurred on days with mean temperatures above the threshold temperature T_T (and, thus, being assumed to be rain), with intensities of at least 5 mm per day (i.e., excluding drizzle or negligible amounts). Note that the calibration of the T_T parameter was a part of the general calibration process described in Sect. 2.3.

2) Simulated mean SWE for a given day reaching at least 10 mm, detecting the thick snowpack layer on the ground.

In addition to the RoS day definition mentioned above, multi-day RoS periods, referred to as RoS events here, were identified at a catchment scale to assess hydrological implications and changes in a hydrological response caused by such RoS events. In this study, RoS events were defined as multi-day events, which start from the initial RoS day (the first day when both conditions given above were met), and end day, when the first local maximum runoff was simulated. RoS events may include both, RoS days and non-RoS days. The maximum RoS-driven response time was limited to six days, similar to Freudiger et al. (2014). RoS events were defined in the same way as in Hotovy et al. (2023) and were used for hydrological response analyses (Sects. 2.6 and 3.7).

2.5 Sensitivity to climatic variations

A sensitivity analysis assessed how incremental changes in climate variables affect RoS occurrence and their runoff response. In this study, we modified two main climate parameters governing snow storage and RoS events: air temperature (T) and precipitation (P). The modifications consider future changes in these climate variables projected for the central European region by climate models (Gutiérrez et al., 2021). A total of 24 combinations (projections) of increasing air temperature and precipitation change were used for simulations relative to the reference conditions (hereafter referred to as T0_P1). The referenced (current) air temperature (T0) was manually increased by 1-4 °C (T1, T2, T3, T4), and changes in precipitation from a 20 % decrease to a 20 % increase were applied (P08 = -20 %, P09 = -10 %, P11 = +10 %, P12 = +20 %). These 24 combinations cover most of the projected changes in air temperature and precipitation from less warm to warm and from dry to wet conditions. Mean air temperatures and precipitation totals for all catchments in both regions are listed in Table S1 in the Supplementary material. Temperature and precipitation modifications were applied to the entire daily data series.

2.6 Assessment of RoS-related variables

As a basis for further analyses, several hydroclimatic statistics (Table 2) were calculated from simulations for each catchment (67+26 catchments) and all 25 projections. These statistics included mean seasonal (Nov-Apr) air temperatures (T_{mean}), precipitation sums (P_{sum}), annual mean snow water equivalents (SWE_{mean}), annual maximum snow water equivalents (SWE_{max}), the annual sum of snowfall (S_{sum}) and annual snowfall fraction (S_f). These annual or seasonal values were then correlated with the number of RoS days. For this, Spearman's correlation coefficient was used to detect mutual correlations between variables, as the variables were not normally distributed based on the results of a Shapiro-Wilk test. Correlation analyses were performed based on all 25 projections, averaged per catchment, separately for each of the two main geographical regions. Table S2 in the Supplementary material shows modeled values of all variables for distinct projections. To evaluate the RoS-related hydrological response and its changes for all climate projections, the total runoff (Q_{event}) during RoS events was calculated, and the total direct runoff (Q_{direct}) was calculated for each RoS event (Table 2). A fraction of the total runoff during RoS events to the total runoff was then calculated to describe the relative contribution of the RoS runoff to the total catchment runoff. Moreover, the relative changes in the total direct runoff were evaluated for individual projections.

Table 2: List of climate and snow variables and hydrological parameters used in the analyses.

Variable	Description
T_{mean}	Nov-Apr mean air temperature [$^{\circ}\text{C}$]
P_{sum}	Nov-Apr precipitation sum (rainfall and snowfall) [mm]
SWE_{mean}	Nov-Apr mean snow water equivalent [mm]
SWE_{max}	Nov-Apr maximum daily/weekly snow water equivalent [mm]
S_{sum}	Nov-Apr snowfall sum [mm]
S_f	Nov-Apr snowfall fraction, a ratio of snowfall water equivalent to total precipitation [-]. The threshold temperature calibrated by the HBV model has been used for separating snowfall and rainfall.
Q_{event}	Total runoff during RoS event [mm]
Q_{direct}	Direct runoff (sum) during RoS event [mm] calculated as an outflow from the upper groundwater box of the HBV model, which is considered to be a fast runoff component

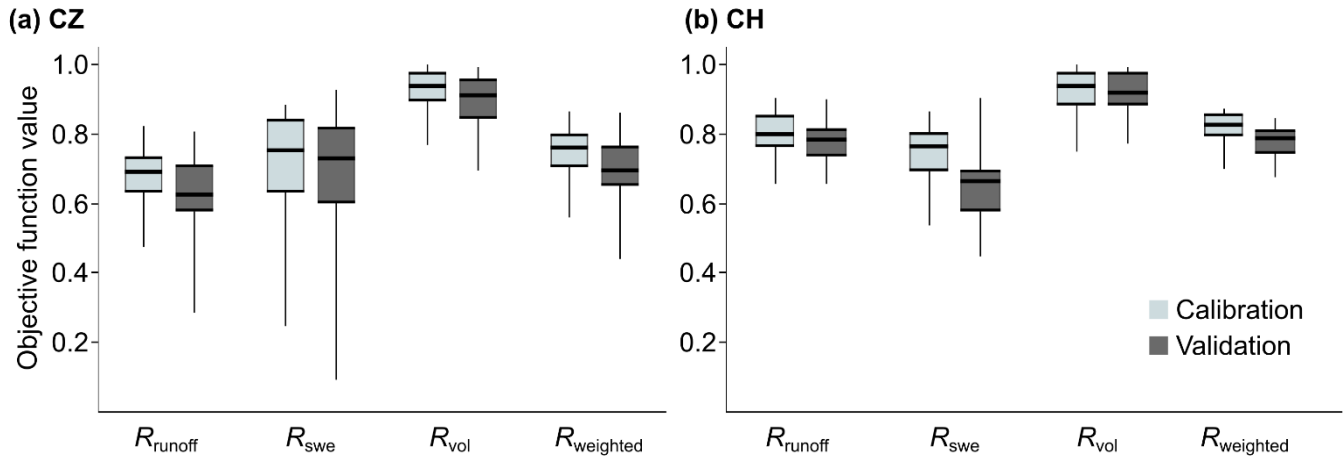
3 Results

3.1 HBV model evaluation

Overall model performance was evaluated using a combination of selected goodness-of-fit criteria with different weights (Fig. 2). The median objective function value resulting from 100 parameter sets was 0.76 for model calibration for the Czech catchments and 0.83 for the Swiss catchments (values ranged from 0.56 to 0.86, and 0.70 to 0.87 respectively). Results for model validation reached 0.70 for the Czech catchments, and 0.79 for the Swiss catchments (values ranged from 0.44 to 0.86, and 0.68 to 0.85 respectively). More model testing of SWE simulations and RoS occurrence was carried out by Jenicek

195 et al. (2021), Nedelcev and Jenicek (2021), and Hotovy et al. (2023), who all worked with a similar set of catchments in their studies. Hotovy et al. (2023) also tested the HBV model performance during RoS events and concluded that the HBV model, despite its conceptualization of the snowmelt process, may be used for RoS analyses, specifically for the assessment of interannual variability and trends of RoS events.

200



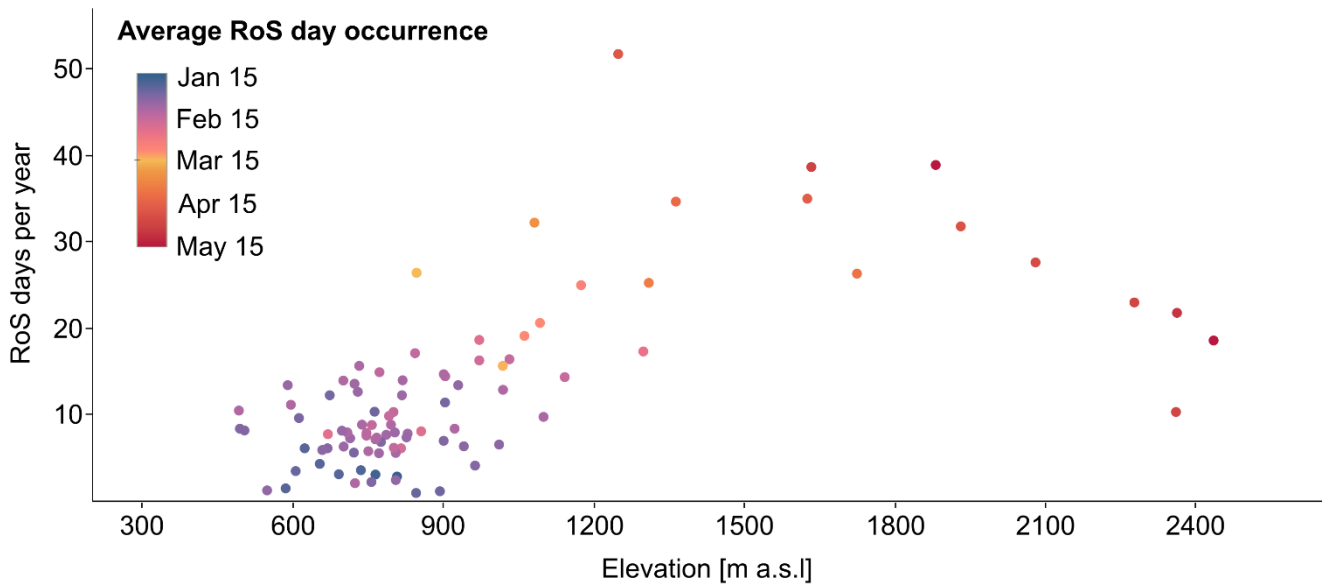
205

Figure 2: Model performance for all 93 study catchments within both Czech (a) and Swiss (b) regions evaluated by the combination of selected objective criteria, including the logarithmic Nash-Sutcliffe efficiency for runoff (R_{runoff}), Nash-Sutcliffe efficiency for SWE (R_{swe}), and volume error (R_{vol}). These criteria were weighted ($R_{weighted}$) to calculate the overall objective function of the model. Boxplots represent the variation among catchments, with the 25th and 75th percentiles within a box, the median as a thick line and the whiskers represent maximum and minimum values.

3.2 RoS day occurrence

According to the RoS day definition given in Sect. 2.4, RoS occurrence within individual study catchments and elevations is shown in Fig. 3. The displayed values represent the annual number of RoS days during 30 cold seasons (1980-2010), corresponding to the RoS frequency in the reference scenario T0_P1. Values shown in Fig. 3 are valid for mean elevations of individual catchments.

The total number of RoS days for each catchment varied from 31 to 1554 in the entire study period. The lowest occurrence was observed at Blanice catchment (CZ-115), where only one RoS day occurred each season on average. In contrast, the Sitter catchment (CH-114) experienced frequent RoS with 52 days each season on average. Generally, the highest number of RoS days appeared within the elevation range of 1000-2000 m a.s.l., including high-elevation Swiss catchments in particular. At lower elevations, typically for the Czech catchments which experienced the shorter snow season, RoS days occurred less frequently. The number of RoS days decreased at those catchments with the highest mean elevation, likely due to the lack of rainfall during the winter season (results not shown). Distinct catchments saw the average RoS occurrence at different times of the year from mid-January to mid-May, reflecting the increase in elevation.

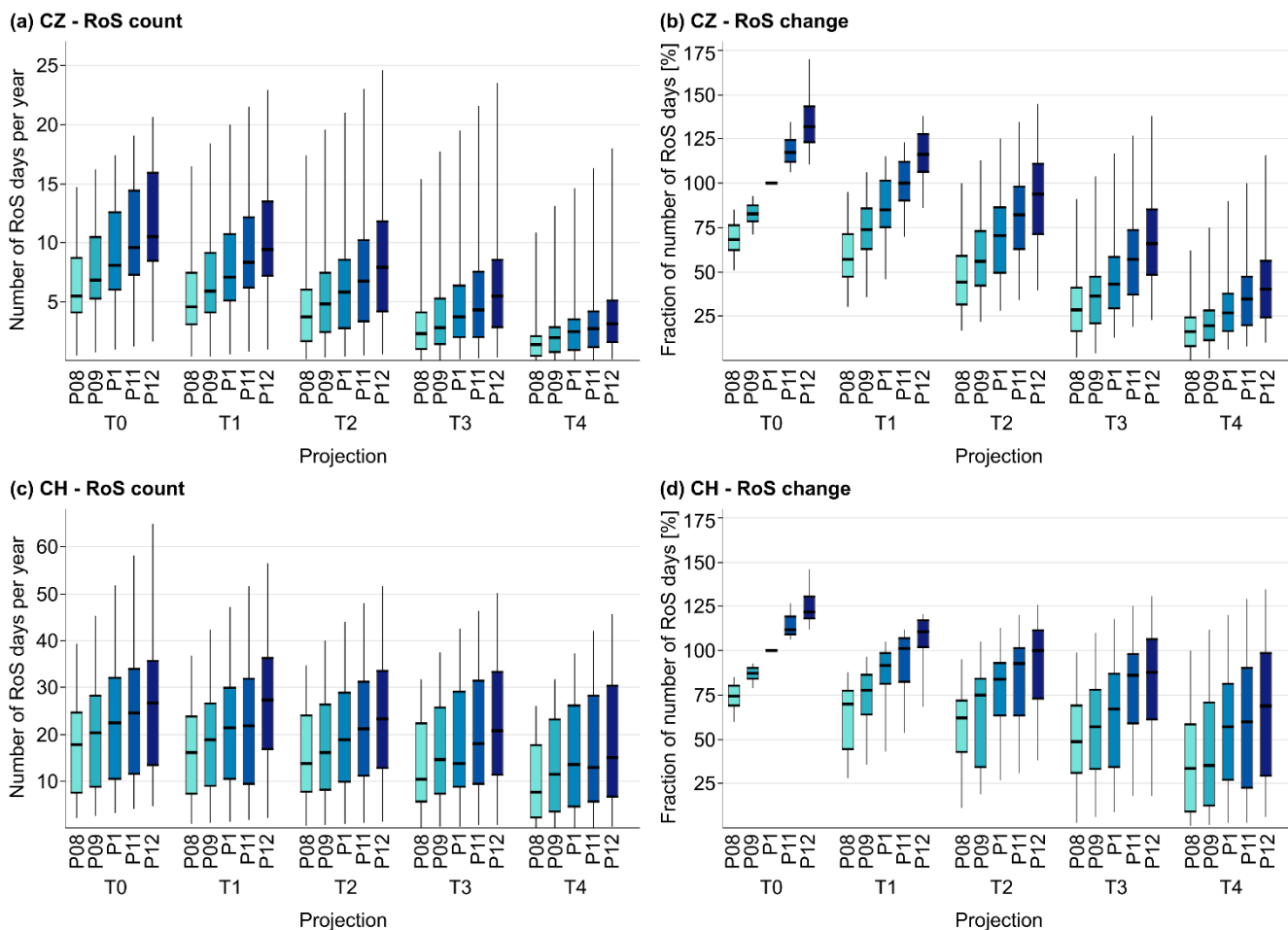


220

Figure 3: The annual number of RoS days in all 93 study catchments between 1980 and 2010, corresponding to the reference scenario T0_P1. Each dot represents one catchment and is colored according to the average RoS occurrence throughout the year. Individual catchments are characterized by mean catchment elevation (shown in Table S1).

3.3 Regional changes in RoS days for different climate projections

225 The numbers of annual RoS days were found to vary regionally and for the 25 projections (Fig. 4). The changes in the median values of all catchments within each region suggest that only four projections for the Czech dataset, and five projections for the Swiss dataset, will lead to an increase in the number of RoS days. The number of RoS days increased only for the projections with a 1 °C temperature increase combined with a precipitation increase (projections T0_P11, T0_P12, T1_P11, T1_P12). In most of the projections, the number of RoS days is expected to decline (Figs. 4a and 4c), especially for
 230 projections with a relatively large temperature increase amplified by precipitation decrease. Projections with a temperature increase of 4 °C suggested a decrease of RoS days by about 75 % for the Czech catchments (Fig. 4b). For the high-elevation Swiss catchments, the number of RoS days decreased less (Fig. 4d). However, there were large variations among the individual study catchments in each region.

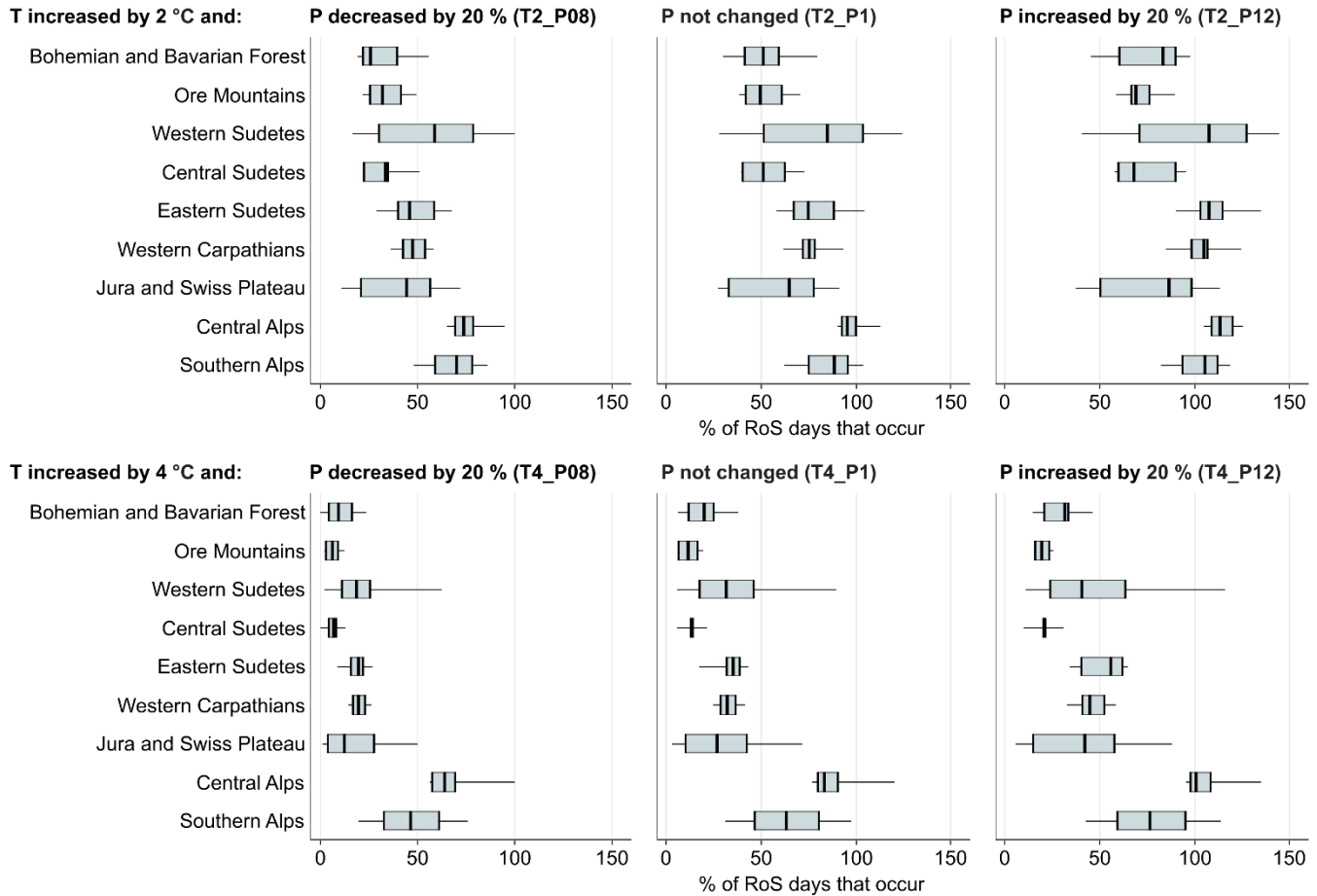


235 **Figure 4: Number of RoS days per year in both Czech (a, b) and Swiss (c, d) regions for all projections (a, c), and a fraction of the number of RoS days relative to reference conditions in both regions for all projections (b, d). Boxplots represent the variation among catchments, with the 25th and 75th percentiles represented by each box, the median as a thick line and the whiskers showing the maximum and minimum values. Boxes are grouped and colored according to the temperature (T) and precipitation (P) projections.**

240 The above-mentioned differences and projected changes across regions are supplemented by the evaluation across individual mountain ranges (Fig. 5). Results showed that catchments are generally less sensitive to changes in precipitation compared to the increase in temperature. This was shown by projections assuming a temperature increase by 4 °C, where similar RoS decreases were suggested among individual mountain ranges, independent of changes in precipitation.

Overall, there were large differences between the individual mountain ranges and selected projections. Regionally, the catchments located in the Western Sudetes will be relatively unaffected by the temperature increase by 2 °C, however, additional temperature rise (T4 projections) may result in sudden RoS decline, which will be more pronounced compared to the Eastern Sudetes and Western Carpathians. In Switzerland, the catchments located in the Central and Southern Alps showed higher resistance to changes in air temperature and precipitation than those in the Jura and Swiss Plateau, which

250 behave similarly to those in Czechia. In general, southern and western mountain ranges experienced larger RoS decreases in both regions.



255 **Figure 5: Percent of RoS days that occur due to the temperature (T) increase and precipitation (P) changes in selected combinations, compared to reference scenario T0_P1. Boxplots represent the variation among catchments located in the individual mountain ranges, with the 25th and 75th percentiles within a box, the median as a thick line and the whiskers representing maximum and minimum values.**

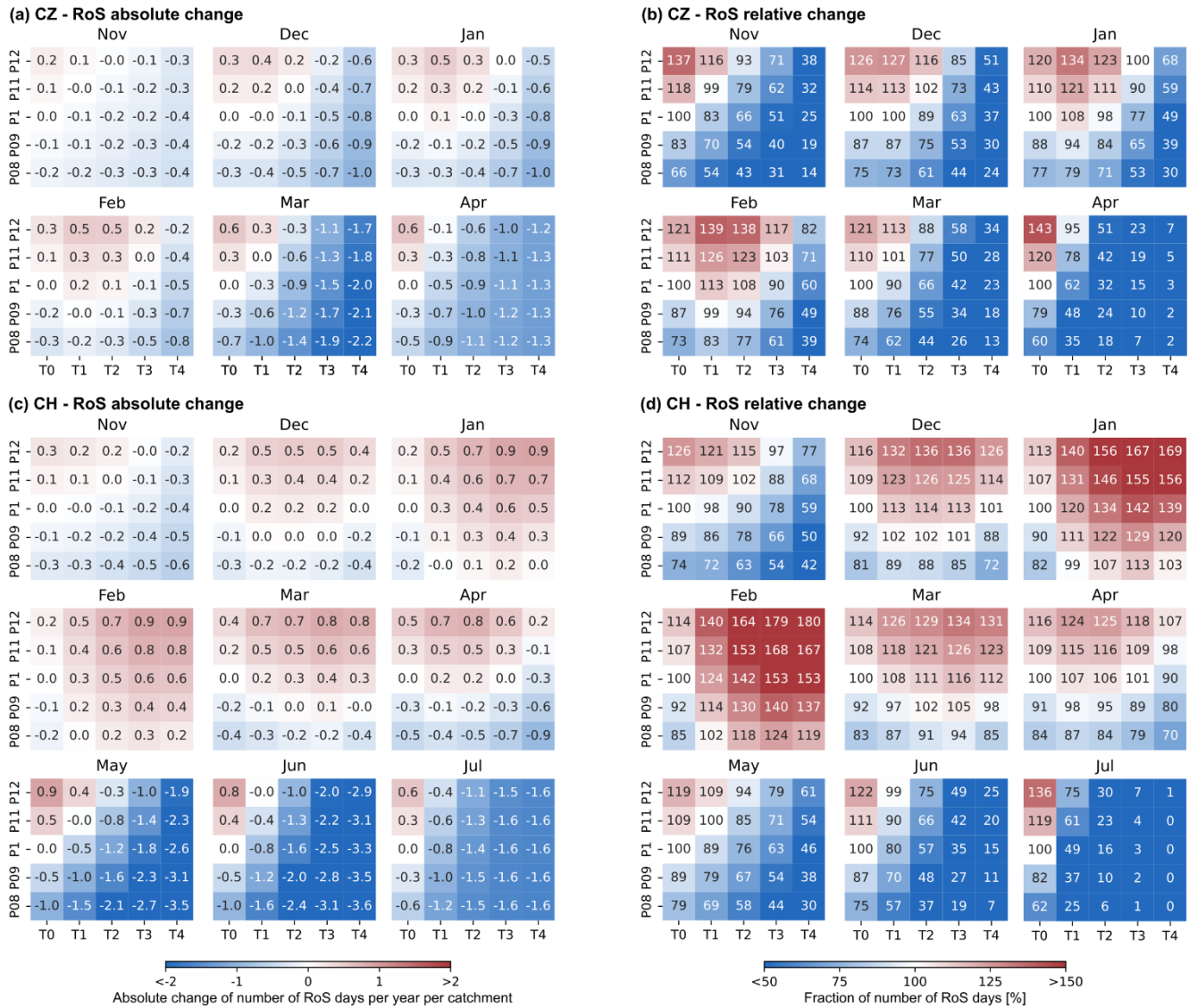
3.4 Seasonal RoS changes for different climate projections

Results showed that changes in RoS occurrence will likely differ considerably for different months of the cold season. A notable RoS increase was detected in January and February across the Swiss catchments (Fig. 6d) and this mid-winter trend was more pronounced than in Czechia. In these winter months, only two projections resulted in a slight RoS decrease in Switzerland. Across the Czech catchments, a RoS increase was limited only to projections leading to wet conditions and a moderate increase in air temperature (Fig. 6b).

260

Towards the end of the winter, with an earlier snowmelt period onset in Czechia, a decrease in RoS days was simulated for most projections (Figs. 6a and 6b). Projections leading to the temperature increase by more than 2 °C led to a slight RoS

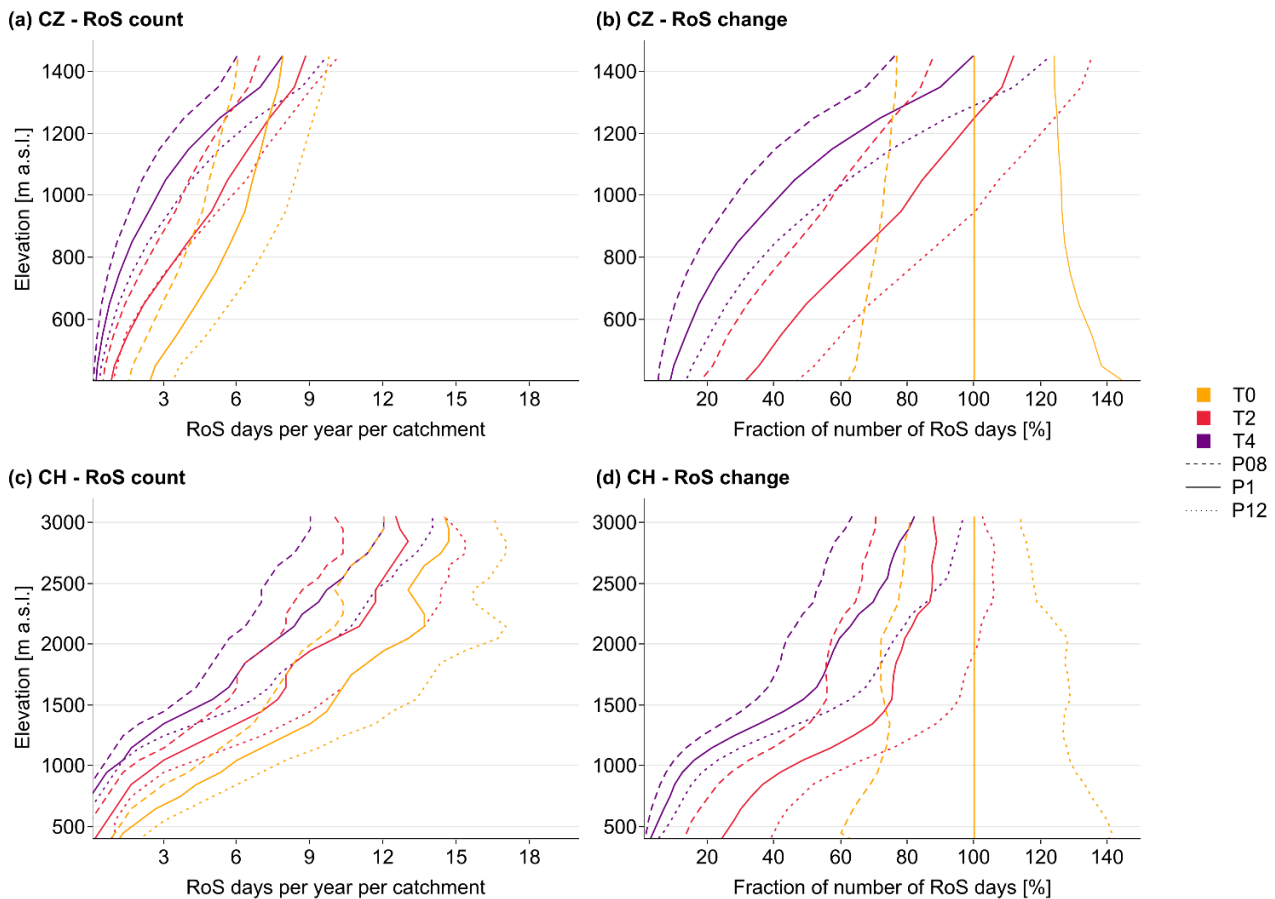
265 increase only for the wetter months of January or February. Only a few projections, representing wetter conditions and a temperature increase limited to 2 °C, predicted an increase in the number of RoS for the Czech catchments for other months during the cold season (November, December, March, and April). A similar pattern, although for more projections and with a more substantial RoS increase, was simulated across the Swiss region (Figs. 6c and 6d). This RoS increase resulted from the compensating effect of increased precipitation for projections with a moderate increase in air temperature.



270 **Figure 6: Absolute (left column, a and c) and a fraction of the number of RoS days (right column, b and d) for all projections (T and P combinations) in both Czech (top row, a and b) and Swiss (bottom row, c and d) regions. Note that changes are related to reference conditions T0_P1 and selected months (May-Oct for CZ, Aug-Oct for CH) are not shown here due to having only a few RoS days.**

3.5 RoS changes across elevation zones

275 Elevation-based differences in the occurrence of RoS days (Fig. 3) were further analyzed in more detail. We identified considerable patterns in RoS variations across elevation zones (Fig. 7), evaluating all RoS days expected to occur in the study catchments (Figs. 7a and 7c). The wettest projection with no temperature change (T0_P12) is the only projection that suggested a RoS increase for all elevations in both geographical regions (Figs. 7b and 7c). All other projections simulated RoS decline below 1000 m a.s.l. for both study regions, whereas the decline for the Swiss catchments is more pronounced below this elevation level. More than an 80 % decrease may occur below 600 m a.s.l. for the Czech catchments for the projections with the highest air temperature increase (T4). A similar relative decrease in RoS days occurs for the Swiss catchments at elevations even below 1000 m a.s.l. Another difference between the two study regions was indicated at the highest elevations in Czechia (above 1300 m a.s.l.), where the warmest and wettest projections suggested the RoS increase. In contrast, such an increase was not seen in the simulations for the Swiss catchments.



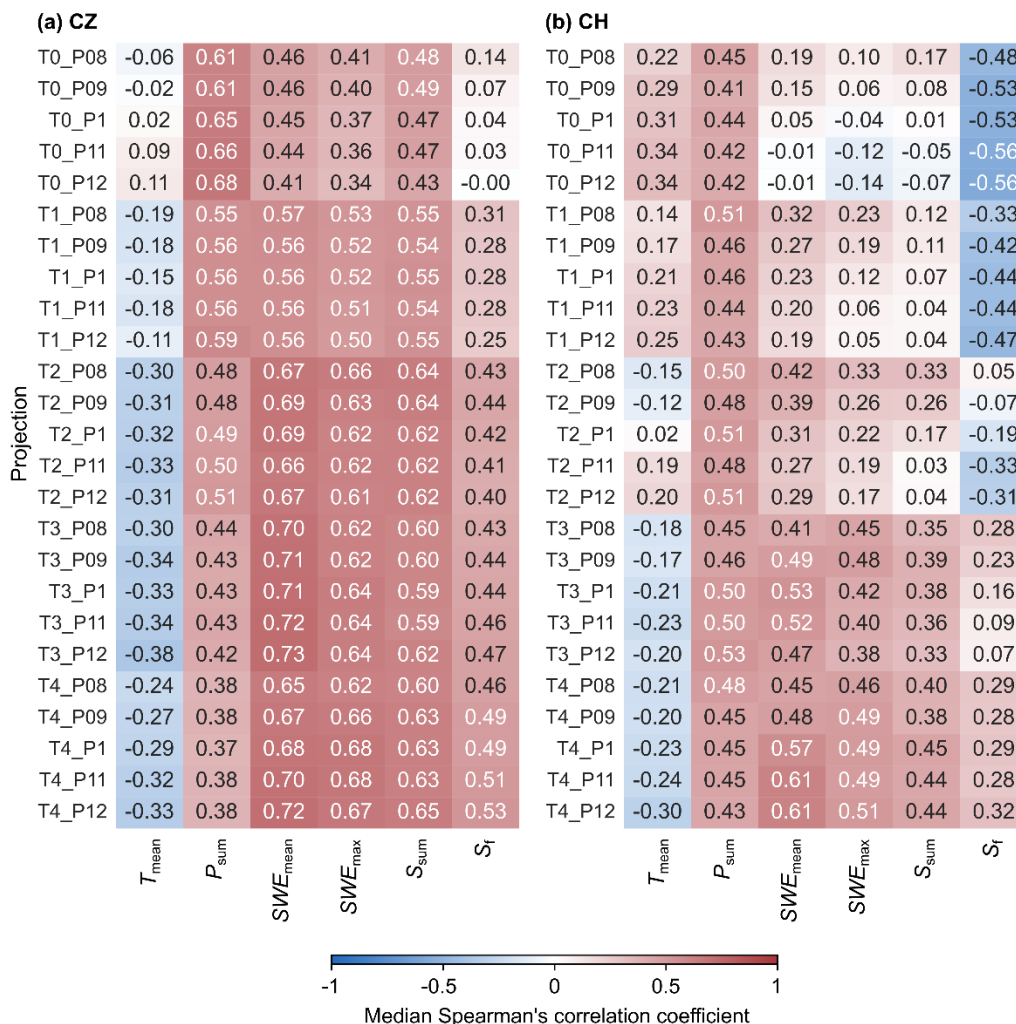
285

Figure 7: RoS day occurrence (a and c) and a fraction of the number of RoS days for selected projections compared to reference conditions T0_P1 (b and d) for distinct elevation zones in both Czech (a and b) and Swiss (c and d) regions. The absolute RoS numbers were weighted by the number of catchments within the individual elevation zones. Line colors and styles represent selected temperature (T) and precipitation (P) projections.

290 3.6 Effect of seasonal characteristics on the RoS occurrence

Several climate and snow parameters defined in Sect. 2.6 were assessed for their relation with the occurrence of RoS days based on the values of Spearman's correlation coefficient (Fig. 8). Results showed some interesting differences between the main regions and individual parameters. Interestingly, a correlation between the occurrence of RoS days and air temperature (T_{mean}) was relatively weak (values up to -0.38), but tended to be more negative and thus stronger with projected temperature increase in both regions. Results also indicated that the sum of precipitation (P_{sum}) plays a more important role in the occurrence of RoS days compared to air temperature. In Czechia, relatively strong positive correlations with precipitation totals became less important for warmer projections, which may be associated with the decrease in snowfall totals causing an overall RoS decrease for warmer projections. In Switzerland, seasonal snowfall totals (S_{sum}) were detected as the less important driver for RoS occurrence compared to the seasonal sum of all precipitation, regardless of the projection. Parameters related to SWE (SWE_{mean} , SWE_{max}) were shown as the most important factor for the Czech catchments, showing an increasing positive relation for the warmer projections.

Similar to the Czech catchments, the importance of SWE increased with the temperature increase in Switzerland. However, the positive correlation was relatively lower, particularly for the projections with a relatively lower increase in air temperature. Snowfall fraction (S_f) was identified as the parameter with the largest fluctuations across projections and regions. Positive correlations increasing with the warmer projections were detected in Czechia while increasing snowfall fraction led to fewer RoS days in projections characterized by a temperature increase of up to 1 °C. Overall, results suggested that RoS events are sensitive to different changes in individual parameters among both regions and individual projections.



310 **Figure 8: Median Spearman's correlation coefficients indicated by color and number for all projections in both Czech (a) and Swiss (b) regions valid for the selected climate and snow characteristics: Seasonal mean air temperature (T_{mean}), sum of precipitation (P_{sum}), mean snow water equivalent (SWE_{mean}), maximum snow water equivalent (SWE_{max}), sum of snowfall (S_{sum}) and snowfall fraction (S_f).**

3.7 Runoff response to RoS

315 To assess RoS event-related runoff response and its changes for different projections, the total RoS runoff (Q_{event}) for each RoS event was calculated (Sect. 2.6) and shown as a ratio to the total annual runoff in both regions (Fig. 9). The results show that RoS-driven runoff contributes to the total runoff with different volumes in both regions, and these contributions are expected to change for different projections. In the reference conditions (T0_P1), RoS events contributed on average by 10 % to the total annual runoff in the Czech catchments, with the highest contribution of 19 % for some catchments (Fig. 9a). In

320 Switzerland, where the variability was much higher, RoS events contributed on average 18 % to the total annual runoff with some catchments contributing up to 35 % (Fig. 9b). The results indicated that the RoS contributions will likely decrease in

the future following a temperature increase. For instance, model simulations suggested that RoS events will be responsible for 5-9 % of the total annual runoff in Czechia for a temperature increase of 2 °C, and 11-16 % in Switzerland. Projections with a temperature increase of 4 °C would reduce the runoff fractions to 2-4 % across the Czech catchments, and 5-9 % for the Swiss catchments. Nevertheless, the RoS runoff decrease caused by the increased air temperature may be partly compensated by the precipitation increase. Despite the expectations that the RoS impact on the total runoff will be lower in the future, extreme hydrological response and flooding triggered by RoS events may still occur.

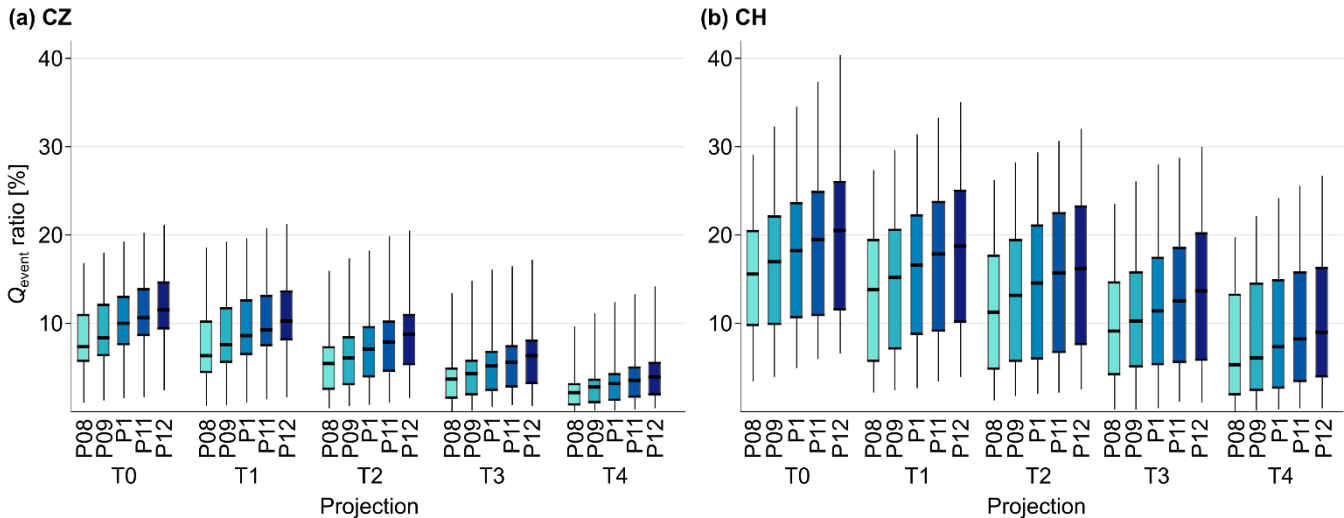


Figure 9: Fractions of ROS-driven runoff (Q_{event}) to the total annual runoff in both Czech (a) and Swiss (b) regions for all projections. Boxes represent the 25th and 75th percentiles, with the median from all catchments indicated as a thick line. Whiskers represent maximum and minimum values. Boxes are grouped and colored according to the temperature (T) and precipitation (P) projections.

The regional differences in the annual RoS runoff fractions were further investigated for individual months during the cold season, showing the relative changes in the direct runoff during RoS days (Q_{direct}) for all projections (Fig. 10). These relative changes, in parallel to the changes in hydrological response, were consistent with relative changes in the number of RoS days shown in Figure 5. For the Czech catchments, a relative increase of at least 25 % was projected only for two projections (T0_P11 and T0_P12) for all months (Fig. 10a). Note that May to October (for Czechia) and August to October (for Switzerland) were excluded from the analysis due to a low number of RoS events, which does not allow for a robust analysis.

In Switzerland, changes in RoS-related direct runoff and RoS occurrence correlated even better, and hydrological impacts generated by RoS events were generally more pronounced (Fig. 10b). In contrast to the Czech catchments, the mid-winter months (December to March) were assessed to be the most hazardous for increased RoS-related runoff response. A notable direct runoff increase of more than 50 % was projected for warmer and wetter projections throughout December to February. For January and February, higher RoS-related runoff was predicted even for some drier projections. With the expected more

345 frequent RoS events during these months, Swiss catchments, particularly high-elevated ones, may face more extreme RoS-related flood events in the future.

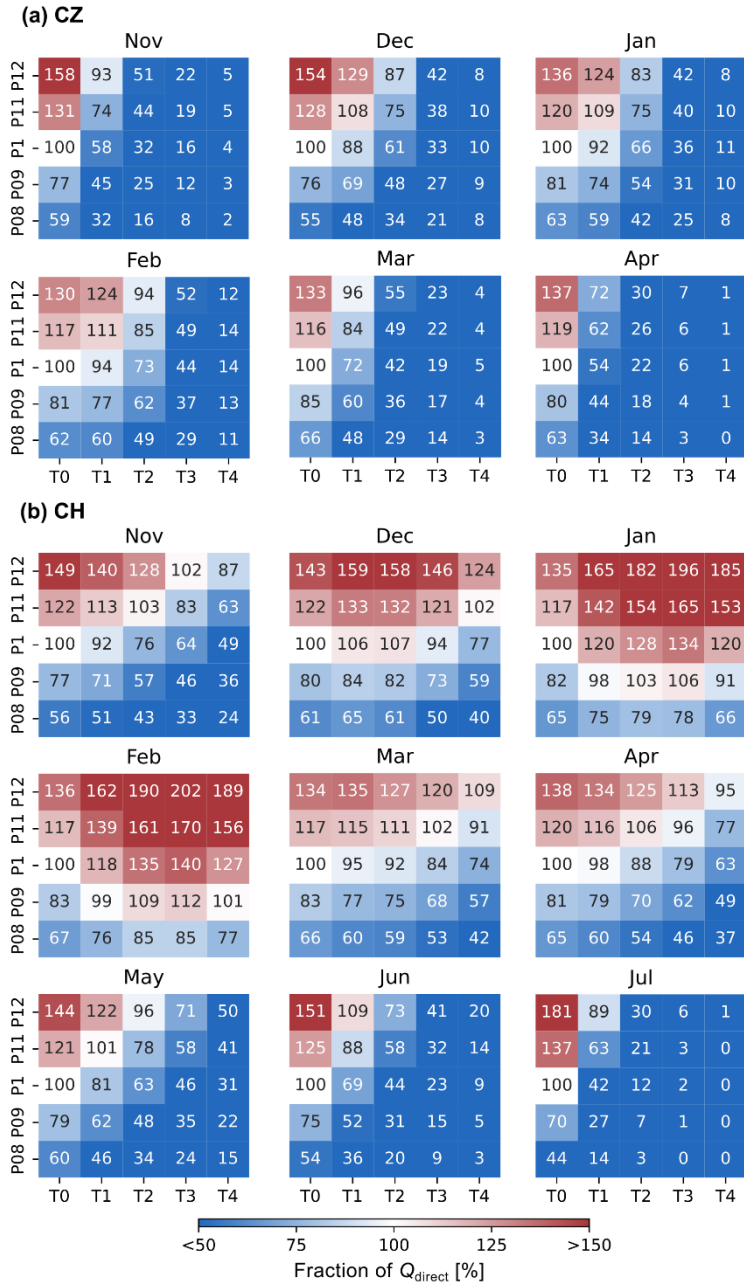


Figure 10: Monthly fraction in RoS-driven direct runoff (Q_{direct}) relative to reference conditions T0_P1 (100, white entries, first column, third row) for all projections (T and P combinations) in both Czech (a) and Swiss (b) regions.

4.1 HBV model uncertainty

To determine rainfall-runoff components and thus to identify RoS days, RoS events, related variables, and all projected changes, a semi-distributed hydrological model HBV was employed in this study, similar to Freudiger et al. (2014), Juras et al. (2021) and Hotovy et al. (2023). Model calibration, validation and testing were performed in the previous studies using similar datasets (Jenicek and Ledvinka, 2020; Jenicek et al., 2021). Consistently with these studies, multi-criteria model calibration and reiterated calibration runs were performed to reduce the overall parameter uncertainty. Nash-Sutcliffe efficiency values over 0.7, which were also reached for the extended dataset in this study, represent one of the acceptable test criteria (Moriassi et al., 2015).

Since the presented results are based on modeled SWE to define RoS situations, uncertainties arising from the model parametrization need to be addressed. The assessment of the model's ability to simulate SWE and thus detect RoS days correctly was investigated by Hotovy et al. (2023), who compared counts of observed and simulated RoS days, as well as simulated runoff and SWE during RoS events specifically, and did not find major inconsistencies in the model runs and assumed that the model provided sufficiently good simulations. Differences between observed and modeled values may result from the lack of SWE measurements and representativeness of the measurement location, particularly across the Czech catchments. More detailed testing of SWE simulations for the Czech catchments was carried out by Jenicek et al. (2021) and Nedelcev and Jenicek (2021). For example, Nedelcev and Jenicek (2021) compared simulated and observed trends in air temperature, precipitation, and SWE, concluding that the model can provide overall reliable simulations of the above variables, which are temporally and spatially consistent with observed data. SWE simulations were not explicitly evaluated for the Swiss catchments. However, overall model performance is better in simulating SWE for the Swiss catchments, since daily gridded SWE data combining snow depth station data and a snow density model has been used for model calibration (Magnusson et al., 2014).

The HBV model uses the modified degree-day approach, which may raise further questions about model simplification. However, this simplified method, which is based on a near-linear relationship between snowmelt and air temperature, was hard to outperform at a catchment scale using more sophisticated models, accounting for the entire energy balance of the snowpack (Seibert and Bergström, 2022). Moreover, the complex energy balance approach demands specific data, which is difficult or even impossible to use at a regional scale with various types of catchments. Despite the possible limitations of these bucket-type approaches, several studies have demonstrated that the degree-day method is adequate to be used for snow storage simulation at a catchment scale under a changing climate (Addor et al., 2014; Etter et al., 2017; Juras et al., 2021). Girons Lopez et al. (2020) confirmed that the current HBV snow routine provides results at a catchment level that can hardly be improved despite increasing the physical representation. The above studies confirmed that the model can correctly simulate and distribute all selected snow-related parameters for study catchments adequately to trends in time series. Results

presented in the previous studies showed that model setup, procedures, and derived parameters can satisfactorily represent the actual natural processes, including specifics of RoS events.

4.2 RoS definitions

385 Variations of the threshold values set to identify individual RoS days/events may significantly affect the total number of recognized situations. A unified RoS definition does not exist in the literature. Different authors use different parameters and thresholds in their studies. The average temperature, duration of snow cover, and the dominant phase of precipitation are expected to be the main factors that explain the variation in the sensitivity of RoS to climate warming (López-Moreno et al., 2021).

390 As for air temperature, several studies (Bieniek et al., 2018; Crawford et al., 2020; Surfleet and Tullos, 2013) used the threshold of 0 °C for the daily mean air temperature, while numerous recent studies did not specify the temperature threshold for detecting RoS (Mooney and Li, 2021; Pall et al., 2019; Schirmer et al., 2022; Yang et al., 2022). In this study, we determined the air temperature threshold as one of the RoS-defining parameters, which has been calibrated separately for each of the study catchments. This approach appeared to be a valuable addition to the previous definition used by Hotovy et al. (2023), who used zero as the temperature threshold. The varying threshold temperature may buffer local climatic conditions affected by different catchment properties, such as elevation range, topography or vegetation, and thus reduce one of the sources of potential errors when identifying RoS days and events. However, we found only minor local differences in the number of RoS days in this presented research as well as in the study performed by Hotovy et al. (2023).

Derived threshold temperatures applied in this study varied from -1.9 to 1.6 °C within all study catchments (Sect. 2.3). This threshold temperature range is comparable to the one presented by Jennings et al. (2018), who identified the temperature range between -0.4 and 2.4 °C to be valid for 95 % of the stations across the Northern Hemisphere, and indicating the air temperature at which rainfall and snowfall are in equal frequency. Lower temperature thresholds occurred particularly at high-elevated catchments, where snowfall occurs more often than rainfall. The temperature threshold is a challenging criterion that is used in the model to distinguish the phase of precipitation. This can be especially challenging during days when the air temperature fluctuates around the freezing point and consequently, the snowfall fraction is even more sensitive to the changes in air temperature.

4.3 Sensitivity analysis approach

In this study, we investigated potential RoS changes due to variations in climate variables, namely air temperature and precipitation, assessing regional and seasonal changes, future changes at different elevations, and changes in RoS-related runoff response.

To limit uncertainties related to the climatological modeling, a sensitivity analysis was applied in this study instead of the complex climatological modeling approach to assess how air temperature and precipitation changes affect RoS occurrence and extremity. Different sources of uncertainty resulting from the modeling approach were considered in several RoS

studies, with natural climate variability being seen as the primary source of uncertainty in RoS projections (Schirmer et al.,
415 2022). A sensitivity analysis approach for RoS-related research was performed by López-Moreno et al. (2021), who used this
method to demonstrate the effects of the warming climate.

In this study, climate variables were altered with regard to the expected future climate variations presented by various
respected sources (Gutiérrez et al., 2021). A total of 24 combinations covered a large range of possible future climate
behavior. These projections were related to the given reference period, representing the current climate conditions that are
420 already even more than 1 °C warmer compared to the air temperature in the pre-industrial era. Selected temperature
projections cover more optimistic ranges with an air temperature increase up to 2 °C but also pessimistic projections with a
temperature increase close to 4 °C. Since the direction of precipitation changes is uncertain for the regions of central Europe,
projecting both increases and decreases using different climate models, a range from a 20 % decrease to a 20 % increase was
applied in this study to cover a wide range in potential future climate.

425 **4.4 Observed and future changes in RoS**

Studies investigating RoS occurrence are usually limited to specific regions (Li et al., 2019; Yang et al., 2022) since the
spatial and temporal distribution of RoS days and events is controlled by current and local weather conditions. Thus, a
comparison of RoS occurrence across different regions may be challenging. Notable regional differences within both study
regions and individual subregions and mountain ranges were also detected in this study. Local climate variability and
430 uncertainty in climate model projections (discussed more in detail in Sect. 4.3) are other factors that make climate change-
driven variations in RoS even more challenging to assess. The sensitivity of RoS to climate change is highly variable among
sites and also with different elevations, aspects, and slopes in each basin (López-Moreno et al., 2021).

Our results were consistent with the conclusions presented by Schirmer et al. (2022) or Mooney and Li (2021), who found
climate change signals towards more intense and frequent RoS events for an RCP 8.5 scenario (closest to the warmest
435 projections in our study assuming an increase in temperature of 4 °C) at high elevations. Many studies (Il Jeong and
Sushama, 2017; Li et al., 2019; Mooney and Li, 2021; Musselman et al., 2018; Sezen et al., 2020; Trubilowicz and Moore,
2017) evaluating and modeling RoS events for different climate scenarios predict an increase of RoS events, particularly at
higher elevations (usually valid for catchments above 1500 m a.s.l.). In contrast, their results showed a general RoS decrease
with lower hydrological extreme responses at lower elevations (usually covering catchments below 1000 m a.s.l.). These
440 broader elevation-based behaviors were more pronounced in the Czech catchments in our study. Results also showed
seasonally-dependent changes in RoS occurrence. Most of the projections suggested a decrease in the number of RoS days
towards the end of winter (particularly April and May), which supports the findings presented by Sezen et al. (2020). The
signals towards more frequent RoS events, more pronounced in the Swiss catchments, were detected in the middle of the
snow season. This RoS increase is likely driven by changes in precipitation since more precipitation is expected to occur as
445 rain rather than snow (Nedelcev and Jenicek, 2021).

There is still limited knowledge on how RoS-driven hydrological response will be affected by climate change (Myers et al., 2023). Therefore, RoS-related runoff projections presented in this study are very beneficial. Sikorska-Senoner and Seibert (2020) identified an overall decreasing trend of RoS-related flooding for 27 Swiss catchments between 1980 and 2014, which agrees with our general results for the Swiss study catchments and throughout the entire year. In our study, we found
450 that these general trends may not be present for winter months (January, February and March) due to expected changes in air temperature and precipitation patterns. Beniston and Stoffel (2016) concluded that the frequency of floods triggered by RoS may increase by 50 % in Switzerland with a temperature increase of 2-4 °C. However, an air temperature increase of more than 4 °C may result in a RoS-driven flood decrease due to the decline in snowpack duration.

Runoff projections presented in this study did not specifically assess changes in the extreme hydrological RoS-related
455 response. Thus, these possible climate-driven changes remain uncertain. Such extreme hydrological events triggered by RoS may occur. However, the probability will likely be lowered with gradual warming, although significant RoS runoff events remain an important flood risk, especially for moderate warming up to 2 °C compared to the reference period. The relative increase in RoS-driven runoff was projected to be even less frequent than the relative increase in the number of RoS days in January and February. This fact may indicate that more frequent RoS occurrence does not necessarily result in increased
460 runoff with potential flooding. All projections with a temperature increase above 2 °C, which seem realistic for the future climate, show an expected decrease in RoS runoff response for all months.

According to López-Moreno et al. (2021), the hydrological importance of RoS is not expected to decrease, although the overall frequency of RoS drops. Their model runs showed that maximum runoffs caused by RoS may increase due to warmer snowpack during future RoS events, and more accelerated snowmelt enhanced by energy inputs. The above-mentioned
465 inconsistency between relative changes in RoS numbers (Fig. 6) and relative changes in runoff response (Fig. 10) was evident in our analyses. The initial snowpack properties and related snowpack retention capacity can also play an important role in runoff formation during RoS events (Garvelmann et al., 2015; Würzer et al., 2016). Consequently, some RoS events do not increase runoff (Juras et al., 2021; Wayand et al., 2015).

5 Conclusions

470 We evaluated potential regional and seasonal variations in RoS occurrence that are projected to occur in the future due to climate change. We performed a sensitivity analysis using a conceptual hydrological model simulating the change in RoS situations and their runoff response to precipitation and air temperature changes. Based on the results, we can draw the following conclusions.

The mean number of RoS days per season varied from one to more than 50 RoS days at a catchment scale, with the most
475 frequent RoS occurrence in the elevation range from 1000 to 2000 m a.s.l. Regarding the elevation, distinct catchments saw the average RoS occurrence at different times of the year from mid-January to mid-May. March was the month with the highest RoS occurrence.

The results showed that climate change-driven RoS changes are highly variable over regions and sub-regions, across elevations, and within the cold season. In general, RoS days are expected to occur less frequently with further warming, particularly at lower elevations. The warmest projections suggested a decrease of RoS days by about 75 % for the Czech catchments. High-elevation Swiss catchments may respond less sensitively, at least in projections leading to wetter conditions, compared to the reference period. However, the number of RoS days may increase, specifically during the mid-winter (January, February) and at higher elevations following moderate warming, which may be further enhanced by increased precipitation.

Various seasonal climate and snow characteristics may control RoS occurrences. The RoS occurrence was identified as more sensitive to changes in snowfall in the Czech catchments, while seasonal precipitation totals (regardless of snowfall or rainfall) appeared to be the primary driver in Switzerland. Surprisingly, the correlation between RoS and air temperature was relatively weak in both regions.

The results suggested that RoS contribution to annual runoff will likely be reduced from the current 10 % to 2-4 % for the warmest projections in Czechia, and from 18 % to 5-9 % in Switzerland. However, the RoS contribution to runoff may increase in winter months in Switzerland, for almost all projections with the same or higher amount of precipitation, regardless of air temperature increase. With the expected more frequent RoS events during these months, Swiss catchments, particularly high-elevation ones, may face more extreme RoS-related flood events in the future. For Czech catchments, the winter runoff increase is expected only for wet projections with a relatively small air temperature increase. Despite the expectations that the overall RoS impact on runoff will be lower in the future, extreme hydrological response and flooding triggered by RoS events may still represent a significant flood risk.

Data availability

The HBV model outputs were published as an open dataset (Jenicek et al., 2024).

Author contribution

OH and MJ initiated the study and designed the research; OH, ON and MJ prepared and analyzed data; OH and ON produced the figures and tables; all authors contributed to interpreting the results; OH wrote the manuscript with the contribution of all co-authors.

Competing interests

At least one of the (co-)authors is a member of the editorial board of Hydrology and Earth System Sciences.

505 **Disclaimer**

Publisher's note: Copernicus Publications remains neutral with regard to jurisdictional claims made in the text, published maps, institutional affiliations, or any other geographical representation in this paper. While Copernicus Publications makes every effort to include appropriate place names, the final responsibility lies with the authors.

Acknowledgments

510 The authors wish to thank Tobias Jonas for preparing and providing SWE data for the Swiss catchments. Many thanks are due to Tracy Ewen for improving the language.

Financial support

This work was supported jointly by the Czech Science Foundation and Swiss National Science Foundation (project MountSnow, no. GAČR 23-06859K and SNSF 200021E_213165), Charles University Grant Agency (project no. GAUK 515 316821), Technology Agency of the Czech Republic (project SS02030040) and the Johannes Amos Comenius Programme (P JAC; project No. CZ.02.01.01/00/22_008/0004605; Natural and anthropogenic georisks).

References

- Addor, N., Rössler, O., Köplin, N., Huss, M., Weingartner, R., and Seibert, J.: Robust changes and sources of uncertainty in the projected hydrological regimes of Swiss catchments, *Water Resour. Res.*, 50, 7541–7562, 520 <https://doi.org/10.1002/2014WR015549>, 2014.
- Bartsch, A., Kumpula, T., Forbes, B. C., and Stammler, F.: Detection of snow surface thawing and refreezing in the Eurasian arctic with QuikSCAT: Implications for reindeer herding, *Ecol. Appl.*, 20, 2346–2358, <https://doi.org/10.1890/09-1927.1>, 2010.
- Bartsch, A., Bergstedt, H., Pointner, G., Muri, X., Rautiainen, K., Leppänen, L., Joly, K., Sokolov, A., Orekhov, P., Ehrlich, 525 D., and Soininen, E. M.: Towards long-term records of rain-on-snow events across the Arctic from satellite data, *Cryosphere*, 17, 889–915, <https://doi.org/10.5194/TC-17-889-2023>, 2023.
- Beniston, M. and Stoffel, M.: Rain-on-snow events, floods and climate change in the Alps: Events may increase with warming up to 4 °C and decrease thereafter, *Sci. Total Environ.*, 571, 228–236, <https://doi.org/10.1016/j.scitotenv.2016.07.146>, 2016.

- 530 Berghuijs, W. R., Harrigan, S., Molnar, P., Slater, L. J., and Kirchner, J. W.: The Relative Importance of Different Flood-Generating Mechanisms Across Europe, *Water Resour. Res.*, 55, 4582–4593, <https://doi.org/10.1029/2019WR024841>, 2019.
- Beven, K.: An epistemically uncertain walk through the rather fuzzy subject of observation and model uncertainties I, *Hydrol. Process.*, 35, 1–9, <https://doi.org/10.1002/hyp.14012>, 2021.
- Bieniek, P. A., Bhatt, U. S., Walsh, J. E., Lader, R., Griffith, B., Roach, J. K., and Thoman, R. L.: Assessment of Alaska
535 rain-on-snow events using dynamical downscaling, *J. Appl. Meteorol. Climatol.*, 57, 1847–1863, <https://doi.org/10.1175/JAMC-D-17-0276.1>, 2018.
- Blahušiaková, A., Matoušková, M., Jenicek, M., Ledvinka, O., Kliment, Z., Podolinská, J., and Snopková, Z.: Snow and climate trends and their impact on seasonal runoff and hydrological drought types in selected mountain catchments in Central Europe, *Hydrol. Sci. J.*, 65, 2083–2096, <https://doi.org/10.1080/02626667.2020.1784900>, 2020.
- 540 Blöschl, G., Bierkens, M. F. P., Chambel, A., Cudennec, C., Destouni, G., Fiori, A., Kirchner, J. W., McDonnell, J. J., Savenije, H. H. G., Sivapalan, M., Stumpff, C., Toth, E., Volpi, E., Carr, G., Lupton, C., Salinas, J., Széles, B., Viglione, A., Aksoy, H., Allen, S. T., Amin, A., Andréassian, V., Arheimer, B., Aryal, S. K., Baker, V., Bardsley, E., Barendrecht, M. H., Bartosova, A., Batelaan, O., Berghuijs, W. R., Beven, K., Blume, T., Bogaard, T., Borges de Amorim, P., Böttcher, M. E., Boulet, G., Breinl, K., Brilly, M., Brocca, L., Buytaert, W., Castellarin, A., Castelletti, A., Chen, X., Chen, Y., Chen, Y.,
545 Chiffard, P., Claps, P., Clark, M. P., Collins, A. L., Croke, B., Dathe, A., David, P. C., de Barros, F. P. J., de Rooij, G., Di Baldassarre, G., Driscoll, J. M., Duethmann, D., Dwivedi, R., Eris, E., Farmer, W. H., Feiccabrino, J., Ferguson, G., Ferrari, E., Ferraris, S., Fersch, B., Finger, D., Foglia, L., Fowler, K., Gartsman, B., Gascoin, S., Gaume, E., Gelfan, A., Geris, J., Gharari, S., Gleeson, T., Glendell, M., Gonzalez Bevacqua, A., González-Dugo, M. P., Grimaldi, S., Gupta, A. B., Guse, B., Han, D., Hannah, D., Harpold, A., Haun, S., Heal, K., Helfricht, K., Herrnegger, M., Hipsey, M., Hlaváčiková, H.,
550 Hohmann, C., Holko, L., Hopkinson, C., Hrachowitz, M., Illangasekare, T. H., Inam, A., Innocente, C., Istanbuloglu, E., Jarihani, B., et al.: Twenty-three unsolved problems in hydrology (UPH)—a community perspective, *Hydrol. Sci. J.*, 64, 1141–1158, <https://doi.org/10.1080/02626667.2019.1620507>, 2019.
- Brunner, M. I. and Fischer, S.: Snow-influenced floods are more strongly connected in space than purely rainfall-driven floods, *Environ. Res. Lett.*, 17, 104038, <https://doi.org/10.1088/1748-9326/ac948f>, 2022.
- 555 Crawford, A. D., Alley, K. E., Cooke, A. M., and Serreze, M. C.: Synoptic climatology of rain-on-snow events in Alaska, *Mon. Weather Rev.*, 148, 1275–1295, <https://doi.org/10.1175/MWR-D-19-0311.1>, 2020.
- Cui, G., Anderson, M., and Bales, R.: Runoff response to the uncertainty from key water-budget variables in a seasonally snow-covered mountain basin, *J. Hydrol. Reg. Stud.*, 50, 101601, <https://doi.org/10.1016/j.ejrh.2023.101601>, 2023.

- Earman, S., Campbell, A. R., Phillips, F. M., and Newman, B. D.: Isotopic exchange between snow and atmospheric water vapor: Estimation of the snowmelt component of groundwater recharge in the southwestern United States, *J. Geophys. Res.*, 111, D09302, <https://doi.org/10.1029/2005JD006470>, 2006.
- 560 Etter, S., Addor, N., Huss, M., and Finger, D.: Climate change impacts on future snow, ice and rain runoff in a Swiss mountain catchment using multi-dataset calibration, *J. Hydrol. Reg. Stud.*, 13, 222–239, <https://doi.org/10.1016/j.ejrh.2017.08.005>, 2017.
- 565 Freudiger, D., Kohn, I., Stahl, K., and Weiler, M.: Large-scale analysis of changing frequencies of rain-on-snow events with flood-generation potential, *Hydrol. Earth Syst. Sci.*, 18, 2695–2709, <https://doi.org/10.5194/hess-18-2695-2014>, 2014.
- Garvelmann, J., Pohl, S., and Weiler, M.: Variability of Observed Energy Fluxes during Rain-on-Snow and Clear Sky Snowmelt in a Midlatitude Mountain Environment, *J. Hydrometeorol.*, 15, 1220–1237, <https://doi.org/10.1175/JHM-D-13-0187.1>, 2014.
- 570 Garvelmann, J., Pohl, S., and Weiler, M.: Spatio-temporal controls of snowmelt and runoff generation during rain-on-snow events in a mid-latitude mountain catchment, *Hydrol. Process.*, 29, 3649–3664, <https://doi.org/10.1002/hyp.10460>, 2015.
- Girons Lopez, M., Vis, M. J. P., Jenicek, M., Griessinger, N., and Seibert, J.: Assessing the degree of detail of temperature-based snow routines for runoff modelling in mountainous areas in central Europe, *Hydrol. Earth Syst. Sci.*, 24, 4441–4461, <https://doi.org/10.5194/hess-24-4441-2020>, 2020.
- 575 Grenfell, T. C. and Putkonen, J.: A method for the detection of the severe rain-on-snow event on Banks Island, October 2003, using passive microwave remote sensing, *Water Resour. Res.*, 44, 3425, <https://doi.org/10.1029/2007WR005929>, 2008.
- Gutiérrez, J. M., Jones, R. G., Narisma, G. T., Alves, L. M., Amjad, M., Gorodetskaya, I. V., Grose, M., Klutse, N. A. B., Krakovska, S., Li, J., Martinez-Castro, D., Mearns, L. O., Mernild, S. H., Ngo-Duc, T., van den Hurk, B., and Yoon, J. H.: Atlas, in: *Climate Change 2021 – The Physical Science Basis*, Cambridge University Press, 1927–2058, <https://doi.org/10.1017/9781009157896.021>, 2021.
- 580 Hale, K. E., Jennings, K. S., Musselman, K. N., Livneh, B., and Molotch, N. P.: Recent decreases in snow water storage in western North America, *Commun. Earth Environ.*, 4, 1–11, <https://doi.org/10.1038/s43247-023-00751-3>, 2023.
- Hotovy, O. and Jenicek, M.: The impact of changing subcanopy radiation on snowmelt in a disturbed coniferous forest, *Hydrol. Process.*, 34, 5298–5314, <https://doi.org/10.1002/hyp.13936>, 2020.

- Hotovy, O., Nedelcev, O., and Jenicek, M.: Changes in rain-on-snow events in mountain catchments in the rain–snow transition zone, *Hydrol. Sci. J.*, 68, 572–584, <https://doi.org/10.1080/02626667.2023.2177544>, 2023.
- Jenicek, M. and Ledvinka, O.: Importance of snowmelt contribution to seasonal runoff and summer low flows in Czechia, *Hydrol. Earth Syst. Sci.*, 24, 3475–3491, <https://doi.org/10.5194/hess-24-3475-2020>, 2020.
- 590 Jenicek, M., Hnilica, J., Nedelcev, O., and Sipek, V.: Future changes in snowpack will impact seasonal runoff and low flows in Czechia, *J. Hydrol. Reg. Stud.*, 37, 100899, <https://doi.org/10.1016/j.ejrh.2021.100899>, 2021.
- Jenicek, M., Nedelcev, O., and Hotovy, O.: Supplementary data: Rain-on-snow events in mountainous catchments under climate change (Version 1) [Data set]. Zenodo. <https://doi.org/10.5281/zenodo.12772038>, 2024.
- Jennings, K. S., Winchell, T. S., Livneh, B., and Molotch, N. P.: Spatial variation of the rain-snow temperature threshold across the Northern Hemisphere, *Nat. Commun.*, 9, 1–9, <https://doi.org/10.1038/s41467-018-03629-7>, 2018.
- 595 Il Jeong, D. and Sushama, L.: Rain-on-snow events over North America based on two Canadian regional climate models, *Clim. Dyn.*, 50, 303–316, <https://doi.org/10.1007/s00382-017-3609-x>, 2017.
- Juras, R., Blöcher, J. R., Jenicek, M., Hotovy, O., and Markonis, Y.: What affects the hydrological response of rain-on-snow events in low-altitude mountain ranges in Central Europe?, *J. Hydrol.*, 603, 127002, <https://doi.org/10.1016/j.jhydrol.2021.127002>, 2021.
- 600 https://doi.org/10.1016/j.jhydrol.2021.127002, 2021.
- Li, D., Lettenmaier, D. P., Margulis, S. A., and Andreadis, K.: The Role of Rain-on-Snow in Flooding Over the Conterminous United States, *Water Resour. Res.*, 55, 8492–8513, <https://doi.org/10.1029/2019WR024950>, 2019.
- Li, Z., Chen, Y., Li, Y., and Wang, Y.: Declining snowfall fraction in the alpine regions, Central Asia, *Sci. Rep.*, 10, 1–12, <https://doi.org/10.1038/s41598-020-60303-z>, 2020.
- 605 Lindström, G., Johansson, B., Persson, M., Gardelin, M., and Bergström, S.: Development and test of the distributed HBV-96 hydrological model, *J. Hydrol.*, 201, 272–288, [https://doi.org/10.1016/S0022-1694\(97\)00041-3](https://doi.org/10.1016/S0022-1694(97)00041-3), 1997.
- López-Moreno, J. I., Pomeroy, J. W., Morán-Tejeda, E., Revuelto, J., Navarro-Serrano, F. M., Vidaller, I., and Alonso-González, E.: Changes in the frequency of global high mountain rain-on-snow events due to climate warming, *Environ. Res. Lett.*, 16, 094021, <https://doi.org/10.1088/1748-9326/ac0dde>, 2021.

- 610 Magnusson, J., Gustafsson, D., Hüsler, F., and Jonas, T.: Assimilation of point SWE data into a distributed snow cover model comparing two contrasting methods, *Water Resour. Res.*, 50, 7816–7835, <https://doi.org/10.1002/2014WR015302>, 2014.
- Maina, F. Z. and Kumar, S. V.: Diverging Trends in Rain-On-Snow Over High Mountain Asia, *Earth’s Futur.*, 11, <https://doi.org/10.1029/2022EF003009>, 2023.
- 615 Mooney, P. A. and Li, L.: Near future changes to rain-on-snow events in Norway, *Environ. Res. Lett.*, 16, 064039, <https://doi.org/10.1088/1748-9326/abfdeb>, 2021.
- Morán-Tejeda, E., López-Moreno, J. I., Stoffel, M., and Beniston, M.: Rain-on-snow events in Switzerland: Recent observations and projections for the 21st century, *Clim. Res.*, 71, 111–125, <https://doi.org/10.3354/cr01435>, 2016.
- Moriasi, D. N., Gitau, M. W., Pai, N., and Daggupati, P.: Hydrologic and water quality models: Performance measures and evaluation criteria, *Trans. ASABE*, 58, 1763–1785, <https://doi.org/10.13031/trans.58.10715>, 2015.
- 620 Mott, R., Winstral, A., Cluzet, B., Helbig, N., Magnusson, J., Mazzotti, G., Quéno, L., Schirmer, M., Webster, C., and Jonas, T.: Operational snow-hydrological modeling for Switzerland, *Front. Earth Sci.*, 11, 1–20, <https://doi.org/10.3389/feart.2023.1228158>, 2023.
- Musselman, K. N., Lehner, F., Ikeda, K., Clark, M. P., Prein, A. F., Liu, C., Barlage, M., and Rasmussen, R.: Projected increases and shifts in rain-on-snow flood risk over western North America, <https://doi.org/10.1038/s41558-018-0236-4>, 2018.
- 625 Myers, D. T., Ficklin, D. L., and Robeson, S. M.: Hydrologic implications of projected changes in rain-on-snow melt for Great Lakes Basin watersheds, *Hydrol. Earth Syst. Sci.*, 27, 1755–1770, <https://doi.org/10.5194/hess-27-1755-2023>, 2023.
- Nedelcev, O. and Jenicek, M.: Trends in seasonal snowpack and their relation to climate variables in mountain catchments in Czechia, *Hydrol. Sci. J.*, 66, 2340–2356, <https://doi.org/10.1080/02626667.2021.1990298>, 2021.
- 630 Notarnicola, C.: Hotspots of snow cover changes in global mountain regions over 2000–2018, *Remote Sens. Environ.*, 243, 111781, <https://doi.org/10.1016/j.rse.2020.111781>, 2020.
- Ohba, M. and Kawase, H.: Rain-on-Snow events in Japan as projected by a large ensemble of regional climate simulations, *Clim. Dyn.*, 55, 2785–2800, <https://doi.org/10.1007/s00382-020-05419-8>, 2020.

- 635 Oudin, L., Hervieu, F., Michel, C., Perrin, C., Andréassian, V., Anctil, F., and Loumagne, C.: Which potential evapotranspiration input for a lumped rainfall-runoff model? Part 2 - Towards a simple and efficient potential evapotranspiration model for rainfall-runoff modelling, *J. Hydrol.*, 303, 290–306, <https://doi.org/10.1016/j.jhydrol.2004.08.026>, 2005.
- Pall, P., Tallaksen, L. M., and Stordal, F.: A climatology of rain-on-snow events for Norway, *J. Clim.*, 32, 6995–7016, <https://doi.org/10.1175/JCLI-D-18-0529.1>, 2019.
- 640 Parajka, J., Bezak, N., Burkhart, J., Hauksson, B., Holko, L., Hundecha, Y., Jenicek, M., Krajčí, P., Mangini, W., Molnar, P., Riboust, P., Rizzi, J., Sensoy, A., Thirel, G., and Viglione, A.: Modis snowline elevation changes during snowmelt runoff events in Europe, *J. Hydrol. Hydromechanics*, 67, 101–109, <https://doi.org/10.2478/johh-2018-0011>, 2019.
- Poschlod, B., Zscheischler, J., Sillmann, J., Wood, R. R., and Ludwig, R.: Climate change effects on hydrometeorological compound events over southern Norway, *Weather Clim. Extrem.*, 28, 100253, <https://doi.org/10.1016/j.wace.2020.100253>, 2020.
- 645 Schirmer, M., Winstral, A., Jonas, T., Burlando, P., and Peleg, N.: Natural climate variability is an important aspect of future projections of snow water resources and rain-on-snow events, *Cryosph.*, 16, 3469–3488, <https://doi.org/10.5194/tc-16-3469-2022>, 2022.
- 650 Seibert, J. and Bergström, S.: A retrospective on hydrological catchment modelling based on half a century with the HBV model, *Hydrol. Earth Syst. Sci.*, 26, 1371–1388, <https://doi.org/10.5194/hess-26-1371-2022>, 2022.
- Seibert, J. and Vis, M. J. P.: Teaching hydrological modeling with a user-friendly catchment-runoff-model software package, *Hydrol. Earth Syst. Sci.*, 16, 3315–3325, <https://doi.org/10.5194/hess-16-3315-2012>, 2012.
- Sezen, C., Sraj, M., Medved, A., and Bezak, N.: Investigation of rain-on-snow floods under climate change, *Appl. Sci.*, 10, <https://doi.org/10.3390/app10041242>, 2020.
- 655 Sikorska-Senoner, A. E. and Seibert, J.: Flood-type trend analysis for alpine catchments, *Hydrol. Sci. J.*, 65, 1281–1299, <https://doi.org/10.1080/02626667.2020.1749761>, 2020.
- Surfleet, C. G. and Tullos, D.: Variability in effect of climate change on rain-on-snow peak flow events in a temperate climate, *J. Hydrol.*, 479, 24–34, <https://doi.org/10.1016/j.jhydrol.2012.11.021>, 2013.
- 660 Suriano, Z. J.: North American rain-on-snow ablation climatology, *Clim. Res.*, 87, 133–145, <https://doi.org/10.3354/cr01687>, 2022.

- Trubilowicz, J. W. and Moore, R. D.: Quantifying the role of the snowpack in generating water available for run-off during rain-on-snow events from snow pillow records, *Hydrol. Process.*, 31, 4136–4150, <https://doi.org/10.1002/hyp.11310>, 2017.
- Urban, G., Richterová, D., Kliegrová, S., and Zusková, I.: Reasons for shortening snow cover duration in the Western Sudetes in light of global climate change, *Int. J. Climatol.*, 43, 5485–5511, <https://doi.org/10.1002/joc.8157>, 2023.
- Wayand, N. E., Lundquist, J. D., and Clark, M. P.: Modeling the influence of hypsometry, vegetation, and storm energy on snowmelt contributions to basins during rain-on-snow floods, *Water Resour. Res.*, 51, 8551–8569, <https://doi.org/10.1002/2014WR016576>, 2015.
- Würzer, S., Jonas, T., Wever, N., and Lehning, M.: Influence of Initial Snowpack Properties on Runoff Formation during Rain-on-Snow Events, *J. Hydrometeorol.*, 17, 1801–1815, <https://doi.org/10.1175/JHM-D-15-0181.1>, 2016.
- Yang, T., Li, Q., Hamdi, R., Chen, X., Zou, Q., Cui, F., De Maeyer, P., and Li, L.: Trends and spatial variations of rain-on-snow events over the high Mountain Asia, *J. Hydrol.*, 614, 128593, <https://doi.org/10.1016/j.jhydrol.2022.128593>, 2022.
- Yang, Z., Chen, R., Liu, Y., Zhao, Y., Liu, Z., and Liu, J.: The impact of rain-on-snow events on the snowmelt process: A field study, *Hydrol. Process.*, 37, e15019, <https://doi.org/10.1002/hyp.15019>, 2023.